

THE UNIVERSITY OF HULL

Detection and Measurement and of Repolarisation Features in Atrial Fibrillation  
and Healthy Subjects

being a Thesis submitted for the Degree of

Doctor of Philosophy

in the University of Hull

by

Marwa Saeb Al-Karadi BSc MSc

July 2019

# Abstract

Major cardiac organisations recommended U wave abnormalities should be reported during ECG interpretation. However, U waves cannot be measured in patients with atrial fibrillation (AF) due to the obscuring fibrillatory wave.

The first aim of the research was to provide a validated algorithm to clean the ECGs of AF patients by removing the atrial fibrillatory waves so that the characteristics of ventricle repolarisation components, U and T waves, could be detected and measured accurately without fibrillatory wave contamination.

Having established a validated algorithm to measure the waveform features, the second aim was to use this algorithm to investigate the effect of beat interval dependency on the repolarisation waves, especially U waves, during AF and to compare them to those in sinus rhythm (SR) of healthy subjects. The research could provide mechanistic insight into the origin of U waves since AF is unique in its rapidly changing ventricular beat intervals. The preceding beat interval has a direct impact on ventricular filling dynamics and hence also on mechano-electrical coupling, one of the leading hypotheses of U wave genesis.

Algorithms were developed to remove the contaminating fibrillatory waves in AF recordings and to measure features of the ventricular repolarisation waves.

The ventricular repolarisation features, U and T waves, are measurable and dependent on preceding beat interval in AF and SR. The beat interval dependency of repolarisation features, especially the U wave, supported the mechano-electrical hypothesis during AF and SR.

The research provides tools to facilitate the detection and reporting of U waves and their abnormalities in AF patients and provides mechanistic insight into rate dependency of ventricular repolarisation features.

# Acknowledgement

Firstly, I would like to express my sincere gratitude to my first supervisor Dr. Philip Langley for the continuous support of my PhD study, for his patience, inspiration, and immense knowledge. His guidance helped me in all the time of research and writing of this thesis. I could not have imagined having a better advisor and mentor for my PhD study.

My profound appreciation to my second supervisor Dr. Antony J. Wilkinson for all the support and encouragement he gave me. Without his guidance and constant feedback this PhD would not have been achievable. I will forever be thankful to his help, advise, motivation, and enlightening from the first month of the study till the last moment.

I gratefully acknowledge the funding received towards my PhD from the University of Hull, Faculty of Science and Engineering. I dared to dream, and the University helped to make it true.

My sincere thanks also go to Dr. Jane Caldwell from Castle Hill Hospital and NHS Trust who provided the research with the databases and the valuable consultation during the PhD study.

Finally, I would like to express my appreciation to all the unconditional love, limitless support and utmost encouragement in every single minute during this journey: to my beloved mother, father and brother.

# Contents

Abstract.....	1
Acknowledgement .....	2
Contents .....	3
List of Abbreviation.....	8
Publications.....	9
Introduction.....	10
Chapter 1. Literature Review .....	13
1.1. Introduction.....	13
1.2. Cardiac Anatomy and Physiology.....	14
1.2.1. The Heart Anatomy.....	14
1.2.1.1. Location of the Heart .....	14
1.2.1.2. Heart Walls .....	14
1.2.1.3. Chambers and Valves of the Heart.....	16
1.2.1.4. The Cardiovascular Circuits and Blood Flow .....	17
1.2.2. Cardiac Electrophysiology .....	20
1.2.2.1. Electrical Activity of the Heart .....	20
1.2.2.1.1. The Cardiac Conduction System.....	20
1.2.2.1.2. Depolarisation and Repolarisation of Cardiac Cells .....	21
1.2.2.1.3. Cardiac Action Potential .....	22
1.2.2.1.3.1. The Interval-Duration Relation .....	25
1.2.2.1.3.2. Afterdepolarisation.....	25
1.2.2.2. Cardiac Muscle Cells Structure (Histology) .....	27
1.2.2.3. Excitation Contraction Coupling.....	30
1.2.2.4. Electrocardiogram .....	32
1.2.2.4.1. ECG Components (Waves, Intervals and Segments ).....	33
1.2.2.4.2. ECG Normal Characteristics.....	34
1.2.2.4.2.1. Heart Rate .....	34
1.2.2.4.2.2. Cardiac Rhythm .....	35
1.2.2.5. ECG Lead System.....	35
1.2.2.5.1. The 12 Lead ECG System.....	35
1.2.3. Cardiac Mechanical Properties .....	39
1.2.3.1. Cardiac Cycle and Mechanical Events.....	39

1.2.3.2. Cardiac Performance (Cardiac Output).....	41
1.2.3.2.1. Preload and End Diastolic Volume (EDV) .....	43
1.2.3.2.2. Contractility and Afterload .....	43
1.2.3.3. Frank-Starling Law of the Heart .....	44
1.2.3.4. Ventricular Pressure-Volume Relationship.....	46
1.2.4. Principles of Heart Physiology During Exercise .....	47
1.2.4.1. Cardiovascular Response to the Exercise .....	48
1.2.4.2. ECG During Exercise.....	51
1.3. U wave in Electrocardiogram .....	52
1.3.1. The Characteristics of U Wave .....	53
1.3.2. Origin of U Wave.....	55
1.3.3. The Hypotheses of U Wave Genesis.....	56
1.3.3.1. Hypothesis 1: Delayed Repolarisation for His-Purkinje System .....	56
1.3.3.2. Hypothesis 2: Delayed Repolarisation of Certain Regions of the Ventricular Myocardium.....	57
1.3.3.3. Hypothesis 3: Mechano-Electrical Coupling .....	59
1.3.4. U Wave Pathology .....	60
1.3.4.1. Abnormalities of U Wave .....	60
1.3.4.1.1. U Wave Inverted .....	60
1.3.4.1.2. Prominent U Wave.....	61
1.4. T Wave in Electrocardiogram .....	62
1.4.1. Characteristic of T Wave in Normal ECG .....	62
1.4.2. Origin of T Wave .....	63
1.4.3. Abnormalities of T Wave.....	64
1.4.3.1. QT Interval.....	65
1.5. Abnormal Heart Rhythm.....	66
1.5.1. Types of Arrhythmias .....	66
1.5.2. Atrial Fibrillation (AF).....	68
1.5.2.1. Atrial Fibrillation Characteristics.....	69
1.5.2.2. Cardiac Activity Difference Between Normal Rhythm and AF .....	70
1.5.2.3. Classification of Atrial Fibrillation .....	72
1.5.2.4. Atrial Fibrillation Symptoms, Causes, Factors and Risks.....	73
1.5.2.4.1. Symptoms .....	73
1.5.2.4.2. Causes, Factors and Risks .....	73
Chapter 2. Research Ethics and ECG Recordings .....	76
2.1. Introduction.....	76

2.2. Research Ethics .....	77
2.3. Descriptions of the ECG Databases .....	77
2.3.1. Long Duration AF Database .....	77
2.3.2. AF/SR Database .....	78
2.3.2.1. PhysioNet Recordings .....	78
2.3.2.2. Local Hospital Acquired Recordings .....	79
2.3.3. SR Exercise Recordings .....	79
Chapter 3. Development of Techniques which Enable the Measurement of Ventricular Repolarisation Features in the ECGs of Patients with Atrial Fibrillation .....	81
3.1. Introduction .....	81
3.2. Candidate Techniques .....	82
3.2.1. Principal Component Analysis .....	86
3.2.1.1. PCA Basic Model .....	86
3.2.1.2. ECG Processing .....	87
3.2.1.3. Implementation Examples .....	89
3.2.2. Independent Component Analysis .....	98
3.2.2.1. ICA Basic Model .....	98
3.2.2.1.1. FastICA Algorithm .....	100
3.2.2.2. ECG Processing .....	100
3.2.2.3. Implementation Examples .....	101
3.2.3. Beat Averaging Technique .....	104
3.2.3.1. ECG Processing .....	104
3.2.3.2. Implementation Examples .....	107
3.3. Comparison Study Between BA, PCA and ICA Techniques .....	111
3.3.1. Method .....	111
3.3.2. Results .....	113
3.3.3. Discussion .....	115
3.4. Chapter Summary .....	117
Chapter 4. Validation of the Ventricular Repolarisation Measurement Techniques .....	119
4.1. Introduction .....	119
4.2. Validation of Automatic Measurements for Ventricular Repolarisation Features Against Manual Measurement .....	120
4.2.1. Method .....	120
4.2.1.1. ECG Database .....	120
4.2.1.2. ECG Processing .....	121
4.2.1.2.1. ECG Pre-processing .....	121

4.2.1.2.2. Automatic Measurement .....	121
4.2.1.2.3. Manual Measurement.....	123
4.2.1.3. Statistical Comparison .....	125
4.2.2. Results.....	127
4.2.2.1. Comparison Between Automatic and Manual Measurements .....	127
4.2.2.2. Inter-observer Variation.....	129
4.2.3. Discussion.....	131
4.3. Validation Study for the Beat Averaging Technique to Extract U Waves in AF Patients by Comparison with U Waves in the Same Patients During SR.....	133
4.3.1. Method .....	133
4.3.1.1. ECG Recordings .....	133
4.3.1.2. ECG Processing .....	133
4.3.1.2.1. AF Recording Analysis.....	134
4.3.1.2.2. SR Recordings Analysis.....	135
4.3.1.3. The Validation Assessment.....	135
4.3.1.4. U Wave Measurement.....	136
4.3.2. Results.....	136
4.3.3. Discussion.....	140
4.4. The Number of Beats Required to Remove the Atrial Fibrillatory Activity to Allow the Effective Measurement of the U Wave in AF.....	142
4.4.1. Method .....	143
4.4.1.1. ECG Recordings .....	143
4.4.1.2. ECG Processing .....	143
4.4.2. Results.....	145
4.4.3. Discussion.....	148
4.5. Chapter Summary .....	149
Chapter 5. Investigation of Rate Dependency of Ventricular Repolarisation Features in Atrial Fibrillation Patients and Healthy Subjects .....	151
5.1. Introduction.....	151
5.2. The Effect of Beat Interval on Ventricular Repolarisation Characteristics in Atrial Fibrillation .....	152
5.2.1. Methods.....	152
5.2.1.1. ECG Recordings .....	152
5.2.1.2. ECG Processing .....	152
5.2.1.3. Statistical Analysis.....	153
5.2.1.4. ‘Preceding’ vs ‘Current’ Beat Interval.....	154
5.2.2. Results.....	155

5.2.2.1. The Effect of the Preceding Beat Interval on Ventricular Repolarisation Features ...	155
5.2.2.1.1. U Wave Amplitudes.....	157
5.2.2.1.2. T wave Amplitudes .....	160
5.2.2.1.3. Analysis of the Relative U Wave and T Wave Amplitude Changes with Respect to Preceding R-R Interval.....	164
5.2.2.1.4. R-T and T-U Intervals.....	165
5.2.2.1.5. TUn Amplitude and R-TUn Interval.....	170
5.2.2.2. ‘Preceding’ vs ‘Current’ Beat Interval.....	171
5.2.3. Discussion .....	174
5.2.3.1. Rate Dependency of U Wave Features .....	177
5.2.3.2. Rate Dependency of T Wave Features.....	178
5.3. The Effect of the Heart Rate Changes Due to Exercise on the U and T Waves Amplitudes in Healthy Subjects .....	181
5.3.1. Method .....	181
5.3.1.1. ECG Recordings .....	181
5.3.1.2. ECG Processing .....	181
5.3.1.2.1. Pre-Exercise Analysis .....	181
5.3.1.2.2. Post-Exercise Analysis.....	182
5.3.2. Results.....	184
5.3.2.1. U Wave Amplitudes.....	184
5.3.2.2. T Wave Amplitudes .....	184
5.3.3. Discussion.....	188
5.4. Chapter Summary .....	191
Chapter 6. Future Perspectives.....	193
6.1. Introduction.....	193
6.2. U wave Abnormalities in Atrial Fibrillation .....	193
6.3. Further Investigation of U Wave Genesis (Cellular Basis).....	193
6.3.1. Intracellular Calcium Dynamics and the U Wave.....	193
6.3.2. The Imaging for U Wave in LQTS .....	194
6.4. The Depression of P-R (PQ) Interval in Healthy Subjects .....	194
Chapter 7. Research Summary and Final Discussion .....	197
References.....	200
Appendix A.....	214
Appendix B .....	216
Appendix C .....	225
Appendix D.....	227

## List of Abbreviation

Abbreviation	Explanation
AF	Atrial fibrillation
AV	Atrioventricular
BA	Beat averaging
bpm	Beats per minutes
BSS	Blind source separation
CO	Cardiac output
DAD	Delayed afterdepolarisation
DOR	Dispersion of repolarisation
EAD	Early afterdepolarisation
EC	Excitation-contraction
ECG	Electrocardiographic signal
EDPVR	End-diastolic pressure–volume relationship
EDV	End diastolic volume
EF	Ejection fraction
ESPVR	End-systolic pressure–volume relationship
ESV	End-systolic volume
HR	Heart rate
ICA	Independent component analysis
ICs	Independent components
LAD	left anterior descending artery
LV	Left ventricular
LQTS	Long QT syndrome
MEC	Mechano-electrical coupling
PAF	Paroxysmal atrial fibrillation
PCA	Principal component analysis
PCs	Principal components
SA	Sinoatrial node
SNR	Signal to noise ratio
SQTS	Short QT syndrome
SR	Sinus rhythm
SV	Stroke volume
TdP	Torsade de pointes

## **Publications**

**Al-Karadi MS**, Wilkinson AJ, Caldwell J, Langley P. Validation of an algorithm to reveal the U wave in atrial fibrillation. *Sci Rep* 2018; **8**: 11946.

**Al-Karadi MS**, Wilkinson AJ, Langley P. The Effect of Beat Interval on Ventricular Repolarisation in Atrial Fibrillation. *Comput. Cardiol.* 2018; **45**. doi:10.22489/cinc.2018.294.

# Introduction

The thesis consists of *seven* chapters which present the studies and investigations to address the aims of the research.

*Chapter one* reviews the literature associated with the investigations and to support the theories proposed to explain the thesis finding and its outcome. The chapter includes five main parts. The first is the introduction and the second part introduces the anatomy and electrophysiology of the normal heart. The cardiac mechanical properties are considered as they play a significant and essential role to understand the underlying mechanisms for the proposed theories. Additionally, the physiological and electrical principles of cardiovascular response during exercise are described as exercise was used to modulate heart rate in one of the studies.

As the main focus of the research was to investigate ventricular repolarisation features, particularly the challenging U, the third part of this chapter contains a review of the U wave of the electrocardiogram, exploring the wave's characteristics, controversial genesis, pathology and abnormalities.

In the fourth part of this chapter, the T wave of the electrocardiogram is described. Since the thesis seeks to present a wide view of the repolarisation characteristics in AF and healthy subjects, the characteristics of the normal T wave are described, and the wave's origin and abnormalities reviewed. Additionally, QT interval is reviewed due to its association to the interval between R wave and T wave peaks (R-T interval) that was investigated as part of this research.

Atrial fibrillation is one of the most common arrhythmias and can affect people's lives severely. It is famous for its rapid heart rate changes which makes it a unique model to investigate the beat interval dependency of ventricular repolarisation features. Thus, the last part of this chapter focuses on cardiac arrhythmias and atrial fibrillation particularly. Atrial fibrillation characteristics, classification, symptoms, causes and risk are reviewed.

In *Chapter two*, all research ethics and ethical approvals are presented along with descriptions of the ECG databases used in the studies.

*Chapter three* proposes three potential techniques to clean the atrial fibrillation recordings from the atrial activity and provide clean beats to allow ventricular repolarisation components to be measured without the contamination by these atrial fibrillatory waves. This is important because in atrial fibrillation, the atrial fibrillatory waves contaminate the ventricular repolarisations components, completely obscure the U wave, and prevent the accurate measurement of their features. Therefore, it is essential to remove these atrial fibrillatory waves before any analysis or measurements. The three techniques: principal component analysis (PCA), independent component analysis (ICA) and beat averaging technique (BA), were examined, and their ability to remove the atrial activity was evaluated. It was found that the beat averaging technique offered an effective tool to remove the atrial fibrillatory activity in

atrial fibrillation recordings and was used for this purpose in the subsequent studies of this research.

*Chapter four* deals with validation and implementation details of the computerised measurement techniques used throughout the research.

First, an algorithm for automatic measurement of the ECG repolarisation features is introduced and validated against manual measurements. Repolarisation features include U and T wave amplitudes and the intervals between R wave and T wave peaks (R-T interval) and between T wave and U wave peaks (T-U interval).

Second, validation of the beat averaging algorithm is presented. It demonstrates the presence of U waves in SR and AF recordings for the same individuals. Significant differences in the amplitudes of U waves between AF and SR recordings were measured suggesting that U waves might be influenced by heart rate.

In the final and third part of this chapter, since the quality of the extracted ventricular repolarisation waveforms is dependent upon the number of beats used in the beat averaging algorithm, the number of beats to remove atrial fibrillatory waves effectively is established.

Much of the work presented in this chapter was published under the title ‘Validation of an algorithm to reveal the U wave in atrial fibrillation’ [1].

Providing efficient and validated algorithms to clean and measure ventricular features in AF and SR, facilitated the possibility to inspect the effect of rate dependency on the repolarisation characteristics in AF and healthy subjects. Therefore, the thesis continues in *Chapter five* with two significant investigations. Both demonstrate the importance of considering the preceding beat interval as a major influence on the repolarisation features in AF and healthy subjects. However, the rate dependency of ventricular repolarisation features in AF is shown to be different to that in healthy subjects. The observed rate dependencies suggest that mechano-electrical coupling plays a significant role in determining U and T wave features.

*Chapter six* presents the perspective of future works and *Chapter seven* provides a comprehensive summary and discussion dealing with all studies mentioned above.

# **Chapter 1**

## **Literature Review**

# Chapter 1. Literature Review

## 1.1. Introduction

This chapter reviews the literature associated to the conducted studies. The chapter is divided into four main parts. The *first* part (section 1.2) reviews the cardiac anatomy and electrophysiology, mechanical properties of the heart, and the principles of heart physiology during the exercise. The *second* part of the chapter (section 1.3) focuses on the U wave in the ECG as it represents the main investigated repolarisation feature in the conducted studies. It describes U wave characteristics, and the controversial hypothesis of the wave's origin. Additionally, the section reviews the U wave pathology and the importance of its abnormalities from the clinical perspective. The *third* part (section 1.4) reviews the T wave in ECG as the second main repolarisation feature investigated during the research. The T wave characteristics, origin and the abnormalities are reviewed in this part. The *fourth* and last part in this chapter (section 1.5) reviews cardiac arrhythmias with a focus on atrial fibrillation (AF) as it plays a significant role during the research since the main investigation is to detect and measure repolarisation features in this arrhythmia. This part reviews AF characteristics, types, symptoms, factors and risks.

## 1.2. Cardiac Anatomy and Physiology

### 1.2.1. The Heart Anatomy

#### 1.2.1.1. Location of the Heart

The human heart is located in the chest and occupies a small region between the third and sixth ribs in the central portion of the thorax cavity of the body as Figure 1.1-a shows. The heart rests on the diaphragm behind the sternum, between the lower parts of the lungs [2,3] as illustrated in Figure 1.1-b.

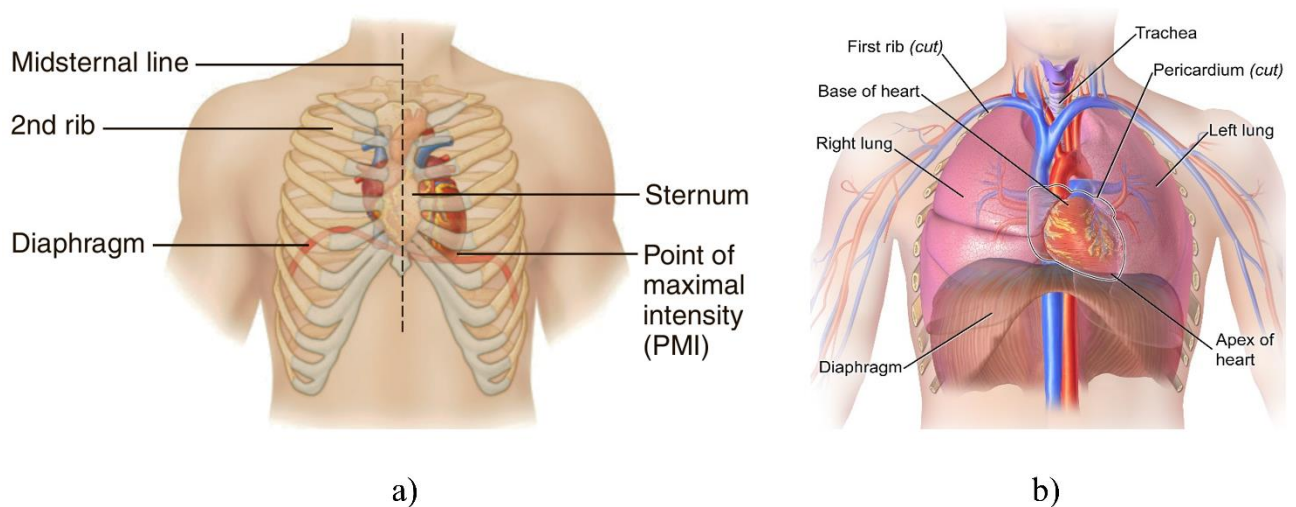


**Figure 1.1:** Location of heart within the thorax cavity (anterior view), where **a)** shows the position of the heart relative to sternum and ribs, and **b)** shows the great vessels location above the heart [2,3].

A typical adult heart has an inverted conical shape, measures approximately 12.5 cm from the base (top) to the apex (bottom) and 7.5 cm at its widest point, leaning towards the left side of the body and slightly forward [2,3]. The right atrium and right ventricle dominate an anterior view of the heart. The great vessels are located above the heart, and they are: the left and the right of pulmonary arteries and veins (two on both sides), the superior and inferior vena cava and the aorta [2,3]. Figure 1.2 displays the frontal section of the heart.

#### 1.2.1.2. Heart Walls

The heart is a muscle organ self-adjusting pump which works in harmony to propel the blood to all tissues of the body [4]. The heart muscle is enclosed in a protective sac known as the *pericardium*, illustrated in Figure 1.3, which protects and stabilises its position. The ultimate

purpose of the heart is to provide the tissues with the oxygen. The hearts chambers play the main part in this process [4].

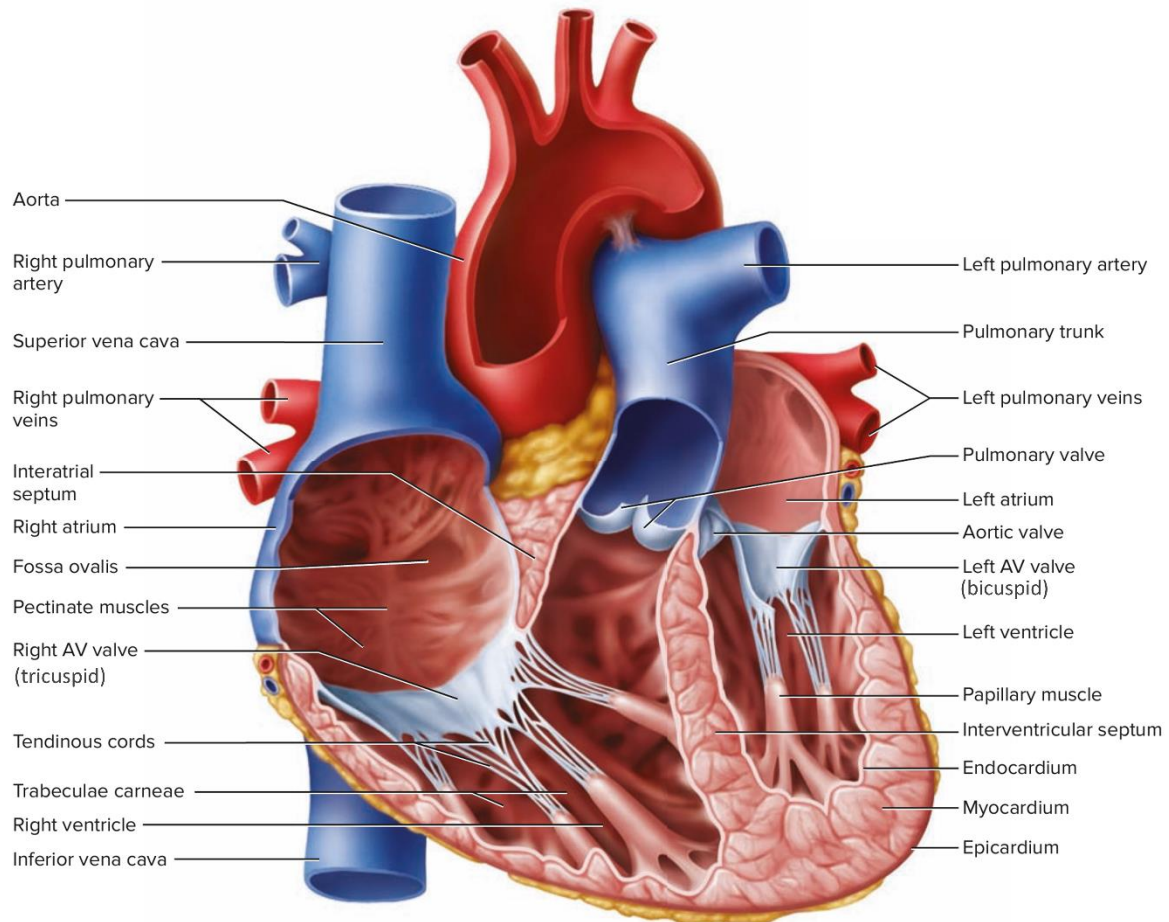


**Figure 1.2:** Internal Anatomy of the heart (frontal section of the heart, anterior view) [3].

The walls of the heart are composed of cardiac muscle and have *three* distinct layers shown in Figure 1.3. The wall layers are: [4,5].

- 1) The *Epicardium* is the outer thin membrane (visceral pericardium) that covers the outer surface of the heart and contains the lymphatic and blood vessels that supply the myocardium.
- 2) The *Myocardium* is the cardiac muscle tissue (middle) and forms the atria and ventricles. This layer is the thickest and responsible for the pumping action of the heart.
- 3) The *Endocardium* is the inner thin membrane lining inside the cardiac muscle, it gives a smooth lining for the hearts chambers and covers the valves too.

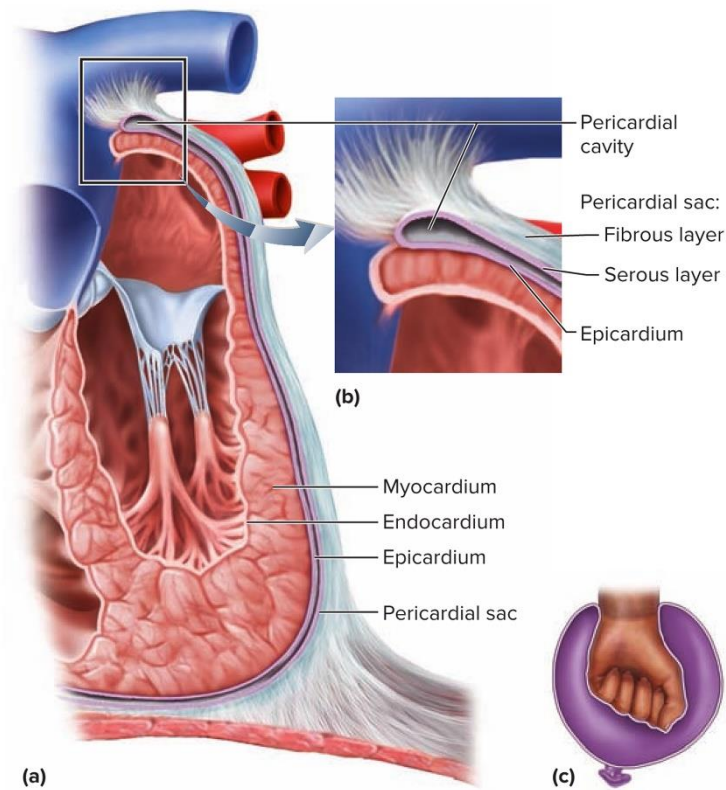


**Figure 1.3:** Pericardium and heart wall. **a)** the three layers of the heart wall and relationship to pericardium, **b)** pericardial sac details and **c)** a fist in balloon illustrates, by analogy, how the pericardium wraps around the heart [3].

### 1.2.1.3. Chambers and Valves of the Heart

The human heart has four chambers, the right and left *atria* and *ventricles* (Figure 1.2). The two smaller superior chambers are receiving chambers, called left atrium and right atrium divided by the *interatrial septum*. They receive blood from blood vessels and contract to push the blood into the lower chambers. The two inferior chambers called ventricles, are divided by a thick wall called the *interventricular septum* and are primarily responsible to eject blood out of the heart into blood vessels called arteries and keep it flowing around the body [3,6,7].

Ventricular muscles anatomically are thicker than atrial muscle [3,8]. This comes from the fact that the ventricles pump blood over long distances through vasculature relative to atria, thus they must work harder to push the blood. Further, the left ventricular free wall and the septum are much thicker than the wall of the right ventricular (two to four times). This is necessary since the left ventricle pumps blood to all organs through systematic circulation (except lungs), and that essential to generate higher pressure than the right ventricle. The right ventricle pumps the blood to the lungs only through the pulmonary circulation [7,8]. Figure 1.2 and 1.4 shows the difference between the thickness of atrial and ventricular muscles.

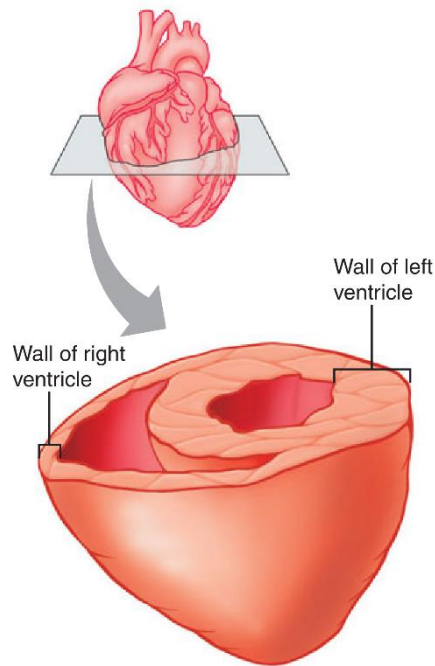


**Figure 1.4:** The thickness of the right and left ventricle muscles [8].

The heart needs valves to pump the blood efficiently and ensure one-way flow. It has four *valves*, which they are divided into two categories: *atrioventricular* valves and *semilunar* valves (Figure 1.2). The atrioventricular (AV) valves are, the *tricuspid* valve (right AV valve) sited between the right atrium and ventricle, and *mitral* (bicuspid, left AV valve) valve between the left atrium and ventricle. The semilunar valves are, the *pulmonary* (pulmonic) valve lies between the right ventricle and the pulmonary artery, whereas the *aortic* (aortic semilunar) valve locates between the aorta and the left ventricle [4,7].

The right side of the heart receives poorly oxygenated blood from the body during systemic circulation and pumps it through pulmonary valve to the lungs for oxygenation during *pulmonary circulation*. The right side does not need to work very hard to drive the blood through the pulmonary circulation, thus it works with low pressure in comparison to the left side of the heart [5,7]. The left side of the heart receives rich oxygenated blood from lungs and pumps it through the aortic valve to the aorta for distribution to the body. The left side does most of the work as has been mentioned, and functions with high pressure to push the blood to the whole *systematic circulation* to the entire body (except lungs) [6,7,9].

#### 1.2.1.4. The Cardiovascular Circuits and Blood Flow

For healthy adults, cardiac circulatory system forms a closed loop of two circuits, both generated and terminated in the heart. The blood pumped out of the heart via set of vessels and returns to the heart by a different set [9]. The two circuits are divided into two halves lengthwise [10].

Figure 1.5 displays the circulatory system showing the two circulations. The *pulmonary circulation* contains blood pumped from right ventricle via the lungs and then pushed to the left atrium. The blood then pumped through the *systemic circulation* from the left ventricle through the body organs and tissues (except the lungs) back then to the right atrium [10]. The vessels that carry the blood from the body organs and tissues towards the heart are called *veins* whereas those carry the blood away from the heart called *arteries* [9,10].

The blood in systemic circuit leaves the left ventricle through a large artery, the *aorta* as Figure 1.5 shows. The arteries of the systematic circulation divided into progressively smaller arteries branch *arterioles* to smallest *capillaries* in which they unite to form large diameter vessels the *venules*. Then the venules in the systemic circulation unite to construct the veins. The veins unite from different organs and tissues to form two large veins, the *inferior vena cava* and *superior vena cava*. The inferior vena cava collects from below the heart whereas the superior vena cava collects the blood from above the heart, see Figure 1.5. The blood is returned to the right atrium through these two veins [10].

In the pulmonary circulation, blood leaves the right ventricle through large *pulmonary trunk* which divided into two pulmonary arteries, one for the right lung and the other for the left lung. Through four pulmonary veins, the blood leaves the lungs and is pushed into the left atrium [8-10].

The blood flows via the lung capillaries where it collects oxygen ( $O_2$ ) that is provided to the lungs via breathing. Hence the blood in pulmonary veins, systemic arteries and left side of the heart are highly oxygenated. The oxygen diffuses to be used by cells as the blood flows through the organs and tissues resulting in lower oxygen ( $O_2$ ) content. In other words, in normal cardiac circulations, the blood pumps to the lungs in order to exchange the  $O_2$  and  $CO_2$  during the pulmonary circulation. Whereas the heart pumps the blood to all other tissues through systematic circulation [9-11], see Figure 1.5.

The blood flows from the heart in one direction (unidirectional) achieved by the valves arrangements, and occurs by the dilatation of the aorta and its branches during ventricular contractions (*systole*) and by elastic regression of the large arteries walls with blood forward pushing during the ventricular relaxation (*diastole*) [11-14]

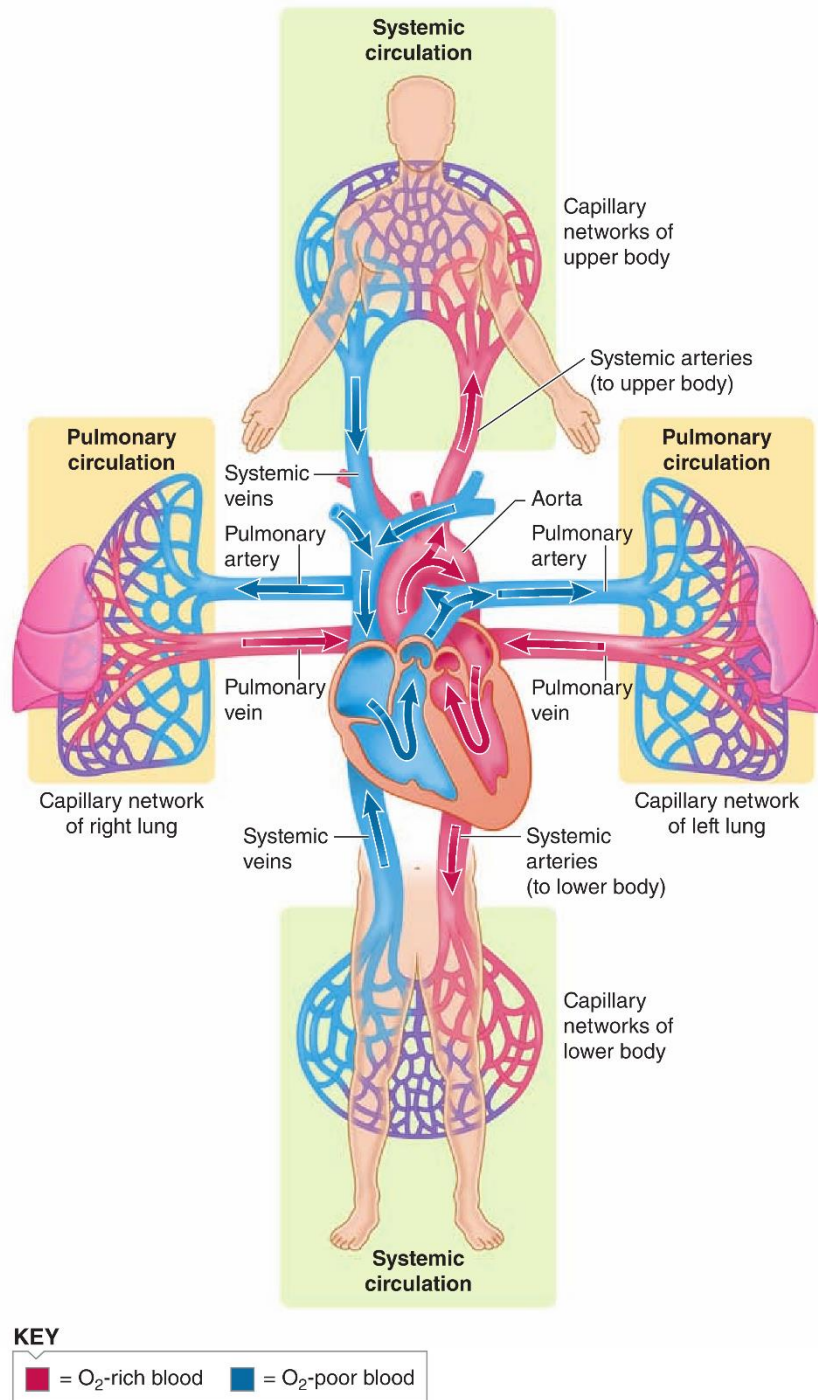


**Figure 1.5:** The systemic and pulmonary circulations. The circulatory system comprises of two separate vascular loops, the systemic circulation which carries blood between the heart and the organ system, and the pulmonary circulation which carries blood between the heart and the lungs [15].

## 1.2.2. Cardiac Electrophysiology

### 1.2.2.1. Electrical Activity of the Heart

The cardiac muscle is unique among other types of muscles, in being able to generate and conduct its own electrical impulses or its action potentials without hormonal or neural stimulation. This property known as *automaticity* which is essential to excite the muscle fibre throughout the myocardium and produce the conduction which helps generate the current that spread through the entire body [4,16].

The cells that initiate and distribute the stimulation through the heart to contract are part of a network of specialised cardiac muscle cells known as the *cardiac conduction system* that initiate and distribute the electrical impulses of the heart [4,16].

#### 1.2.2.1.1. The Cardiac Conduction System

The cardiac conduction system in Figure 1.6 consists of the following components [8,14,16]:

- 1) The **sinoatrial (SA) node**, is embedded in the wall of the right atrium, near the entrance of the superior vena cava (SVC) and contains the *pacemaker cells*.

Normally cardiac excitation starts from the SA node. The nodes' cells have no stable resting potential. However, they depolarise to threshold spontaneously, creating the pacemaker potential, and establishing the *heart rate* (HR). When the pacemaker potential reaches the threshold, it will trigger the *action potential*. Each action potential propagates from the SA node through the atria cell by cell as Figure 1.7 shows. After the action potential, both atria contracts at the same time.

- 2) The **atrioventricular (AV) node**, located at the junction between the atria and ventricles in the internal septum.

After conducting along the atrial muscle cells, action potential arrived at the AV node, where it significantly slows due to the differences of cells structure and the impulse takes about 100 ms to pass through AV node. This delay (the AV nodal delay) is important to the atria to give them time to contract before the ventricles.

- 3) The **atrioventricular (AV) bundle**

The bundle called also **bundle of His**, it is the only electrical connection between atria and ventricles. The action potential enters the AV bundle coming from the AV node, and that take place only if the action potential succeeds to conduct from atria to the ventricles.

- 4) The **right and left bundle branches**

The action potential enters the right and the left bundle branches after the propagation goes through the AV bundle, and continue towards the apex of the heart. The left bundle branch supporting the massive left ventricle; therefore, they are larger than the right bundle branch.

Both branches extend to the apex of the heart, and at the end they diverge and conduct to Purkinje fibres through moderator band and papillary muscles.

## 5) Purkinje fibres

Purkinje fibres are the extensive network of branches spread through the ventricular myocardium taking place from the apex upward towards the cardiac valves [8]. At the final stage, the Purkinje fibres rapidly conduct the action potential starting at the apex of the heart to the rest of the ventricular myocardium, causing the contraction at the ventricles and pushing the blood upward to the pulmonary and aortic (semilunar) valves [9].

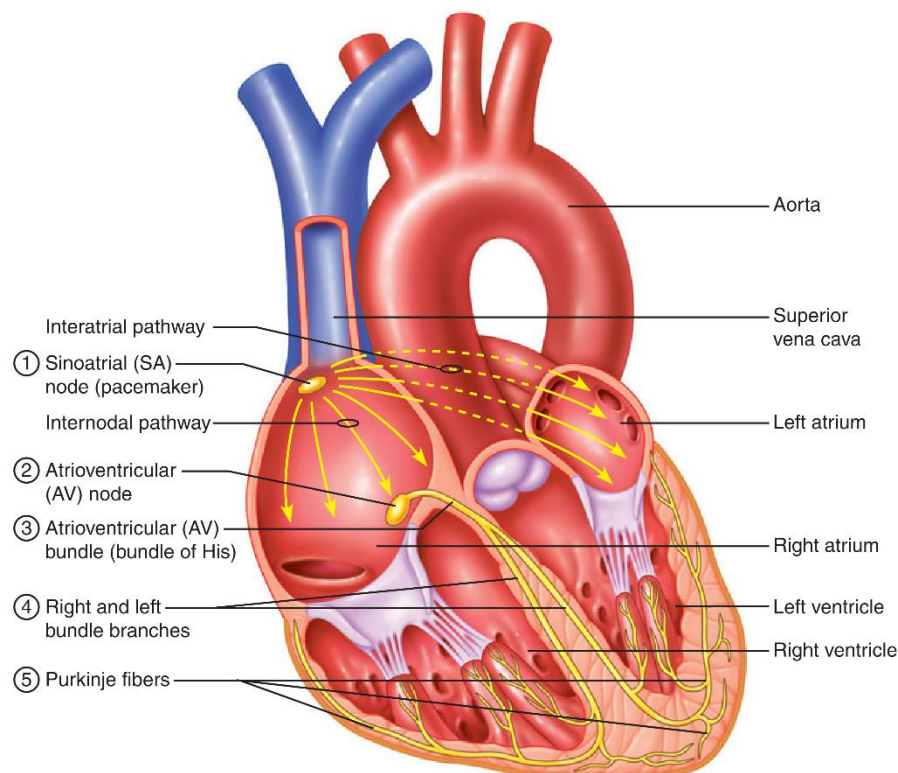


**Figure 1.6:** The conduction system of the heart showing the initiation of depolarisation wave by sinoatrial (SN) node passes via atrial myocardium to the atrioventricular (AV) node, right and left bundle branches, and finally to Purkinje fibres in ventricular walls [8].

### 1.2.2.1.2. Depolarisation and Repolarisation of Cardiac Cells

The cardiac cells are surrounded and filled by many ions. The major three ions are sodium ( $\text{Na}^+$ ), potassium ( $\text{K}^+$ ) and calcium ( $\text{Ca}^{2+}$ ). During the cell resting period, the inside of the cell membrane is considered negatively charged (-) whereas the outside of the cell membrane is positively charged. The movement of these ions from inside and across the cell membrane

initiates the flow of electrical activity that generates electrical signal known as electrocardiography ECG [17,18].

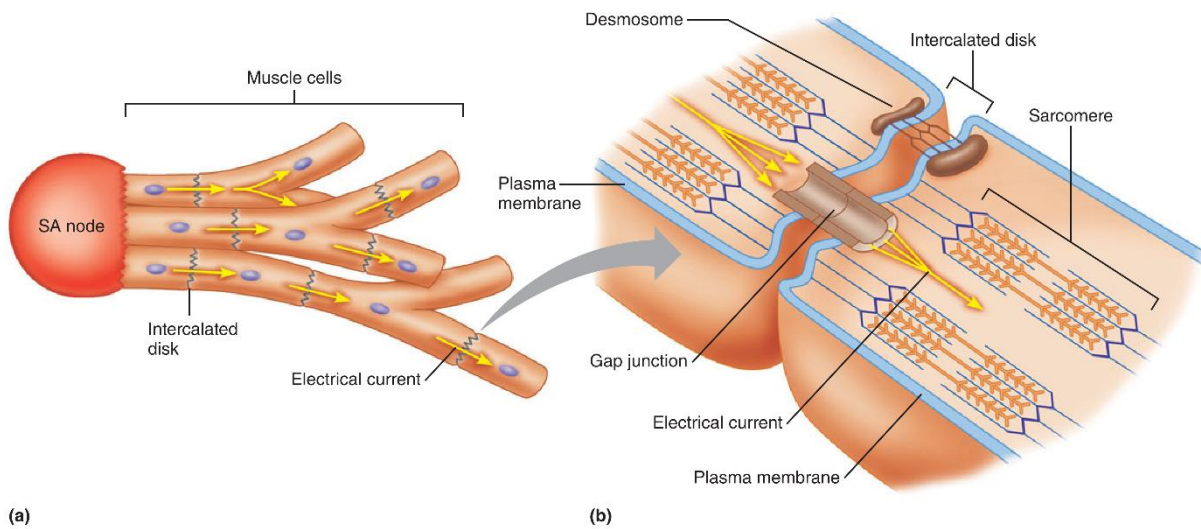


**Figure 1.7:** The electrical connections among cardiac muscle cells, where **a)** shows an action potential generated by the cells of SA node spontaneously and spreading to the adjacent cells via electrical current passing through gap junction in intercalated disks, and **b)** shows a schematic view between two adjacent cells presenting the gap junction their desmosome [8].

When an electrical impulse is initiated in the heart, the inside of the cell quickly becomes positive relative to the outside of the cell. This excitation state occurs because of this electrical impulse and accordingly it changes the polarity of the cell which is known as *depolarisation*. The electrical impulse starts at one end of the cardiac cell, the repolarisation wave propagates through the cell to the opposite side (the other end).

The return of the stimulated cell to its resting state is known as *repolarisation*. In this phase, the cell recovered allowing the inside of the cell to return to its normal negativity (resting state). Repolarisation starts at the cell that just depolarised and the resting state is preserved until the new arrival of the next wave of depolarisation [17,18]. Figure 1.8 shows the depolarisation and repolarisation of cardiac cells. It is important to note that once the cells have been depolarised, the depolarisation second wave cannot arise until the first one is entirely finished. This is known as *absolute refractory period* [17].

### 1.2.2.1.3. Cardiac Action Potential

In the normal condition the SA node is the pacemaker for the entire heart, where its depolarisation initiates the action potential that leads to depolarisation of all other cardiac cells

[10]. The electrical excitation is coupled with the mechanical contraction of the cardiac muscle (check excitation coupling section 1.2.2.3), hence the rate of discharge of the SA node determine and controls the heart rate [10].

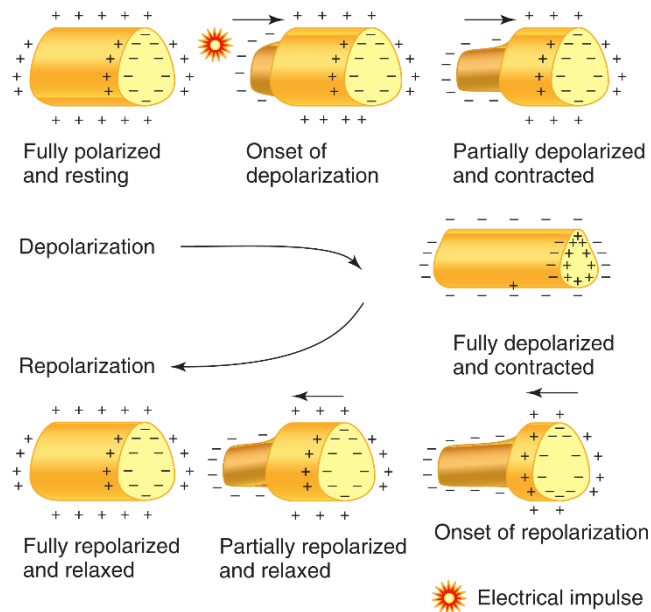


**Figure 1.8:** Depolarisation and repolarisation of cardiac cells [18].

The action potential generated by the SA node travels through the conduction system and spreads to excite the atrial and ventricular muscle fibres. These fibres, called the *contractile* fibres, are where the action potential takes place. Cardiac muscle has long action potential due to  $\text{Ca}^{2+}$  entry which plays a very important role. The rapid depolarisation phase is the results of  $\text{Na}^+$  entry while steep repolarisation phase is due to  $\text{K}^+$  leaving the cardiac cells.

The action potential has five phases and by convention they start with phase 0. Figure 1.9 shows the action potential phases for the contractile cells [10,14]. Note that the main study focuses on the contractile cells behaviour during the action potential, therefore the action potential for these cells have addressed rather than the pacemaker cells and their action potential.

The *typical* action potential phases of the contractile cardiac cells are (Figure 1.9) [10,14]:

#### **Phase 4: Resting membrane potential**

The cardiac contractile cells have stable resting potential of around -90 mV [10,14].

#### **Phase 0: Depolarisation**

The membrane potential becomes more positive when a wave of depolarisation moves into a contractile cell via gap junctions. Voltage-gated  $\text{Na}^+$  channels open allowing  $\text{Na}^+$  to enter the cell and consequently depolarise it rapidly. Before the  $\text{Na}^+$  channels close, the membrane potential reaches about +20 mV [10,14].

### Phase 1: Initial repolarisation

When the  $\text{Na}^+$  channels close, the cell begins to repolarise as  $\text{K}^+$  leaves through open  $\text{K}^+$  channels [10,14].

### Phase 2: The plateau

The initial repolarisation is very brief. Then the action potential flattens to a plateau due to the results of two actions: a decrease in  $\text{K}^+$  permeability and the increase in  $\text{Ca}^{2+}$  permeability. The voltage gated  $\text{Ca}^{2+}$  channels activated according to the depolarisation where they have been slowly opened during phases 0 and 1. The  $\text{Ca}^{2+}$  enters the cardiac cell when their channels finally opened. During the same time, some *fast*  $\text{K}^+$  channels close. Due to both the influx of  $\text{Ca}^{2+}$  and the decreased of  $\text{K}^+$  efflux causes the flattened the action potential and produce the plateau phase. The influx of  $\text{Ca}$  lengthens the total duration of the cardiac action potential [10,14].

### Phase 3: Rapid repolarisation

The plateau phase finishes when  $\text{Ca}^{2+}$  channels close and  $\text{K}^+$  permeability increases. The *slow*  $\text{K}^+$  channels are responsible for this phase. When the channels of slow  $\text{K}^+$  open, the  $\text{K}^+$  exits quickly in which help the cell to return to the resting potential (i.e. phase 4) [10,14].

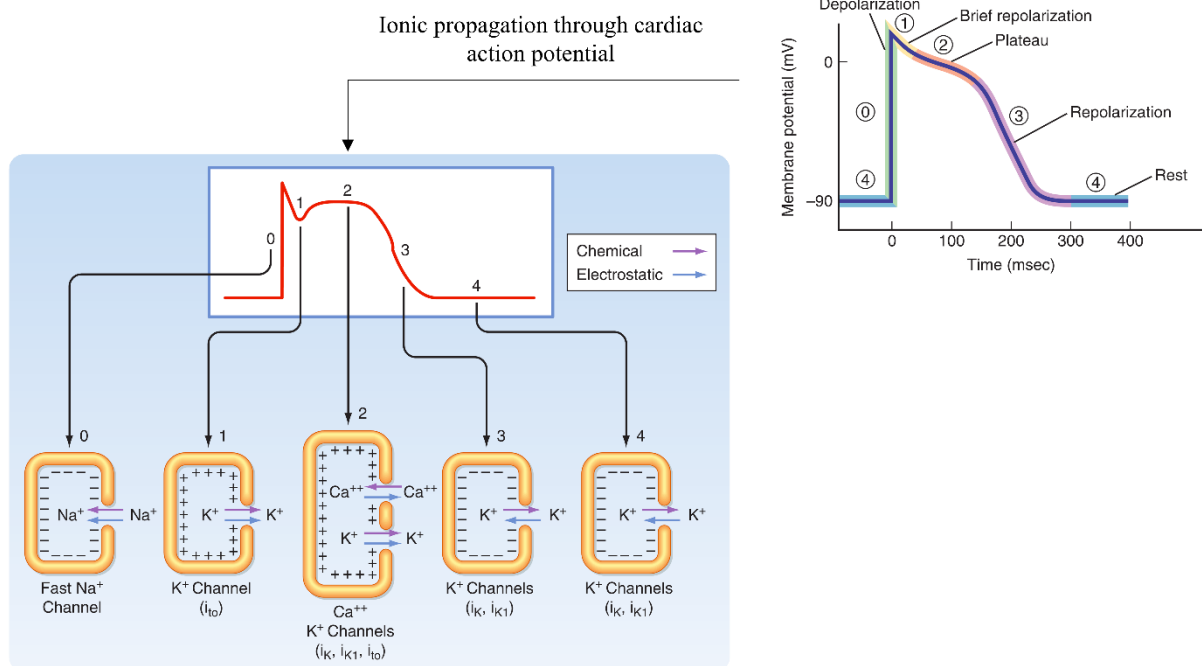


**Figure 1.9:** The cardiac action potential from ventricular muscle cell showing the principal ionic currents and channels during the phases. **Phase 0** shows the entry of  $\text{Na}^+$  into the cell through fast  $\text{Na}^+$  channels to generate the upstroke. **Phase 1** shows the efflux of  $\text{K}^+$  to generate early partial repolarization. **Phase 2**, the plateau phase, shows the net influx of  $\text{Ca}^{2+}$  through  $\text{Ca}^{2+}$  channels is balanced by the efflux of  $\text{K}^+$ . **Phase 3** shows the efflux of  $\text{K}^+$  and  $\text{Ca}^{2+}$  channels close. **Phase 4** shows the efflux of  $\text{K}^+$  and returning to resting membrane potential [8,11].

### 1.2.2.1.3.1. The Interval-Duration Relation

The interval-duration relationship is a physiological mechanism where the duration of cardiac action potential prolongs when the heart rate slows and shortens at faster heart rates. This response is significant during rapid heartbeats, where the shorter cardiac cycle needs to allow adequate time for the ventricles to fill [19].

The normal action potential duration for the ventricle when the heart rate 75 beat/minute (bpm) is approximately 0.35 s (total cycle length is 0.8 s). So far, the athletes can reach to a heart rate 180 bpm where the total cycle length is 0.33 s [19]. This is important during rapid heart rate when the need to activate the cardiac myocytes is increased, the action potential must become shorter to produce an inverse relationship between the cycle length and heart rate known as *interval-duration relationship*, this will allow a long diastolic interval to prolong the subsequent action potential, and shortens the action potential that succeed the short diastolic intervals [19]. Figure 1.10a-b shows an example for action potential response to slow and fast heart rates respectively.

With an irregular cardiac heart rhythm such that exhibited by the patients with atrial fibrillation (AF), the effect of the preceding diastolic interval on the duration of the following action potential is govern by interval-duration relationship where the long diastolic intervals are followed by longer action potential and similarly short diastolic intervals followed by shorter action potential. Such a response known as the *Ashman phenomenon* is typically seen in atrial fibrillation beats [19]. Figure 1.10-c shows an illustration of irregular action potential for variable heart rhythm.

There are several possible reasons for the interval-duration relationship. The shortening of the action potential for fast heart rates, where the diastolic interval is short could be due to the incomplete decrease of the delayed rectifier current  $i_{Kr}$  and  $i_{Ks}$ . Also, the plateau phase is shortened due to the slow recovery of the  $Ca^{2+}$  channel that had been activated by the preceding beat interval. Further, action potential could be shortened due to the increase of the frequency of  $i_{Na}$  channel opening which increase the cytosolic Na concentration and that leads to early repolarisation [19].

### 1.2.2.1.3.2. Afterdepolarisation

Afterdepolarisation and triggered activity are abnormal action potential. Afterdepolarisation is spontaneous depolarisation that can occur during the repolarisation on phase 3 or early in phase 4 after the cell repolarised [19,20]. Afterdepolarisation can arise when the heart becomes calcium overloaded, in which can be related to the inward current generated by Na-Ca [19,20]. There are two types of afterdepolarisation, first, *early afterdepolarisation* (EAD) and second, *delayed afterdepolarisation* (DAD). Figure 1.11 compares between the normal action potential, EAD and DAD.

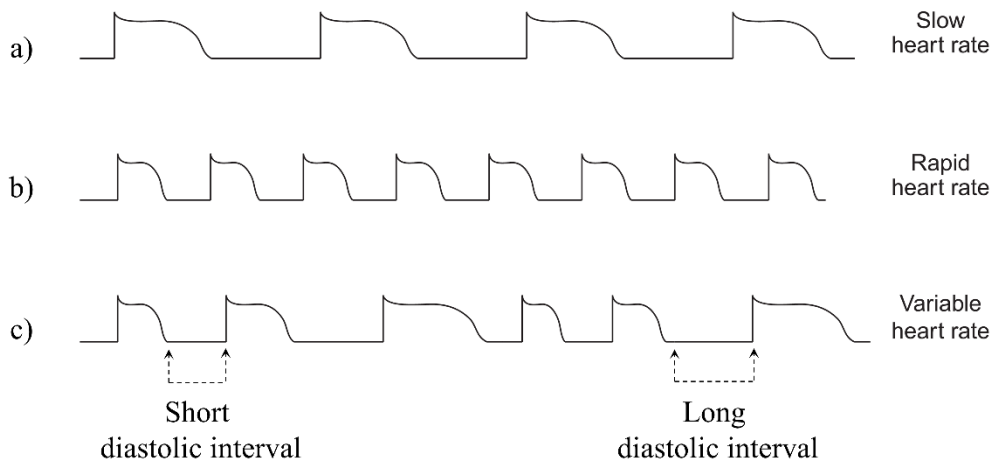


**Figure 1.10:** Interval-duration relationship. **a)** the action potential for slow heart rate, **b)** the action potential for fast heart rate and **c)** irregular action potential for variable heart rate [19 edited].

The EAD are depolarisation that occurs before the end of action potential (before the complete repolarisation) when the potential of cell membrane ranges between -10 and -30 mV during phase 2 or phase 3 (Figure 1.11-b) [21]. Thus, conditions that associated to prolonging action potential duration and QT intervals enhance the EAD development [21,22]. Note that EAD is mostly thought to be the mechanism that underlies the torsade de pointes (TdP) [22].

The DAD can occur after the of phase 3 or early in phase 4 when membrane potential returned to its resting state i.e. when the membrane completely repolarised (Figure 1.11-c) [20,21]. The DADs are mainly associated with the conditions such as digitalis toxicity and ischemia [21].

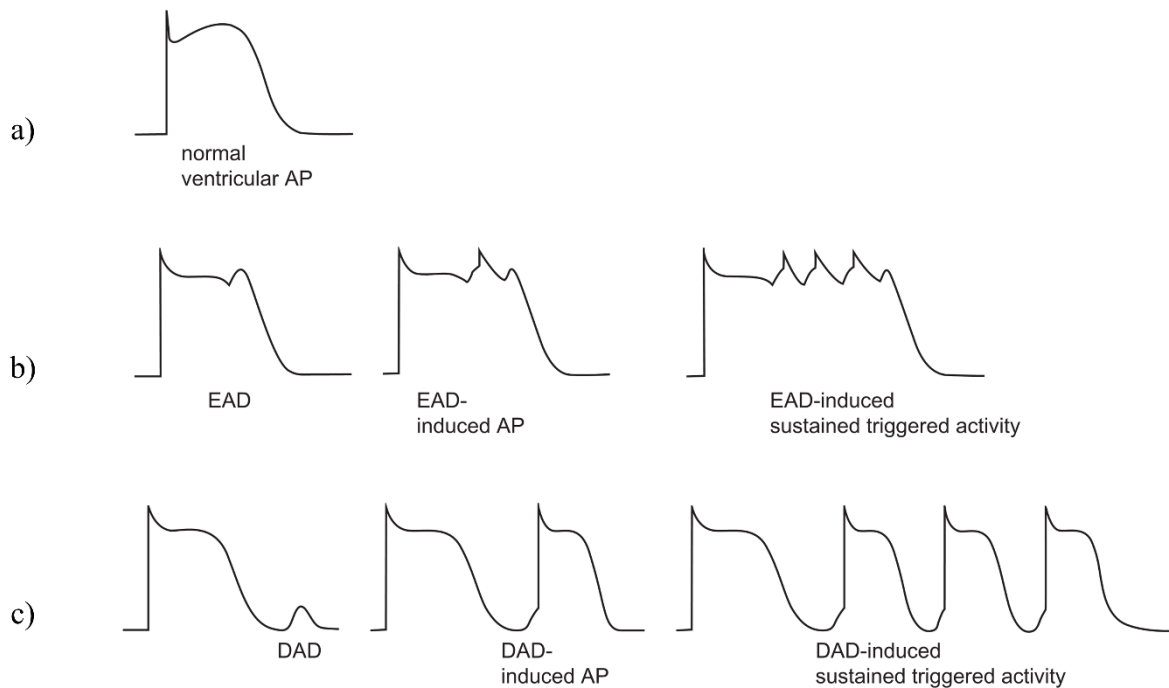


**Figure 1.11:** Illustration of cardiac action potential. **a)** Normal ventricular action potential (AP), **b)** early afterdepolarisation (EAD) are interruption of repolarisation before it completed. EAD are assumed to be the results reactivation of calcium current or Na-Ca exchanger current. **c)** delayed afterdepolarisation (DAD) are membrane depolarisation that arise after the end of the repolarisation. If the DAD is of adequate amplitude, it may trigger single or runs of action potentials [20 edited].

### 1.2.2.2. Cardiac Muscle Cells Structure (Histology)

The heart is composed of special cardiac muscle cells known as myocardium [14]. Mostly, the cardiac muscle is contractile, however, only 1% of the myocardial cells are have unique property to generate action potential spontaneously without any outside signal. Impressively, the heart is capable to contract without a connection to the other parts of the body organs because the contraction signal is myogenic. In other words, the signal originates in the muscle tissue itself rather than from a nerve impulse. As has been explained in conduction system section 1.2.2.1.1, the signal of myocardial contraction comes from the special pacemaker cells instead of the nervous system and they set the cardiac heartbeat rate. These cells are different anatomically from the contractile cells as they are smaller and have fewer contractile fibres since they do not contribute to the contractile force of the heart [14]. The study focuses on the repolarisation process; therefore, this section focuses on the cardiac contractile cells structure as they represent mainly the ventricles cells.

Typically, the contractile cells are striated muscle in which the contractile fibrils in the cells are aligned in parallel bundle. The muscle fibres organised into *sarcomeres* [5,14]. Figure 1.12 shows the muscle structure in which have the following properties [5,14]:

- 1) Cardiac muscle has small fibres and usually have a single nucleus for each fibre.

- 2) The individual muscle cells diverge to branches and join the adjacent cells end to end to create a complex network as Figure 1.12-a shows. The junction between the cells are known as *intercalated discs* which contain the interdigitated membranes. The intercalated discs consist of two components: *desmosomes* and *gap junctions*. The desmosomes represent strong connections that can tie the neighbouring cells together and allow force that created in one cell to be transferred to the neighbouring cell (see Figure 1.7 for closer look) [14].
- 3) Gap junctions in the intercalated discs connect the cardiac muscle cells electrically and chemically from one to another. These junctions allow the depolarisation waves to spread quickly from cell to cell in which help the muscles cells to contract nearly at the same time [14]. (see Figure 1.7 for closer look).
- 4) The transverse tubules (t-tubules) are where they branch inside the myocardial cells.
- 5) Myocardial sarcoplasmic reticulum is an extensive branching network close to t-tubules. This structure regulates intracellular  $\text{Ca}^{2+}$  concentrations which is essential for the relaxation and contraction [5,14].
- 6) Mitochondria take about one-third from the cell volume of the contractile fibre. This reflects the fact that muscle cells demand high energy. Presumably, the cardiac muscle cells consume around 70-80% of  $\text{O}_2$  that delivered to them through the blood [14].

If there is increase in the activity, the heart nearly uses all the  $\text{O}_2$  that is transferred by the coronary arteries. Accordingly, the only way to get more  $\text{O}_2$  is to exercise the cardiac muscle to increase the blood flowing [14]. In cardiac muscles, the action potential initiates *excitation-contraction coupling* (EC coupling) which is essential to complete the mechanism of the cardiac muscle fibres contraction. This process will be discussed in the section 1.2.2.3 as part of the mechanical activity of the heart. To understand how the excitation-contraction coupling works, it is important to understand the structure of *sarcomeres* and how they work.

Each muscle fibre includes thousands of myofibrils that form most of the intracellular volume. Each myofibril consists of several types proteins ordered into repeating contractile structure known as *sarcomere*. Myofibril proteins include the motor protein *myosin* which forms *thick filaments*, and the microfilament *actin* forms the *thin filaments*. See Figure 1.12-b. the myosin has the ability to create the movement and helps to determine the muscle's speed of contractions [14].

Each *sarcomere* contains the following elements [5,14] (Figure 1.12-b):

- 1) **Z discs:** One sarcomere is formed by two Z discs, filaments found between them. The Z disc is a protein with zigzag structure. It serves as the attachment position of the thin filaments.
- 2) **I bands:** The lightest colour bands of the sarcomere which represents the region that taken place only by thin filaments. The Z disc take place through the middle of I band, hence each half of an I band belongs to a different sarcomere.
- 3) **A band:** The darkest band of the sarcomere and occupies the entire thick filament. The thick and thin filaments overlapped at the outer edge of A band.
- 4) **H zone:** The central region of A band

- 5) **M line**: the protein that forms the attachment region of thick filaments. It is equivalent to the Z disc of the thin filaments. The A band divided by the M line.

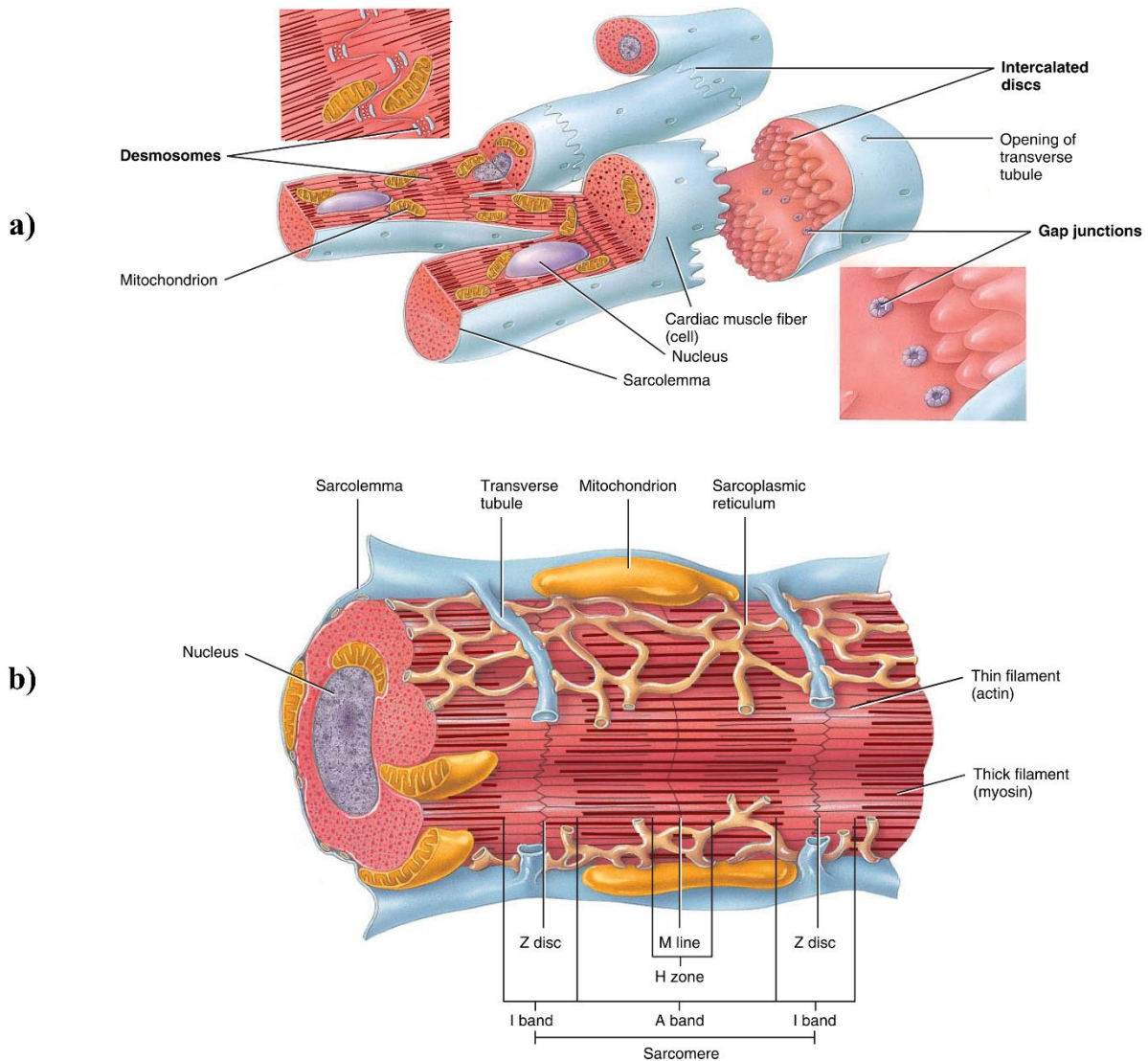


**Figure 1.12:** Cardiac muscle tissue histology. **a)** Cardiac muscle fibres where they connected to their neighbouring fibres via intercalated discs which contain desmosomes and gap junctions. **b)** Cardiac muscle fibres components showing the sarcomere structure [5 edited].

The distinction of the cardiac muscle structure helps the muscle fibres to contract in a remarkable process that enable the muscle to create a force to move or resist a load in which physiologically called the *muscle tension* [5]. The contraction is defined as the tension that created in the muscle and it requires energy input, whereas the relaxation is defined as the release of this tension that created by the contraction [5,14]. One of the major steps that is essential for the cardiac muscle contraction is excitation-contraction coupling [5].

### 1.2.2.3. Excitation Contraction Coupling

The excitation-contraction coupling (EC coupling) is the process where the cardiac action potential stimulates the contraction by initiating the calcium signals that activate a contraction-relaxation cycle [8,14]. In other words, it is the mechanism that takes place from the electrical excitation of the cardiac myocyte to the contraction of the heart where the blood pushed out [22].

The process of the EC coupling starts when the action potential stimulus in the cardiac muscle cells. Figure 1.13 illustrates the EC coupling step by step. This stimulus is a current coming through the gap junction. The action potential enters a contractile cell and spreads across the plasma membrane down into the t-tubules cleft. This opens the voltage-gated L-type  $\text{Ca}^{+2}$  in cell membrane. During this and through these channels, the  $\text{Ca}^{+2}$  enters the cell shifting down their electrical activity (this process is responsible for the plateau phase of the action potential as it sensitive to calcium) [8,14,22].

The calcium that passes inside the cell during the plateau phase works on the voltage-sensitive channels that trigger  $\text{Ca}^{+2}$  release in sarcoplasmic reticulum and stimulates them to remain open for longer period. The rise of calcium entry opens *ryanodine receptor  $\text{Ca}^{+2}$  release channels* (RyR). Consequently, sarcoplasmic reticulum releases more calcium with each action potential. This process of EC coupling is known as *calcium-induced calcium release* (CICR) [8]. When the channels RyR open, the stored  $\text{Ca}^{+2}$  influx out the sarcoplasmic reticulum and moves into the cytosol. This creates a  $\text{Ca}^{+2}$  spark, and multiple sparks initiated from different RyR channels sum to generate a  $\text{Ca}^{+2}$  signal [8].

Calcium excites contraction of the cardiac muscle where the calcium released provides nearly 90% of the calcium needed for the contraction and the remained 10% enters the cell from extracellular fluid [8]. Calcium diffuses to the contractile components in which the ion binds to the troponin (globular protein complex involved in muscle contraction) and initiate the cycle of crossbridge formation and movement [8].

Contraction then takes place using the *sliding filament movement* theory [8,14]. In this theory, overlapping actin and myosin filaments of fixed length slide, exceed one another in an energy required operation in which results to contract the muscle [8,14]. With closer look to the myofibril structure in Figure 1.14-a where it presents the sarcomere *resting* state, the end of the thick (myosin) and thin (actin) filaments slightly overlapped. In *relaxed* state, the sarcomere has a large I band (thin filament), and the A band length is in the same length of thick filament. On the other hand, when the muscle contract (Figure 1.14-b), both thin and thick filaments slide past each other, and the sarcomere's Z discs move closer together and in which results to shortening the sarcomere length. The I band and the H zone (area where actin and myosin do not overlap during the resting state) were almost disappeared.

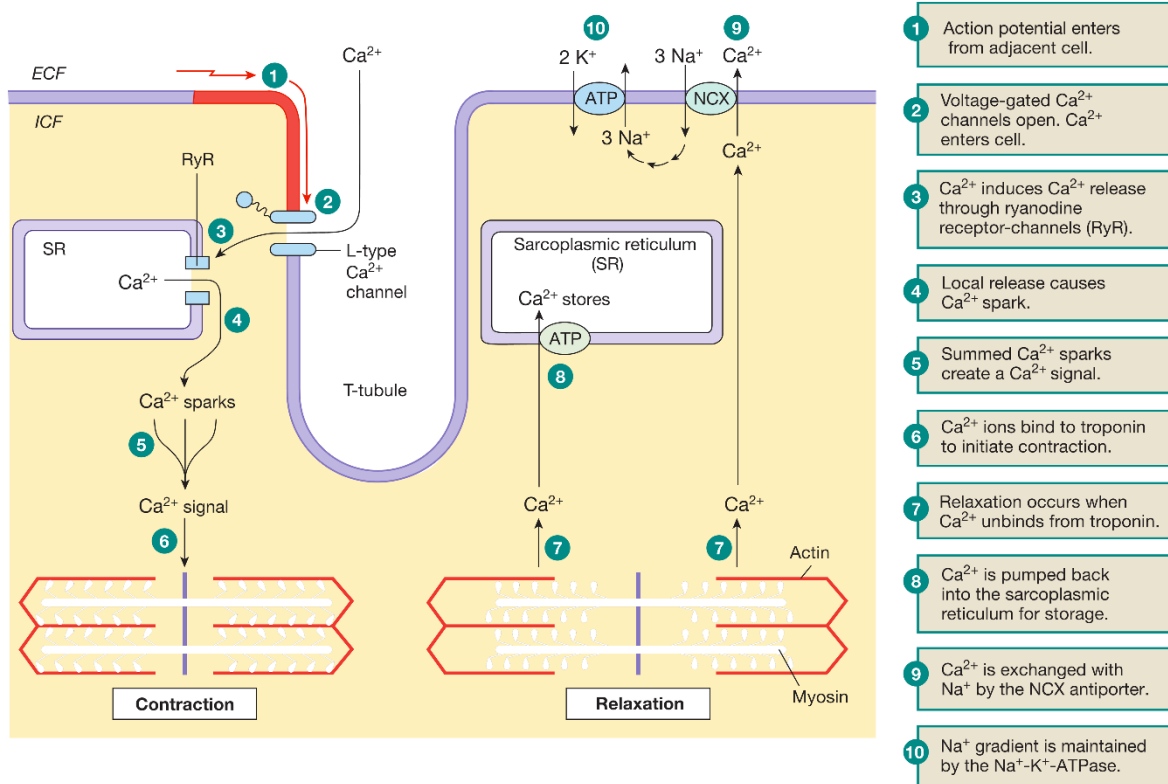


**Figure 1.13:** Excitation-contraction coupling in cardiac muscle. The illustration shows the cellular events in the cardiac muscle that leads to the contraction and relaxation in the contractile cells [14].

The relaxation process requires the removal of the calcium from the cytosol of cardiac muscle. When the reduction of cytoplasmic Ca<sup>2+</sup> concentration leads to Ca<sup>2+</sup> unbind from troponin, consequently myosin releases actin, and the contractile filaments slides back to their relaxes location. Then Ca<sup>2+</sup> is transferred back into sarcoplasmic reticulum (i.e. removed from the cardiac cell) by Na<sup>+</sup>-Ca<sup>2+</sup> exchanger (NCX). It is important to note that, calcium release is rapid and does not require energy since the concentration of calcium gradient is large during the diastole. On the contrary, the removal of calcium from the cytosol and unbinding from the troponin is an energy requiring process [14].

Finally, one Ca<sup>2+</sup> moves out of the cell and exchanged by 3 Na<sup>+</sup> entering the cell in which down their electrochemical gradient. Note that the Sodium that entered the cell through this transfer is removed by the Na<sup>+</sup>-K<sup>+</sup>-ATPase [14].

The EC coupling and sliding filament theory illustrate how the cardiac muscle can contract and create force without making movement. According to the theory of sliding filaments, the muscle fibres generates a *tension* which is directly relative to the *force* cross-bridges between the thick and thin filaments [8,14]. In other words, the force generated by the cardiac muscle is relative to the active cross-bridges which they determined according to the bound between the Ca<sup>2+</sup> and troponin [14].

With low cytosolic  $\text{Ca}^{+2}$  concentrations, less cross-bridges are activated which lead to smaller force of contraction. However, if additional  $\text{Ca}^{+2}$  enters the cells from extracellular fluid, more  $\text{Ca}^{+2}$  is released from sarcoplasmic reticulum [14]. Consequentially, more  $\text{Ca}^{+2}$  bind the troponin, increasing the ability to form cross-bridges between the myosin and actin, hence produce additional *force* inside the muscle cells [14].

Additionally, another significant factor that influence the contraction force is the *length* of the sarcomere at the beginning of the contraction (see section 1.2.3.1, the passive filling phase in the cardiac cycle). Fundamentally, in the intact heart, the *stretch* on the individual fibres is defined as the function of how much blood fills in the chambers (i.e. blood volume). The relationship between the ventricular volume and the force will be addressed in section 1.2.3.4 of this chapter as it represents an essential part of explaining the results of the thesis investigations.

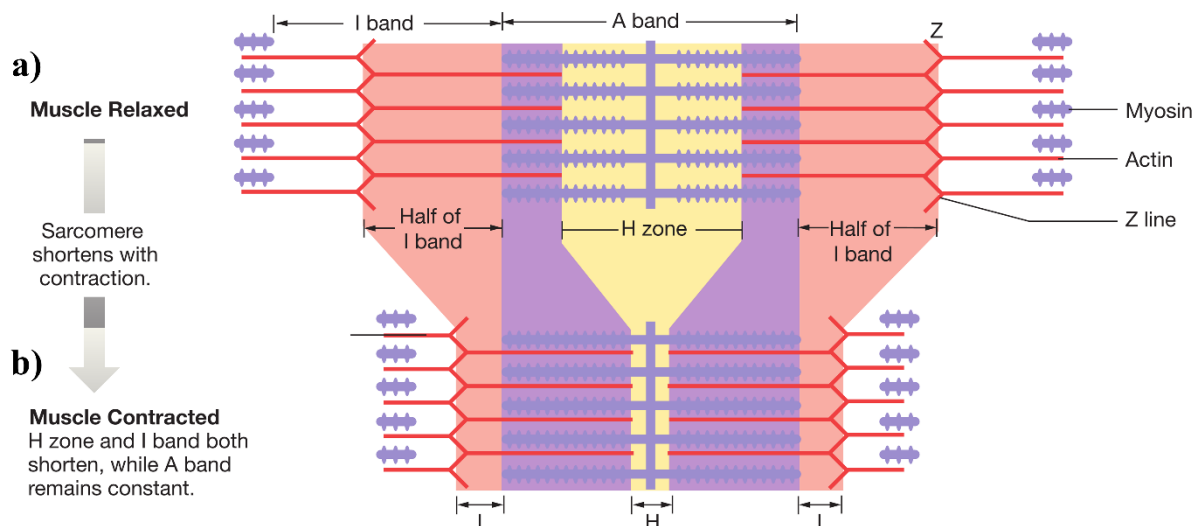


**Figure 1.14:** The length of sarcomere during **a)** the relaxed and **b)** contracted states. During the contraction, the sarcomere shortens, actin and myosin do not change, instead they slide past each another [14].

#### 1.2.2.4. Electrocardiogram

As the action potentials propagate through the cardiac muscle during the depolarisation and repolarisation, they generate electrical current that can be detected on the body surface using recording electrodes placed on the skin [5,8,15]. The measured signal is known as electrocardiogram or ECG (sometimes EKG). The ECG represents electrical current that spread overall the heart as a function of the time during the cardiac cycle (i.e. heartbeat).

Historically, the first human ECG was recorded in 1887 [5], however, it was not processed for clinical use until the early years of the 20<sup>th</sup> century. Willem Einthoven, a Dutch physiologist was considered the father of the of the modern ECG. Where he named the ECG components as we know them today and created the hypothetical ‘Einthoven’s triangle’ [5,8,15].

The ECG electrical signal can be detected by placing electrodes appropriately on the skin, amplified and viewed on the chart recorder or a computer screen. The instrument that used to detect and record the ECG is called electrocardiograph [16]. Figure 1.15-a depicts the typical ECG signal showing the deflection points that are designated by the letters P, Q, R, S, T and U.

Before explaining the ECG components and their formation, it is important to note that the ECG recording represents the surface electrode voltage difference between two points. The normal ECG signal exhibits major components, waves, intervals and segments. Each represents the electrical activity that associated to a specific part of the cardiac muscle during the cardiac cycle. The following section explains these components and their formation [16].

#### 1.2.2.4.1. ECG Components (Waves, Intervals and Segments )

The atria and ventricles depolarise and then at different times contract because of the action potential triggered by the cardiac conduction system along a specific pathway. The phase of contraction is known as *systole* whereas the relaxation phase is known as *diastole* [4,5]. The ECG waves represents the timing of the atrial and ventricles systole and diastole. Figure 1.15-b shows the major ECG components on the ECG graph in a **typical** record, the **waves** are [4,5,23]:

- 1) **P wave**: the first recognisable small wave in the ECG. It represents the depolarisation of the atria.
- 2) **QRS complex**: which arise as the ventricles depolarise. This signal is prominent and strong since the ventricles muscles are bigger than those of the atria. In addition, it forms a complex signal presumably because of the complexity of the pathway that depolarisation propagates through the ventricles. The ventricles begin to contract shortly after the peak of R wave.
- 3) **T wave**: represents the ventricles repolarisation. Note that atrial repolarisation is not visible because it takes place during the ventricle depolarisation i.e. during QRS complex electrical wave [23].
- 4) **U wave**: it has been believed that U wave represents the last phase of the ventricular repolarisation. The wave has controversial origin; however, it usually follows the T wave.

The ECG signal is analysed by measuring the amplitude and duration (time) of the different components. The time between waves is known as *segments* or *intervals*. Fundamentally, the segments defined as the duration from the end of one wave to the beginning of the another [23,24]. The **segments** and **intervals** are [23,24]:

- 1) **P-Q segment** is the time between the beginning of P wave to the beginning of the QRS complex, where it represents the conduction time starting from the atrial excitation to the start of ventricles excitation.

- 2) **P-R interval** begins from the start of the atrial depolarisation to the beginning of QRS when the ventricular depolarised. Lengthening in P-R interval with more than 200 ms indicates a damage of AV node or conduction pathway.
- 3) **S-T segment** starts at the end of S wave and ends at the start of T wave. This segment represents the time when the ventricles muscle depolarised during the plateau phase of action potential. It is worth to mention that S-T segment elevated above the baseline or depressed below it when the heart muscle receives inadequate O<sub>2</sub>.
- 4) **Q-T interval** begins from the start of the QRS complex to the end of T wave. It represents the time of ventricular depolarisation to the end of its repolarisation. The lengthening of the Q-T interval is related to conduction abnormalities, myocardial ischemia or myocardial damage. In addition, the Q-T may indicate a patient with a congenital heart defect which can cause a sudden death [4].

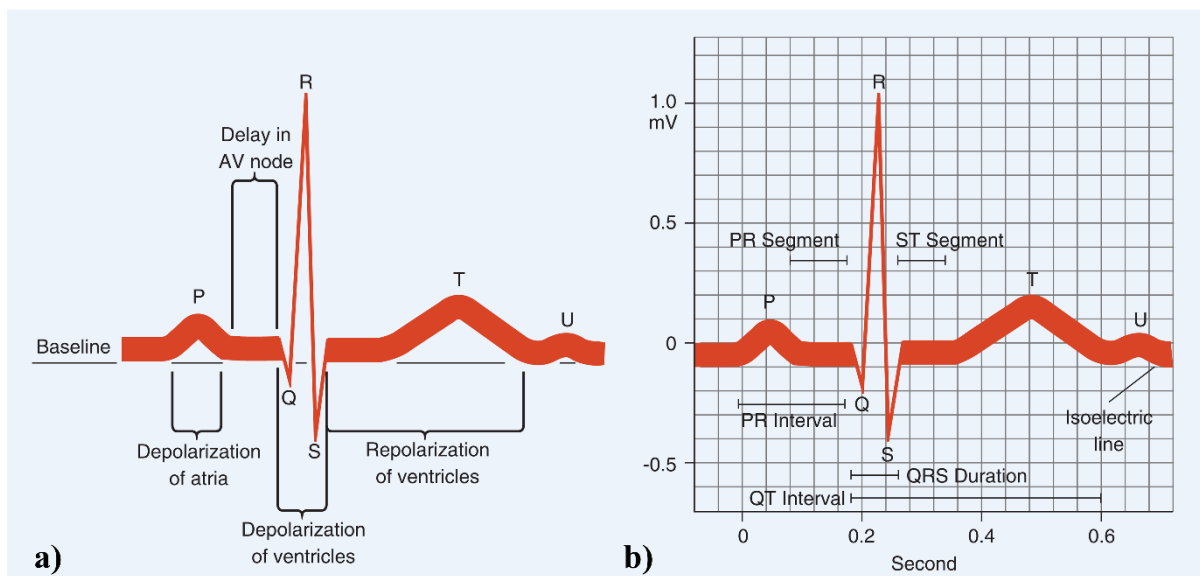


**Figure 1.15:** The ECG signal with six components (P, Q, R, S, T and U) showing **a)** representative phase for the depolarisation and repolarisation of the atria and ventricles, **b)** a strip of graph paper with annotated waves (P, Q, R, S, T and U), intervals (P-R and Q-T) and segments (P-R, and S-T) [16].

## 1.2.2.4.2. ECG Normal Characteristics

### 1.2.2.4.2.1. Heart Rate

The heart rate in the normal sinus rhythm at resting is usually between 60 to 100 bpm. Note that heart rate during the nocturnal sleeping (about 50 bpm) is different from the normal day (average 75 bpm) [23]. There are several methods that can be used to assess the heart rate from the ECG. The most famous method uses graph paper with the standard recording speed of 25 mm/second [16,23].

#### **1.2.2.4.2.2. Cardiac Rhythm**

The cardiac rhythm can be normal which is defined as *sinus rhythm* (SR) which originates from the sinus node. Mainly, P wave presence is the key to decide whether the rhythm is SR or not [23]. Also, there is ectopic rhythm which originates from a site other than sinus node [23]. The abnormal rhythms are described in section 1.5 of this chapter.

#### **1.2.2.5. ECG Lead System**

The conduction system of the heart produces electrical activity (current), and as has been mentioned the potential difference of these currents can be detected and measured through the electrocardiograph [23]. The body served as a conductor of this electrical activity, thus recording electrodes placed on the skin in distance from the heart, for instance chest, wrists, and ankles can detect the voltage that produced by the cardiac currents in which conducted to these places [23,24]. These electrodes convert the ionic current to electron current, so the ECG potential amplify it, record it then display it [25].

The famous way to detect and record the voltage of the heart (electrical potential) is by using the 12 standard leads. However, there are different configuration such as 3 leads system or 5 leads system. Using multiple leads are essential to capture the full picture of the 3D electrical activity of the heart. Each lead presents different angle to the same signal (same activity) [25]. The following section reviews the 12 leads ECG system as it represents an essential part during the study.

##### **1.2.2.5.1. The 12 Lead ECG System**

The routinely and widely used method by cardiologists to diagnose cardiac diseases is 12 lead ECGs system. The 12 lead ECG uses 10 electrodes placed in 10 standard locations on the patient's skin. The 12 leads system uses three types of leads: the *limb leads*, the *augmented leads*, and the *precordial leads* [25]. Figure 1.16 illustrates the placement of the 10 electrodes that produced the 12 leads ECG. The electrodes are positioned on the arms and legs (limb leads) and six positions on the chest (chest leads) to record the ECG [25,26].

The electrical signal of the heart is amplified by the electrocardiograph and produce 12 different tracings from different combinations of the limb and chest leads. Each electrode of limb and chest records electrical activity with a little difference because of the difference in the angles and position relative to the heart. These records help the cardiologists to discover if the heart is enlarged, if a specific region of the heart is damaged, or if the cardiac conducting pathway is abnormal [25,26].

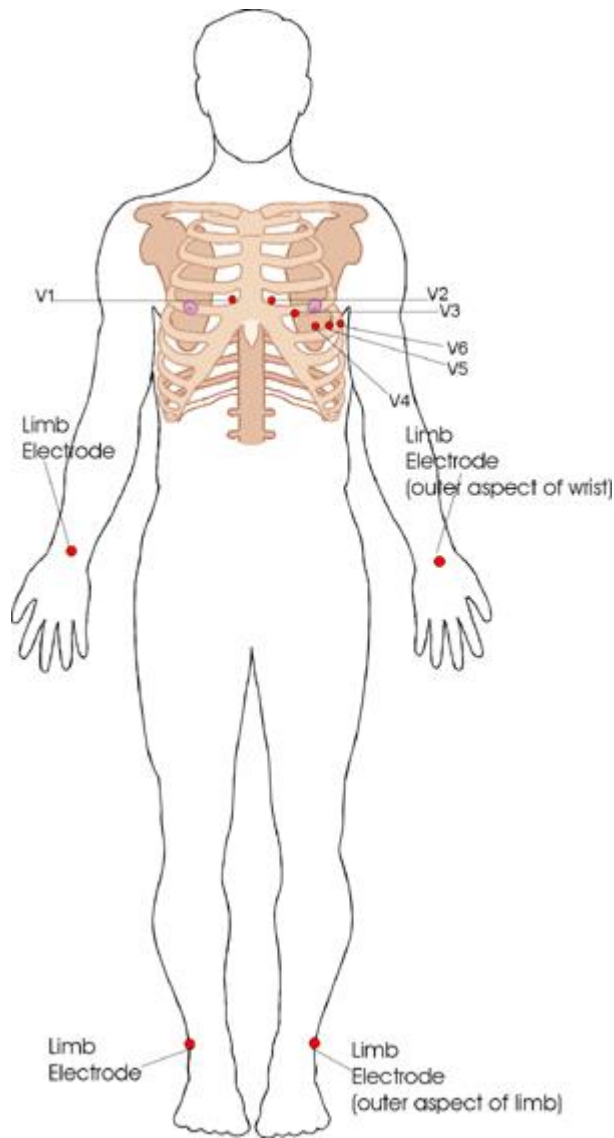


**Figure 1.16:** The 12 Leads ECG system showing the location of the limbs leads and the chest leads (precordial leads) annotated as V1, V2, V3, V4, V5 and V6 [26].

The three limb leads I, II and III record the potential differences between two parts of the body. To record these leads, electrodes are placed on the right arm, left arm, and left foot [27] as Figure 1.17 shows.

These bipolar leads reveal the direction and magnitude in the frontal plane. Lead I records the differences in potential between the left arm (+) and right arm (-). Lead II records the differences in potential between the left leg (+) and right arm (-). Lead III records the differences in potential between the left leg (+) and left arm (-). The potential differences recorded by these leads are explained in Figure 1.18 [28].

The right leg electrode (Figure 1.17) is required for reducing the interference and could be placed anywhere in the body; however, it is placed at this limb by convenience [29]. Lead III

can be found by subtract lead I from lead II. The vector that represents the limb leads known as Einthoven's law as shown in Figure 1.19a-b [25].

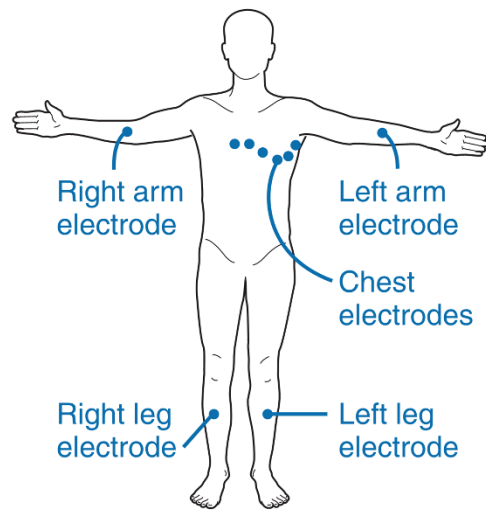


**Figure 1.17:** The placement of the electrodes of the limb leads [28].

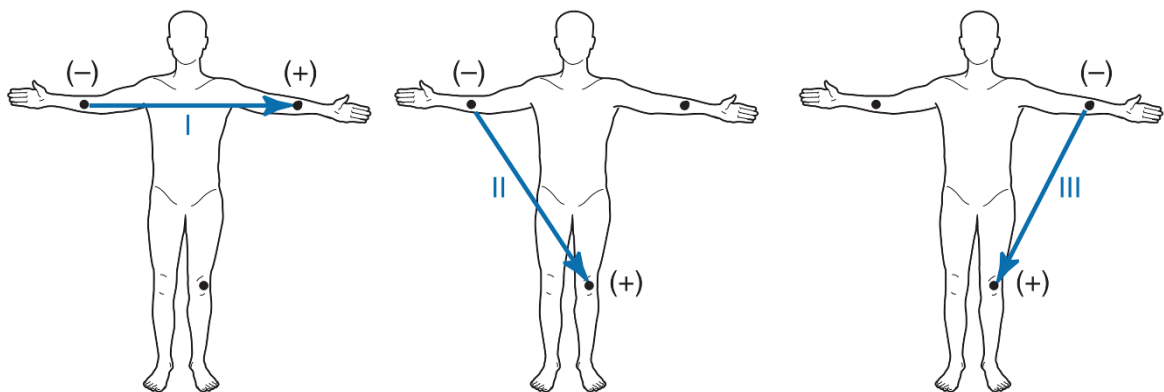


**Figure 1.18:** The bipolar limb leads, i) lead I, ii) lead II and iii) lead III [28].

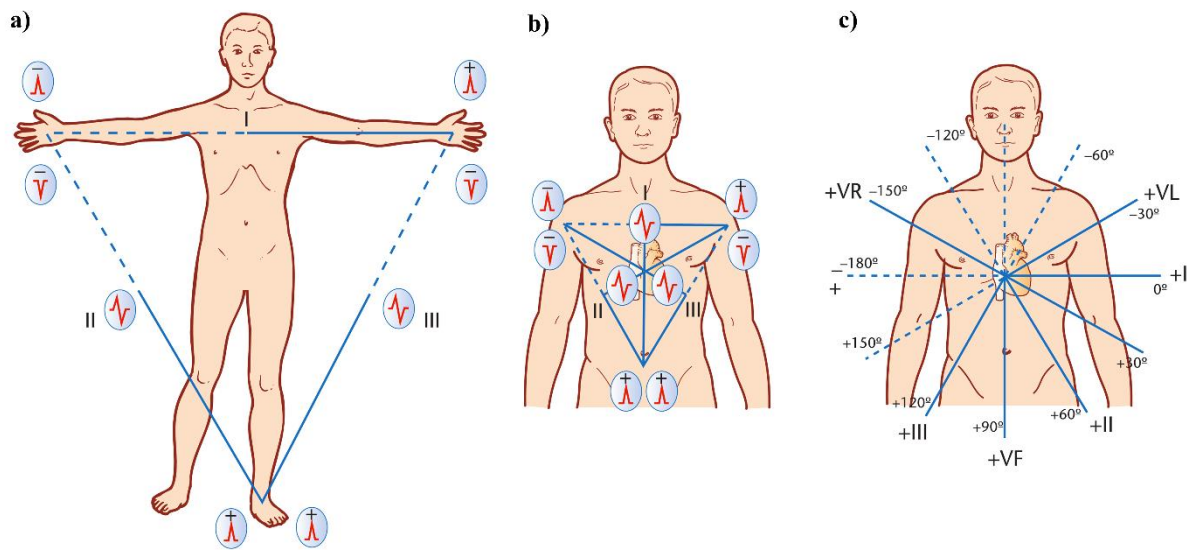


**Figure 1.19:** a) Einthoven's triangle, b) Einthoven's triangle superimposed on the human thorax and c) vector directions of the limb leads and augmented limb leads [30].

The augmented leads known as aVR, aVL and aVF, shown in Figure 1.19-c. The positive electrode for these leads recorded in reference to the average of the other electrodes thus they considered as *unipolar* recordings. Lead aVR, established when the right arm potential is recorded in reference to the average of the left arm and left leg potential. Where lead aVL, the left arm potential is recorded referencing the average of the right arm and left leg potentials. Whereas lead aVF, the left leg potential is recorded relative to the average of the right and left arm potentials. Additionally, the augmented leads can be derived from standard limb leads I and II [25]. Figure 1.19-c shows vector combination of the limb leads, and augmented leads.

The precordial leads consist of six leads named as V1, V2, V3, V4, V5, and V6 as shown in Figure 1.16. The precordial leads are *unipolar* leads that use a reference known as Wilson's central terminal. Wilson's central terminal is defined as the average potential of the right arm, left arm, and left leg electrodes [25]. These six positive electrodes are placed on the chest surface over the heart to record the heart's electrical activity in the horizontal plane perpendicular to the frontal plane as Figure 1.20 displays [31]. Electrode for V1 is placed to the right of the sternum over the fourth intercostal space whilst electrode for V6 is placed laterally on the chest over the fifth intercostal space [31]. According to this placement, lead V1, lies on the top of right ventricular free wall as Figure 1.20 shows whereas lead V6 lies over the left ventricular lateral wall. Lead V1 during the normal electrical activity shows negative deflection whereas as V6 is positive as shown in Figure 1.20 [31].

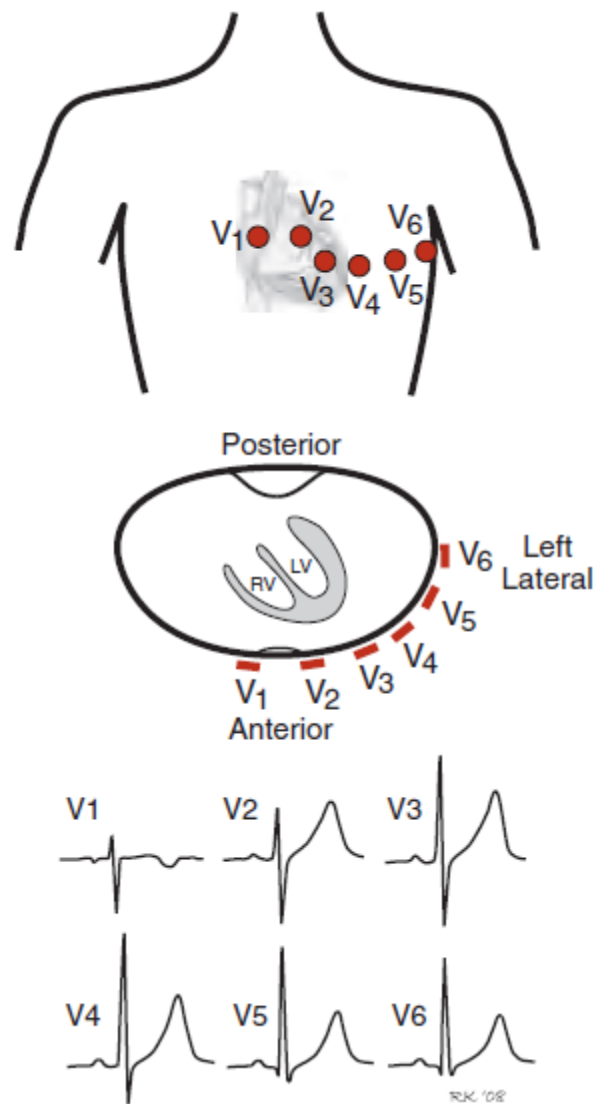


**Figure 1.20:** The six precordial leads (V1-V6) placement and their appearance on the ECG recordings. Leads V3-V6 shows mostly in normal condition high amplitudes [31].

### 1.2.3. Cardiac Mechanical Properties

#### 1.2.3.1. Cardiac Cycle and Mechanical Events

The *cardiac cycle* contains all the events related to the flow of blood through the heart during a one heartbeat. The review in this section concentrates on the following aspects of the cardiac cycle that are needed to explain the study investigation, which includes: the various phases in the pumping action of the heart, the periods of valve opening and closure, the changes in atrial, ventricular, and aortic pressure, as they reflect contraction and relaxation of the heart muscle; and the changes in ventricular volume as it reflect the amount of blood inflowing and leaving the ventricle during each heartbeat [8].

Figure 1.21 depicts *Wigger diagram* that shows the major events and their relationship of the cardiac cycle. The Figure is divided into coloured and numbered bars to match the following phases and to help to explain the phases through the text. Typically, all these events are completed in less than 1 second [3]. The following examination of the cardiac cycle starts from the middle of diastole in which the atria and ventricles fully relaxed [3]:

### 1) Ventricular filling

The ventricles expand during diastole, and their pressure falls below the pressure of atria. Consequently, the AV valves open and blood flows into the ventricles, and that causes ventricular pressure to rise and atrial pressure to fall.

Fundamentally, *Ventricular filling* occurs in three phases (see Figure 1.21) [3]:

**1a)** The first one-third is *rapid ventricular filling* when blood enters the ventricles rapidly.

**1b)** The second one-third, known as *diastasis*, is featured by slower filling. At the end of diastasis, P wave of the ECG can be seen, indicating the depolarisation of the atria.

**1c)** In the last one-third, atrial systole finalises the *filling* process. The right atrium contracts slightly before the left as it receives the signal firstly from the SA node. At the end of ventricular filling phase, each ventricle contains an *end-diastolic volume (EDV)*. The EDV is the amount of blood in the ventricle at the end of diastole just before a contraction starts [3], more details of the EDV are reviewed in section 1.2.3.2.1.

### 2) Isovolumetric contraction

At this phase, the atria repolarise, relax, and stay in diastole during rest phases of the cardiac cycle. The ventricles depolarise and generate the QRS complex of the ECG, then start to contract. Wave Q indicates the end of ventricular filling while R indicates the transition from atrial systole to isovolumetric contraction of the ventricles. The S takes place during isovolumetric contraction.

The pressure in the ventricles increases sharply and accordingly the pressure gradient between atria and ventricles reverses. The AV valves close as ventricular blood flows back against the cusps. At the beginning of this phase, the heart sound *S1* occurs.

In spite of the ventricles contract, they do not eject blood and their volume has no change. This is why the phase called as *isovolumetric*. The reason is because pressures in the aorta and pulmonary trunk are still larger than the pressures in the corresponding ventricles and thus oppose the opening of the semilunar valves. The cardiomyocytes exert force; however, the blood cannot go anywhere as the four valves closed [3].

### 3) Ventricular ejection

When the ventricular pressure exceeds arterial pressure, the ejection of blood begins, and forces the semilunar valves open. Typically, the pressure peaks at about 120 mm Hg in the left ventricle and around 25 mm Hg in the right. Blood flows out of each ventricle quickly at first (*rapid ejection*), then it flows out more slowly under less pressure (*reduced ejection*). Ventricular ejection takes nearly 200 to 250 ms. It corresponds to the plateau phase of the myocardial action potential but delays somewhat behind it. Late in this phase, T wave occurs at beginning at the moment of peak ventricular pressure.

The ventricles do not eject all their blood. At the resting, each ventricle contains an EDV of around 130 mL, however, the amount ejected is about 70 mL, this is called the *stroke volume (SV)* [3].

This represents about 54% of the EDV, the percentage called the *ejection fraction (EF)*. The blood that remained behind, around 60 mL in presented case, is known as *the end-systolic volume (ESV)*. The  $EDV - SV = ESV$ . In strong exercise, the EF can reach 90%. Ejection fraction is a significant measure of cardiac health [3].

#### 4) **Isovolumetric relaxation**

This phase represents the early ventricular diastole. The T wave ends, and the ventricles begin to enlarge.

At the onset of ventricular diastole, some blood from the aorta and pulmonary trunk flows backward via the semilunar valves. The backflow, however, rapidly fills the cusps and closes them, generating a minor pressure rebound that appears as the *dicrotic notch* of the aortic pressure curve (the top curve in the Wiggers diagram). Heart sound *S2* occurs at this phase when the semilunar valves closed, and the ventricles expand.

This phase is known as *isovolumetric* because the semilunar valves are closed, the AV valves have not yet opened, and hence the ventricles are taking in no blood. When the AV valves open again, ventricular filling (phase 1) starts again. If occurs, the heart sound *S3* supposed to be a result from the transition of expanded empty ventricles to rapid blood filling [3].

During the resting when the heart beats at 75 bpm, atrial systole takes around 0.1 s, ventricular systole takes 0.3 s, and the period when all four chambers are in diastole (*quiescent period*) takes around 0.4 s. Therefore, the total duration of the cardiac cycle is 0.8 s [3].

### **1.2.3.2. Cardiac Performance (Cardiac Output)**

The heart's efficiency as a pump is measured in terms of *cardiac output* which is the amount of blood that heart pumps each 1 minute. The cardiac output CO (sometimes termed as Q) is determined as the product of the amount of blood that the heart ejects with each beat known as stroke volume (SV) and the heart rate (HR) when the heart beats each minute (i.e.  $CO = SV \times HR$ ) [3,16].

In the normal condition, many factors influence the cardiac output such as the body size, temperature and the metabolic needs of the muscle tissues. It increases with physical activity (e.g. exercise) and decreases during rest and sleep. The value of cardiac output can increase to high level during maximum exercise (e.g. in the highly trained athlete) [3,16].

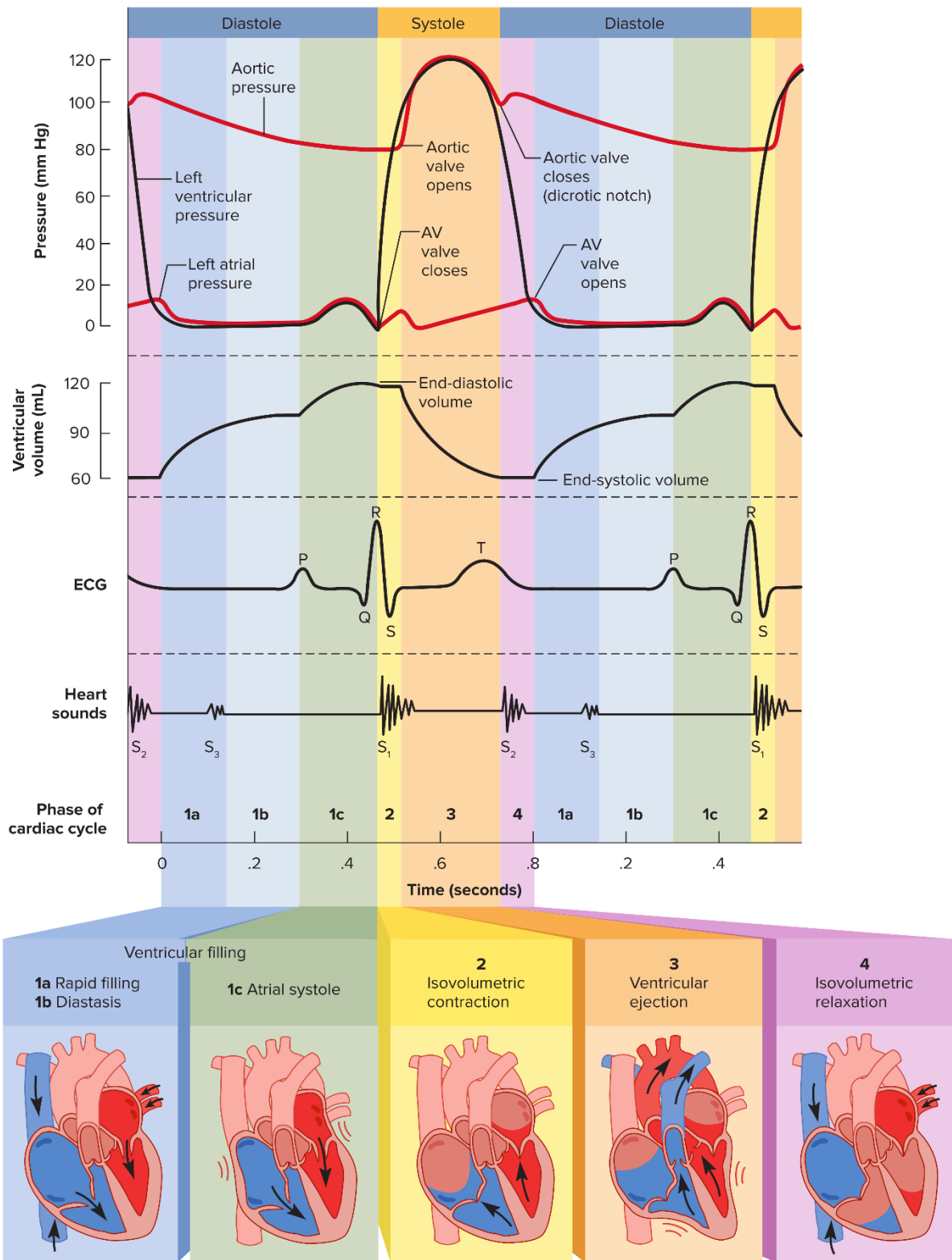


**Figure 1.21:** The phases of the cardiac cycle showing two cycles, Wiggers diagram (modified) [3].

The ability of the heart to regulate the SV or to increase its output according to body needs is mainly govern by four factors: i) the *preload* or ventricular filling, ii) the *afterload* or defined

as the resistance to the ejection process of blood from the heart, iii) *cardiac contractility*, and finally iv) the *heart rate*. The heart rate and contractility are mainly cardiac factors, i.e. they are originated in the heart, despite they are governed by various neural and humoral mechanisms. On the other hand, preload and afterload, are reliant on the performance of both the heart and blood vessels [3].

The review will focus on the factors that are associated to study proposed theories, such the preload and its relation to the heart rate, however the other factors will be reviewed briefly as the study demands.

### **1.2.3.2.1. Preload and End Diastolic Volume (EDV)**

The *preload* represents the amount of tension (stretch) in the ventricular myocardium immediately before it begins to contract [5, 31]. The term preload is used because it represents the load imposed on the heart before the contraction begins. As more blood enters the heart, a greater stretching occurs in the myocardium according to the length–tension relationship (see the details in section 1.2.3.3) [5, 31]. Consequently, as more blood fills the heart during diastole, the greater the force of contraction during systole [3,5, 31]. This relationship is known as the *Frank–Starling law of the heart*.

The preload is related to the *end-diastolic volume* (EDV) which is defined as the volume of blood that fills the ventricles at the end of diastole [3,5]. Typically, the greater the EDV, the more forceful the next contraction. There are two factors that regulate EDV, first, the duration of ventricular diastole (considered in this study) and second, the venous return (represents the volume of blood returning to the ventricle) [3,5, 31].

Less filling time in the ventricles means a smaller EDV, and the ventricles possibly contract before they are sufficiently filled. In contrast, when venous return increases, a larger volume of blood flows into the ventricles, and consequently the EDV is increased. In the fast heart rate when it exceeds 160 bpm, SV generally declines due to the short filling time. At such fast heart rates, EDV is less, and the preload is lower [3,5].

Therefore, patients with slow resting heart rates mainly have large resting SV due to the prolongation of filling time, and preload is larger. The *heart's Frank–Starling law* equalises the output of both right and left ventricles and preserves the same volume of blood to flow for both the systemic and pulmonary circulations [5, 31].

### **1.2.3.2.2. Contractility and Afterload**

The SV is directly relative to *contractility*, when the ventricles contract more forcefully, they propel more blood. To eject blood, the generated pressure in a ventricle when it contracts must be higher than the pressure in the arteries as blood flows only from higher pressure to lower pressure. When blood starts to be ejected from the ventricle, the added volume of blood in the

arteries causes an increase in pressure presented by the peripheral resistance. The total peripheral resistance consequently generates an impedance to the ejection of blood from the ventricle known as *afterload*. This is medically important because a person with a high total resistance has a high arterial blood pressure, and hence high afterload imposed on the ventricular muscle [3,5, 31]. The SV is inversely related to the total peripheral resistance, where the greater the peripheral resistance, the lower the SV [3,5, 31,32]. Figure 1.22 shows the determination of cardiac output by the SV and the heart rate, and how SV is determined by preload, afterload, and contractility [32].

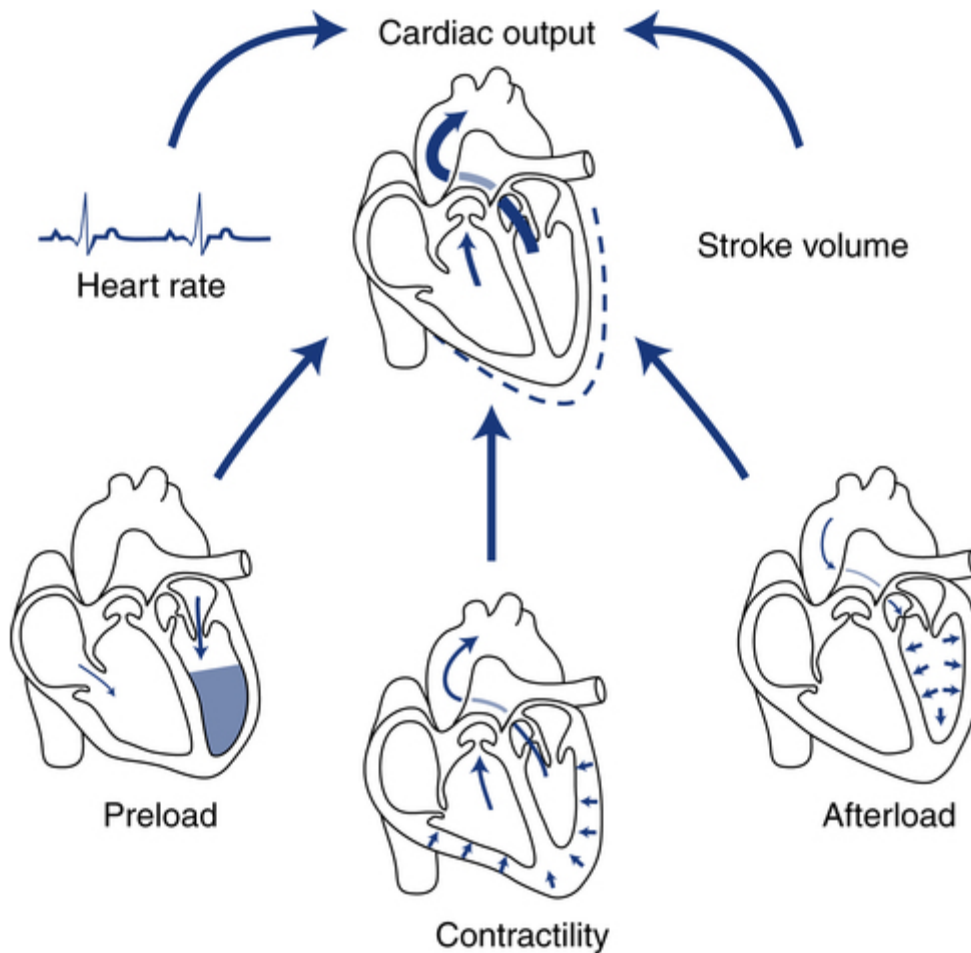


**Figure 1.22:** An illustration shows the cardiac output is determined by both stroke volume and heart rate. Stroke volume is determined by preload, afterload, and contractility [33].

### 1.2.3.3. Frank-Starling Law of the Heart

The Frank-Starling law (or sometimes called Frank-Starling mechanism) elucidates the relationship between the contraction force and the initial length of muscle cells, in other words the heart's ability to increase its force of contraction when stretched [11,31].

It stated that “*ability of the heart to change its force of contraction and therefore stroke volume in response to changes in venous return*” [31]. Simply, it stated that SV is directly related to

the EDV. Which means the ventricles tend to expel as much blood as they receive, and the more they stretch the harder they contract on the next beat [3].

In fact, when the ventricles fill with blood, the cardiac muscle wall (myocardium) stretches so that the actin overlap with myosin only at the edges of the A bands as Figure 1.23 illustrates. This process increases the number of interactions between actin and myosin, which allows additional force to be established during contraction. As the overlapping of actin and myosin is more valuable via stretching of the ventricles, and because the level of stretching is controlled by the level of filling (EDV), hence the strength of contraction is intrinsically regulated by the EDV [32].

The muscle length (i.e. the sarcomere length) is strongly affected by the contraction strength (force). This is assumed to be due to an increased sensitivity of stretched cardiac muscle to the stimulation impacts of  $Ca^{2+}$  [11].

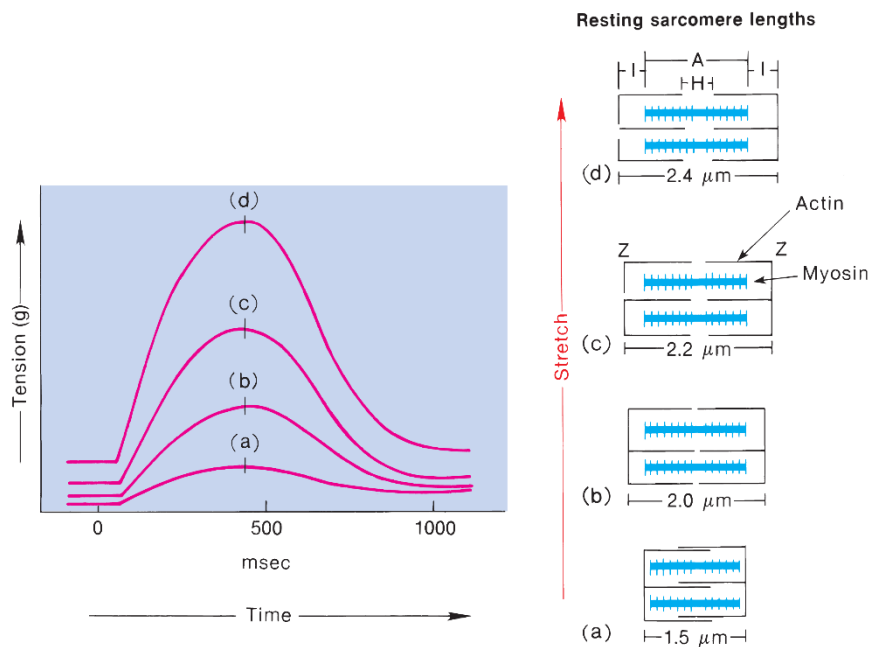


**Figure 1.23:** The Length-Tension relationship according to the Frank-Starling mechanism. If the heart muscle is exposed to an increasing degree of stretch (*a* through *d*), it contracts more forcefully. The y-axis as the tension indicates contraction strength. Interestingly, the time required to achieve maximum contraction remains constant, regardless of the level of stretch [32].

#### 1.2.3.4. Ventricular Pressure-Volume Relationship

The pressure volume loop gives a powerful tool to analyse the cardiac cycle and characterise the ventricular function as a pump [31].

Figure 1.24 shows pressure–volume loops and the mechanical event of the cardiac cycle, where the loop in Figure 1.24a-b is generated by plotting left ventricular pressure against left ventricular volume at various time points during a complete cardiac cycle. The cardiac cycle phases are annotated in Figure 1.24-a. Figure 1.24-c illustrates the loop of the mechanical events for one cardiac cycle to follow the description during the pressure-volume diagram explanation. The EDV (the largest volume reached) at the end of filling, and ESV (residual volume) of the ventricle shown at the end of ejection (Figure 1.24-a). Thus, the difference between EDV and ESV is represented by the width of the loop which is the stroke volume (SV) [31-35].

The filling phase passes along the *end-diastolic pressure–volume relationship* (EDPVR) as shown in Figure 1.24-b, or as it is known a passive filling curve for the ventricle. The highest pressure that can be established by the ventricle at any given left ventricular volume is defined as the *end-systolic pressure–volume relationship* (ESPVR) as displayed in Figure 1.24-b [31,35].

Figure 1.24-a shows the hemodynamic changes during a one cardiac cycle. The rise in ventricular pressure during the phase of filling ends when the mitral valve closes, and reflects the compliance of the ventricular wall. During the phase of isovolumic contraction, pressure increases sharply while volume stayed constant [31,35].

Ventricular pressure increases to a level to exceed the aortic pressure; accordingly, the aortic valve opens, and blood is ejected. Ventricular ejection phase (i.e. systole) continues until ventricular pressure decreased below aortic pressure and the aortic valve closes. The phase of isovolumic relaxation follows, which is recognised by a sharp fall in pressure and without change in the volume. Accordingly, the mitral valve then opens, hence completing one cardiac cycle [31,35].

The end-systolic points in Figure 1.22-b in the series of loops emulate a *linear* relationship of pressure-volume with the ESPVR. The End-systolic elastance ( $E_{es}$ ) describes the slope of ESPVR. On the other hand, the diastolic pressure-volume points (Figure 1.24-b) define a non-linear end diastolic relationship (EDPVR). Typically, a constant contractility and afterload, leads to progressive reduction in preload which causes the loops to shift toward smaller volumes at end-systole and end-diastole, which leads to a decrease in stroke volume SV [31,35].

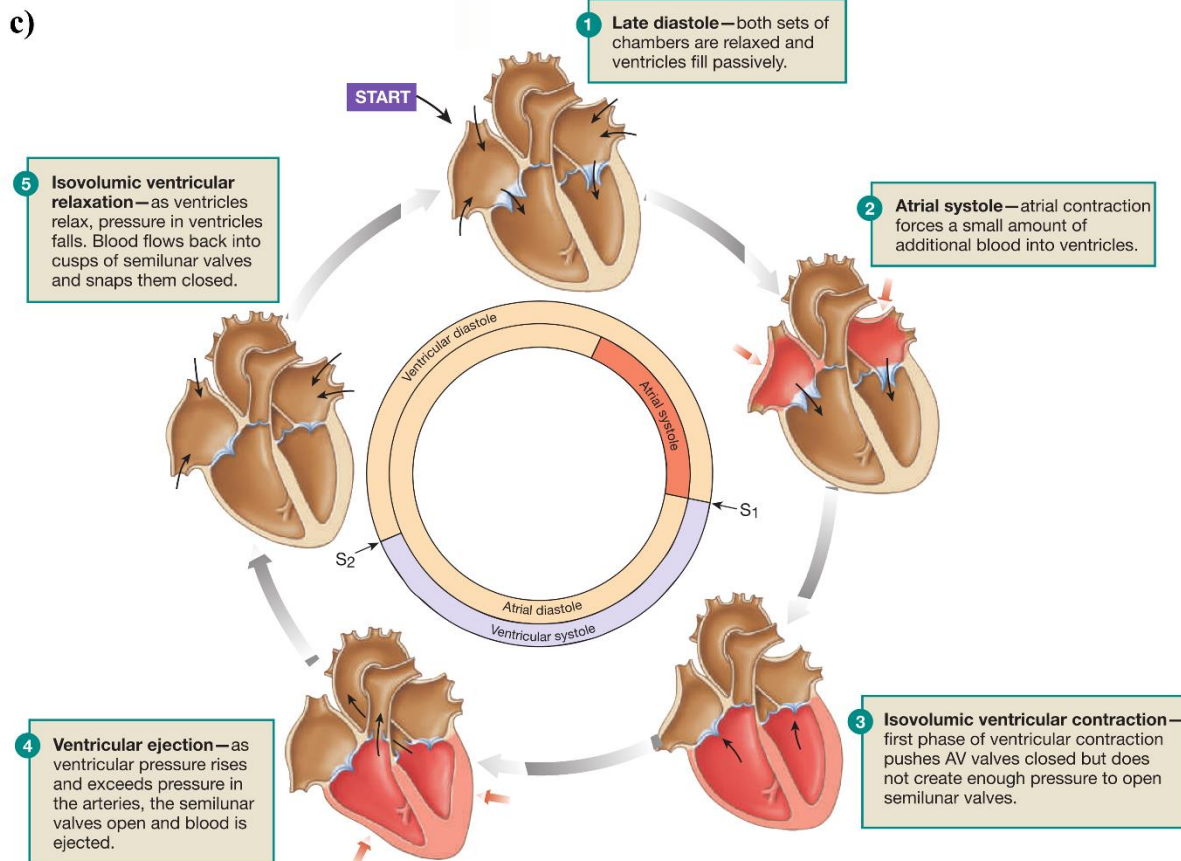
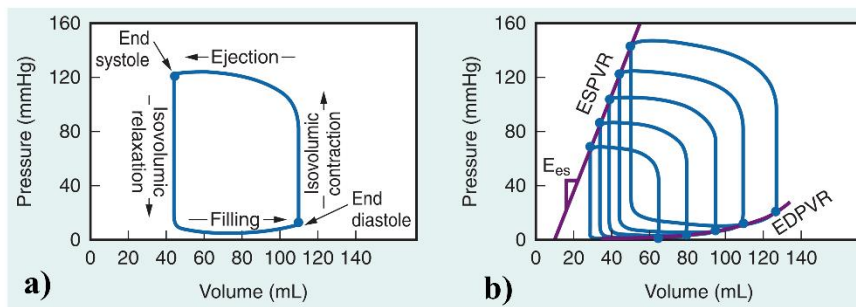


**Figure 1.24:** The pressure–volume loops and the mechanical event of the cardiac cycle. **a)** Pressure–volume loop of the left ventricle [35]. **b)** Multiple pressure–volume loops generated by progressive reductions in preload. **c)** The mechanical event of one cardiac cycle [14].

### 1.2.4. Principles of Heart Physiology During Exercise

All types of the movement regardless of the duration, the intensity or the mode, demand power and energy above the resting rate. Oxygen plays a big role to provide more energy to the working muscles, and to achieve this, cardiovascular and respiratory systems work together.

There are many types of physical exercises, however there are two main general groups of exercise: dynamic exercise (e.g. running, walking, swimming and cycling) and isometric exercise (e.g. plank and side bridge and many yoga poses such as chair and tree poses). The isometric exercises involve holding a position rather than moving as is the case with dynamic exercise [36,37].

The dynamic exercise has the major effect on the cardiovascular and respiratory systems in many ways during the individual life. The study of exercise physiology can provide a useful insight to understand the circulatory system behaviours and response, and how the system interacts with the respiratory system since they have a strong bond of working together. There is strong relationship between the exercise intensity and the cardiorespiratory parameters, such as heart rate, left ventricle stroke volume, cardiac output, atrial pressure, and atrial and venous blood oxygen contents. Clinically, exercise stress is used to diagnose, assess and quantify the intensity of the cardiovascular/respiratory disease [37].

Since the variation of heart rate is one of the factors of the exercise activity, therefore it could provide a useful model to investigate the effect of this changes on the electrocardiogram (ECG) and the cardiac phases including the waves of depolarisation and repolarisation.

So far, there are several studies investigated the effect of the heart rate changes on the T wave, however there are no studies about U wave behaviours with respect to these changes in healthy subjects. In the study (see section 5.3 of Chapter five), the effect of the heart rate changes was investigated on the repolarisation waves.

#### **1.2.4.1. Cardiovascular Response to the Exercise**

Exercise is a powerful physiological exertion leads to a disturbance in entire body homeostasis. In response to exercise, neural and hormonal alteration results in the inotropic (force or speed alteration of the muscle contraction) and chronotropic (effects that changes the heart rate) state of the heart [2]. The influence of these changes results in increased cardiac output to plateau within two minutes, to reach a ‘steady-state’ as a result of increased heart and stroke volume (cardiac output (Q) = HR × SV) [36,38-40], as Figure 1.25-a. shows. This reflects the fact that cardiac output is adequate to transport the demanded oxygen to support the metabolic needs during the activity [36,38,39].

Heart rate increases directly at the onset of the exercise due to the repaid withdrawal to the parasympathetic system (vagal tone). Simultaneously, sympathetic nerve activity starts to contribute to increase the heart rate following the beginning of exercise and becomes progressively significant as heart rate increases [36,38,39].

Typically, when the cardiorespiratory system meets the requirements of the body’s metabolism, the exercise is often called the “steady-state” or “steady-rate”. During the steady state, the energy provided to cardiovascular system is balanced to energy required to the working muscles [36].

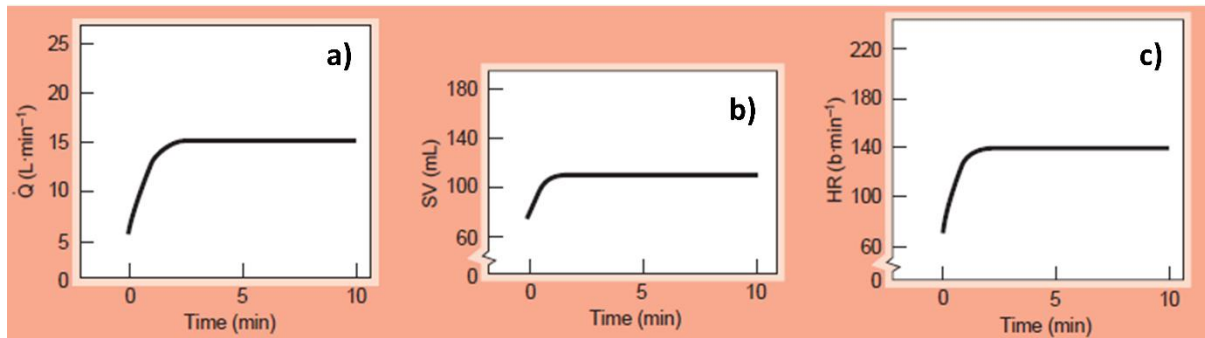


**Figure 1.25:** Cardiovascular response to submaximal exercise, **a)** Cardiac output ( $Q$ ), **b)** Stroke volume ( $SV$ ), and **c)** Heart Rate ( $HR$ ) [36].

The changed action potential duration, contractile velocity and conduction velocity, related to the increase in heart rate results in several ECG changes during exercise (reviewed in the following section). Similar to heart rate, stroke volume  $SV$  also increases during exercise (Figure 1.25-b and c). The increase in  $SV$  is associated with changes in end diastolic volume ( $EDV$ ) and ‘sympathetic stimulation and adrenaline’ control [36].

Exercise results in an increased  $EDV$  combined with an increased return of blood to the heart, and rapidly changing intrathoracic pressure. The increased  $EDV$  leads to an increased  $SV$  associated with an increased length of myocardial fibre i.e. sarcomere length (see section 1.2.3.3). This capacity to increase stroke volume has a higher limit associated with the maximum myocardial length [36,38,39]. Figure 1.26 illustrates the difference of ventricular volume during the supine, standing and during exercise conditions.

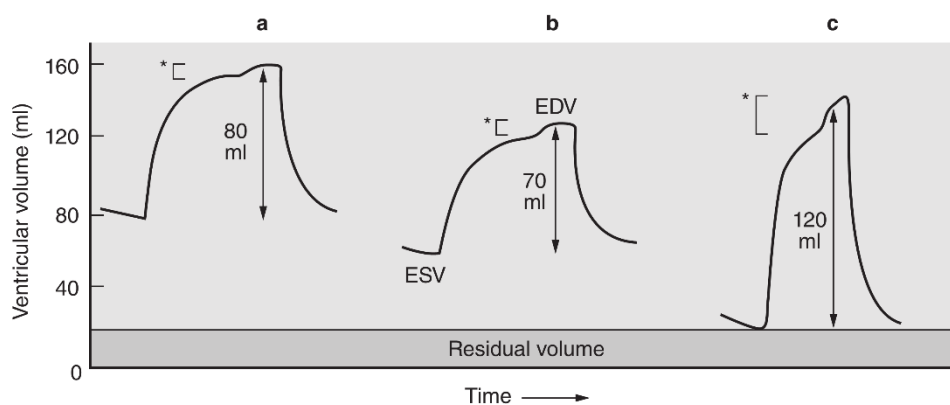


**Figure 1.26:** Illustration shows the volumes of the heart during **a)** supine, **b)** while standing, and **c)** during exercise. \* indicates atrial contribution to ventricular filling [40].

The ventricles’ rapid filling during early diastole (see section 1.2.3.1) is substantial during exercise when the heart rate increases, and diastole is significantly reduced. An increased sympathetic input associated with raised circulating adrenaline results in an increased

myocardial contractility. Increased atrial contractility increases EDV, while increased ventricular contractility decreases end systolic volume (ESV) due to the increased force and velocity of contraction. The result is an increased ejection fraction (EF) during exercise in which results in an increased SV [40].

At higher heart rates, despite a reduction in systole, the fast ejection of blood during early systole results in a minimal effect on stroke volume. EDV, however, at maximal exercise remains close to resting values although a sympathetic-derived increase in ventricular relaxation due to the reduced time for the slow phase of diastolic filling (diastasis) and the AV valves resistance to higher flow rates [36-40]. As a result, SV increases during light and moderate exercise but then followed by plateau once the steady state is achieved [36-40]. Figure 1.27. illustrates the changes of EDV and ESV to initiate the SV during the rest and the exercise.

The consumption of the myocardial oxygen rises during the exercise, because the heart must do more work to increase cardiac output and then provides the working muscle with the needed oxygen. Consequently, the myocardial blood flow increased dramatically (workload) to the working muscles to support the energy production [36].

Figure 1.28. shows the oxygen consumption through time changes from the beginning of the exercise to the recovery state. At the start of the exercise, oxygen consumption starts to increase, and then continue to raise at the first minute of sustained exercise, and then plateaus as oxygen uptake matches the muscles and tissues need. At the end of the exercise, the oxygen consumptions start to decrease gradually during recovery period [37].

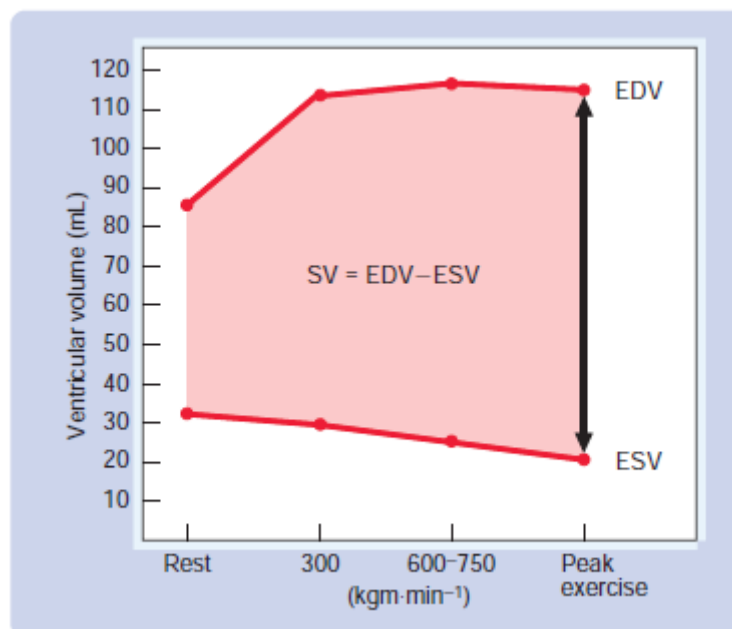


**Figure 1.27:** The changes of end-diastolic volume (EDV) and end-systolic volume (ESV) to initiate the stroke volume (SV) during the rest and the exercise [37].

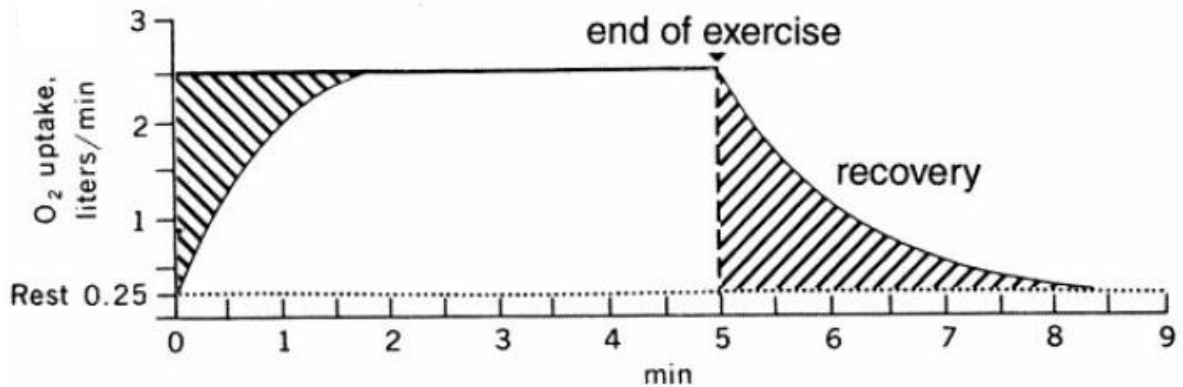


**Figure 1.28:** Oxygen consumption ( $O_2$  uptake) as a function of time during and after steady-state, dynamic exercise. With initiation of the exercise (at time 0), oxygen uptake increases over the first 1–2 minutes and levels off at a steady-state value. During the first minute of exercise, oxygen uptake does not match oxygen requirement, resulting in an oxygen deficit (crosshatched area, upper left). During the plateau, oxygen need of the exercise is matched to oxygen supply. During recovery period, there is a gradual decrease in the oxygen uptake down to resting levels [37].

Notably, cardiovascular physiological response to the dynamic exercise has the same behaviour for both genders. However, the magnitude of the response varies according to variables associated to the differences in the body size and structure, and factors such as duration, intensity, the environmental conditions and frequency of the exercise [36,39,41,42].

#### 1.2.4.2. ECG During Exercise

Exercise is commonly used in the clinical setting to create a strong physiological stress to the cardiovascular system. Examining the cardiovascular system responses to exercise helps clinicians and researchers identify underlying cardiovascular disease and clarify the mechanisms underlying abnormal responses [40]. It has been described in section 1.2.4.1, as exercise intensity increases, the heart rate, arterial blood pressure, stroke volume SV and myocardial oxygen demand increases [40].

Exercise testing can be employed to diagnose underlying diseases of cardiovascular system and evaluate the efficacy of pharmacotherapy. Exercise testing is valuable to understand the cardiorespiratory capacity, diagnostic testing (A diagnostic test is a procedure performed to confirm or determine the presence of disease in an individual suspected of having a disease, usually following the report of symptoms, or based on other medical test results. e.g. angina and dyspnea), and disease severity [40]. One of the efficient methods to view the response of exercise testing is the ECG results as the exercise physiological stress evolves various

responses on the ECG. The ECG response before, during and after exercise plays a significant role in the analysis of the subject condition by the experts.

The changes in the ECG during exercise in normal subjects were first described by Simonson in 1953 [43]. Later, several studies were conducted to describe the ECG components and their response during the exercise or recovery period. However, the main focus was on the P wave, QRS complex, and T wave; or the intervals or segments between them. However, it has been rarely described U wave or quantify it during exercise process. A possible reason is that U wave is a small deflection with low amplitude and has widely reported that with fast heart rate U wave cannot be seen [43].

The change of action potential duration, cardiac conduction velocity, and contractile velocity that associated with the increase in heart rate (HR) during exercise, results in several ECG changes in normal heart of healthy subjects, including the following [40]:

- R-R interval decreases
- P-wave amplitude and morphology experience minor changes
- Q-wave amplitude increases
- R-wave amplitude reduces to a minimum at maximal exercise
- The QRS complex undergoes minimal shortening
- J-point depression occurs
- Tall, peaked T waves occur (becomes symmetrical)
- ST segment becomes upsloping
- QT interval experiences a rate-related shortening (rate dependent)

In the *recovery* period, these changes are mostly reversed [43]. Further, Lloyd-Thomas and Palmer [44,45] briefly reported that inversion of the U wave after exercise was considered to be pathological. Its amplitude increased after exercise in several leads with depression of the T-U segment.

### **1.3. U wave in Electrocardiogram**

The electrocardiographic U wave was firstly described by Willem Einthoven in 1903 [46]. Despite the long period since the wave's description, however, the underlying electrophysiological basis of U wave origin has not been yet fully understood or precisely explained [47-50]. Several hypotheses have been proposed to explain the U wave genesis, however, none of them has been universally accepted [48-50]. The objective of this section is to review the recognised characteristics of the U wave, its genesis related to the proposed hypotheses, its pathology and abnormality.

Observed U waves can have considerable amplitude in pathological cardiac cases, nevertheless it was present in 50% of all persons with normal heart as wave with small amplitude [48,51,52]. He made two observations; firstly, U waves had various amplitudes in all hearts. Secondly, the

end of the U wave lies after the second heart sound [48,49]. In 1912, Lewis and Gilder observed that in 75 % of all ECG. The U wave was distinguishable with an amplitude of around 0.1 mV and a duration of 0.16 s [53]. They considered the U wave as an early diastolic event, because they found that U wave initiation coincides with closure of the semilunar valves and the second heart sound [53].

For long period, the U wave was thought to have no significant diagnostic information in the ECG, and thus it has rarely been included in the routine analysis of the ECG. Unfortunately, that has been reflected in most of the old reports and clinical books where they neglected U wave. Recently, due to the scientific revolution and modernise investigations using computer simulation, echocardiographic inspection and high-resolution ECG, with growing knowledge of the cellular basis of cardiac repolarisation, together have led to new insight into the role and the genesis of the U wave in the cardiac electrophysiology and pathology [49,50].

### **1.3.1. The Characteristics of U Wave**

The U wave is characterised as the last small rounded inconstant diastolic deflection of the ECG, following the T-wave [48,49,52]. The U wave is a separate wave under physiological conditions and starts with the second heart sound during phase 4 of the cardiac action potential, in other words it begins at the beginning of ventricular relaxation [48,49]. Figure 1.29-a illustrates the position of U wave during monophasic action potential and Figure 1.29-b shows its coincidence with the second sound S<sub>2</sub> during the mechanical cycle.

U wave morphology is mainly monophasic positive or negative however it can be biphasic [48,49,52]. According to the recent investigation, the U wave is usually best recognised in the precordial leads V2-V6, when heart rates between 50 and 100 bpm. The wave's timing is identical in all leads. The highest amplitude of the U wave is in leads V2-V3, and seldom exceeds 0.2 mV in human [48,49,51,54,55].

The interval from the end of the T-wave to the peak of the U wave is almost rate independent, which is unlike the QT interval regardless of whether heart rate is raised (e.g. hypercalcaemia or due to digitalis) or decreased (e.g. during atrial fibrillation) [48,50,56]. Nevertheless, the U wave becomes indistinguishable, if the QT interval increases more than 100 ms, this comes under pathophysiological conditions such as long QT syndrome (LQTS) where the U wave can be difficult to discern from the T-wave [48-50,56] or following administration of class III antiarrhythmic drugs [48,49]. The interval from the end of the T-wave to the apex U wave is approximately 90–110ms [48,51], and the duration from Q wave to the U end interval increases with the prolongation of R-R intervals [48-50].

In normal subjects U wave always directed similarly to the polarity of the T wave [48-50,52], hence the U wave is called 'the U wave inverted' if its polarity inverted relative to the T wave and considered diagnostically important [49,57,58]. Regarding the pathological U wave polarity, there are three described categories of U wave: patients with negative T waves and positive U waves are called 'Type I discordance', positive T waves with negative U waves are

called ‘Type II discordance’, and the combination of negative T and negative U waves are called ‘concordant polarity’ [49,57,58].

The U wave under normal conditions is upward except in lead aVR where it is reported negative and occasionally in lead III and aVF [48,49,59]. The U wave in atrial fibrillation (AF), is best seen in the precordial leads V2-V6, however the maximal amplitudes recognised in lead V4 [1,55]. As the main interest of the investigation is to examine U wave particularly in AF, thus U waves were investigated using either 12 leads ECG for multichannel studies or lead V4 for single channel studies, since lead V4 represents optimum lead for observing U waves due to their higher amplitudes [1,31,49,54].

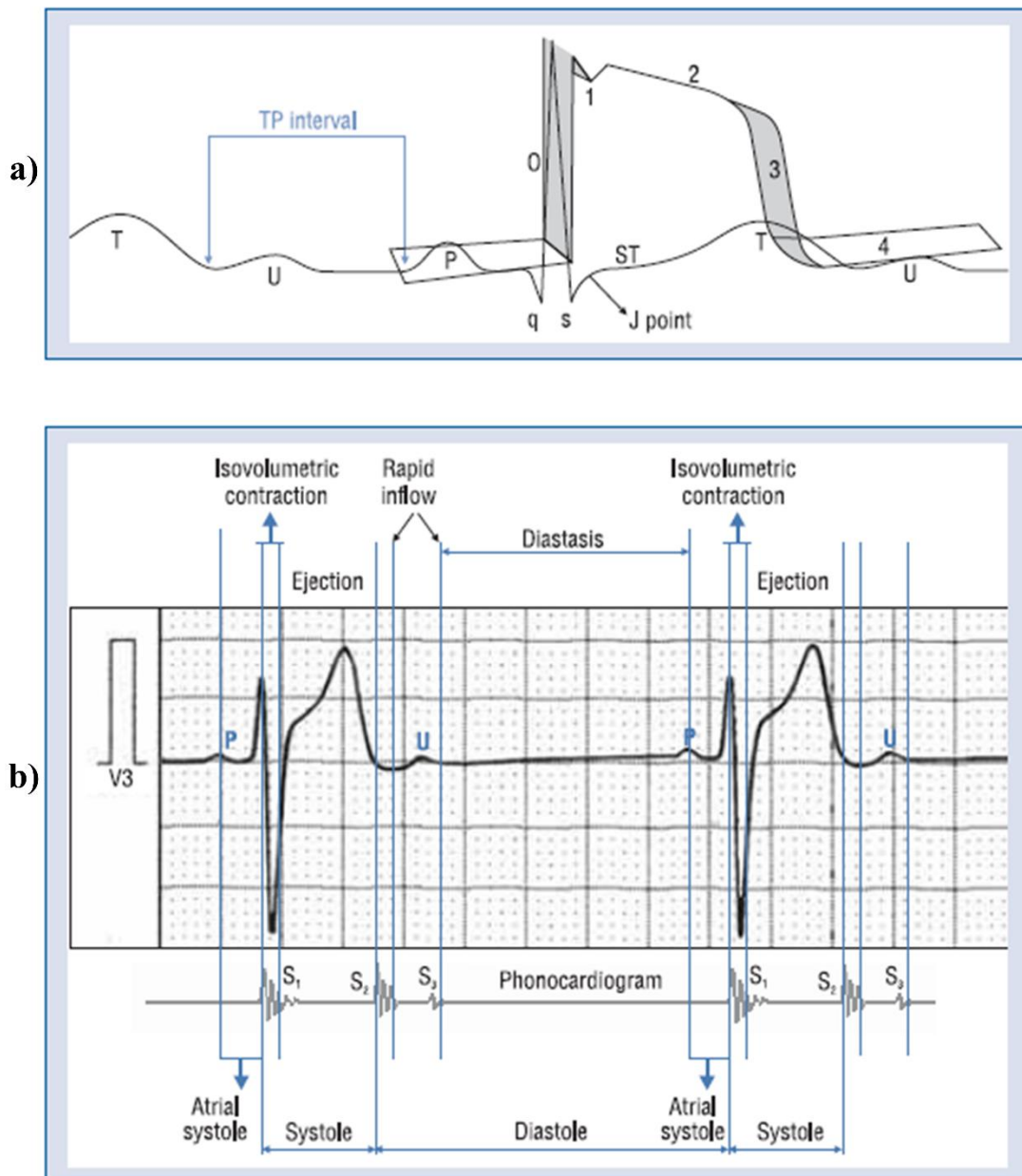


**Figure 1.29:** The U wave of ECG in the cardiac action potential and during the mechanical cycle in normal condition. **a)** The U wave is coincident during phase 4 of the action potential. On the surface ECG, U wave is located on the TP interval. **b)** The U wave during the cardiac mechanical cycle showing its relationship to the second heart sound S<sub>2</sub> [49].

The precordial leads, particularly V2-V4, are best to examine the repolarisation features including U wave. The reason is their placement is close and towards the left and the front ventricular which has large muscle mass [17,31,60] (see Figure 1.20). This helps to record higher electrical activity associated to the repolarisation waves compared to the rest of leads. Interestingly, the instantaneous amplitude of the measured potentials depends upon the direction of the electrode, and the voltage amplitude is directly associated to the mass of cardiac tissue undergoing depolarization or repolarization [17, 31,60]. Figure 1.30 shows the precordial leads placement relative to the ribcage and heart anteriority. Further, a preliminary study to investigate U wave in AF [54] showed that precordial leads V2-V6 have higher amplitudes compared to other leads, and lead V4 was the largest among the 12 leads as shown in Figure 1.31.

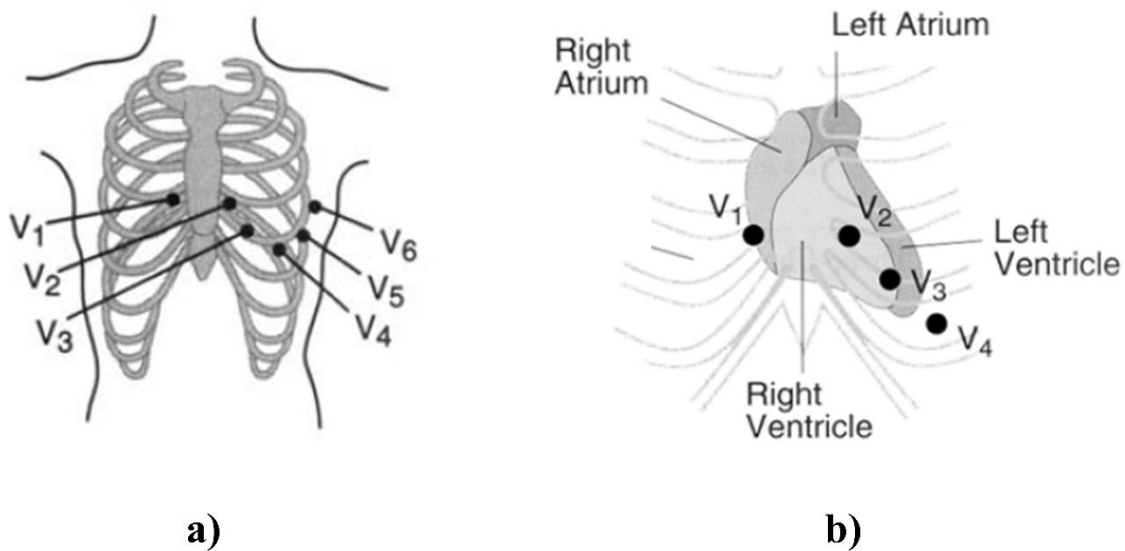


**Figure 1.30:** The precordial leads placement. **a)** Position of the chest electrodes relative to the ribcage [60]. **b)** Diagram illustrating the position of the precordial leads (V1-V4) relative to the heart anteriorly [61].

### 1.3.2. Origin of U Wave

The origin of the U wave is unknown. Since the Einthoven's first description of the U wave 100 years ago, a number of controversial theories have been proposed to explain its origin including papillary muscles, Purkinje system, negative afterpotentials, mechano-electrical feedback and early or delayed afterdepolarisations [48-50,62-64]. However satisfactory clarification is still outstanding, and the debates continue regarding whether the U wave is a purely electrical or mechano-electrical phenomena [48-50,62-64]. This is because the U wave is the only component of the ventricular features of the ECG during the cardiac cycle that cannot be derived evidently or obviously from the ventricular action potential dynamics [63,64].

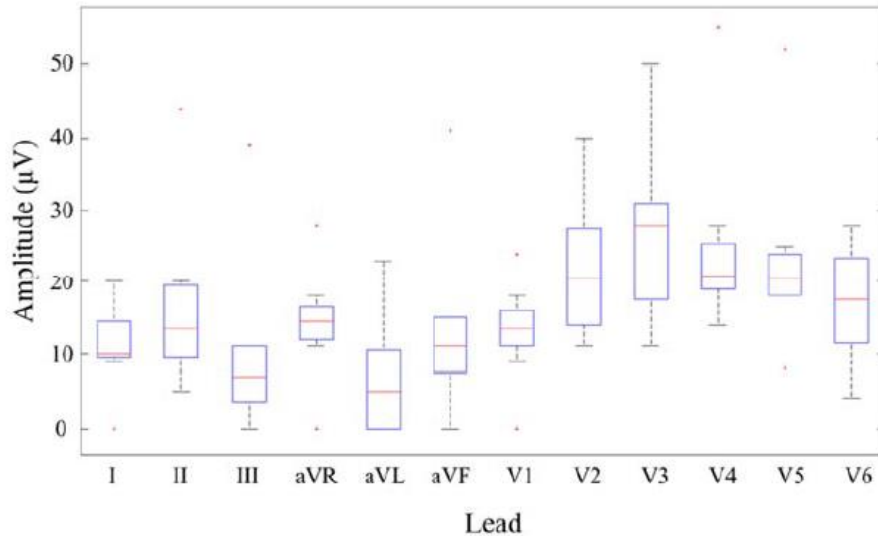


**Figure 1.31:** Amplitude distribution of U waves across the 12 leads in 10 atrial fibrillation patients [54].

There are several hypotheses to explain the genesis of the U wave as mentioned above. However, only three hypotheses were widely investigated, and they are [48-64]:

- i) Delayed repolarisation of the His-Purkinje system [65,66].
- ii) Delayed repolarisation of certain regions of the ventricular myocardium like the papillary muscle or mid-myocardial (M cells) [67-69].
- iii) Stretch-induced delayed after-depolarisations, caused by expansion of the ventricular wall during diastole. The hypothesis currently called mechano-electrical coupling hypothesis or mechano-electrical feedback [48,51,64-71].

The following section discusses the three major hypotheses to explain the genesis of U wave.

### 1.3.3. The Hypotheses of U Wave Genesis

The three major hypotheses to explain the genesis of U wave are:

#### 1.3.3.1. Hypothesis 1: Delayed Repolarisation for His-Purkinje System

The first theory introduced to explain the U wave genesis is “delayed repolarisation of the intraventricular conduction system of the ventricular Purkinje fibres”. It was introduced in 1960 by Hoffman and Cranefield [65]. In this theory, it has been suggested that the U wave might reflect repolarisation of the Purkinje system, since the action potential duration in these fibres are the longest for any cells in the heart [48,49,65].

In canine model experiment using microelectrode techniques, Watanabe [66] conducted a study to compare the action potential of Purkinje and ventricular muscle fibres under conditions

accentuating the U wave. The author concluded that the U wave represents Purkinje fibres repolarisation. The duration of phase 3 was distinctly increased and the difference between Purkinje fibre and ventricular action potential duration significantly increased. These comparisons detected a good temporal correlation between phase 3 repolarisation in Purkinje fibres and the U wave [66].

There are many arguments against His-Purkinje hypothesis which make it implausible theory to explain U wave genesis. The arguments against this theory include the fact that the involved tissue mass of Purkinje relative to the large mass of the ventricles, is too small to be recorded on the surface ECG and generate U waves [72]. Furthermore, the interval between the end of the T-wave and apex of the U wave is heart rate independent, whereas Purkinje fibre action potential duration is heart rate dependent [51]. Moreover, amphibian hearts have no Purkinje fibres, but they do exhibit U waves [48,49]. Additionally, in patients with right bundle branch block, the timing of the U wave correlates better with the presence of right myocardial hypertrophy than with timing of intraventricular conduction [50]. Furthermore, the U wave morphology does not fit the Purkinje fibres repolarisation pattern. The rising limb of the T-wave is longer than its descending limb, which is like the repolarisation pattern of ventricular and Purkinje fibres, while the U wave ascending faster than it decays [48].

### **1.3.3.2. Hypothesis 2: Delayed Repolarisation of Certain Regions of the Ventricular Myocardium**

The delayed ventricular repolarisation of certain regions of the ventricular myocardium like the papillary muscle or mid-myocardial (M cells) is one of the proposed hypotheses to explain the origin of U wave of ECG.

Regarding the papillary muscles region, in 1956, Furbetta and A Bufalari [73] characterised the ‘papillary muscle syndrome’ and assumed that the U wave represents repolarisation of the papillary muscle and neighbouring components. The authors supposed that various papillary muscle abnormalities, whether anatomic or functional, can be detected by modifications of U waves and the T-U segment [51,73].

Regarding this hypothesis from the M cells region perspective, the theory is attributed to the key feature of M cells (located in the mid-myocardium) which is their ability to prolong action potential duration during decreasing of the heart rate more than epicardial or endocardial cardiomyocytes [51]. Figure 1.32 displays the action potential in different cardiac tissues where M cells in midmyocardium has the longest action potential. The M-cells relative to the epicardial or endocardial have different electrophysiological and pharmacological features [51].

Antzelevitch and et al [74] suggested that M cells have abundant tissue mass comparable to Purkinje cells and their delayed afterdepolarisation could be sufficient to give the rise to pathophysiologic U wave in the presence of developed or congenital long QT interval (LQTS).

The discovery of M cells and their electrophysiologic behaviour has an impact to understand the cellular basis for repolarisation and has contributed to further understanding of U-wave genesis [74]. On the contrary, another experiment suggested that M cells may give rise to a second component of the T-wave, as an accentuated or inverted U wave [51]. Antzelevitch and et al suggested to use the terms ‘T1’ and ‘T2’ to describe the two adjoining repolarisation waves, or ‘bifurcated T-wave’, which is separate from the U wave [51,64].

The T and U waves as separate deflections was also found in patients with acute myocardial ischaemia, where the monophasic transformed ventricular complex is independent of the morphology and timing of the U wave [48].

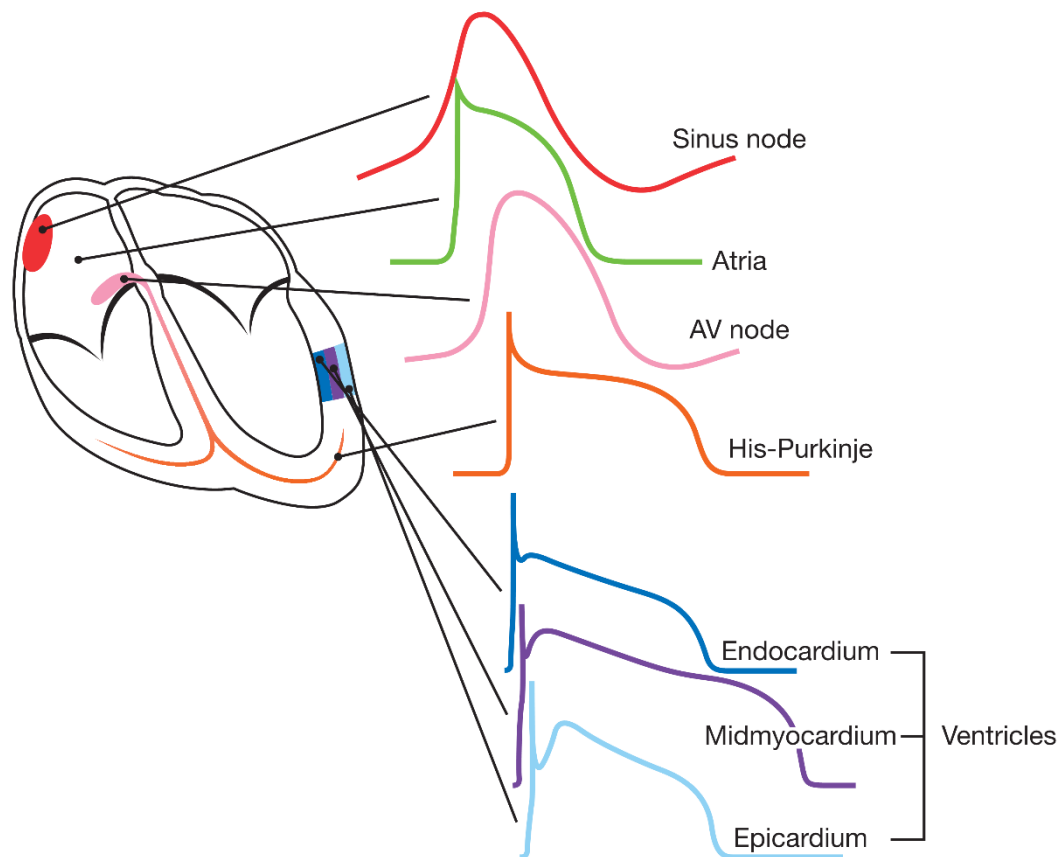


**Figure 1.32:** Different action potential in different cardiac tissues . The His-Purkinje tissue has the fastest upstroke speed for rapid conduction of electrical impulse to activate the ventricles synchronously. The ventricular epicardium, endocardium, and midmyocardium have distinct action potential formations [75].

### 1.3.3.3. Hypothesis 3: Mechano-Electrical Coupling

Lepeschkin in 1957 firstly suggested the concept of mechano-electrical coupling as a contributor to, or a cause of, the U waves [51,76]. As the T wave end coincides with the second heart sound (S<sub>2</sub>), the mechano-electrical hypothesis suggests that after potentials caused by stretching of the cardiac muscle layers of the left ventricle would give rise to the U wave [51,53,77]. The mechano-sensitive ion channels transduce the changes in the cardiomyocytes mechanical environment into electrical signals [51,78-80]. Up to now, there is no decisive proof to support the U wave via mechano-electrical hypothesis. However, this hypothesis produced principally because it links between the timing of U wave and ventricular relaxation which makes it more favourable among the other hypotheses [51].

Schimpf et al. [63] found in echocardiographic measurements that the presence of the U wave in short QT syndrome (SQTS) patients synchronised with aortic valve closure and isovolumic relaxation, in which supports the hypothesis that the U wave is associated to mechanical stretch.

Clinically, there is a considerable dissociation between the ventricular repolarisation and the mechanical systole termination in SQTS patients. The coincidence of the U wave with ending of mechanical systole provides a favourable support for the mechano-electrical coupling hypothesis for the genesis of the U wave [63].

There is a reason to believe the U wave is generated due to triggered potential by stretching of cardiac ventricular muscle during the time of rapid blood filling into the ventricles [48]. In other words, the combination of the afterpotential with the triggered activity are presumably contributed to the wave's genesis [48]. Afterpotentials (see section 1.2.2.1.3.2) arise in stretched cardiac fibres and physiologically the endocardial tissue is subjected to a greater stretch than the epicardial muscle.

Also, Lepeschkin [76] assumed that U waves were initiated by the potential differences between larger negative afterpotentials and smaller afterpotentials of the cardiac muscle. Further, Di Bernardo and Murray [81] proposed a simple process to model repolarisation in the left ventricle and its corresponding T waves on the surface ECG. They modelled the action potentials of the cardiac cell in the left ventricle with differences in only the duration of the plateau phase. The authors concluded that repolarisation of the left ventricle can be demonstrated independently of the depolarisation sequence and action potential duration gradients. This method has produced an easy and powerful instrument to characterise the repolarisation ventricular features. The same authors using their left ventricle repolarisation computer model have demonstrated that the delay of repolarisation in different regions of the heart cannot explain the U wave. Whereas the presence of after potentials on the cardiac cells does explain the polarity of U wave and other characteristic and features. additionally, the authors also found that the timing of abnormal after-potential correlated with abnormal U wave inversion [82].

### **1.3.4. U Wave Pathology**

#### **1.3.4.1. Abnormalities of U Wave**

The U wave in the normal subjects has the same polarity as the T wave [48-50,57,58]. Typically, the U wave is lower than the 50% of the width and between 3 to 24% (average 11%) of the preceding T wave amplitude [48,49]. Therefore, if the U wave inverts with the respect to the T wave polarity or exceeds 1.5 mm, it considered abnormal and diagnosed as clinically important as it may be the earliest and the only marker of heart disease [48,49,64]. Major cardiac organisations such as American Heart Association (AHA) and Heart Rhythm Society (HRS) and American College of Cardiology (ACC) recommended that all U wave abnormalities should be reported during ECG interpretation [49,52].

There are two types of U wave abnormalities [48,49]:

##### **1.3.4.1.1. U Wave Inverted**

An inverted or negative U wave appears in various pathological conditions and around 93% in ECG abnormalities of cardiac diseases. In the normal condition, the negative U wave appears in the standard ECG lead aVR and occasionally III and aVF. It is rarely occurring in the absence of heart disease or other ECG abnormalities [48,49,73,83].

The U wave inversion has been reported during attacks of variant angina pectoris and during exercise testing [73,80]. The lone inverted U wave after exercise is highly predictive of significant coronary artery disease [49,84]. Generally, in cases of hypertensive, ischemic, or left-sided valvular heart disease, the inverted U wave is reported in the left precordial leads; however, in patients with right ventricular hypertrophy the inverted U wave is usually reported in the right precordial leads [49,84,85].

Moreover, negative U waves is a significant sign of ischemia and related with coronary artery disease (CAD) stenosis, usually in the LAD artery [48,86]. Also, it associated with hypertension (high blood pressure nearly 40% cases), and congestive heart disease [48,86]. The association of negative U waves and stroke is dependent on the presence of CAD [86]. Additionally, inverted U wave can be seen in hyperthyroidism, primary cardiomyopathy [48,49,86]. Figure 1.33 presents an example of inverted U wave in lead V2 and V3.

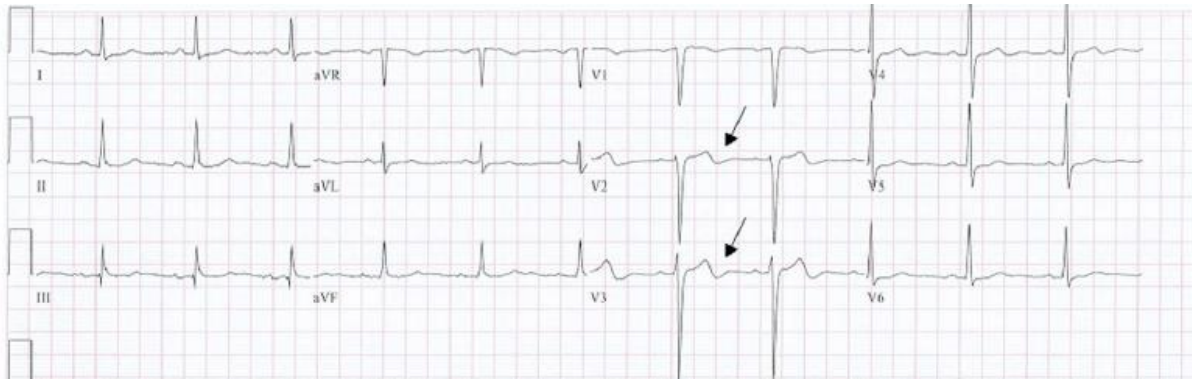


**Figure 1.33:** An example of ECG showing inverted U waves in the leads V2 and V3 as annotated by the arrows [87].

### 1.3.4.1.2. Prominent U Wave

If the U wave reaches 1.5 mm/0.15 mV or 25% of the amplitude of the T wave or more, it is considered a high or ‘prominent’ U wave [49]. However, it could be 2 mm (0.2 mV) in the lead II, and the precordial V2-V4 [48,49].

It has been reported that the amplitude of U wave is inversely related to the heart rate (1/R-R), thus it can be seen readily in bradycardia [49,83]. The amplitude of the U wave increases during slow rates which is associated with the increase in ventricular filling and longer ejection period. This is clear in the cases of long QT interval [49,83].

Also, hypokalemia is one of the conditions famous for prominent U waves and distinctive changes in the ST-T complex. It may produce a combination of ST depressions with prominent U waves and overall prolonged repolarisation [88]. Figure 1.34 displays an example ECG with different hypokalemia’s patterns showing prominent U waves. Typically, the U waves with hypokalemia become enlarged and may even exceed the amplitude of the T waves [88]. In the hypokalemia, the repolarisation process is prolonged, and clinically represented by the prominent U waves, however the QT interval may remain normal. Technically, because the T wave and U wave frequently merge, the measurement of the QT interval cannot always be accurate, the term ‘T-U fusion’ wave can be applied in this case [88].

Furthermore, there are many other causes of prominent U waves including: early repolarisation variant, hypomagnesemia, hypocalcaemia, hypothermia, digitalis effect, mitral valve prolapses, endocranial hypertension, and cardiomyopathies. Additionally, U wave represents a significant sign to identify the congenital long QT syndrome [59,89].

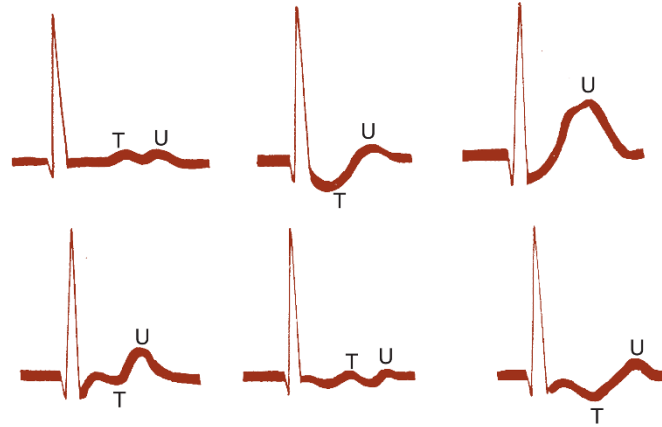


**Figure 1.34:** Example presents ECG patterns that may be seen with hypokalemia showing the appearance of prominent U waves, sometimes with ST segment depressions or T wave inversions [88 edited].

## 1.4. T Wave in Electrocardiogram

### 1.4.1. Characteristic of T Wave in Normal ECG

The electrocardiographic T wave represents the period of ventricular repolarisation corresponds to phase 3 of the cardiac action potential [62,90,91]. Because of the slow rate of repolarisation compared to depolarisation, the T wave is wide, has a slow rising, and returns rapidly to the isoelectric line that follows its peak. In other words, it has slow rising and rapid falling. Hence, the T wave is asymmetric with a rounded peak, and the amplitude is variable [52,90,91].

The T wave in normal adults, is positive in most limb and precordial leads except leads aVR, aVL, III and V1; and its higher voltage is reported in leads V2 and V3 [94,95]. Otherwise, Opposite direction of T wave and QRS complex (discordance) could be due to pathology [91-93]. The T wave can be seen as positive and negative as mentioned, also can be seen biphasic. The variation of T wave amplitude or shape in periodic beat to beat is called T wave alternans [52,64, 91-93].

T wave amplitudes and morphology are influenced directly by the heart rate. T wave becomes more symmetrical with higher amplitudes with the increasing of the heart rate due to the increasing of dispersion of the repolarisation as the action potential are linearly correlated to heart rate [94,95]. Additionally, T wave amplitude is affected by the pressure, where the pressure increases the T wave amplitude increases due to stretch of the left ventricular repolarisation by mechano-electrical coupling [96,97].

### 1.4.2. Origin of T Wave

The T wave represents the ventricular repolarisation. Depolarisation starts at the cardiac endocardial surface and propagates to the cardiac epicardium, whereas repolarisation starts at the epicardial surface and propagates to the endocardium, which means the direction of ventricular depolarisation is opposite to that of ventricular repolarisation. Consequently, in the normal condition the T wave polarity on the ECG is similar to the direction of the QRS [52,64,90-92]. In other words, the QRS and T wave axes are usually concordant. T wave discordance is due to pathology and various diseases [92,97].

In the last decades, many studies were conducted [92,98] to understand the T wave formation. However, the ionic and cellular basis for the genesis of the transmural gradient was not recognised until 'M cells' were discovered by Antzelevitch and his colleagues in the early 1990 [98].

The three myocardial layers, epicardial, endocardial and M cells; histologically are similar, however electro-physiologically and pharmacologically they are different, mainly due to their repolarisation properties [98]. The distinction of M cells is tended to prolong more than the cells of epicardium or endocardium during slow heart rate, or in response to the prolongation of the action potential due to drugs. This plays an essential role in abnormal ventricular repolarisation such as long QT syndrome (LQTS) [92,99].

The electrical interaction among these three myocardial layers during ventricular repolarisation underlies the genesis of various T wave morphologies as demonstrated in the isolated arterially perfused ventricular wedge preparation under both physiologic and pathologic conditions. [92,99,100].

For the positive T wave on the ECG trace, always the peak of the T wave is corresponding with the repolarisation of epicardium [92] while the end of T wave is associated with either the repolarisation of M cells or by the repolarisation of the endocardium [92,99]. Figure 1.35 illustrates the T wave formation regarding the difference between the action potential of the myocardial layers. Nevertheless, the interval from the T wave peak to the T wave end represents the maximum transmural dispersion of repolarisation of the ventricle. Technically, the T peak-T end interval shows a rate dependence in humans [93,97,101] and has played a significant index in the assessment of arrhythmic risk in patients with the LQTS [102,103].

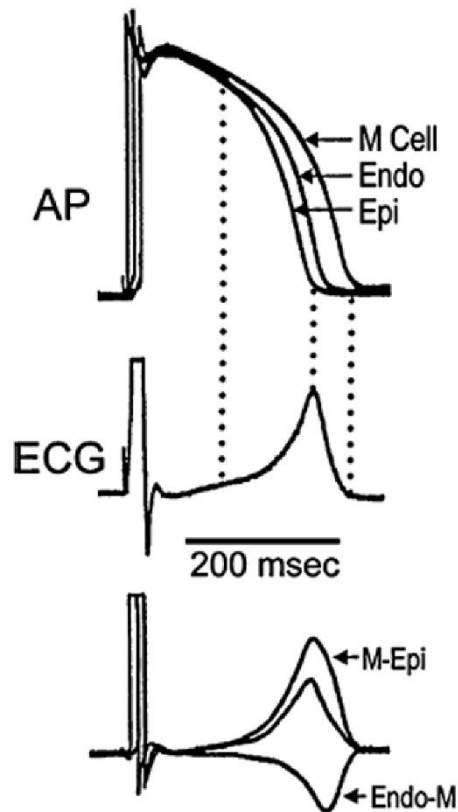


**Figure 1.35:** The inscription of the T wave from the voltage gradients of the action potential of myocardial layers. The top shows action potentials recorded from endocardial, epicardial, and M cells of an arterially perfused canine left ventricular wedge preparation. The middle presents the ECG recorded across the wedge, and the bottom exhibits the computed voltage differences between the M region and epicardial ‘M-Epi’ action potentials and between the M region and endocardium ‘Endo-M’ responses [64 edited].

### 1.4.3. Abnormalities of T Wave

Abnormalities of the T wave are associated with a variety of cardiac conditions and diseases and can be life threatening or can be sign for the risky cardiac conditions [52]. The abnormalities of T-waves can be seen in the presence or absence of ST-segment abnormalities.

In normal adults, the T-wave amplitude is most positive in lead V2 or V3. Several terms such as *peaked*, *biphasic*, *symmetrical*, *hyperacute*, *flat*, ‘*camel hump*’ and *inverted* are being used to T wave abnormalities descriptors.

Mainly the T wave abnormalities regarded to quantitative descriptors or the morphology. The negative T-wave in the precordial leads V5 and V6 is clinically important [49]. It is proposed that the T wave amplitude in leads I, II, aVL, and V2 to V6 when its ranging from -0.1 to -0.5 mV is reported as *inverted*, as *deep negative* when the amplitude is from -0.5 to -1.0 mV, and if the amplitude is less than -1.0 mV as *giant negative* [52]. The *inverted* T wave is highly

associated to the myocardial ischemia [52] and seen with many conditions such as bundle branch block, hypertrophic cardiomyopathy, and ventricular hypertrophy [52].

Further, if the T wave amplitude is less than 10% of the R-wave amplitude it is called *low* and *flat* when the T-wave peak amplitude is ranging between 0.1 and -0.1 mV in leads I, II, aVL [52]. *Flattened* T wave can be caused by hypokalemia or due to digitalis which leads to prominent U wave [52]. Additionally, *biphasic* T wave can be caused by myocardial ischemia and hypokalemia. Moreover, it is difficult to distinguish notching (bifid) of the T wave from a U wave that is superimposed on the downslope of an upright T wave. Note, it is rare to find the notched T wave in all 12 leads, and usually the interval between the two peaks of a notched T wave is less than the interval between the peak of a monophasic T wave and the following U wave [52].

#### **1.4.3.1. QT Interval**

The QT interval represents the duration of ventricular systole during the cardiac cycle [83]. It is measured from the start of the QRS complex to the end of T wave [83]. To obtain an accurate measurement of QT, multichannel recorders are used as it allows more accurate determination of the QRS onset and the T wave end. The QT interval is inversely related to the heart rate, where it decreases when the heart rate increases [83]. Short and long QT intervals represent pathophysiologic state. Abnormal shortening of QT interval occurs as a result of a shortened or absence of ST segment. It is rarely distinguished except in hypercalcemia and due to digitalis effects [83,103]. So far, the short QT syndrome that associated with the sudden death became more distinguishable with the channelopathy [83,88].

On the other hand, lengthening of the QT interval is more common clinically, and might occur because of increasing QRS duration or the lengthening of repolarisation [83]. Both the congenital and acquired forms of long QT syndrome are mainly associated with sudden death due to the cardiac arrest or death after acute myocardial infraction [83,104,105]. Additionally, lengthening of QT interval could contribute to arrhythmias, or are associated with the risk of torsade de pointes (TdP) [83].

Moreover, the QT interval is affected by the left ventricular pressure, where the pressure increases the QT interval is prolonged due to the increase of the dispersion because of stretch of repolarisation by mechano-electrical coupling [96].

It is important to note; the thesis study did not investigate the QT intervals either in atrial fibrillation or healthy subjects. Instead, RT intervals and R-TU nadir intervals were examined and associated with the QT interval.

## 1.5. Abnormal Heart Rhythm

The normal rhythm of heartbeats, initiated by the SA node, is known as *normal sinus rhythm*. The defect in the cardiac conduction system leads to establish irregular rhythm, this abnormal heart rhythm called *arrhythmia* [5].

The heart could beat irregularly, erratically, too quickly, or too slowly. This leads to many symptoms including chest pain, dizziness, light-headedness, shortness of breath and fainting. Many factors may stimulate the heart and cause arrhythmia, such as stress, cocaine, alcohol, nicotine, and specific drugs that include caffeine or other stimulants [5]. Furthermore, arrhythmia may also be produced by a congenital defect, myocardial infarction, coronary artery disease, defective heart valves, hypertension, hyperthyroidism, or potassium deficiency [5].

### 1.5.1. Types of Arrhythmias

Arrhythmias are characterised by their rhythm, speed, and disorder origin and categorised into several types. If the heart rate is slow and below 50 bpm, it called *Bradycardia*. Whereas *tachycardia* refers to a fast heart rate with over 100 bpm; and *fibrillation* refers to rapid, uncoordinated heartbeats. If the arrhythmias begin in the atria, they are called *supraventricular* or *atrial* arrhythmias; while those that initiate in the ventricles are called *ventricular arrhythmias* [3,5].

The study has focused the ventricular features in one of the supraventricular arrhythmias known as *atrial fibrillation* (AF) which will be reviewed in depth during this chapter. However, the most famous arrhythmias can be classified as [3,5,8]:

#### 1) Atrial fibrillation (AF)

Atrial fibrillation AF is a common arrhythmia, mostly affecting elderly adults. In AF the contraction of the atrial fibres is asynchronous (not in harmony). The atria may beat 300–600 bpm and the ventricles may also accelerate, which results in a rapid ventricular rate up to 160 bpm [3,5,8]. Typically, the ECG characteristics of subjects with AF has no clear P waves combined with irregularly occurring QRS complexes (i.e. irregular R-R intervals). Atrial fibrillation can cause stroke [3,5,8], since blood may stagnate in the atria and generate blood clots. A stroke occurs when part of a blood clot blocks an artery that supplies the brain [3,5,8]. More detail of AF and its symptoms, causes and physiology are reviewed in the following sections of this chapter. Figure 1.36 presents an example of ECG with AF compared to normal beat.

#### 2) Atrial flutter

Atrial flutter has rapid but regular atrial contractions (around 240–360 bpm) combined by an atrioventricular AV block in which few of the nerve impulses from the SA node is conducted through the AV node [3,5,8]. Figure 1.36 presents an example of ECG with atrial flutter.

### 3) Heart block

This arrhythmia occurs when the electrical pathways between the atria and ventricles are blocked, resulting in the slow transmission of nerve impulses. The common location of the blockage is the atrioventricular node. This condition is called *atrioventricular (AV) block* and is classified into several degrees. *first degree AV block*, the interval P-Q is prolonged (Figure 1.36), usually due to the slow conduction through the AV node compared to the normal. In *second-degree AV block*, some of the action potentials from the SA node are not conducted via the AV node, which results in dropped beats as the excitation does not always reach the ventricles. Accordingly, there are fewer QRS complexes compared to the presence of P waves on the ECG (Figure 1.36). In *third degree (complete) AV block*, the SA node action potentials cannot get through the AV node. The fibres in the atria and ventricles pace the upper and lower chambers individually. With third degree (complete) AV block, the rate of ventricular contraction is less than 40 bpm (Figure 1.36) [3,5,8].

### 4) Ventricular premature contraction

This arrhythmia occurs when a region of the heart other than the conduction system (an ectopic focus), becomes more excitable than normal and accordingly causes an occasional abnormal action potential to arise. As a wave of depolarization propagates outward from the ectopic focus, it causes a ventricular premature contraction (i.e. ectopic beat) [3,5,8]. Figure 1.36 shows an example of ECG with ventricular premature.

### 5) Ventricular tachycardia (VT)

This arrhythmia originates in the ventricles, where it is characterised by four or more ventricular premature contractions. VT causes the ventricles to beat rapidly at a minimum 120 bpm, see Figure 1.36. VT is idiopathic; however, it is correlated with cardiac disease or a recent myocardial infarction. Continued VT is dangerous because the ventricles do not fill appropriately and therefore do not pump enough blood. The result may produce low blood pressure and heart failure [3,5,8].

### 6) Ventricular fibrillation (VF)

VF is the deadliest arrhythmia in which ventricular fibres contractions are completely asynchronous; therefore, the ventricles shiver rather than contract in a harmonised way. Consequently, ventricular pumping stops, blood ejection stops, and circulatory failure and death occur unless there is immediate medical intervention [3,5,8]. During VF, the ECG has no clear P waves, QRS complexes, or T waves (see Figure 1.36). The most common cause of VF is insufficient blood flow to the heart because of coronary artery disease, as occurs during a myocardial infarction. Other causes include cardiovascular shock, electrical shock, drowning, and very low levels of potassium. VF causes unconsciousness in seconds and, if untreated, seizures occur, and irreversible brain damage may happen after 5 minutes. Death soon follows [3,5,8].

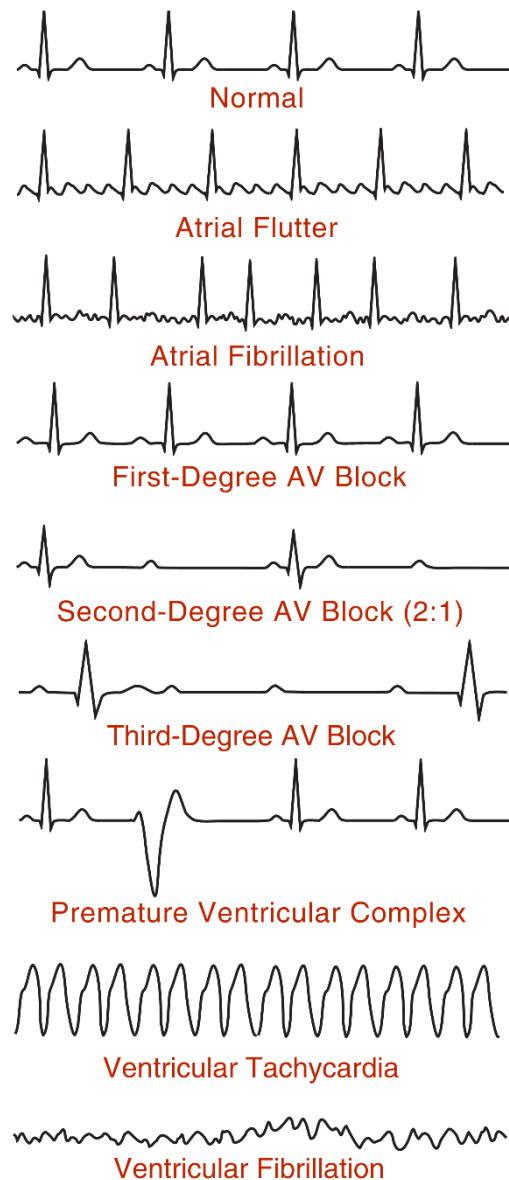


**Figure 1.36:** Examples of ECGs with normal and abnormal rhythms (Arrhythmias). AV = atrioventricular [31].

### 1.5.2. Atrial Fibrillation (AF)

In the clinical practice, atrial fibrillation (AF) is the most common arrhythmia in adults which needs therapeutic interventions [106,107]. Its prevalence is increasing and the number of patients with AF is growing along with the aging population [106-108]. The impact of atrial fibrillation is on the quality of life due to the rapid irregular heartbeats or palpitation attacks. It is also one of the most prevalent risk factors of ischemic stroke which may lead to the death. Mostly, AF requires therapeutic interventions, in contrast to many other arrhythmias in clinical practice, even for patients who are not subjected to the discomfort from their arrhythmia [106-108].

The prevalence of atrial fibrillation increases with aging where it estimated as 0.5% in individuals below 50 years, 1.5–2% in 50–60 years, and around 3% and higher in patients above 70 years [106,109] as Figure 1.37 present. Generally, AF is significantly more common among men, especially at a young age, nevertheless, gender-related variances decrease with increasing age (Figure 1.37).

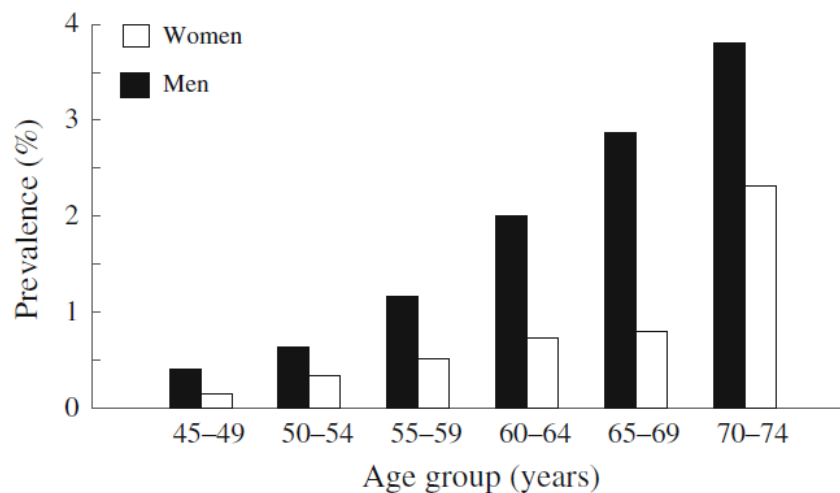


**Figure 1.37:** The AF prevalence with respect to age and gender [106].

The following sections provide an overview of basic concepts related to the AF characteristics, underlying mechanisms, classification of AF, symptoms, causes and its risks and impact on the human health.

### 1.5.2.1. Atrial Fibrillation Characteristics

Atrial fibrillation is a supraventricular tachyarrhythmia [106,110]. It is characterised by uncoordinated atrial electrical activation and accordingly leads to inefficient atrial contractions. In many cases, AF diagnosis is based on three morphological features in the ECG [106,110]:

- a) Irregular R-R intervals (irregular heart rate)
- b) Absence of P waves
- c) Presence of fluctuating atrial waveforms known as fibrillatory waves or ‘f’ waves.

Figure 1.36 presents an example ECG with atrial fibrillation (third row) compared to the normal ECG (first row). Irregularity of R-R intervals were considered a key feature of AF where their irregularity is detectable by the human eye [106,110]. In addition, the absence of P waves is controversial in subjects with low-amplitude f waves. However, large-amplitude f waves can mimic P waves, particularly in the right precordial leads V1 and V2 [106,110].

### 1.5.2.2. Cardiac Activity Difference Between Normal Rhythm and AF

It is necessary to understand the mechanism and the normal physiology of the conducting cardiac system to understand the mechanism of AF. The AF mechanism is complicated and needs a combination of triggers, usually characterised by ectopic atrial firing which enhance perpetuation of AF.

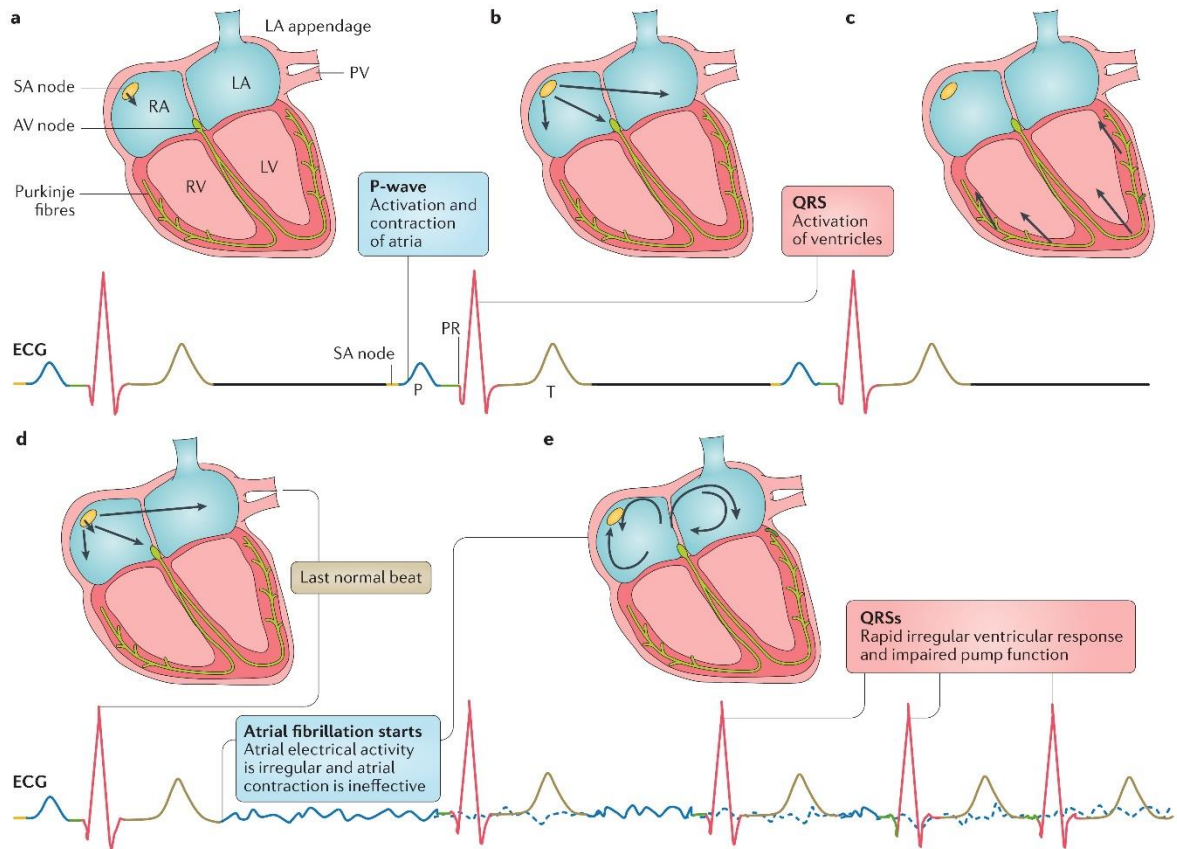
The conduction system and electrical pathways of the heart during sinus rhythm (SR) has been explained extensively in section 1.2.2.1.1. However, both electrical pathways, during SR and AF will be reviewed to understand the difference between them.

Figure 1.38 shows the electrical conduction during sinus rhythm (SR) and atrial fibrillation (AF). Primarily, the heart rate and rhythm are controlled by the electrical conduction system of the heart. The normal heart rhythm SR originates in SA node (Figure 1.38-a), which it acts as the physiological pacemaker [111]. The impulse propagates from the SA node through the atria as Figure 1.38-b illustrates, then it travels through the Purkinje fibres. These fibres convey the impulse through the AV node (between the atria and the ventricular) to reach the ventricles (Figure 1.38-c) causing the cardiac muscle contraction [111].

Figure 1.38-d displays the ‘last normal beat’ before the onset of AF episode in Figure 1.38-e. In contrast to the atrial activation in SR, in AF the atrial activity is very fast and irregular. There is no synchronised atrial contraction; and the ventricles response is irregular and rapid and depends on the filtering effect of the AV node [111].

The electromechanical consequences of AF have significant clinical implications [111]. The absence of efficient atrial contraction increases the risk of blood coagulation and thrombosis, especially in the left atrial (LA) appendage (see Figure 1.38-a). The irregular and rapid ventricular rate during AF episodes affects the ventricular contraction by decreasing its efficiency and may worsen to develop heart failure or sometimes even causing ‘de novo’ heart failure [111].

The AF rapid and irregular rhythm can be maintained by each of three main mechanisms [111-113] that are illustrated in Figure 1.39. *First*, in this mechanism one or more firing atrial ectopic foci may be present (Figure 1.39-a), leading to irregular conduction towards the rest of the atria creating irregular fibrillatory activity. *Second*, one or a small number of ‘primary re-entry’ circuits (or rotors which arise when an action potential travels through a potential conducting circuit in a continuous fashion) may initiate rapid local activation as shown in 1.39-b with fibrillatory conduction in which causes AF episodes [111-113]. *Finally*, AF may be preserved by *many* functional ‘re-entry’ waves or rotors with irregular forms and no consistent activation pattern [111-113] as illustrated in Figure 1.39-c.



**Figure 1.38:** Schematic diagrams of electrical conduction pathway during sinus rhythm (SR) and atrial fibrillation (AF). The cardiac mechanisms (top of each row) and electrocardiograms (ECGs; bottom of each row) in normal SR (parts a–c) and AF (parts d and e). **a)** The SA node is located in the upper wall of the right atrium (RA), originates the electrical impulses. **b)** Impulses are spread through the heart, firstly through working atrial muscle cells and then through the conduction system (in green), in which depolarise the cardiomyocyte membrane and causing subsequent contraction. On an ECG, atrial depolarisation and contraction is represented by the P wave. **c)** The AV node delays the conduction between the atria and the ventricles, to ensure that atrial contraction, and blood propelling into the ventricles precedes ventricular contraction. On an ECG, ventricular depolarisation is denoted by the QRS complex, ventricular repolarisation by the T wave and the span taken for the electrical impulse to travel from the SA through the AV node is represented by PR interval (measured from the beginning of the P wave to the start of the QRS). **d)** The ‘last normal beat’ before the start of AF. **e)** AF is characterised by fast and uncoordinated atrial activity in which causing ineffective atrial contraction. Consequently, the ventricles respond with irregular and fast electrical activity that makes the contractions weaker than normal. LA: left atrium; LV: left ventricle; PV: pulmonary vein; RV: right ventricle [111].

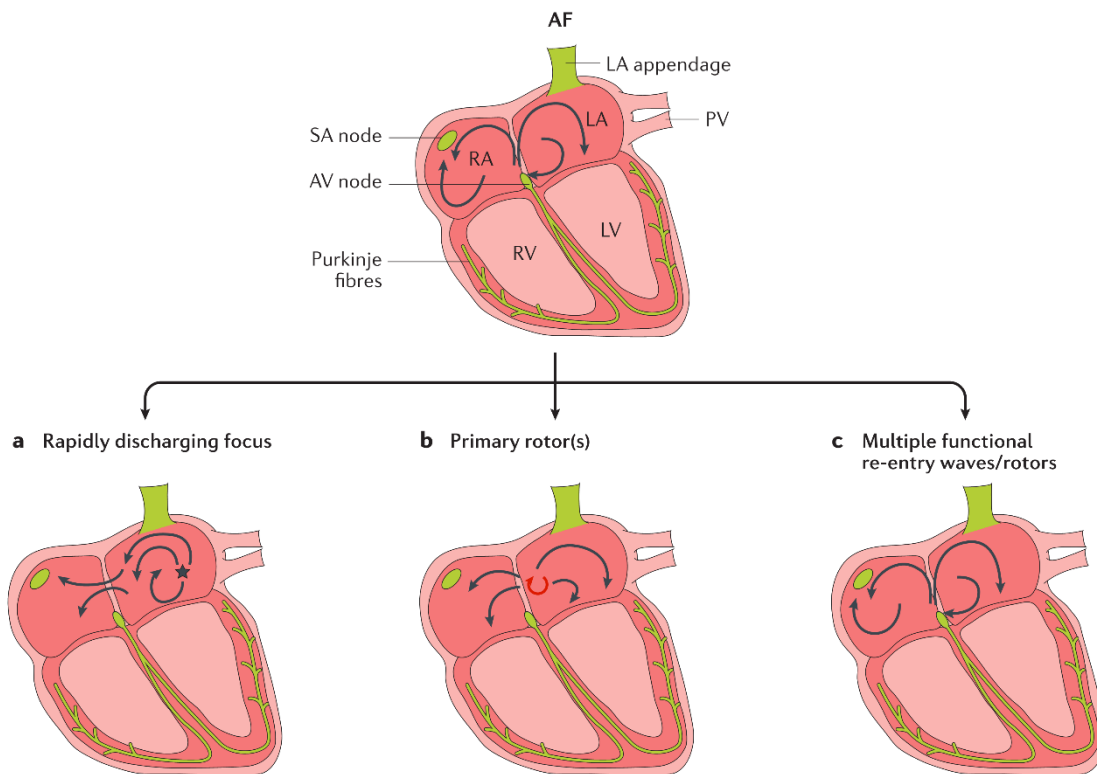


**Figure 1.39:** The three mechanisms that can maintain atrial fibrillation (AF). Ectopic electrical impulses that spread throughout the atrial myocardium cells in an irregular way can be maintained through different mechanisms. **a)** A rapidly discharging atrial focus. **b)** A primary re-entrant rotor. **c)** Multiple functional re-entry circuits. AV: atrioventricular; LA: left atrium; LV: left ventricle; PV: pulmonary vein; RA: right atrium; RV: right ventricle; SA: sinoatrial. [111]

### 1.5.2.3. Classification of Atrial Fibrillation

Atrial fibrillation is classified into three main categories in general practice.

The main categories are [114,115]:

i) Paroxysmal atrial fibrillation

In this category of AF, the episodes of arrhythmia are self-terminating and last for less than 7 days [114,115]. Typically, this begins in the 50s-60s age group but can start earlier in life. If AF paroxysms are going to self-terminate, they usually last 24 to 48 hours. This type of AF may be associated with mitral valve disease, ischaemic heart disease and thyrotoxicosis [114,115].

ii) Persistent atrial fibrillation

In this category of arrhythmia, the AF episodes lasts for more than 7 days but either self-terminates, need drugs or direct current cardioversion (DC cardioversion) for their termination [114,115].

iii) Permanent atrial fibrillation

When the arrhythmia has been long standing for more than one year it is classified as permanent AF. Typically, the treatments to restore AF rhythm back to SR are unsuccessful.

Despite of the three AF categories above, AF may occur in a *single episode* which may be due to cardiac surgery, chest infection, pulmonary embolus, or electrolyte disturbance; and once this cause has been removed, the AF episode does not return [114,115].

Generally, patients diagnosed with paroxysmal AF can develop persistent AF because episodes become more regular. Similarly, people diagnosed with persistent AF are vulnerable to develop permanent AF. Increasing the frequency of episodes and with longer the duration, leads to remodelling the heart.

Furthermore, many patients have no specific cause or underlying detectable diseases; this is known as ‘idiopathic’ or “lone” AF. It commonly diagnosed in younger people and can affect those diagnosed with paroxysmal AF (about < 20% ) [114,116].

#### **1.5.2.4. Atrial Fibrillation Symptoms, Causes, Factors and Risks**

##### **1.5.2.4.1. Symptoms**

Patients with AF may experience various symptoms. The most common symptoms include palpitations, tiredness or fatigue, shortness of breath, generalized weakness, dizziness or light-headedness, exercise intolerance and irregular pulse [117,118]. Furthermore, severe symptoms include hypertension, chest pain (angina), and decompensated heart failure (causes respiratory distress) [117,118].

Some of these symptoms may be related to the natural ageing process, however taking patients history in the consultation may lead to suspicions of AF [117,118]. If any individual presents palpitations, shortness of breath and light-headedness, a health investigation should take place since they considered warning signs. Diagnosis and assessment are significant in such cases so that a risk assessment can take place, and then appropriate treatment planned to avoid any complications associated with AF [117,118].

##### **1.5.2.4.2. Causes, Factors and Risks**

Atrial fibrillation is usually associated with underlying structural abnormalities of the heart [117,119]. There are many causes for AF that can be classified as cardiac (e.g. Ischaemic Heart

Disease, hypertension, cardiomyopathy and heart failure) or non-cardiac (e.g. thyroid disease, acute infections, and chronic lung diseases such as asthma) [117,119].

The possible causes are the result of heart tissue damage itself, which may produce extra impulses or stimuli. Also, stretching and remodelling of cardiac muscle tissue can increase atrial pressure, which increases the pressure on the pulmonary veins. This is believed to be a contributing factor in other causes associated with atrial fibrillation, for instance valve disease, heart failure, left ventricular hypertrophy (related to hypertension), atherosclerosis and obesity [119].

On the other hand, alcohol, smoking, caffeine, medication, drug use, high-intensity sport and psychological and physical stress are thought to be stimulants that can trigger AF [120]. Also, aging is a common risk factor for AF. There is evidence to show that obesity, metabolic syndrome, and diabetes can be risk factors for cardiovascular disease leading to AF [121]. Furthermore, research shows that genetic factors may be associated with AF. Where some families tend to develop AF, especially in younger patients, including long and short QT syndromes, Brugada syndrome, and some cardiomyopathies [121].

Significantly, AF can lead to heart failure and embolic strokes, causing either severe disablement or death [121,122]. The reason is when atria are fibrillating, the blood flow from the ventricles becomes slow, which increases the risk of developing a 'blood clot', see Figure 1.40. If the clot is pumped out of the heart, it could travel to the brain and increases the risk of stroke [122].

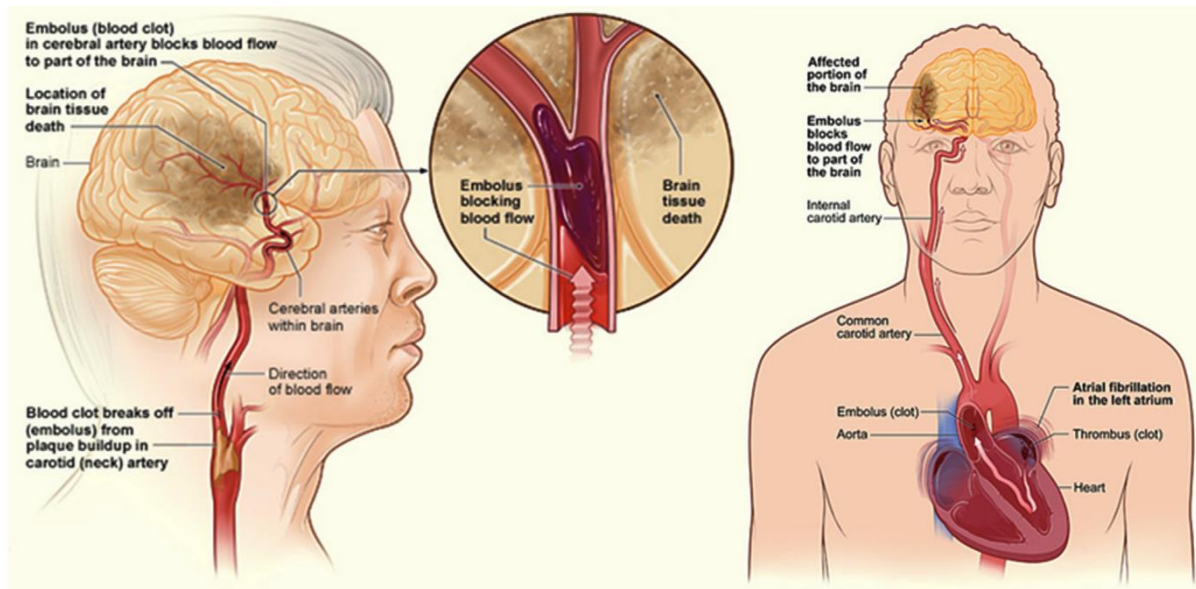


**Figure 1.40:** Mechanisms of stroke in atrial fibrillation, showing the clot formation resulting from blood stasis in the poorly contracting left atrial during atrial fibrillation episodes [122].

## **Chapter 2**

# **Research Ethics and ECG Recordings**

## Chapter 2. Research Ethics and ECG Recordings

### 2.1. Introduction

This chapter outlines the research ethical considerations and the ethical approvals obtained, then describes the ECG databases that were used to conduct the research studies in the thesis.

Three databases were utilised to accomplish the research. The first database includes historical data for long duration AF recordings. The second database contains recordings for which both AF and SR in the same patients were available. The third database contains recordings that were recorded in healthy subjects both before and after treadmill exercise. Table 2.1 summarises the databases and lists the studies within this thesis to which they contribute. The full details of the databases are described in section 2.3.

**Table 2.1.** Summary of the ECG databases

Database name	Long duration AF database	AF/SR database				SR exercise database	
Feature		PhysioNet recordings		Locally acquired recordings		Pre-exercise	Post-exercise
		AF	SR	AF	SR		
No. of subjects	10	14		11		20	
Length (minutes)	15	5	30	4		0.5	6
Sampling rate (Hz)	500	128		1953		500	
Resolution ( $\mu\text{V}$ )	5	-		-		4.9	
No. of leads	12 leads	2 leads		V4		12 leads	
Data used in	<ul style="list-style-type: none"> <li>▪ Chapter 3</li> <li>▪ Chapter 4</li> <li>▪ Chapter 5</li> </ul>	Chapter 4		Chapter 4		Chapter 5	

## **2.2. Research Ethics**

Medical ethics are the moral principles and practices that control the conduct of the physicians and researchers in the treatment of patients [123]. They help to govern the difference between acceptable and unacceptable behaviours and avoid misconduct during the research. The ethical considerations and standardisation are very important in any research because they prevent against the fabrication or falsification of data and hence, promote the knowledge which represent the main objective of research [124,125].

Ethical behaviour is critical for cooperative work and investigations because it enhances an environment of trust, responsibility, and mutual respect among researchers. This is particularly significant when considering issues related to data-sharing, authorship, copyright strategies, confidentiality, and many other issues [124,125].

It is essential to adhere to ethical standards in order for the public and scientific committees to support and believe in the research and to be assured that researchers in their works and investigations followed the guidelines for issues such as human rights, animal welfare, compliance with the law, conflicts of interest, safety, and health standards [123-125]. The ethical issues critically impact the integrity of the research project and investigations [125,126].

The PhD research including all the investigated studies and publications [127] is compliant with all ethical standards and adheres to the ethical requirements of the research [127-129]. The ethical approval for the PhD study and uses of existing recordings was by the Faculty of Science and Engineering. The research approvals are provided in appendix A.

## **2.3. Descriptions of the ECG Databases**

### **2.3.1. Long Duration AF Database**

These recordings were 12 lead ECGs for 10 patients in AF. The recordings are 15 minutes in length. The database was recorded with a sampling rate of 500 Hz and amplitude resolution of 5  $\mu$ V. The recordings were used before in a preliminary study [54].

It has been used mainly in the following analysis and studies:

- i)** Development of techniques which enable the measurement of ventricular repolarisation features in the ECGs of patients with atrial fibrillation (Chapter 3).
- ii)** Validation of automatic measurements for ventricular repolarisation features against manual measurements (Chapter 4).
- iii)** The number of beats required to remove the AF activity to allow effective measurement of the U wave in AF (Chapter 4).
- iv)** The effect of beat interval on the ventricular repolarisation features (Chapter 5).

### 2.3.2. AF/SR Database

This database contains recordings from the same patient in both AF and SR, allowing the comparison of ventricular repolarisation features in both rhythms. Recordings from two sources are in this database.

#### 2.3.2.1. PhysioNet Recordings

The PAF database recordings were openly available from the PAF Prediction Challenge database from PhysioNet [130].

The database contains recordings from 25 patients for which both AF and SR recordings in the same patient were available. Recording duration for AF and SR were 5 and 30 minutes respectively; the recordings had a sampling rate of 128 Hz.

From the recordings of 25 patients, only 14 were suitable for use in this research. 11 recordings from the database had poor quality ECG signals with strong baseline wander and unrecognisable AF characteristics (e.g. no obvious rapid heartbeat changes) so were not used. The recordings are from two unspecified leads, named as  $E_1$  and  $E_2$ . As the reason for using these recordings is to investigate U wave and ventricular features, the lead with the most prominent U wave was analysed.

Table 2.2 summarises the 14 PhysioNet subjects that has been processed, and which ECG channel has analysed in accordance with U wave presence.

**Table 2.2.** Summary of 14 PhysioNet subjects, shows the analysed ECG channels.

Subject	PhysioNet Record	Lead analysed
<b>1</b>	P02	$E_2$
<b>2</b>	P06	$E_2$
<b>3</b>	P08	$E_2$
<b>4</b>	P10	$E_1$
<b>5</b>	P14	$E_1$
<b>6</b>	P20	$E_1$
<b>7</b>	P24	$E_2$
<b>8</b>	P30	$E_1$
<b>9</b>	P32	$E_1$
<b>10</b>	P34	$E_2$
<b>11</b>	P38	$E_2$
<b>12</b>	P40	$E_1$
<b>13</b>	P48	$E_1$
<b>14</b>	P50	$E_2$

### **2.3.2.2. Local Hospital Acquired Recordings**

Similar to the PAF database described above (section 2.3.2.1), these recordings had both AF and SR for the same patient but were standard 12-lead ECG and were acquired specifically for this PhD study during routine electrophysiological studies at Castle Hill Hospital, Kingston upon Hull.

The recording duration for AF or SR was 4 minutes with sampling rate of 1953Hz. Lead V4 was used as part of the data analysed in study 4.3 of Chapter four.

### **2.3.3. SR Exercise Recordings**

These recordings were 12-lead ECGs from 20 healthy subjects previously acquired for other research studies [131]. For each subject there were pre-exercise recordings at rest and during post-exercise recovery after a treadmill exercise to age-adjusted maximum heart rate [131]. The sampling rate was 500 Hz, and amplitude resolution was  $4.9 \mu\text{V}$ . The pre and post-exercise recording durations were 30 and 360 seconds respectively.

This database was used in the investigation ‘The effect of heart rate changes due to exercise on U and T waves amplitudes in healthy subjects’ for which full study details can be found in Chapter five.

## **Chapter 3**

### **Development of Techniques which Enable the Measurement of Ventricular Repolarisation Features in the ECGs of Patients with Atrial Fibrillation**

## **Chapter 3. Development of Techniques which Enable the Measurement of Ventricular Repolarisation Features in the ECGs of Patients with Atrial Fibrillation**

### **3.1. Introduction**

This chapter investigates the cleaning atrial fibrillation (AF) ECG recordings by examining three different techniques and evaluating their abilities to remove the atrial fibrillatory waves that contaminate the ECG signal.

The chapter initially presents three techniques separately, i) principal component analysis (PCA), ii) independent component analysis (ICA), and iii) beat averaging (BA) as potential processing tools to remove the atrial fibrillatory waves. This is followed by a comparison study for the performance of these three techniques to reveal the ventricular repolarisation features in AF recordings.

The aim of this study is to establish an algorithm capable of cleaning AF recordings of atrial fibrillatory waves that contaminate the ECG signals. Removing the atrial activity would offer the opportunity to accurately measure the ventricular repolarisation features such as T waves, and particularly the most challenging feature the U wave, which is almost always undetectable in the ECGs of AF patients.

## 3.2. Candidate Techniques

The ECG signal in patients with AF is contaminated by the atrial activity which makes it impossible to observe the U wave as it is masked by the atrial fibrillatory waves [1,53,132]. T waves are also affected by the presence of atrial activity. Figure 3.1 presents an example of ECG signal with AF activity in which it is impossible to recognise the U wave.

The conventional filtering schemes, such as low and high pass filters [133,134], to filter the ECG recordings have the potential to change the ECG frequencies or shift the phase of the low amplitude components [135,136]. Since this study requires unadulterated observations of ventricular repolarisation features, particularly the U wave in AF, such filtering techniques are to be avoided as they could obscure the signal or distort its features. Therefore, it was necessary to find alternative schemes to clean noise from AF recordings including the atrial activity without deforming the ECG signal.

The techniques *principal component analysis* (PCA) and *independent component analysis* (ICA) are famous statistical techniques universally known as blind source separation (BSS) methods [137-141]. Both techniques are commonly used for signal and noise separation [137-141]. These two techniques employ the signal data representation in a statistical domain rather than time or frequency domain, so the data are projected onto a new set of axes where they are presumed orthogonal (according to PCA) or independent (according to ICA) [137,138]. Orthogonality of two vectors implies a lack of dependence. This lack of dependence, in turn, implies a lack of correlation [142]. Any projection onto an alternative combination of axes is fundamentally a method for data separation into separate components (or sources). This helps to view clearly a significant structure in a specific projection, and that helps to increase the signal to noise ratio for a particular signal source and can produce effective filtering to the desired signal [138,141]. Hence, PCA and ICA techniques attempt to find a combination of axes which are independent from each other and contain the desired properties of the signal.

In medical research, the PCA technique is widely used for different ECG analyses, such as, feature extraction, noise reduction, beat detection and classification, and source separation [139,144,145]. Recently, the PCA technique has become an important tool in ECG processing where it is used as a ‘source separator’ during atrial fibrillation to separate the activities, ‘atrial activity’ and ‘ventricular activity’, and both activities can be characterised and studied with reduced noise interference [133,136]. Such separation is based on the assumption that the atrial and ventricular activities originated from two different bioelectrical sources [133,136,138] but they are overlapped in time and frequency during AF episodes [133,136,139]. Several PCA algorithms have been demonstrated to separate atrial and ventricular components of the ECG in atrial fibrillation (AF) [160]. These algorithms fall into two categories: those which exploit the dissociation between the atrial and ventricular components, and those which exploit the concept that the AV activities are generated from different bioelectric sources [160]. The authors in [159] used the PCA method to separate the atrial and ventricular activities in AF recordings. Their aim was to retrieve the information about the atrial rhythm non-invasively from the body ECG and investigate the stability of this arrhythmia. In their experiment, they have used 12

lead ECG recordings of AF subjects. They stated that the PCA reduces the number of variables when the variables are correlated.

It is reasonable to use 12 leads ECG in the PCA processing. The PCA lends itself to 12-lead ECG analysis since all electrodes measure the same source of electrical activity (the heart) and leads are correlated [145]. Additionally, in [159] the PCA was applied to each of the 12-lead data to derive 12 orthogonal data components. Each principal component describes a proportion of the variability in the 12-lead ECG [159]. Principal component 1 describes the greatest proportion and principal component 12 the least. The authors effectively extract different features of the ECG and assigns them to specific principal components dependent upon their relative dominance across the 12-lead signals.

Also, the PCA algorithm was proposed in [158] as a method to analyse beat to beat changes of the ECG features. Their PCA algorithm showed the ability to track beat to beat changes in different ECG features. However, their work used to extract the respiration activity from the ECG recordings.

Similarly, independent component analysis (ICA), is a BSS method [138,140-143], used extensively in medical research [138,141,143]. The technique has a major contribution to electroencephalography (EEG) and magnetoencephalography (MEG) studies [131]. Furthermore, the technique is also used widely with ECG applications, such as the fetal ECG extraction from the maternal recordings [144], separating breathing artefacts from the ECG, and recently used to extract the atrial activity from the atrial fibrillation recordings [145,146].

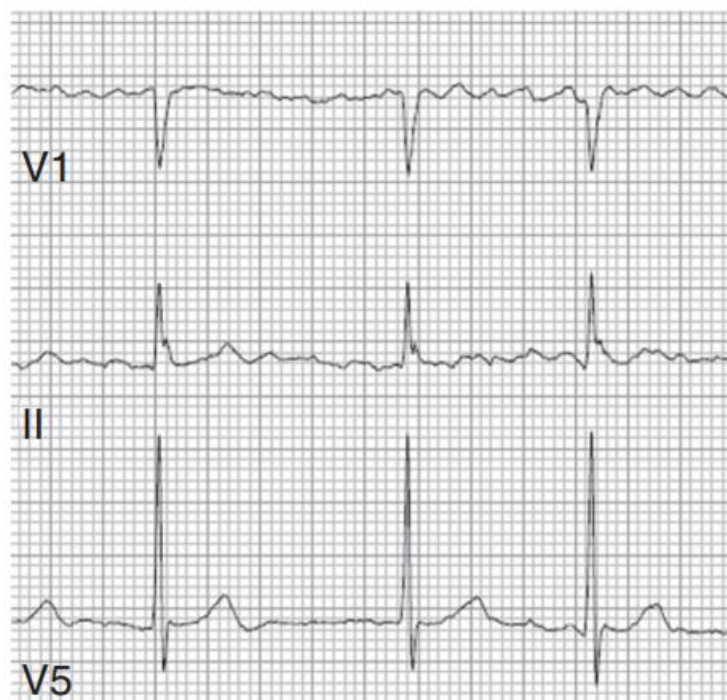


**Figure 3.1:** Example of ECG signal with atrial fibrillation for leads V1,II and V5. P waves are absent and replaced by irregular electrical activity, the ventricular rate is irregular. U wave is impossible to recognise, and T wave is affected by the atrial fibrillatory waves [143].

The ICA algorithm was firstly developed in 1984 [147], but it remained relatively unused until 1994 when the algorithm was introduced with a new concept [140] and became universally well-recognised. The ICA method is considered to be an extension of the PCA technique [139,140]. The PCA uses *variance* to determine the axes and adjusts the covariance matrix of the datasets leading to a set of the orthogonal axes which represents the second order statistics where the data are decorrelated (i.e. the covariance matrix is diagonalised). ICA uses higher order statistics known as *kurtosis* (kurtosis is the fourth moment; mean, variance and skewness are the first three statistical moments) [139,140,145]. It is based on the non-Gaussianity without the necessity of orthogonal axes. The PCA finds uncorrelated components (principal components ‘PCs’) whilst ICA technique finds the independent components (ICs) [139,140].

The ICA algorithm, similar to PCA, has been proposed as a potential technique to separate the wanted ventricular activity from undesirable atrial fibrillatory waves during the AF episodes [139]. Several ICA techniques have been proposed mainly based on higher order statistics HOS (the fourth order cumulant or *kurtosis*) due to their ability to measure statistical independence [145,161]. For instance, FastICA [141,148,149], JADE ICA [150], and infomax [151]. In the current investigation, the ‘FastICA’ algorithm has been applied to AF recordings to separate the two overlapped activities. The algorithm was chosen due to its performance and fast convergence in previous studies [141,148,149].

Rieta et al [145] extracted the atrial activity (AA) of AF recordings using ICA method. The authors argued that AA and ventricular activity (VA) are generated by independent sources of bioelectric activity. This activity exhibits non-Gaussian character [145]. In their experiment, the ICA method is applied to real recordings (12 leads) obtained from patients suffering from AF.

Furthermore, Castells et al [162,163] and Rieta et al [164], described the statistical characteristics of AA and VA sources in AF, and presented the ICA as a suitable separation method that separates them to study AA. They described that VA sources are the ECG components with highest amplitudes. These components have high amplitude during ventricular depolarisation and repolarisation (QRS complex and T wave respectively). However, the rest of the time, they have low values close to zero due to the non-activity period of the ventricular cells. Thus, VA sources are described as a super-Gaussian signal. In AF episodes, AA consists of small and continuous wavelets and considered as a random variable with a pdf described as a sub-Gaussian signal [164].

In the section 1.5.2.2. of Chapter one, the AF mechanisms were explained during the cardiac cycles compared to the normal cycle of healthy heart. This uncoordinated operation of AA and VA during an AF episode makes it reasonable to regard both activities as physically independent and, in turn, as generated by statistically independent sources of cardio-electric activity [145].

Therefore, in our research, we proposed the two techniques of blind source separation: PCA and ICA to separate the desired ventricular activity from the unwanted atrial activity. The two techniques were proposed to clean AF and track the ventricular characteristics changes beat by beat. Regarding the ECG baseline wander, in [161,165] the ECG signal was denoised through the fast ICA with multiple adjustments to improve the baseline drift estimation of ICA algorithm.

The third potential technique to clean AF recordings is the *beat averaging algorithm* (BA). Signal averaging is widely used to reduce noise from the signal without deforming the waveforms. It increases the signal to noise ratio which facilitates the detection of the low amplitude bioelectric potentials [133,152,153]. The technique was originally used for extracting the encephalographic signals (EEG) from noise [136,154]. The studies of Scherlag et al were a milestone in electrocardiography, where they used the technique with ECG to separate, non-invasively, atrial and His-bundle activity, and later for ventricular late potential [154-53]. Over time, the technique was developed and used for differentiating the maternal from fetal ECG, and separate ECG signal from movement artefacts during exercise [154].

In fact, the signal averaging method has been used widely to separate repetitive epochs of signal from uncorrelated noise [25,133]. However, the processing required the following conditions i) the desired signal to be repetitive and invariable, therefore any premature or ectopic beats should be removed before the process, ii) the desired signal should be aligned to a timing reference point (fiducial) such as the peak of the QRS complex in the ECG signal since it meets the condition and easily detectable, and iii) the wanted signal and the noise must be uncorrelated and remain independent during the averaging [1,25,133].

In the current investigation, the beat averaging algorithm (BA) developed uses the signal averaging concept, where, i) the fixed length window relative to fiducial point, ii) the timing reference, fiducial, is identified as the R wave, and iii) the unwanted atrial fibrillatory waves and other types of unwanted components ‘noise’ such as electromagnetic interference (EMI) and power line artefacts are assumed to be uncorrelated with R-R intervals.

The BA algorithm was utilised to generate an average ventricular beat free from the atrial activity as well as the noise. By averaging fixed length windows of ventricular beats after aligning them carefully to their R wave peaks (time reference), the amplitude of uncorrelated noise is decreased and averaged out while the desired ventricular signal is recovered without noise in the resulting average beat. In theory, the reduction of noise level, depends on the number of the averaged signal epochs ( $N$ ), where it can be reduced by the factor of  $\sqrt{N}$  [133]. Therefore, the quality of the averaged beat depends upon the number of beats that are used to generate it [1,136,152].

Finally, the aim of this chapter is to find, from the potential candidate techniques above, which are capable of cleaning the AF recordings of the atrial fibrillatory activity to enable the accurate detection and measurement of ventricular repolarisation features. The three techniques PCA, ICA, and BA have been examined in the following sections to discover their capabilities to

fulfil the aim of the study. The most challenging ventricular repolarisation feature is the U wave since it is impossible to measure it during AF, the focus from hereon is on how well each of the proposed techniques are able to reveal the U wave in AF.

### 3.2.1. Principal Component Analysis

Principal component analysis (PCA) has the potential to clean the AF recordings by separating the atrial and ventricular activities of the ECG signals. The following section explains the PCA statistical approach as an ECG separation tool and the algorithm concept.

#### 3.2.1.1. PCA Basic Model

Principal component analysis (PCA) is a statistical multivariate method. It is used to reduce the dimensionality of a vector of random variables, to describe the total variation with fewer orthogonal combinations of the original variables. The purpose is to find a smaller set of variables with less redundancy that would give as good a representation as possible. The redundancy is measured by correlations between variables. The new orthogonal combinations of variables are found by diagonalising the second order statistics (*covariance*) of the original data [157].

Consider a set of random variables  $\{X_i, i = 1, \dots, N\}$ . In this thesis, random variables are usually ECG samples from a specific time from different channels. The covariance matrix  $\Sigma$  of this set of variables is given by:

$$\Sigma_{ij} = E[(X_i - \bar{X}_i)(X_j - \bar{X}_j)^*]$$

where  $E[\ ]$  is the expected value,  $\bar{X}_i = E[X_i]$  and \* denotes complex conjugate. The covariance matrix is often estimated from measured data. Let  $\mathbf{D} \in R^{N \times M}$  be a matrix with columns being  $M$  samples of a  $N$ -vector of zero-mean random variables. The covariance matrix may be estimated by:

$$\Sigma \approx \frac{1}{M} \mathbf{D} \mathbf{D}^t$$

The singular value decomposition of  $\mathbf{D}$  yields:  $\mathbf{D} = \mathbf{U} \mathbf{\Lambda} \mathbf{V}^t$  where  $\mathbf{U}$  and  $\mathbf{V}$  are orthonormal matrices and  $\mathbf{\Lambda}$  is a diagonal matrix of singular values. Consequently:

$$M \Sigma = \mathbf{U} \mathbf{\Lambda} \mathbf{V}^t (\mathbf{U} \mathbf{\Lambda} \mathbf{V}^t)^t = \mathbf{U} \mathbf{\Lambda} \mathbf{V}^t \mathbf{V} \mathbf{\Lambda} \mathbf{U}^t = \mathbf{U} \mathbf{\Lambda}^2 \mathbf{U}^t \quad (1)$$

where  $\mathbf{U}$  is a matrix whose columns are eigenvectors and  $\mathbf{\Lambda}^2$  is a diagonal matrix of eigenvalues. When  $\mathbf{\Sigma}$  is a covariance matrix then the eigenvectors and eigenvalues are known as principal components and principal variances respectively.

PCA can be applied to multi-channel ECG recordings in an attempt to separate components of the signals exhibiting different correlations. Each ECG (differential) channel is treated as a random variable. Electrical processes in the heart are measured simultaneously on all electrodes but after distortion/filtering due to the position of the electrodes and intervening tissue. Atrial activity produces larger amplitude signals on electrodes near the top of the heart while ventricle activity is larger below the heart. Noise processes often produce uncorrelated signals on all channels. This suggests that different processes would have different correlation patterns across channels, and could possibly be separated by PCA. In particular, intermittent processes, like AF, will have quite low correlations as they occur for small proportions of the time. SR patterns, with high amplitude QRS waves, are highly correlated across channels.

The following sections (3.2.1.2 and 3.2.1.3) present the implementation of the PCA algorithm and a qualitative assessment of its ability to remove the contaminating fibrillatory wave from AF recordings.

### **3.2.1.2. ECG Processing**

The database used for testing all the proposed techniques (PCA, ICA and BA) was the Long Duration AF Database which contains 12 lead ECGs of 10 atrial fibrillation (AF) patients. The database details were described in section 2.3.1 of Chapter two.

Figure 3.2 demonstrates the source separation methods including PCA and ICA to separate the ECG activities and noise in AF recordings.

In the analysis, PCA was applied to 12 lead ECGs to derive 12 orthogonal data components (principal components,  $PC_1$  to  $PC_{12}$ ) as Figure 3.3 illustrates, where each principal component (PC) describes a combination of the variability in the 12 leads ECG.

For each recording, the filtered 12 differential ECG channels were used to calculate the covariance and hence the principal component decomposition. The reconstructed signals (RS) were then calculated from a linear combination of PCs with weights that passed the first three PCs and tapered down to zero over PCs 4 to 9. The aim was to remove or reduce low correlation signals as these are likely to be dominated by noise and intermittent AF processes. At the same time passing high correlation signals dominated by strong ventricular activity and SR signals that occur in the majority of beats. The filter cut-off and taper were chosen by visual inspection of the explained covariance. The reconstructed 12 lead ECGs were assessed by the ability of an expert to identify U-wave activity.

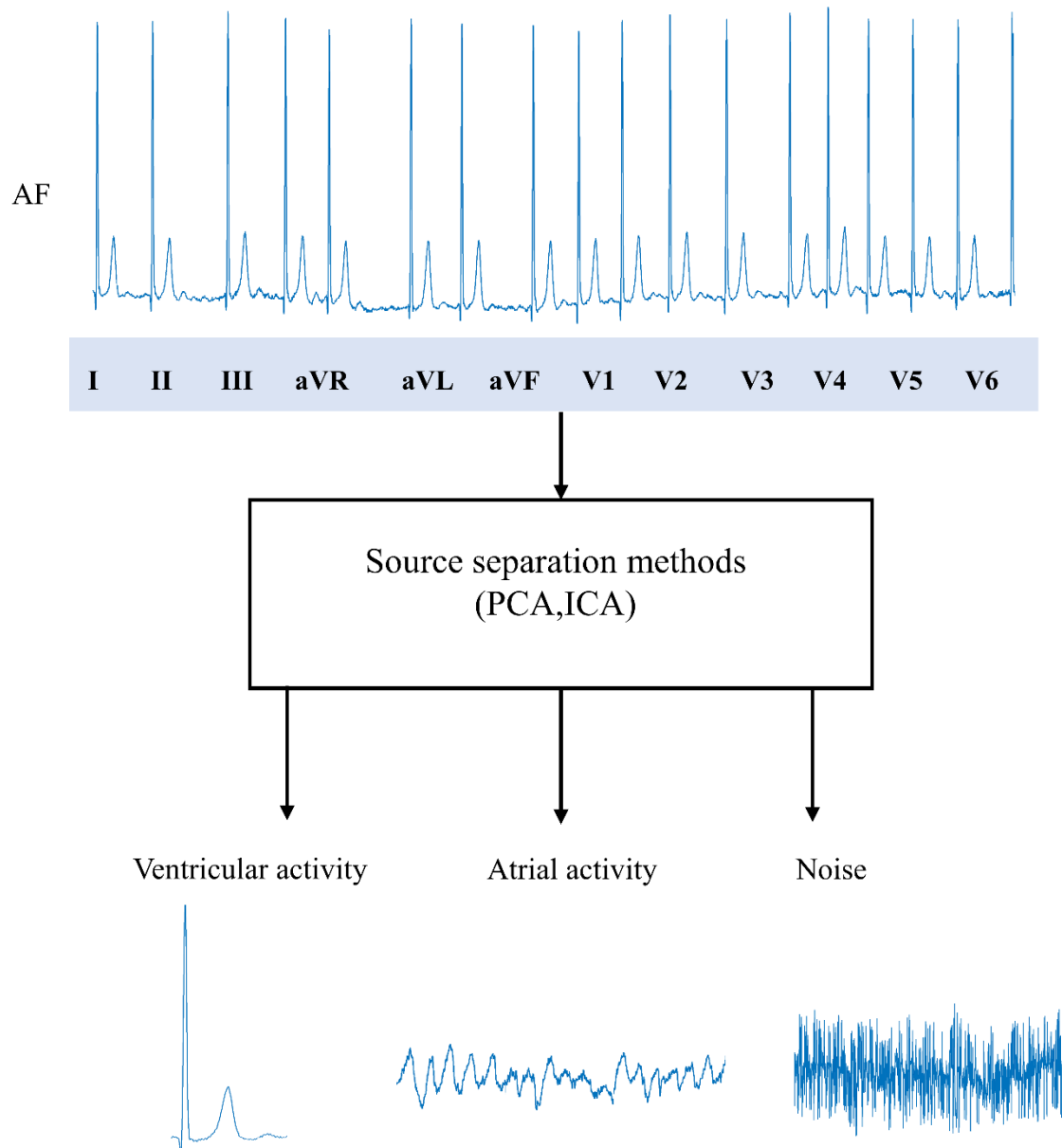


**Figure 3.2:** An illustration for source separation method including the principal component analysis (PCA) and independent component analysis (ICA). The source separation method applied to 12 leads to separate the ventricular activity, the atrial activity and reduce the noise from AF recordings.

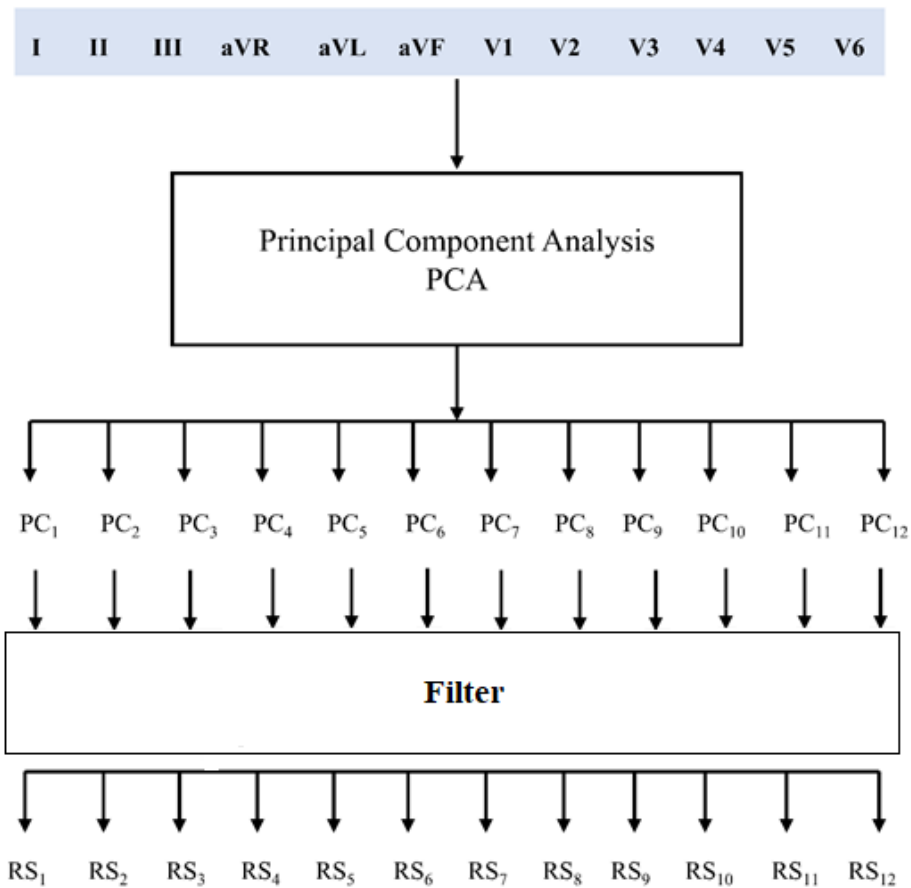


**Figure 3.3:** Illustration for the method workflow using the PCA processing. For each recording, 12 leads  $\{I, \dots, V6\}$  were input to PCA algorithm. 12 principal components  $\{PC_1, \dots, PC_{12}\}$  were derived from the 12 leads during the processing. The principal components are ordered according to the explained variance. A linear combination of principal components were used for the ECG reconstruction to establish 12 reconstructed signals  $\{RS_1$  to  $RS_{12}\}$ .

### 3.2.1.3. Implementation Examples

Figure 3.4 illustrates an example of a 12 lead ECG for one of the AF recordings used in the study. The signals have been band-pass filtered to remove baseline wander and high frequency non-heart signals. This is essential to estimate the covariance matrix as otherwise covariance is dominated by baseline wander. Each subplot shows a 3-second segment of ECG in AF where atrial fibrillatory waves spread through the signal and the U wave is obscured by the atrial activity. It is difficult to distinguish whether or not there is a U wave.

Figure 3.5 shows 12 principal components ( $PC_1$  to  $PC_{12}$ ) derived from the 12 lead ECGs presented in Figure 3.4. Note that the PCA components are zero-mean, unit norm, and mutually orthogonal (orthonormal), consistent with equation (1). The components with the largest contribution to covariance put highest weights on the high number channels where the ventricle signal is strongest. These weights can change sign between channels as differential

measurements can have the QRS complex peaking positive or negative. The PCA analysis is not changed by multiplying a component by -1, and so the polarity of these changes is not important. The higher-order components become more random and are largely determined by noise.

Each subplot in Figure 3.6 presents the principal component weight (or score) for each sample time. The measured signals can be reconstructed by summing the principal components ( $PC_1$  to  $PC_{12}$ ) after weighting with each component score. The PCA components are normalised and so dimensionless, while the scores have units of mV. For the high-order components, both the components and scores become random. Note that the scores are associated with PCA components and not channels, and so are not associated with a physical electrode location.

Figure 3.7 illustrates the variance of each principal component. There is a large step between components 8 and 9, with the last four components describing random noise at the third significant figure in the ECG data. These components can be removed without distorting the heart signal and increasing the signal-to noise ratio (*SNR*). The first 8 components decline rapidly, approximately as component number to the power of -4. These observations suggest the filter weights of zero for components 9 to 12, weights of 1 for the first 3 components reducing smoothly to zero by component 9. The smooth transition of weights greatly reduces Gibbs ringing in the PCA filtered traces.

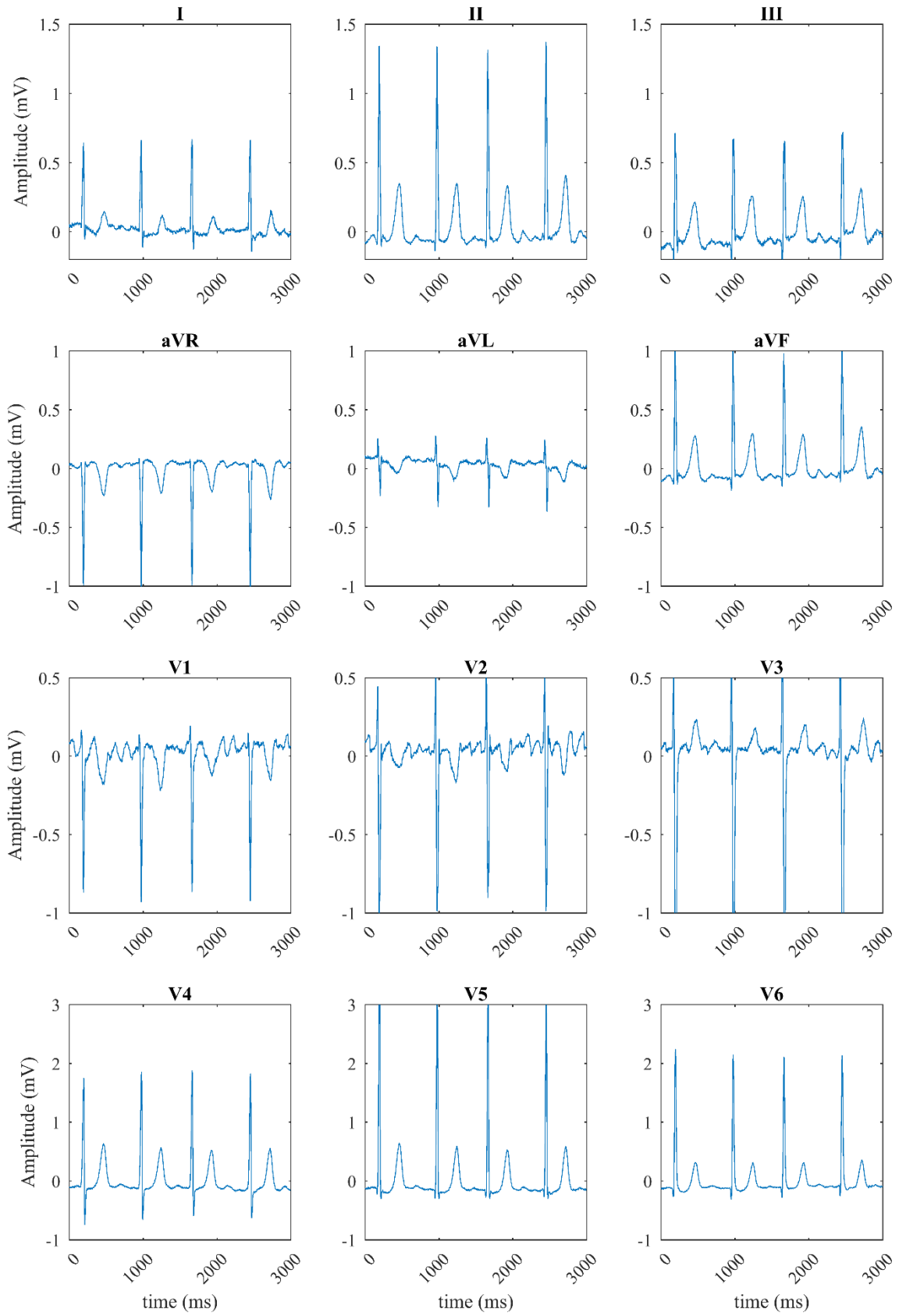
The 12 reconstructed ECG signals (reconstructed leads) are presented in Figure 3.8. Each subplot represents a 3-second interval of the reconstructed differential channel that corresponds to the original leads (presented in Figure 3.4). The observation for the reconstructed ECG signals showed clearly that atrial activity and noise was reduced in most of beats. However, not all the beats were ‘fully’ clean from the unwanted atrial activity. In fact, there were still residual fibrillatory waves covering a considerable number of the reconstructed beats, hence, masking U wave.

Figure 3.9 displays an example to compare few beats for one of the AF recordings (lead I), compared to the same beats after the reconstruction process. Figure 3.9-a displays a 4 second interval of ECG in AF, where the 4 beats show clearly the atrial fibrillatory waves and the difficulty discerning U waves, while Figure 3.9-b displays the corresponding reconstructed beats where generally the noise has been reduced, and AF activity reduced. In Figure 3.9-b the reconstructed beats 1, and 2 showed less noise than beats 3 and 4, and most likely, U waves were visible in both despite of the residual noise. While in beats 3 and 4, the noise level has been reduced but the atrial activity remaining after reconstruction, obscures the beat, covered underneath the U wave, and decreases the ability to detect the U wave.

Since the atrial activity has not ‘fully’ removed, the clarity of the reconstructed beats is poor, hence U wave detection becomes difficult and uncertain. The U waves were visible and discernible in a large number of beats despite of the small level of noise contamination; however, this level of noise can affect the accuracy of the U wave measurement and hence the clinical implication.

The results have demonstrated that PCA technique was able to reduce the atrial activity and the noise in the AF recordings and reduce their propagation among the ECG beats. The technique has partially separated the desired ventricular activity (ventricular beats) of AF recordings as the method suggested, however, the separation was imperfect. This was clear since the fibrillatory waves remained visible for a large number of beats after the reconstruction process, as the example shows (Figure 3.9).

Based on the qualitative visual examination, many ventricular beats were cleared from the atrial activity and had a reduced but variable level of the residual noise. On the other hand, several others had kept the fibrillatory waves and different levels of noise. In section 3.3 a statistical quantitative analysis of the ability of the PCA algorithm to reveal the U wave in comparison to the other techniques (ICA and BA) is presented.



**Figure 3.4:** An example for 12 leads in one AF patient. Each subplot shows 3 seconds strip of ECG in AF where the atrial activity is clear and masking the U wave.

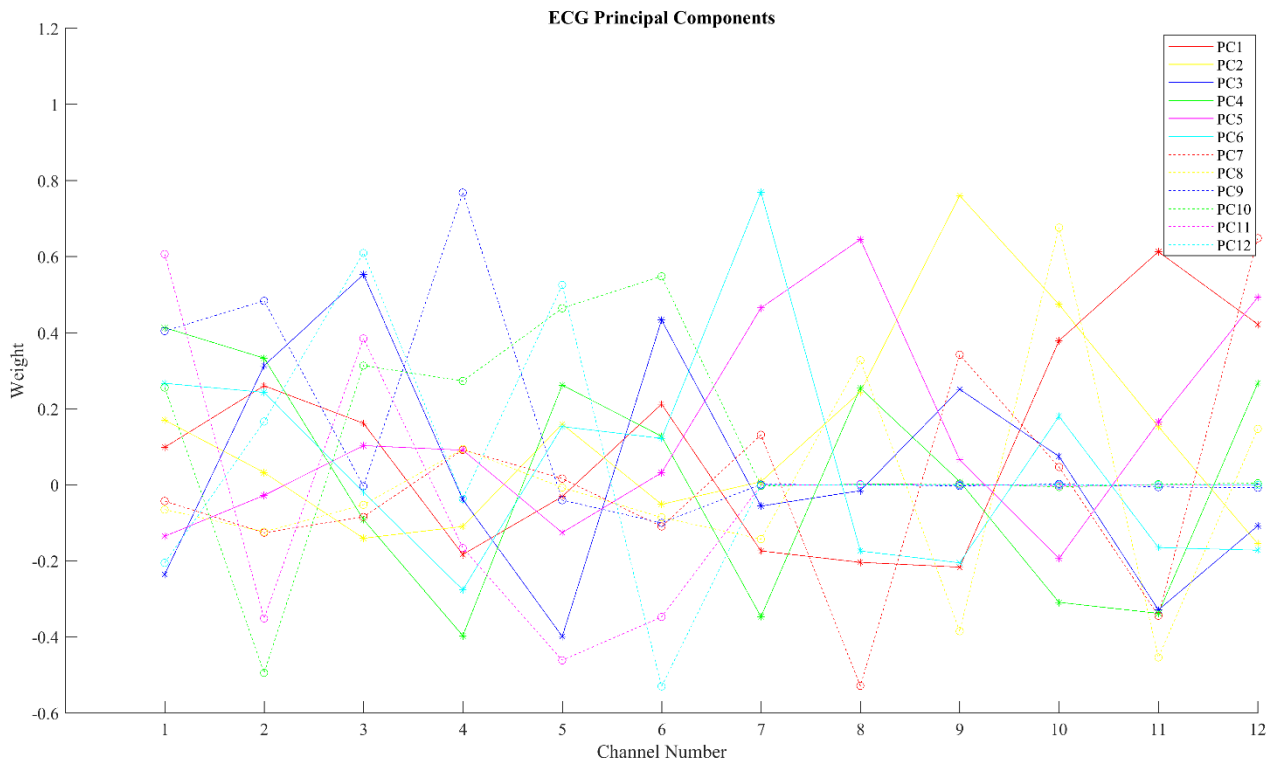


**Figure 3.5:** PCA components.

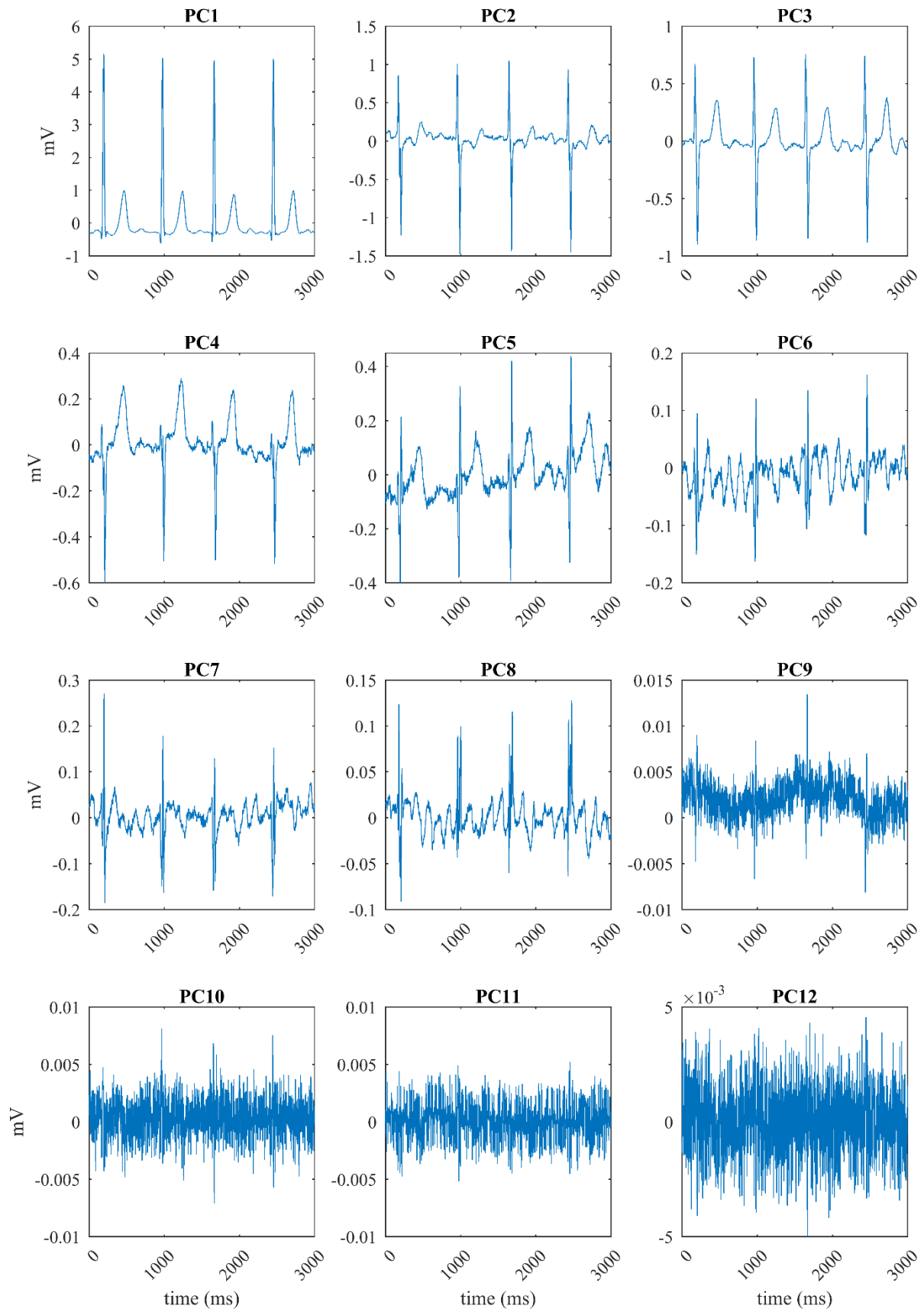


**Figure 3.6:** The weight, or score, time-series of PCA components to reconstruct the measures 12-lead ECG data.

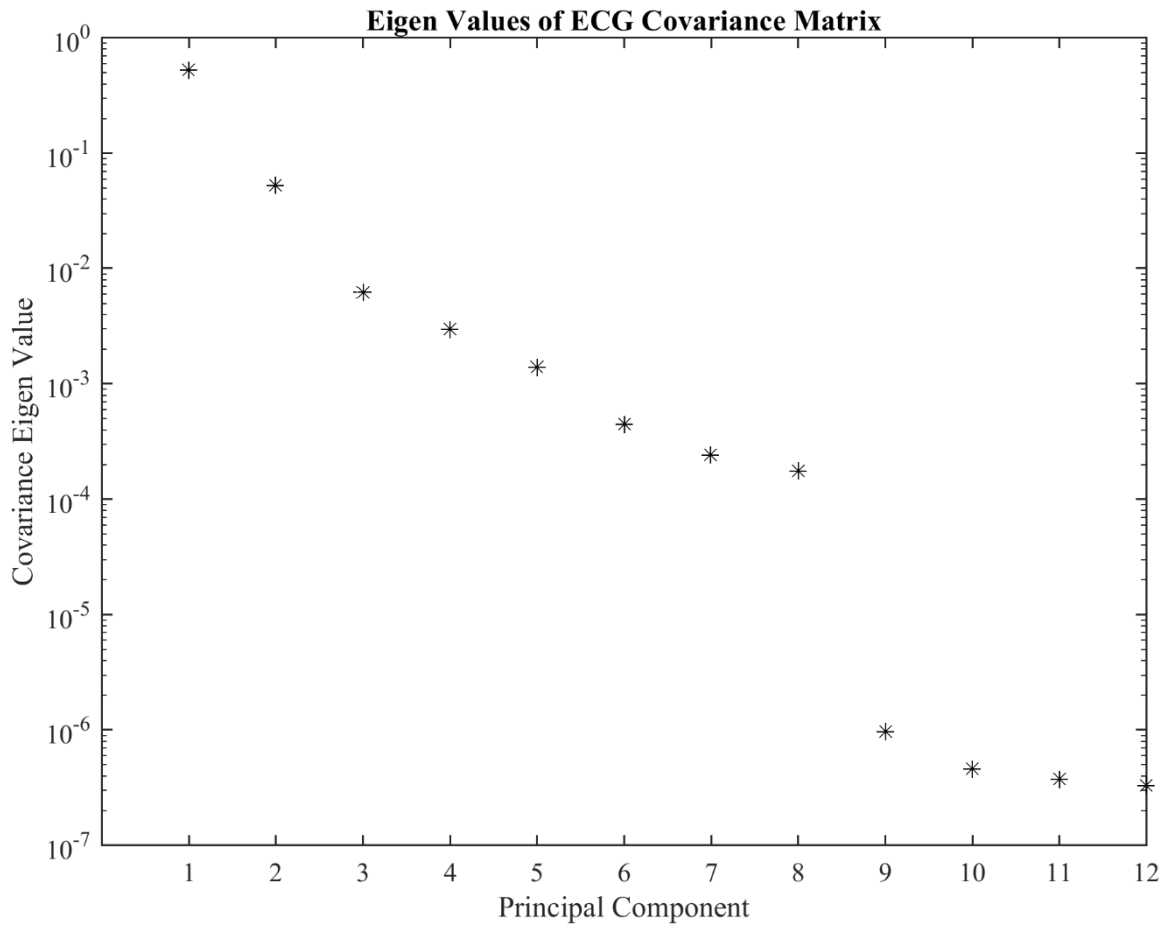


**Figure 3.7:** The Eigenvalues of the ECG covariance matrix describing the amount of the total variance explained by each principle component.

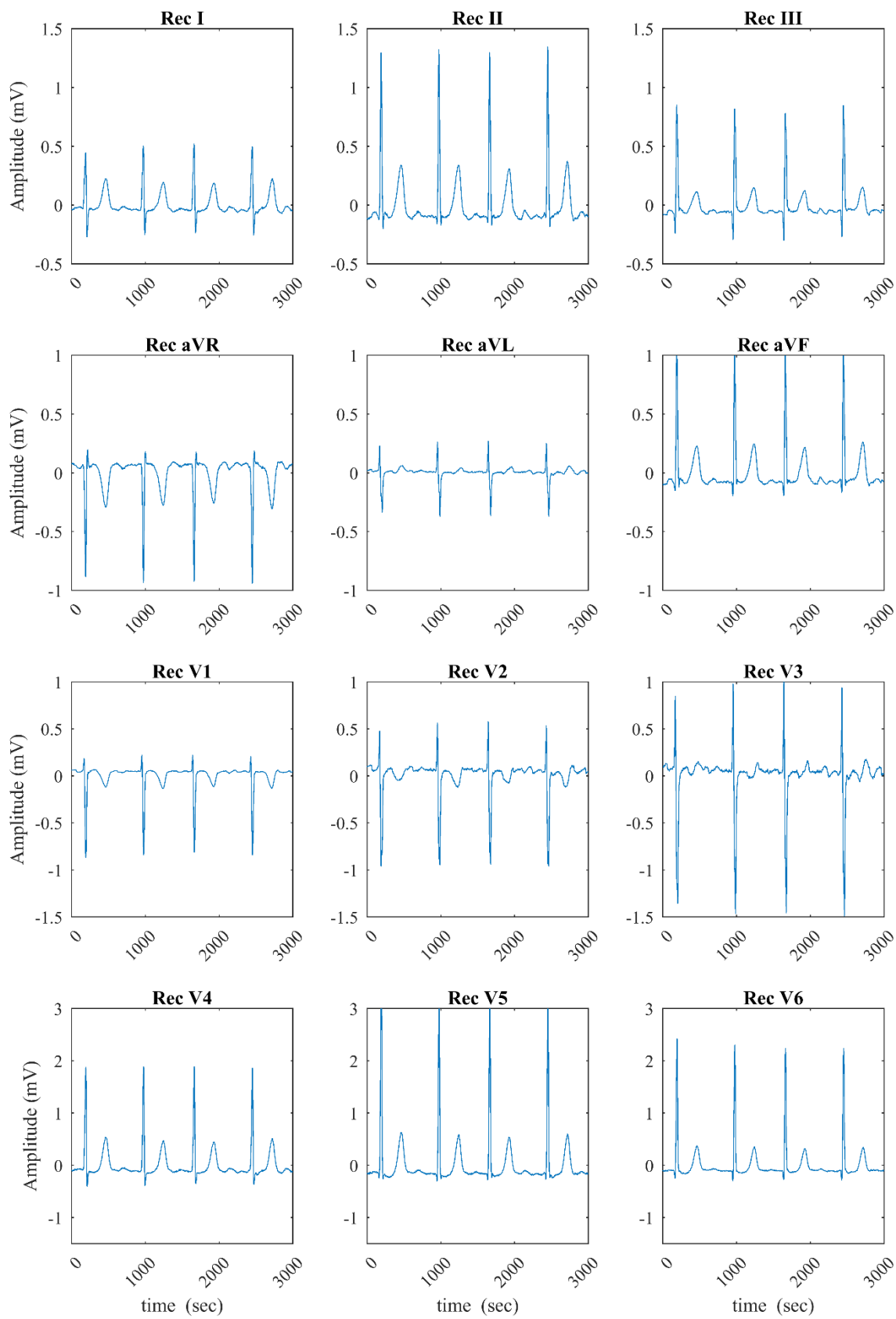


**Figure 3.8:** The 12 reconstructed ECG signals that associated to the 12 lead ECGs for one AF patient. Each subplot shows 3 second intervals of the reconstructed ECG signal corresponding to the leads in Figure 3.4.

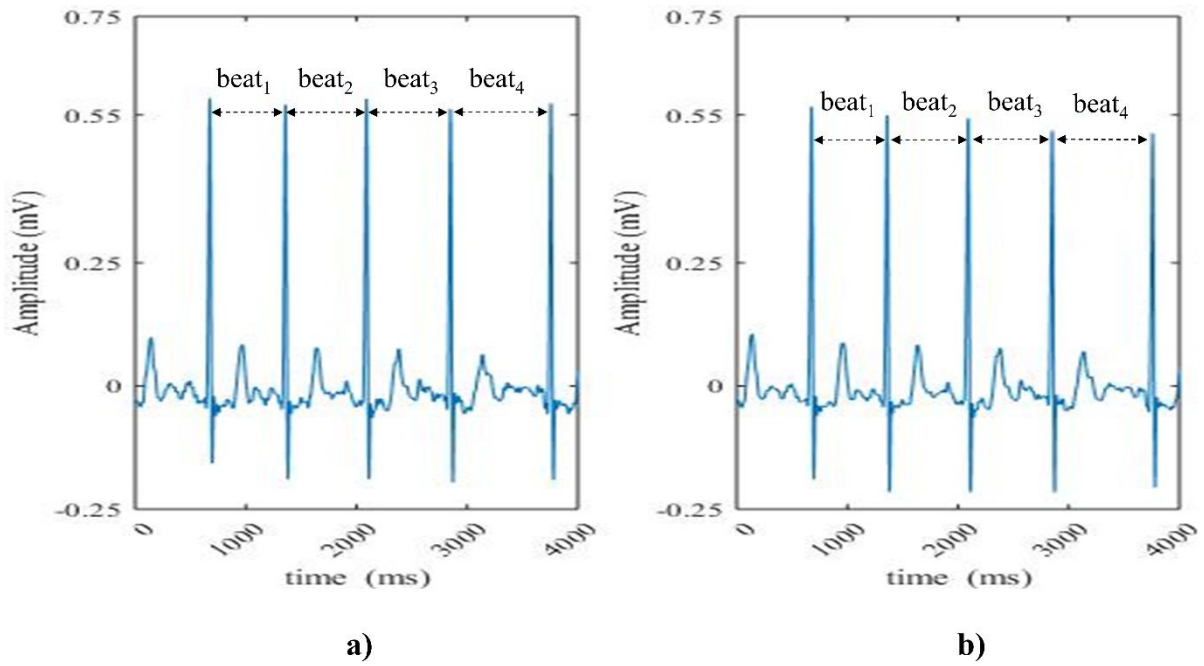


**Figure 3.9:** Comparison example to show the PCA algorithm performance on one AF recording used in the study. **a)** represents a 4 seconds interval including (4 beats) of ECG in AF (lead I) where AF activity is strong, and it is impossible to distinguish the U wave. **b)** the corresponding reconstructed ECG beats where the noise has been reduced, and the atrial activity slightly reduced. In **(b)** the beats 1, 2, the U wave most likely was visible despite the small level of noise, beat 3 showed higher level of noise and glimpse of noisy U wave, and beat 4 showed clear AF activity, hence it is difficult to distinguish U wave.

### 3.2.2. Independent Component Analysis

The following section presents the ICA statistical approach as an ECG separation tool and presents the algorithm concept without the full mathematical details.

#### 3.2.2.1. ICA Basic Model

ICA is a statistical signal processing tool usually used to decompose a set of mixed signals into their components of signals that are mutually statistically independent [143,149,150] by finding the underlying components (factors) from these multidimensional signals [149]. In other words, the ICA tries to find a linear representation for the signals so that the fundamental structure is made more accessible or visible [149,150]. It is worth mentioning that ‘independency’ means the value of one of the components gives no information on the level of the other components [149].

The ICA model forms a linear combination of source signals, [138,143, 149]:

$$\mathbf{x} = \mathbf{A}\mathbf{s}$$

Where  $\mathbf{x}$  represents the mixture of the ‘observable variables’,  $\mathbf{A}$  is the unknown ‘mixing matrix’, and  $\mathbf{s}$  represents the ‘source’ signals. The objective of using ICA is to estimate  $\mathbf{s}$  and  $\mathbf{A}$  from the observation  $\mathbf{x}$  [149]. In order to achieve the source separation process, a linear transformation given by a matrix  $\mathbf{W}$ , so that random variables that are statistically independent can be estimated (i.e. components ), using [138,143,148, 149]:

$$\mathbf{s} = \mathbf{W}\mathbf{x}$$

where matrix  $\mathbf{W}$  is the inverse of the matrix  $\mathbf{A}$ .

As mentioned above, the ICA method aims to estimate source signals  $\mathbf{s}$  that would be as independent as possible, and their linear combinations are the original data. The estimated sources are called ‘components’ (shortly ICs). The components estimation is accomplished by either an iterative algorithm which maximises the metric of independence, or by a non-iterative algorithm which is based on joint diagonalisation of correlation matrices [141].

Interestingly, the ICA method has disadvantage (ambiguity) [140,141]: where the magnitude associated with each component has no order (contrasting the PCA).

In ECG signal processing, the objective of ICA is to obtain the independent component signals that are the original source signals which form the ECG [136,141]. Therefore, in this study, the ICA algorithm is used to decompose the AF ECG signal to extract the desired ventricular activity and separate the unwanted atrial activity from AF recordings, with the goal to be clean enough to investigate ventricular features including U wave.

The ICA requires two main assumptions to make it applicable in the current investigation: **i)** atrial activity and ventricular activity are originated by independent bioelectric sources (atria

and ventricles), and **ii**) the two independent source signals (i.e. activities) are non-Gaussian (non-Gaussianity can be measured by *kurtosis*, the fourth order statistics of the variables) [145].

With respect to the *source independency*; Rieta et al [145] elucidate that during the atrial fibrillation episodes, both activities ‘atrial and ventricular’ are initiated by independent generators (i.e. atria and ventricles) and their amplitude distributions are non-Gaussian [140,145]. Further, regarding the *non-Gaussian behaviour* (statistically), ‘ventricular activity’ shows high amplitude during the heart beats (i.e. QRS complex) compared to low values during the rest of the cardiac cycle, thus the ‘ventricular activity’ revealed a super-Gaussian behaviour, whilst ‘atrial activity’ shows a sub-Gaussian behaviour during the AF episodes [140,145].

The variables that following the Gaussian distribution have zero *kurtosis*. Sub-Gaussian variables (variables whose pdf falls at a slower rate than the Gaussian, for the same variance) have negative *kurtosis*. Super-Gaussian variables (corresponding to pdfs that fall at a faster rate than the Gaussian) have positive *kurtosis* [169].

Thus, if we keep the variance fixed (e.g., for variables normalized to unit variance), maximizing the sum of squared kurtosis, it results in maximizing the non-Gaussianity of the recovered ICs. Usually, the absolute value of the *kurtosis* of the recovered ICs is used as a measure of ranking them. This is important if ICA is used as a feature generation technique [145,169]. Figure 3.10 shows some typical examples of a sub-Gaussian and a super-Gaussian together with the corresponding Gaussian distribution.

The Gaussian distribution is the one that maximizes the entropy under the variance and mean constraints. In other words, it is the most random one, under these constraints, and from this point of view the least informative with respect to the underlying structure of the data. In contrast, distributions that have the least resemblance to the Gaussian are more interesting as they are able to better unveil the structure associated with the data. This observation is at the heart of *projection pursuit*, which is closely related to the ICA family of techniques. The essence of these techniques is to search for directions in the feature space where the data projections are described in terms of non-Gaussian distributions [169].

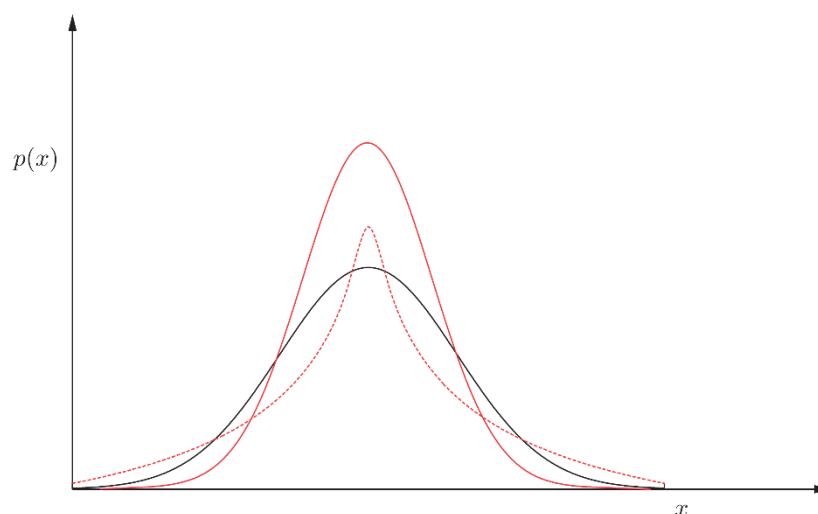


**Figure 3.10:** A Gaussian (full grey line), a super-Gaussian (dotted red line) and a sub-Gaussian (full red line) [169].

### 3.2.2.1.1. FastICA Algorithm

The FastICA algorithm was presented by Hyvarinen and Oja in 2000 [140] employing the ICA method with few modifications based on the target purpose. The algorithm was introduced as a separation tool based on maximising the non-Gaussianity function [140,148,149].

The algorithm is based on the concept of using the ‘central limit theorem’ as a measure of independence, which states “*The distribution of a sum of finite variance independent random variables tends toward a Gaussian distribution*” [170]. In other words, the sum of two independent random variables has a distribution closer to Gaussian than the original two random variables, hence maximising the non-Gaussianity leads to more independent signals [140,141].

Statistically, to find independent sources, the matrix  $\mathbf{W}$  should be de-mixed in the way to maximise the non-Gaussianity of each source.

Notably, the classical way to measure the non-Gaussianity is to use kurtosis [140], which is basically a normalised version of fourth order statistics (moment).

FastICA algorithm has two versions [141] : i) ‘one unit’ algorithm where the algorithm tries to estimate one independent component by maximising the non-Gaussianity, based on a fixed-point iteration scheme, and ii) ‘several units’ algorithm estimates several independent components by using the one-unit algorithm several times.

One of the advantages of the FastICA is that it can estimate both the sub-Gaussian independent components (i.e. atrial activity in AF), and the super-Gaussian independent components (e.g. ventricular activity in AF) [141], a fundamental requirement in the current processing.

Full mathematical details of the FastICA algorithm can be found in [148,149], and a Matlab implementation of the algorithm is available on the internet [171] free of charge and was used in the subsequent implementations.

### 3.2.2.2. ECG Processing

The FastICA algorithm was applied to the 12 leads of the 10 AF recordings to estimate the independent components, resulting in the 12 ICA estimated sources ( $S_1$  to  $S_{12}$ ). Figure 3.2 shows the overview of the separation method using source separation scheme.

To understand the algorithm process based on the basic statistical model, the 12 leads represent the observation matrix  $\mathbf{x}$ . To achieve the separation, the algorithm projects  $\mathbf{x}$  onto orthogonal basis  $\mathbf{W}$  so the estimated sources  $\mathbf{s}$  are maximally independent ( $S_1$  to  $S_{12}$ ), i.e. the independent components. The 12 estimated sources ( $S_1$  to  $S_{12}$ ) were examined visually to decide whether

the algorithm succeeded removing the atrial activity from the AF recordings. Figure 3.11 demonstrates simple illustration for the ICA method employing FastICA algorithm in the analysis.

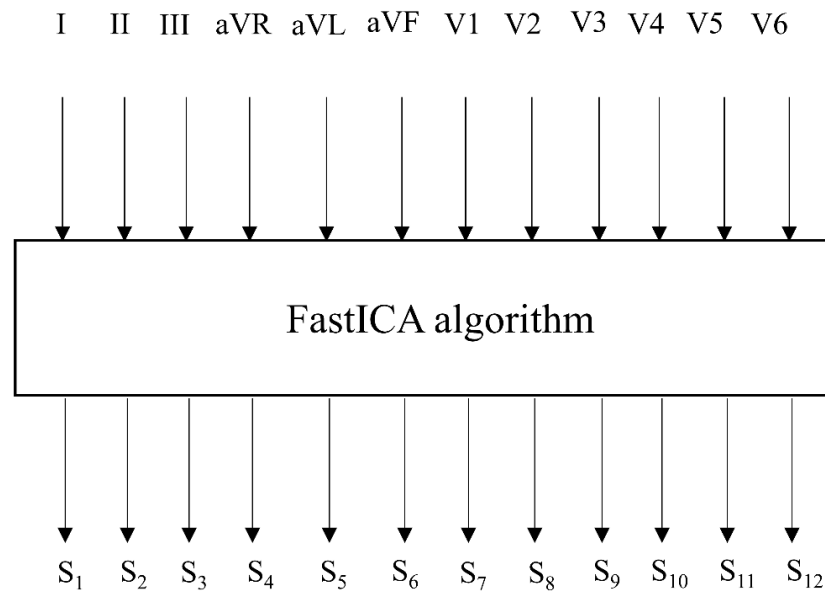


**Figure 3.11:** Simple illustration shows the ICA method using FastICA algorithm. 12 leads ECG applied to the algorithm and the process produces 12 estimated components (sources),  $S_1$  to  $S_{12}$ .

### 3.2.2.3. Implementation Examples

In this section, some implantation examples are presented while a statistical quantitative analysis of the ability of ICA to remove the atrial fibrillatory activity is presented in section 3.3.

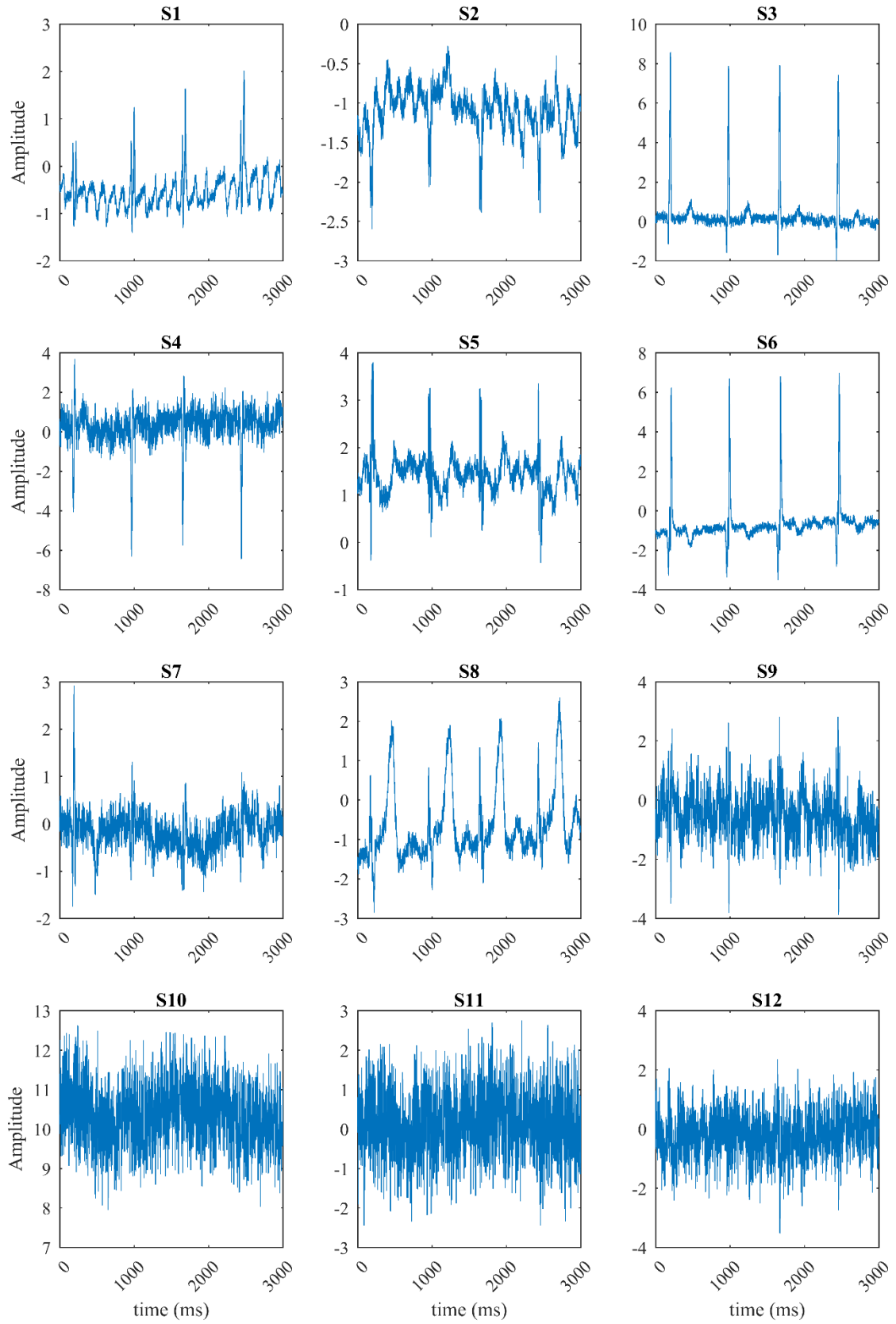
The visual inspection of the results showed the majority of the estimated independent sources ( $S_1$  to  $S_{12}$ ) had kept the atrial activity as well as a high level of noise. However, a few others showed obscured separation and presented intensive level of noise.

Figure 3.4 illustrates an example of 12 leads ECG for the same AF recordings used in the PCA study. Each subplot shows a 3 seconds interval of ECG in AF where the U wave is obscured by the atrial activity and shows the difficulty to distinguish whether there is U wave or not. Figure 3.12 presents the corresponding 12 ICA sources ( $S_1$  to  $S_{12}$ ) estimated from these 12 leads.

It is clear, with the closer look at Figure 3.12, the FastICA algorithm achieved poor separation for both overlapped activities, atrial and ventricular in AF. The estimated sources  $S_3$  and  $S_6$  showed part of the separated ventricular activity by presenting sharp QRS complex waves; however, the T wave is almost indistinguishable in the resultant beats. Despite the reduction in

the presence of atrial activity, considerable noise remains. On the other hand, sources  $S_1$ ,  $S_2$ , and  $S_5$  showed clearly the presence of atrial fibrillatory waves despite the spike of the R waves (i.e. ventricular activity) that appeared in each beat. Interestingly, source  $S_8$ , showed clear noisy T wave in company with the reduction of QRS complex followed by tiny ripple where it is impossible to decide whether this is a U wave or not since the noise was intensive and covered the beats. Sources  $S_4, S_7, S_9-S_{12}$  presented high level of separated noise.

In contrast to the PCA technique where the principal components (PCs) are ordered from the most to the least significant according to their explanation of variance, the ICA technique presented the independent components (estimated sources) randomly with no order. Therefore, subjective visual inspection has a key role to decide whether the two activities had separated successfully, and which source has atrial or ventricular activity, hence if there is a noticeable U wave in the separated ventricular beats.



**Figure 3.12:** The 12 ICA estimated sources ( $S_1$  to  $S_{12}$ ) that associated with the 12 lead ECGs in AF patient.

### 3.2.3. Beat Averaging Technique

The beat averaging (BA) algorithm was the final technique implemented to obtain clean ventricular beats free from the atrial fibrillatory waves that contaminate ECG signals during this arrhythmia. It is described in the following section.

#### 3.2.3.1. ECG Processing

The processing for the beat averaging technique demands long duration recordings, thus long AF recordings were used for the analysis. The database used includes 12 lead ECGs of 10 atrial fibrillation (AF) subjects. The database details were provided in section 2.3.1.

The signal averaging technique has been used to reduce noise from AF signals without deforming the waveforms, by improving signal to noise ratio, so the low amplitude features, such as U waves, can be inspected.

It is important to note; the study assumes that the ‘preceding’ R-R interval has a major influence on the subsequent ventricular characteristics such as T and U wave amplitudes. This is demonstrated in the study presented in Chapter five (section 5.2.1.2). Furthermore, since the technique depends on averaging repetitive epochs of the ECG signal, long ECG durations are essential to collect enough beats for the processing, if there are to be sufficient number of beats to reduce the noise effectively. Since a further objective was to assess the rate dependency of ventricular repolarisation features, it was a requirement that average beats could be generated from beats with a particular beat interval. This placed a further requirement for the use of long duration AF ECG recordings.

To generate an ‘averaged beat’, the algorithm had *four* methodological stages:

- 1) R wave detection
- 2) R-R histogram (to allow selection of individual beats of specific beat interval)
- 3) Beats selection and collection
- 4) Averaged beat calculation.

The methodological details for *each lead* are illustrated in Figure 3.13, and the details are as the follows.

#### 1) R wave detection

R wave peaks were detected automatically using the Matlab function (*findpeaks*). Since the QRS complex represents the most prominent repeating peak in the ECG signal, the Matlab function detects R wave peaks by thresholding the peaks above certain value (e.g. 0.5 mV). The R wave peaks detection was confirmed with visual inspection by plotting the detected points, as illustrated in Figure 3.13-a. If present, ectopic beats and their adjacent intervals were removed.

#### 2) R-R histogram

The R-R histograms with bin size ( $R-R_{bin}$ ) of 50 ms were constructed (Figure 3.13-b), and R-R intervals were identified. Hence, number of beats at particular R-R intervals could be identified.

### 3) Beats selection and collection

Beats were selected from all constructed  $R-R_{bins}$  when they meet selection criteria (Figure 3.13-c). Therefore,  $N$  groups were created relative to  $N R-R_{bin}$ . In other words, each group includes number of beats that belong to one  $R-R_{bin}$ . Figure 3.13-c illustrates for the  $N$  groups, where each group (layer in the Figure) represents the collected beats that belong to the associated  $R-R_{bin}$ .

The selection criteria were chosen to calculate R-R intervals as  $R-R_{i-1} = R_i - R_{i-1}$  as illustrated in Figure 3.13-d. Note that all collected beats in Figure 3.13-d were selected from one  $R-R_{bin}$ .

A careful selection for the beats with respect to the ‘preceding’ R-R interval ( $R-R_{i-1}$ ) were aggregated to build the desired average beat, represented by the interval corresponded to the ‘grey shaded’ area in Figure 3.13-d.

The averaged beat constructed by using all the selected beats within similar ‘preceding’ R-R intervals ( $R-R_{i-1}$ ) that i.e. within the R-R histogram bin ( $R-R_{bin}$ ). In other words, the qualified beats had  $R-R_{i-1} = R-R_{bin} \pm 25$  ms, where  $R-R_{bin}$  was the histogram bin with the selected beats within that interval. A further requirement needed to remove the beats with ‘short’ following R-R intervals ( $R-R_i$ ) (current beat) to avoid the contamination of the averaged U wave with the QRS complex of the following beat. Therefore, beats with  $R-R_i$  less than a threshold ( $R-R_{min}$ ) of 650 ms were excluded, see Figure 3.13-d.

### 4) Average beat calculation

All qualifying beats selected in stage 3 were aligned to their R wave peaks ( $R_i$ ) (Figure 3.13-d) and the ‘averaged beat’ for the collection of beats for each  $R-R_{bin}$  was calculated as the mean amplitude across the beats. The same process of beat collection and averaging was repeated to all R-R bins. Figure 3.13-e shows the averaged beats generated from all R-R bins ( $R-R_{bin}$ ).

The generated averaged beat is illustrated in Figure 3.13-f. All generated averaged beats were inspected visually to decide whether the fibrillatory waves and the noise, were reduced in the AF record.

It is important to note that histogram bins ( $R-R_{bin}$ ) with less than 10 beats were excluded since the number of beats influences the quality and the value of the averaged U wave. For more details, the study in section 4.4 of Chapter four has examined the effect of the number of beats on the quality of the averaged beat and ventricular repolarisation characteristics.

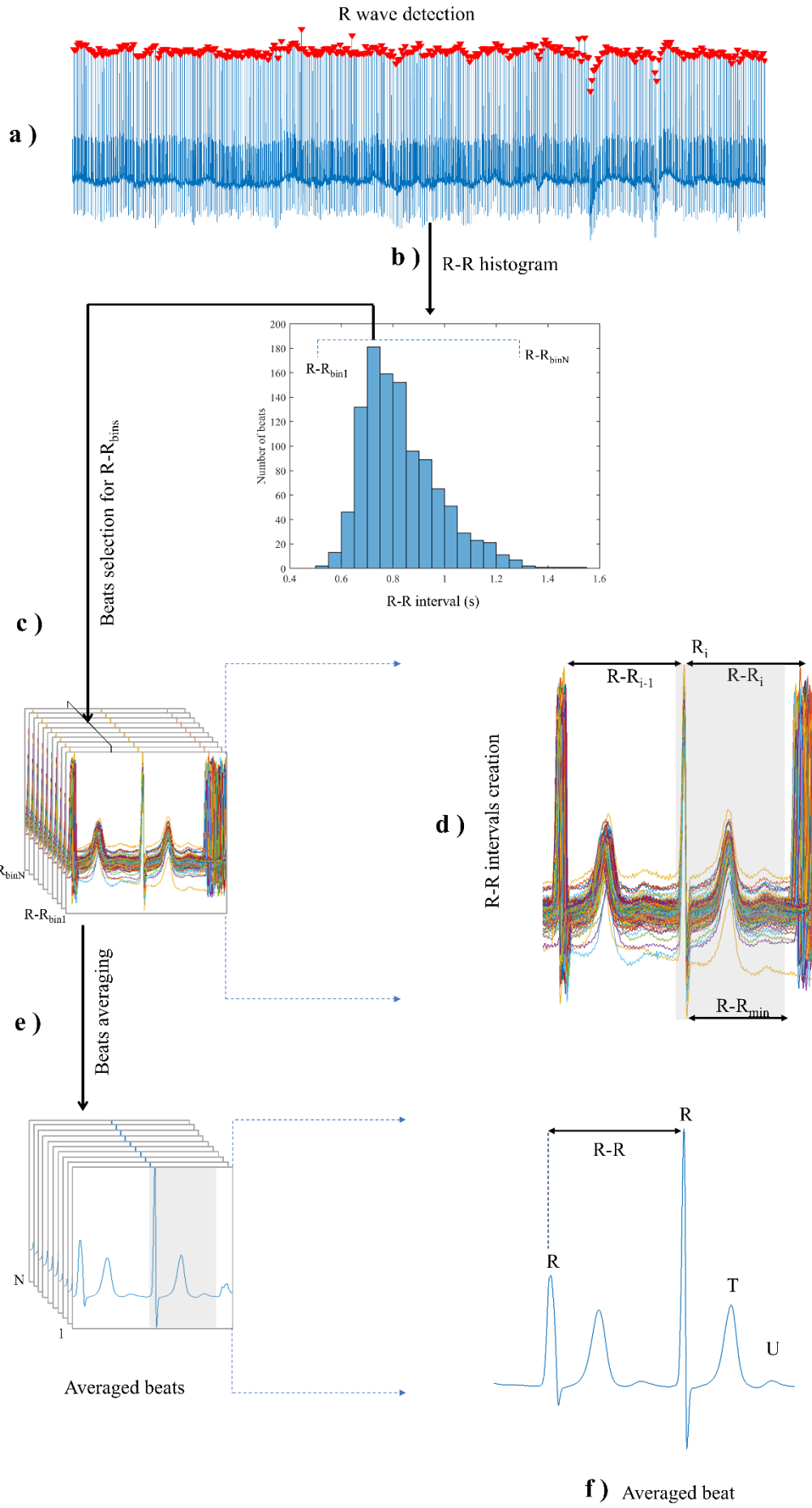


**Figure 3.13:** The signal processing workflow for beat averaging technique to clean AF recordings. **(a)** R wave peaks ( $\blacktriangledown$ ) were detected in the ECG lead. **(b)** the R-R histogram (bin size  $R-R_{bin} = 50$  ms) was created ( $R-R_{bin1}$  to  $R-R_{binN}$ , where  $N = \text{all } R-R_{bins}$ ). **(c)** collect and align the beats from each bin. Collected beats from one of the bins is shown in **(d)**. **(e)** averaged beats for  $N$   $R-R_{bins}$  were calculated resulting in the average beat containing the ventricular repolarisation features (T and U waves) as illustrated in the averaged beat generated from one of the R-R bins in **(f)**.

### 3.2.3.2. Implementation Examples

In this section some implantation examples are presented while a statistical quantitative analysis of the ability of the beat averaging technique to remove the atrial fibrillatory activity is presented in section 3.3.

The beat averaging technique succeeded to clean AF recordings and generate ventricular averaged beats with reduced atrial fibrillatory waves that contaminate the ECG signal. Figure 3.13-f shows a clean averaged beat where the ventricular repolarisation features including U waves were revealed after processing.

Figure 3.4 shows a 5 seconds interval of ECG for 12 leads of the same AF recordings that were used in PCA and ICA analysis. The low amplitudes of the fibrillatory waves are obscuring the ventricular features. Clearly, it is difficult to recognise U waves as they have same morphology and amplitude of the fibrillatory waves.

Figure 3.14 presents the corresponding averaged beats for the 12 leads. It can be seen the noise was reduced including the atrial fibrillatory waves, and the desired ventricular characteristics revealed (corresponding to the grey shaded area), particularly the most challenging feature: The U wave. The averaged beats in the Figure 3.14 were generated using the maximum number of beats ( $R-R_{bin}$  with maximum number of beats, 252 beats) with similar preceding R-R interval ( $725 \pm 25$  ms).

The beat averaging algorithm improved the signal to noise ratio ( $SNR$ ) and the process of creating an averaged beat by careful alignment and summation of a large number of beats helped to separate the uncorrelated noise and atrial fibrillatory waves from the repetitive ventricular beats, without introducing signal distortion. The resultant averaged beats were relatively clean and revealed all desired ventricular characteristics which can facilitate an accurate investigation of the repolarisation waves (e.g. T and U waves) and intervals (e.g. R-T and T-U) in AF.

It is important to note factors that affect the accuracy and quality of the generated averaged beats. *First* the accurate alignment of R waves for the chosen beats (i.e. reference time point where all beats aligned) and *second* the number of beats that averaged during the processing by the algorithm. Hence, it is important to understand their influence on the averaged beats.

To understand the role of the precise alignment for the collected beats to their R wave peaks, Figure 3.13 illustrates the effect of ‘accurate alignment’ and ‘misalignment’ for R waves peaks (fiducial point) on the resultant averaged beat. The example presents two main parts using one of the AF recordings, where i) presents qualified beats collected by the beat averaging algorithm, and ii) the corresponding averaged beat. It has been explained in the method, all chosen beats were aligned carefully to their R wave peak as in Figure 3.15 (i) considering the preceding intervals.

Evidently, all beats are aligned accurately to their R peaks as illustrated in Figure 3.15 (i-C), only noise is reduced and averaged out, while the wanted signal is unchanged as in the resultant averaged beat in Figure 3.15 (ii-C).

However, if the beats are misaligned with the timing reference and then averaged, the signal and the noise will be effected because of reference jitter from beat to beat [132,148], and that leads to an amplitude reduction or distortion of the averaged signal depending on the reference jitter degree (i.e. how many beats misaligned); as an example, Figure 3.15 for the areas (iB) where the beats misaligned to ( $R_k$ ) timing reference, the corresponding area (iiB) for the beats averaged showed a reduction for the ( $R_k$ ) amplitude after the averaging. Similarly, areas (iA, iD) showed strong reference jitter (i.e. strong misalignment) from beat to beat, the averaged results in the corresponding area (iiA and iiD) where both signal and noise were averaged out, causing a distortion to the resultant signal.

The other important factor is the number of beats used for averaging. It has been hypothesised that the number of beats aggregated into the averaged beat has a direct effect on the quality of the resultant beat. In other words, increasing the number of averaged signal epochs would achieve greater noise reduction, and hence higher-quality averaged beat. This has important implications for the algorithm since it demands a long duration of AF recordings. This study has been investigated extensively in study three (section 4.4) of Chapter four.

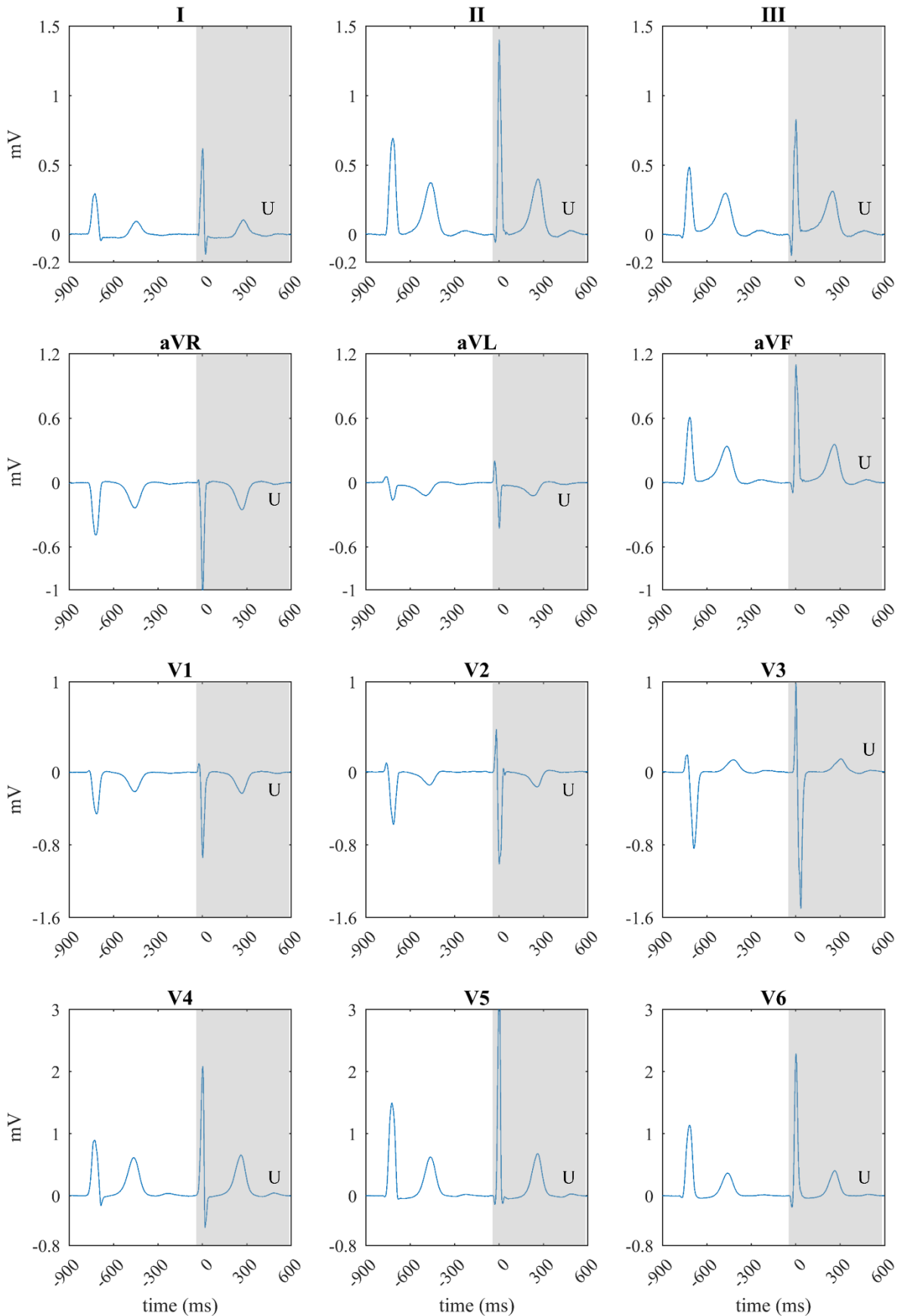


**Figure 3.14:** Example averaged beats for 12 leads for one AF recording. The beats generated by the beat averaging algorithm are free from the atrial fibrillatory waves, and U waves are revealed in the grey shaded area along with uncontaminated T waves.

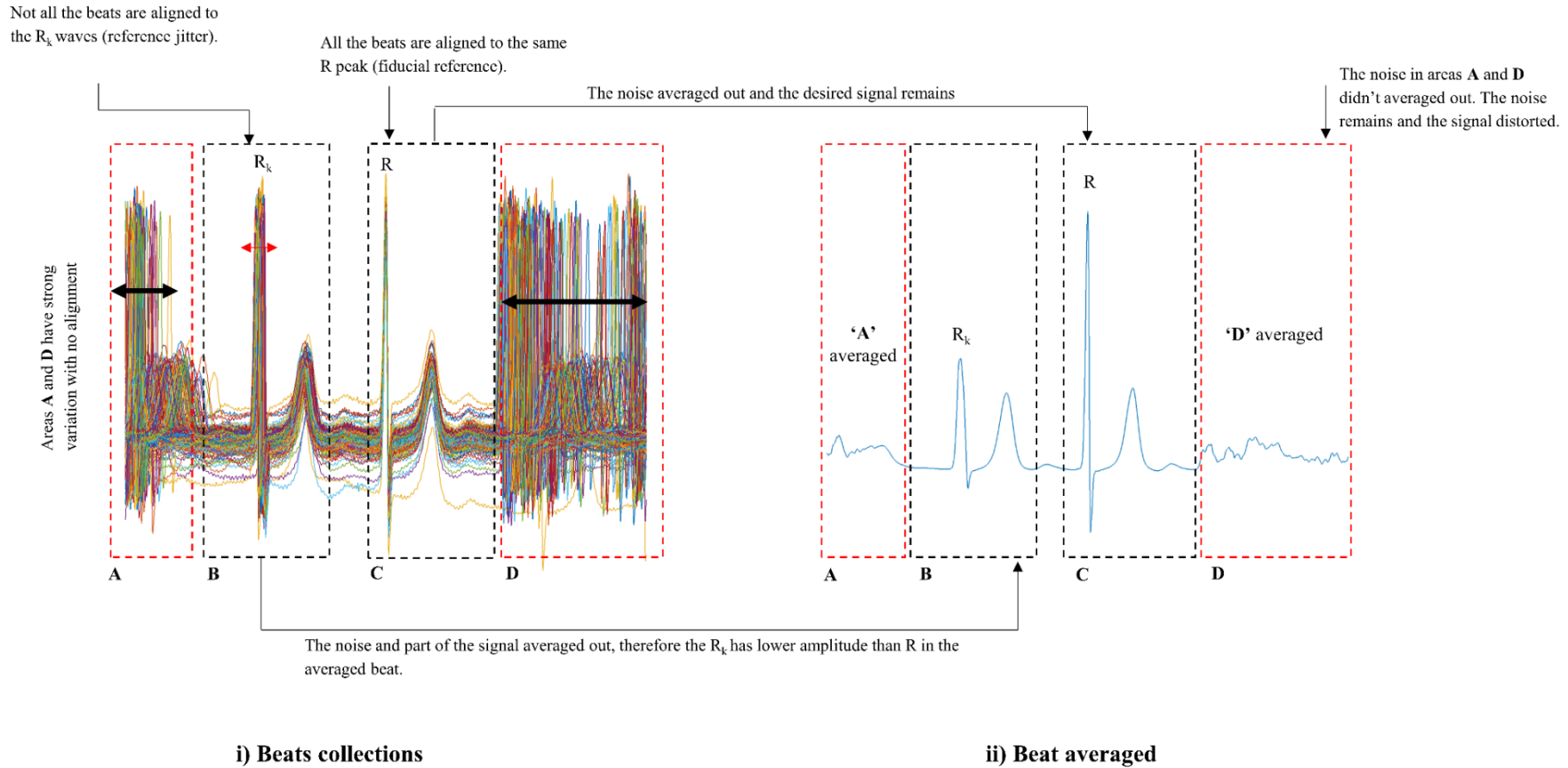


**Figure 3.15:** An example of accurate alignment and misalignment effects on the averaged beats in beat averaging method using one of the AF recording. **i)** represents example of beats collection were aligned to their R wave peaks (part C) where all waves placed accurately to generate an averaged beat with respect the preceding interval ( $R-R_k$ ). The parts A, B, C, and D show different regions of the collected beats during the alignment, part C demonstrates the desired region where all R peaks are aligned carefully. In part B, there is a reference jitter (slight  $R_k$  peaks misalignment), while undesired parts A and D have strong misalignments to the beats' peaks. **ii)** represents the corresponding averaged beat showing the corresponding averaged parts A, B, C and D. In the averaged part C, where all R peaks aligned accurately, the noise averaged out and the desired ventricular beat remains. Part B, the noise and part of the signal averaged out causing lower amplitude for  $R_k$  peak (i.e. lower QRS) because the collected beats in part B have slight peaks misalignment. Parts 'A and D' are noisy and the signal distorted since the corresponding parts A and D in i) have strong variations and misalignments.

### 3.3. Comparison Study Between BA, PCA and ICA Techniques

The aim of this study was to quantitatively assess the three processing techniques PCA, ICA and beat averaging (BA) presented in the previous sections for their ability to clean the AF recordings from the unwanted fibrillatory waves.

#### 3.3.1. Method

The three developed techniques PCA, ICA and BA in the sections (3.2.1, 3.2.2 and 3.2.3), were applied to 12 leads of 10 AF recordings of the Long Duration AF Database to remove the atrial fibrillatory waves from AF recordings and provide clean ventricular beats.

The quality of the resultant beats of the three developed technique was inspected visually. The presence of U wave in these beats was the metric used to compare the techniques' ability to clean AF recordings from the atrial activity, as it represents the most challenging feature of the repolarisation process. Subsequently, the techniques were compared statistically to determine their suitability for further studies to investigate the ventricular features.

To assess the three techniques ability to clean AF recordings, 300 generated beats were examined visually by an expert (PL) to check whether the U wave was visible in these beats. The 300 beats were gathered after applying the 3 techniques on 10 AF recordings.

Each technique was used to provide 100 beats; therefore, the total number of beats were 300. The 300 beats were gathered as the following:

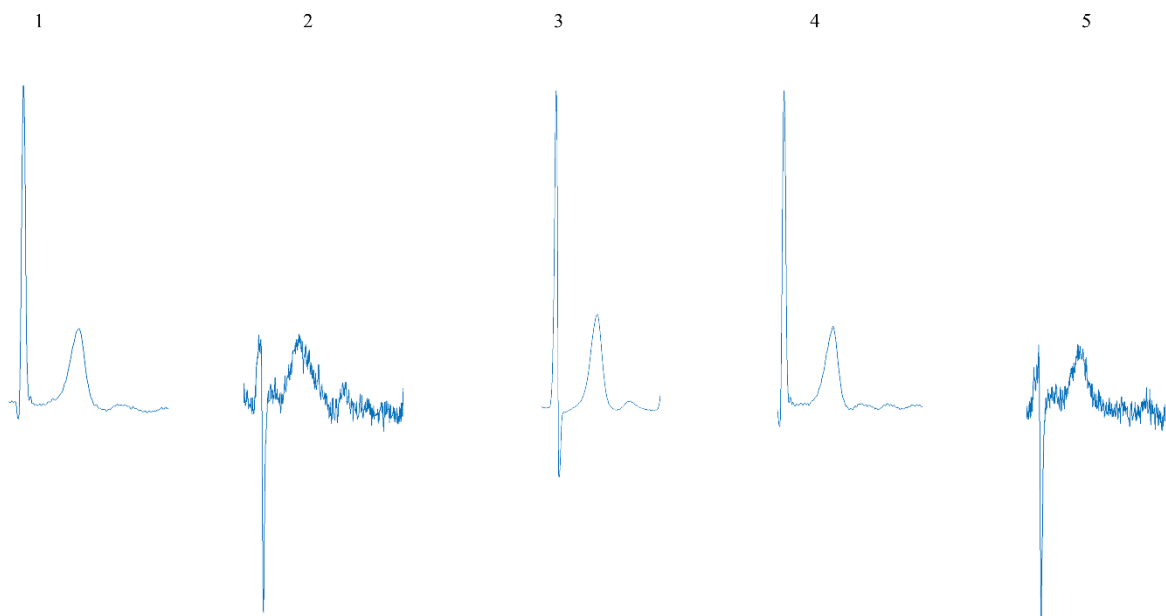
- a) Using the PCA technique (section 3.2.1), 100 beats were gathered from the reconstructed lead V4. The first consecutive 10 beats of reconstructed lead V4 were collected from each AF subject. The reconstructed lead V4 was chosen as the U wave amplitude is known to be higher in this lead (see section 1.3.1).
- b) Using the ICA technique (section 3.2.2), 100 beats were gathered from the visually inspected IC<sub>3</sub>. The IC<sub>3</sub> was chosen as it showed visually less contamination by the remaining atrial activity compared to the other components. The first consecutive 10 beats of IC<sub>3</sub> were collected each AF subject.
- c) Using the BA technique (section 3.2.3), 100 averaged beats were generated using lead V4, the U wave amplitude is known to be higher in this lead (see section 1.3.1). In the processing, 10 different averaged beats were generated from each AF subject.

As has been explained above, in the PCA method, we used the reconstructed lead V4 to provide 10 consecutive beats from each AF subject (total 100 beats = 10 beats x 10 subjects). In ICA method, we used the IC<sub>3</sub> to provide 10 consecutive beats from each AF subject (total 100 beats = 10 beats x 10 subjects). While in BA method, we used the lead V4 to provide 10 different averaged beats from each AF subject (total 100 beats = 10 beats x 10 subjects). The total number of inspected beats was 300 beats.

The 300 collected beats were presented randomly and U wave presence was examined visually in the beats. Figure 3.16 shows representative examples of the examining method. The example shows 5 random beats produced by the 3 techniques. As has been mentioned, the visual examination focused on ‘U wave presence’ to report a decision by answering the question: “*Is U wave visible in the beats?*”

The answers were categorised as:

- i) ‘Yes’ if U wave presence has confirmed in the presented beat.
- ii) ‘No’ if the U wave was not observed in the presented beat.
- iii) ‘Not Sure’ if the U wave presence or absence could not be determined in the presented beat, e.g. there was potentially a U wave, but the expert was not confident due to contaminating noise.



Is U wave visible in the beats?				
1	2	3	4	5
Yes <input type="checkbox"/>				
No <input type="checkbox"/>				
Not sure <input type="checkbox"/>				

**Figure 3.16:** An example illustrates the assessment method for the generated beats, where they presented randomly to be examined visually by an expert. The beats were generated using 3 techniques, BA, PCA and ICA. The total number of examined beats are 300. The visual examination addresses the question “*Is U wave visible in the beats?*”. The answers were categorically classified into ‘Yes’, ‘No’, and ‘Not sure’ depending on certainty of the presence of a U wave.

The frequency of the categorical answers (Yes, No, Not Sure) were gathered and compared among their 3 associated techniques (BA, PCA, and ICA). The results were statistically

assessed using Fisher Freeman-Halton exact test. The test was two sided and  $p$ -values less than 0.05 were considered statistically significant.

Note that the duration of the analysed AF recordings allowed the BA algorithm to provide only 10 generated beats for each lead (check section 5.2 of Chapter five for more details). Therefore, only 10 beats were selected from each lead for all the 3 techniques.

### 3.3.2. Results

The results of the visual inspection showed that ‘beat averaging algorithm’ was the best technique to remove the atrial activity from the AF recordings, compared to the PCA and ICA techniques.

Figure 3.17 shows the statistical results of U wave inspection in 300 beats produced by the 3 developed techniques (BA, PCA and ICA). The triple bars for each technique illustrate the frequency of the state of recognisable U wave during the visual examination, where ‘Yes’ refers to the number of distinguished U wave, ‘No’ refers to the number of unrecognisable U wave, and ‘Not Sure’ refers to the number of indicates the uncertainty of distinguishing U wave.

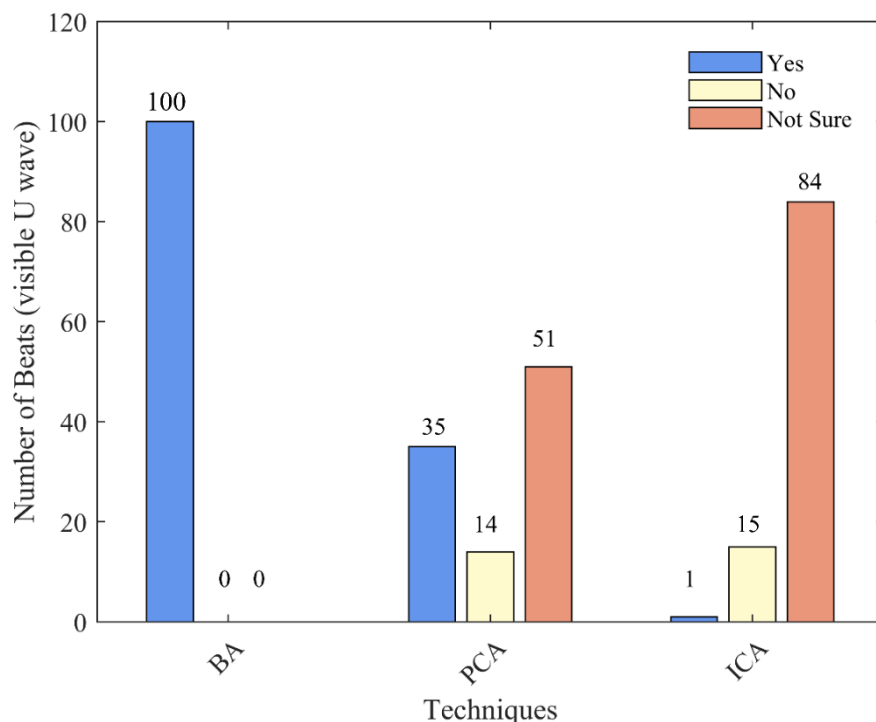


**Figure 3.17:** The frequency of U wave presence that examined visually for 300 produced beats by the techniques beat averaging (BA), PCA, and ICA. The positive, negative and uncertainty outcome to report U wave presence indicated by ‘Yes’, ‘No’ and ‘Not Sure’ respectively.

U waves were discernible for the 100 beats that has been generated by BA technique, and for 35 beats using PCA technique whereas only 1 beat confidently showed visible U wave using the ICA technique, as shown in Figure 3.17. The Uncertainty for distinctive U wave dominated PCA and ICA techniques results with 51 and 84 beats respectively. The difficulties in recognising U wave in many beats associated to PCA and ICA are due to either the remaining fibrillatory waves, or residual noise that obscured the beats, this suggesting a failure to clean the beats from the atrial activity using these two techniques.

Figure 3.18 displays comparison example produced by the 3 techniques BA, PCA, and ICA compared to their associated AF recording. Figure 3.18-a shows a strip of AF signal where it is difficult to distinguish U wave due to spreading atrial activity, 3.18-b illustrates two associated average beats generated by BA technique for i) short beat duration and ii) long beat duration, in both U wave where discernible with high quality since the atrial activity as well as noise were averaged out. Figure 3.18-c presents two beats collected from the reconstructed lead V4 provided by PCA, where the beat in i) suggests an obvious U wave while ii) shows difficulties to distinguish U wave since the beat still suffers from the AF activity according the visual inspection. Similarly, for the beats in Figure 3.18-d where the two presented beats collected form the 3<sup>rd</sup> estimated component (IC<sub>3</sub>) provided by ICA, i) shows potentially a visible U wave despite the considerable level of noise that covered the beat, while ii) shows difficulties to distinguish U wave due to remaining AF activity and high level of noise.

Table 3.1 provides the contingency Table for U waves presence that has been examined for 300 beats related to their generated mechanism (BA, PCA, and ICA). The statistical assessment for the U wave presence among the 3 technique was extremely significant with ( $p=0.000$ ) using the categorical Fisher Freeman-Halton exact test.

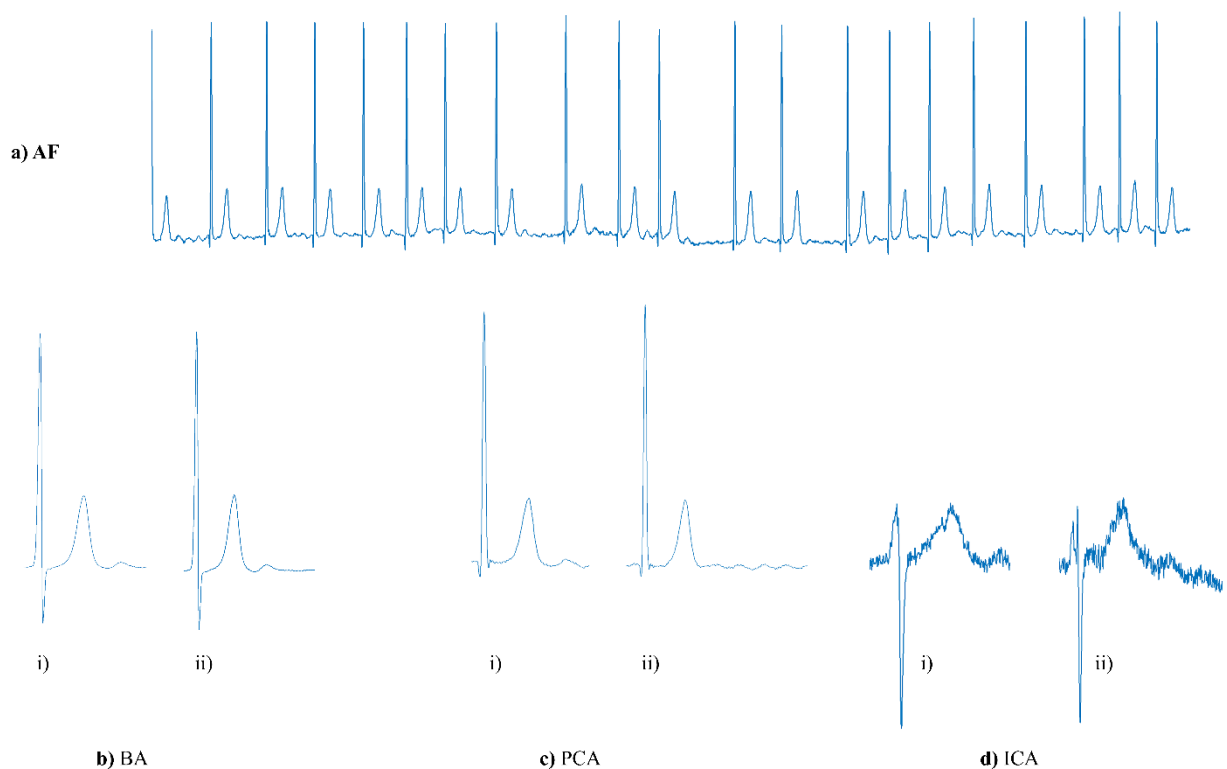


**Figure 3.18:** Example to compare U wave presence in resultant beats by the techniques BA, PCA and ICA to their AF recording. **(a)** an interval of ECG in AF where it is difficult to distinguish U wave, and **(b)** the corresponding two generated averaged beats using BA technique **i)** for short beat duration and **ii)** for long beat duration where in both beat, U wave is visible following T wave. **(c)** two collected beats from the corresponding the reconstructed lead V4 provided by PCA where **i)** shows potentially a clear U wave in the beat while **ii)** shows uncertainty of U wave presence due to the remaining AF activity. **(d)** two collected beats from the corresponding estimated IC<sub>3</sub> provided by ICA technique where **i)** shows potentially discernible U wave in the beat despite of the residual noise whereas **ii)** shows uncertainty of U wave presence due to the remaining AF activity and high level of noise.

**Table 3.1:** Contingency table of the presence of U wave for three techniques BA, PCA, and ICA in AF recording according to the visual examination (using categorical Fisher Freeman-Halton exact test).

Techniques	Visible U wave			Total
	Yes	No	Not Sure	
BA	100	0	0	100
PCA	35	14	51	100
ICA	1	15	84	100
Total	136	29	135	300

### 3.3.3. Discussion

The techniques BA, PCA and ICA were applied to 10 AF ECG recordings. They were applied to remove the atrial activity from the ECG signals and provide clean ventricular beats that can facilitate further investigations of ventricular features in AF including U wave. Their ability to clean AF was compared by examining U wave presence visually in 300 resultant beats obtained by these 3 techniques, 100 beats from each technique. The BA technique produced outputs where a U wave could be observed in all cases compared to the PCA and ICA were far fewer were observable. The U waves were visible for all 100 beats produced by BA, compared to 35 beats for PCA, while only 1 beat showed discernible U wave for ICA (see Figure 3.17).

The presence of U wave was chosen as criteria for the techniques' assessment and efficiency because, on one hand U wave is a desirable ventricular feature for further research studies in AF. On the other hand U wave is a low amplitude deflection compared to other ventricular waves, lies in same amplitude range of atrial fibrillatory waves [54], thus discernible U wave in the resultant ventricular beats can provide a clear indication of the techniques' ability to observe such a small feature as a U wave. In other words, clean visible U wave is a quality measure of the technique ability to provide clean ventricular beats in AF and hence fulfilling the principal aim of the study.

Clearly, BA algorithm succeeded to average out the atrial activity from the AF recordings, reduce the noise, and produced clean ventricular beats with high quality (see Figure 3.18-b). As has been mentioned, U wave was discernible in all averaged beats. This is an interesting finding to find U wave visible in such a condition.

The performance of the PCA technique was less reliable, where only 35 beats showed detectable U waves from 100 inspected beats output by the PCA technique. The technique has separated the atrial activity and the noise from AF recordings; however, many beats preserved their fibrillatory waves, which makes it difficult to observe the U wave during the inspection as the wave is contaminated and masked by the atrial activity, thus making it difficult to observe the U wave in 51 beats (i.e. 'Not Sure').

The ICA technique showed poor ability when removing the atrial activity and noise from the AF recordings compared to the PCA and BA techniques. The beats produced remained contaminated by the atrial activity as well as noise; only one beat showed a noticeable U wave from 100 examined beats despite of the high level of noise. Visible U waves were uncertain for high number of inspected beats (84 beats), this indicates the ICA technique has failed to remove the atrial fibrillatory waves completely from AF recording, which makes it unqualified technique for further studies in AF.

Fundamentally, accuracy in the medical studies is vital, therefore the quality of the produced beats is essential for further studies as they could be used for measurement purposes and medical diagnosis. Hence to evaluate the 3 techniques from the quality point of view, BA technique generated high quality clean beats which qualifies them for further studies of ventricular features. Additionally, for the acceptable beats that produced by the PCA technique, despite the presence of U wave, however, there is a low level of residual noise which varies from beat to beat. Moreover, the beats produced by ICA technique showed poor quality as they were noisy and contaminated by the residual atrial activity combined by considerable level of noise, which make them disqualified for further studies in AF.

In fact, the nature of the PCA and ICA processing presumed can separate the atrial activity from AF recordings and produce clean ventricular beats for the full length of the recordings. This can offer the potential to study the ventricular repolarisation characteristics beat by beat, and track their changes in such arrhythmia (AF) by inspecting the waves T and U, and ventricular intervals. However, the techniques PCA and ICA, were not able to remove the undesired fibrillatory waves and hence cannot facilitate such studies.

The BA technique compared to PCA and ICA provides a favourable candidate to clean AF recordings from the unwanted atrial activity, which can offer a wider potential to study the repolarisation characteristics, including the most challenging feature: U wave in AF. It is important to note a few considerations when using the BA technique to clean AF recordings. The technique demands long duration recordings for higher effectiveness since it depends on collecting a number of beats to be averaged and produce 'one' clean averaged beat. Consequently, the number of beats collected has a direct impact on the quality of the averaged beat, i.e. more beats collected means a higher quality averaged beat. Additionally, producing

one clean averaged beat for certain beat interval can limit the potential to investigate the variation of the ventricular feature changes (such as U wave) from one beat to another. Although the focus of this study has been on the U wave, it is reasonable to assume that any remaining contamination of atrial fibrillatory activity will also be present during the T wave, hence the BA algorithm is likely to provide cleaner T waves than the other evaluated techniques.

### **3.4. Chapter Summary**

The study critically investigated three proposed techniques (BA, PCA, and ICA) to provide a reliable tool to clean AF recordings from atrial activity and provide ventricular beats free from the fibrillatory waves. The BA technique shows a reliable performance with high quality of the generated ventricular beats compared to PCA and ICA techniques. The BA algorithm is highly recommended to clean AF recordings. Consequently, the beat averaging algorithm is used to clean AF recordings in the following chapters as it facilitates further studies in this project. The BA algorithm is validated in Chapter four and used for the research investigations in Chapter five.

## **Chapter 4**

# **Validation of the Ventricular Repolarisation Measurement Techniques**

## **Chapter 4. Validation of the Ventricular Repolarisation Measurement Techniques**

### **4.1. Introduction**

This chapter is dedicated to establish and validate the proposed techniques to detect and measure ventricular repolarisation features in atrial fibrillation. The chapter consists of three essential studies. The *first study* is to develop an algorithm for the automatic measurement of ECG ventricular repolarisation features and to validate it against manual measurements. The *second study* is to validate the ‘beat averaging algorithm’ to reveal the U wave, by comparing the U waves extracted from AF recordings to the U waves that are observable in SR recordings for the same patients. Finally, *third study* is conducted to establish the ‘number of beats’ that are required to extract U waves effectively with high quality using beat averaging algorithm in AF.

## **4.2. Validation of Automatic Measurements for Ventricular Repolarisation Features Against Manual Measurement**

The aim of this study is to develop an algorithm for the automatic measurement of ECG ventricular repolarisation features and to validate it against manual measurements. First, the ECG measurement algorithm is described. Second, a Matlab application to assist the measurement of the same features manually is described. Finally, validation of the algorithm's automatic measurements against manual measurements is presented.

In the previous chapter, the beat averaging algorithm exhibited a strong performance to clean atrial fibrillation (AF) recordings from the contamination of fibrillatory waves and succeeded in providing clean ventricular beats from which ventricular repolarisation wave features (e.g. U and T amplitudes and intervals) can be measured. We now deal with the measurement of these features.

There are two broad approaches to quantify the ECG features, i) manually or ii) automatically [172,173]. Manual measurements have been observed to exhibit large inter-observer variability, while automatic measurements are repeatable because they do not suffer the subjectivity of manual measurement [172,173].

Fundamentally in medical research, visual examination serves as a gold standard of the analysis [173,174]. However, this process is time consuming and cumbersome for large amounts of data. Alternatively, automated measurement provides fast, robust and repeatable analysis for large amounts of data [174]. However, automatic techniques require validation to quantify any measurement bias associated with technical processing.

As the 'automatic ECG feature measurement algorithm' is used throughout the various studies of this project, this study presents a validation of the automatic measurement technique against the 'gold standard' manual technique.

### **4.2.1. Method**

#### **4.2.1.1. ECG Database**

The 10 recordings of the Long Duration AF ECG Database were used in this study. Full details of the database have been described in section 2.3.1 of Chapter two.

Lead V4 was analysed for all 10 AF recordings. V4 was chosen because the amplitude of ventricular waves, particularly the desired U wave, is higher in the precordial leads V2-V4 [54] (see section 1.3.1 of Chapter one) so this aids the visual inspection and manual measurement of the ventricular repolarisation features.

#### **4.2.1.2. ECG Processing**

The validation approach consisted of three methodological stages. First is the recordings pre-processing stage where AF recordings were processed to clean the ECG signal from the contamination of atrial fibrillatory waves to generate clean ventricular beats. The beat averaging algorithm was used in this stage. Second, the ventricular repolarisation features were measured using two approaches, automatically through an automatic measurement algorithm and then manually through bespoke software used by two observers. Finally, the results of the manual and automatic measurements were compared and statistically tested.

Figure 4.1 illustrates the method stages of the validation analysis, demonstrating the three methodological stages in sequence. The following sections describes the processing details of each stage individually.

##### **4.2.1.2.1. ECG Pre-processing**

The objective of this stage is to prepare clean beats to implement the measurement techniques.

The beat averaging algorithm was used to generate 100 ventricular clean averaged beats from 10 AF recordings (total number of generated beats = 10 beats per lead V4 x 10 subjects). For each patient the 10 average beats had different preceding R-R interval. The ventricular repolarisation features of these 100 averaged beats were then measured automatically and manually as described in the following sections.

The full details of beat averaging algorithm processing have been described in section 3.2.3 of Chapter three.

##### **4.2.1.2.2. Automatic Measurement**

An ‘automatic ECG feature measurement algorithm’ was used to measure the ventricular repolarisation features for the 100 ventricular averaged beats in AF.

The algorithm was designed to quantify the desired features automatically. The desired ventricular repolarisation features in the validation study are: U and T wave amplitudes referred to as U amp and T amp, the interval between R and T waves (peak to peak timing points) referred to as R-T, and the interval between T and U waves (peak to peak timing points) referred to as T-U. Figure 4.2 illustrates the desired repolarisation features presented on a generated average beat.

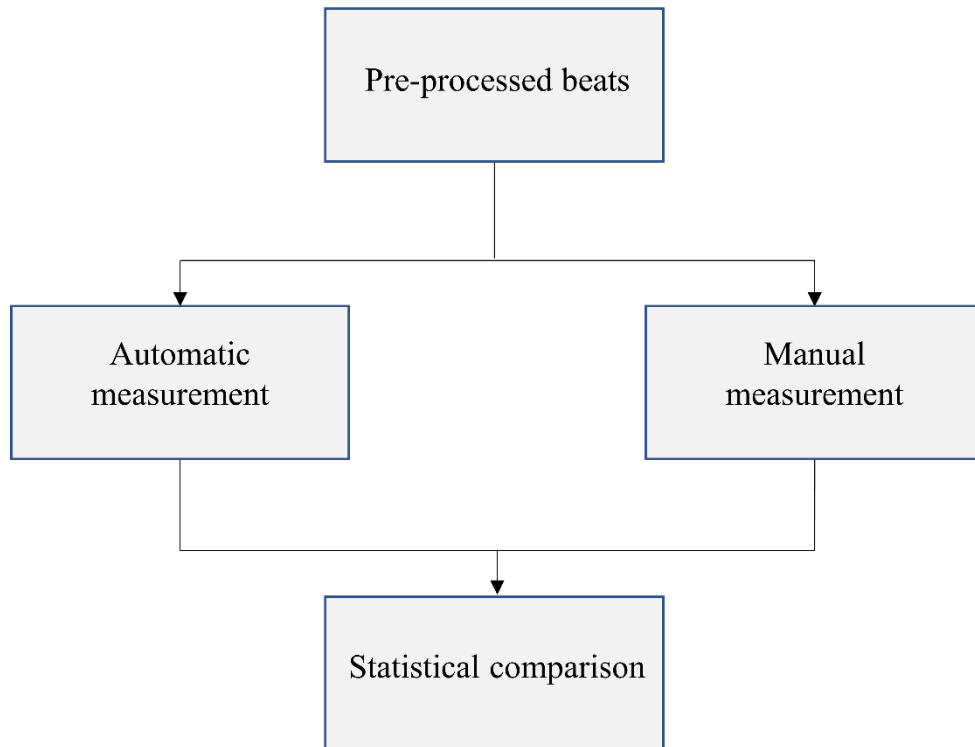


**Figure 4.1:** Illustration of method stages of validation study. Pre-processed averaged beats (100 beats) of 10 AF recordings were prepared for the measurement. Two measurements approaches were implemented to measure the ventricular repolarisation features. Both measurements were compared and statistically tested.

The automatic algorithm measured the amplitudes of the U and T waves from a stable baseline to their peaks. The stable baseline amplitude (referred to as Ref in Figure 4.2) was estimated automatically from a 10-sample point window of the electrically quiescent period before the onset of the QRS complex. The window selection of 10 samples was relative to the location of R wave peak. The location of R wave peak (R) was already known from beat averaging algorithm, therefore by stepping a selected threshold (flexible depending on sampling rate and the type of records i.e. AF/SR) from R wave peak backward to skip the location of Q wave in AF (or P wave in SR), then the stable window of 10 samples was selected. The selected window was visually inspected to confirm its appropriateness.

With the location of the R wave peak in the average beat already known, the location of the T and U wave peaks were detected using the Matlab *findpeaks* function as the next two peaks following the R wave. The *findpeaks* function was used with amplitude and time thresholds to reject small peaks resulting from noise being detected as T or U waves.

The interval between R wave and T wave (R-T) was measured as the duration between their peaks. Similarly, the interval between the T and U waves (T-U) was measured as the duration between their peaks.

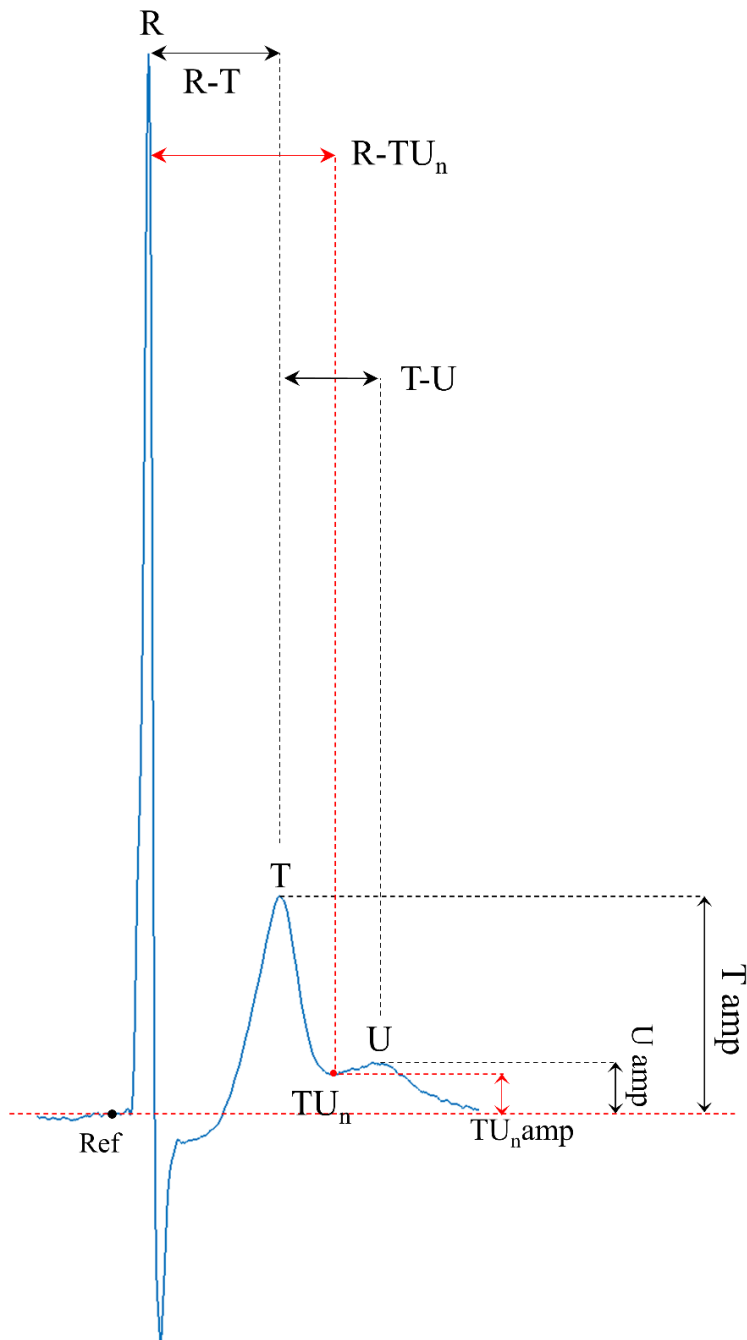


**Figure 4.2:** A representative example of measurement points shows an averaged beat with the repolarisation features indicating T wave amplitude (T amp), U wave amplitude (U amp), R-T interval (R-T), T-U interval (T-U), T wave end amplitude (TU<sub>n</sub> amp) and the intervals (R-TU<sub>n</sub>). Ref = reference for the stable baseline amplitude (electrically quiescent period).

#### 4.2.1.2.3. Manual Measurement

The manual measurement was applied to the same averaged beats used in the automatic measurement to measure the same repolarisation features, T wave amplitude (T amp), U wave amplitude (U amp), R-T interval, and T-U interval.

The measurement was conducted using bespoke Matlab software. The software application was built specifically for this purpose to enable the potential users (e.g. researchers and clinicians) to observe the generated averaged beats on the computer screen and decide the location of the desired features according to their experience.

The measurement of the above features was obtained by two observers (PL, MSA) where they used the software independently to select the repolarisation features manually. The software displayed the averaged beats individually on the computer screen at a size corresponding to ECG paper speed of 50 mm/s and 20 mm/mV. Figure 4.3 shows the GUI main window with one of the averaged beats loaded into software application.

The software enabled the observers to mark independently a stable isoelectric baseline in the period immediately just before the onset of QRS complex, as well as the T peak, and U peak time points. Figure 4.3 illustrates a representative example of these selected marks on the computer screen placed on the loaded averaged beat.

Beside the interest to measure the above main ventricular features, the software application was designed with the flexibility to investigate additional features that cannot be predicted accurately by the automatic measurement algorithm. The additional features are, TU nadir amplitude referred to as TUn amp and its time point, from which the interval between the R wave and TU nadir (referred to as R-TUn) can be calculated. It is important to note that these are not part of the current validation study, thus these will not be presented further in this chapter. However, they represent essential parts of the software application and they have been used in other studies presented in section 5.2 of Chapter five of this thesis.

After the manual selection of the reference baseline window and T peak and U peak time-points the desired features values were calculated based on the manually selected points. The location of R wave peak was already known from beat averaging algorithm since R peak is the reference time point for alignment of multi-beat averaging and always lies in the centre of average beat window. T wave amplitude (T amp), and U wave amplitude (U amp) were automatically calculated from the manual selected baseline to the selected wave peaks. Likewise, T wave end amplitude (TUn amp) was automatically calculated from the manual selected baseline to the TUn point. The intervals R to T wave peaks (R-T), T to U wave peaks (T-U) and R peak to TU nadir (R-TUn) point were automatically calculated from their manually selected points. Figure 4.2 illustrates the mentioned repolarisation features presented on a generated average beat.

The software created is capable of sequential loading of all the generated averaged beats and presenting them on the screen annotated with their recording details (e.g. recording identity, and length of the beat interval) as presented in Figure 4.3. A full description of the software user guide is presented in the appendix B.

### **4.2.1.3. Statistical Comparison**

A statistical comparison and correlation test were applied between manual and automatic measurements associated with each measured feature. In other words, statistical assessments were carried out for the following measurement:

- 1) Manual U amp against automatic U amp
- 2) Manual T amp against automatic T amp
- 3) Manual R-T interval against automatic R-T interval
- 4) Manual T-U interval against automatic T-U interval

The statistical significance of the differences between manual and automatic measurements for each feature was assessed using Wilcoxon signed rank test (paired samples test) following the normality assessment of data distribution for each set by Kolmogorov-Smirnov test. The correlation between manual and automatic measurements for each feature was assessed using Pearson correlation.

Additionally, since the manual measurement was examined by two observes (PL and MSA), inter-observer variation analysis between their measurements was implemented and tested using intra-class correlation (ICC). The average of the two manual measurements for each ECG feature was calculated and was used to validate the automatic measurements.

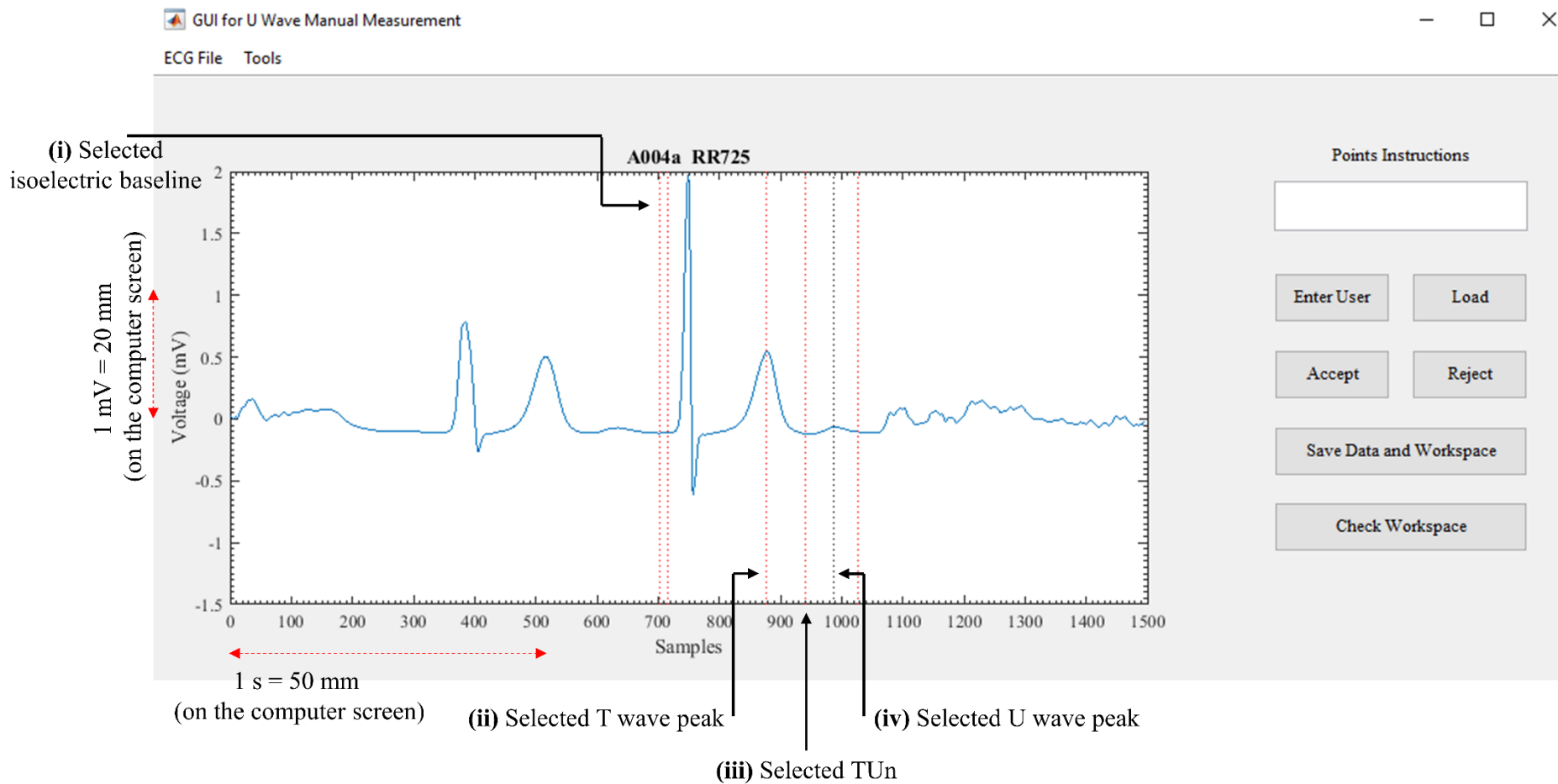


**Figure 4.3:** The GUI main screen of the bespoke Matlab software that was used for manual measurement. It shows an average beat with the manual selected (i) isoelectric baseline window, (ii) T wave peak, (iii) TU nadir (TUn), and (iv) U wave peak.

## 4.2.2. Results

### 4.2.2.1. Comparison Between Automatic and Manual Measurements

Automatic and manual measurements showed a significant positive similarity for all desired repolarisation features.

Figure 4.4 compares the manual and automatic measured ventricular features. Bars and whiskers indicate mean and standard deviation (mean  $\pm$  SD) of the measured values across 100 beats. Table 4.1 presents the statistics for both measurements, where all measured features showed great similarity with no statistical significance difference ( $p > 0.05$ ) between the two sets of measurements.

Statistically, the amplitudes of U waves measured manually and automatically (mean  $\pm$  SD,  $44 \pm 14 \mu\text{V}$  vs  $43 \pm 13 \mu\text{V}$  respectively) showed a strong linear positive correlation, where the correlation coefficient  $R$  was 0.9802. The Wilcoxon signed rank statistical test was not significant with  $p = 0.5708$  between the paired measurements. Similarly, T wave amplitudes were almost identical (manual vs automatic,  $346 \pm 14 \mu\text{V}$  vs  $344 \pm 13 \mu\text{V}$ ) and highly positively correlated where  $R$  was 0.9995. The Wilcoxon signed rank statistical test was not significant with  $p = 0.3075$  between the paired measurements.

Likewise, the manual and automatic measurements of the intervals R-T ( $260 \pm 5$  ms vs  $260 \pm 4$  ms) were positively correlated with  $R$  equal to 0.9794. The Wilcoxon signed rank statistical test between the paired measurements was not significant with  $p = 0.5708$ . The intervals of T-U ( $224 \pm 4$  ms vs  $223 \pm 5$  ms) were positively correlated with  $R$  equal to 0.9893. The Wilcoxon signed rank statistical test between the paired measurements was not significant with  $p = 0.9698$ . Figure 4.5 and Table 4.1 present the correlation between the manual and automatic measurements for the features: U wave amplitudes, T wave amplitudes, R-T intervals, and T-U intervals respectively.

Clearly, there is similarity between the two sets of the measurements (Figure 4.4 and Table 4.1) combined with strong correlation (Figure 4.5) for all the desired features. This indicates that the automatic measurement algorithm performed closely to the standard manual approach. For example, the automatic algorithm underestimated U wave amplitude by an average  $1 \mu\text{V}$  from manual measurement. While for T wave amplitude the mean difference was  $2 \mu\text{V}$ . For the intervals, R-T for both measurements were identical where the average duration was 260 ms, whereas T-U of automatic algorithm underestimated by average 1 ms (see Table 4.1)

**Table 4.1:** Statistical summary of the validation study for manual and automatic measurements of 100 average beats from 10 AF patients using lead V4. *P* value indicates the significance between the paired measurements using the Wilcoxon signed rank statistical test.

Measurement	Manual	Automatic	$\Delta$ value mean $\pm$ SD	<i>p</i> value	Correlation coefficient <i>R</i>
Features	mean $\pm$ SD	mean $\pm$ SD			
U amp ( $\mu$ V)	44 $\pm$ 14	43 $\pm$ 13	1 $\pm$ 3	0.5708	0.9802
T amp ( $\mu$ V)	346 $\pm$ 14	344 $\pm$ 13	2 $\pm$ 4	0.3075	0.9995
R-T (ms)	260 $\pm$ 5	260 $\pm$ 4	0 $\pm$ 2	0.5708	0.9794
T-U (ms)	224 $\pm$ 4	223 $\pm$ 5	1 $\pm$ 2	0.9698	0.9893

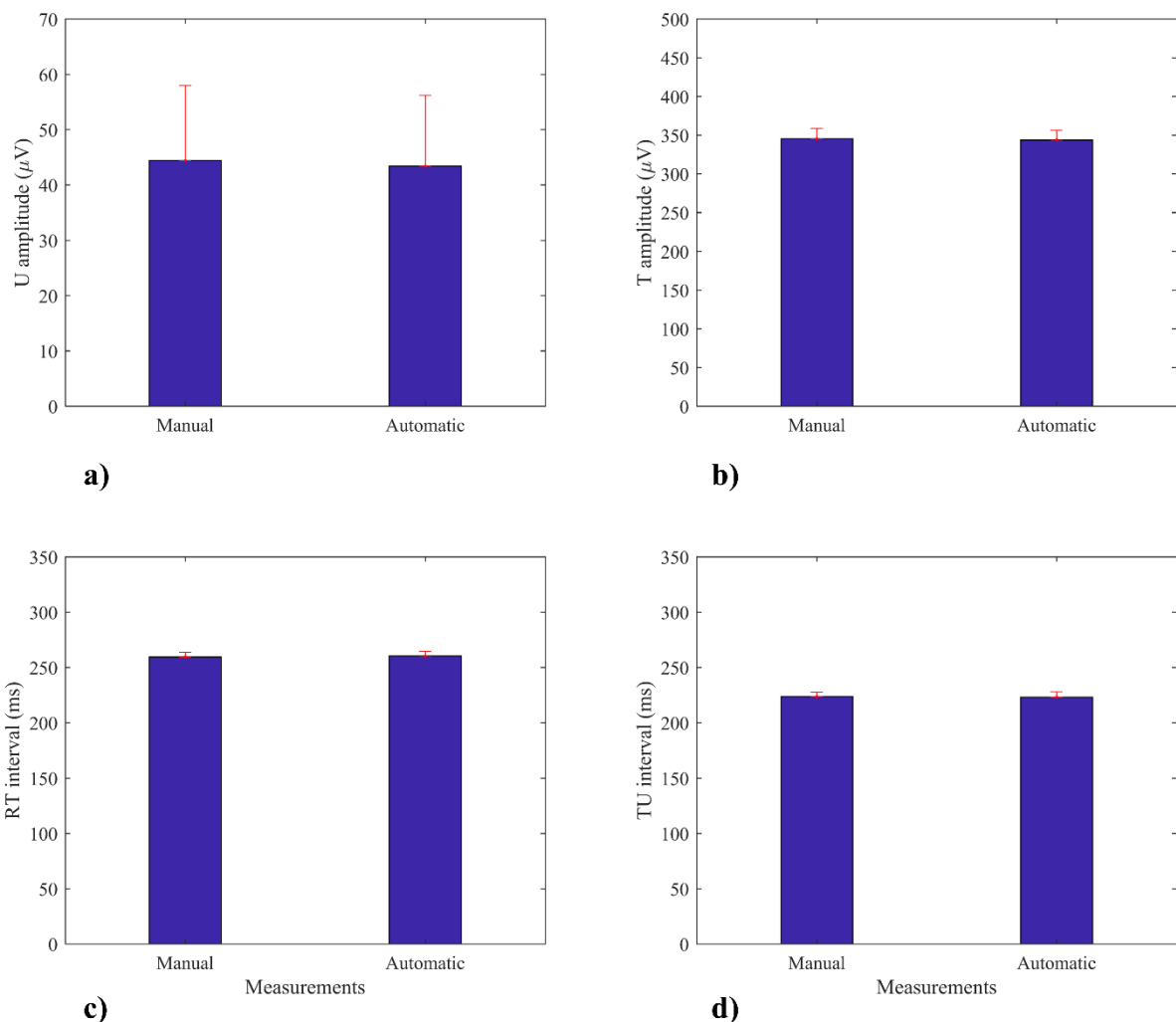


**Figure 4.4:** The automatic and manual measurement results for **a)** U wave amplitude, **b)** T wave amplitude, **c)** R-T interval and **d)** T-U intervals for 100 beats. Bars and whiskers indicate mean and standard deviation (mean  $\pm$  SD) of the values across 100 beats.

### 4.2.2.2. Inter-observer Variation

The repolarisation features measured manually by two observers showed some variation, as expected in any manual measurement, and were positively correlated. Table 4.2 presents the statistics of the measurements of the observer 1 and observer 2. The amplitudes of the waves: U (mean  $\pm$  SD,  $45 \pm 13 \mu\text{V}$  vs  $44 \pm 14 \mu\text{V}$  respectively) and T ( $345 \pm 14 \mu\text{V}$  vs  $346 \pm 14 \mu\text{V}$  respectively), and the interval T-U ( $222 \pm 5 \text{ ms}$  vs  $226 \pm 5 \text{ ms}$  respectively) showed similarity for the measurements of the two observers. The results were positively correlated (Table 4.2) with no statistically significant difference between the paired measurements ( $p > 0.05$ , Wilcoxon signed rank statistical test).

Interestingly, R-T interval presented a significant mean difference ( $p < 0.05$ ) between observers. Figure 4.6 shows the results (mean  $\pm$  SD) for the manually measured features (U and T wave amplitudes, the intervals R-T and T-U), where obviously R-T intervals (Figure 4.6-c) presents differences between observers 1 and 2 ( $265 \pm 5 \text{ ms}$  vs  $254 \pm 5 \text{ ms}$  respectively). On average there was an 11 ms difference in R-T interval measurement between observer 1 and observer 2 (Table 4.2).

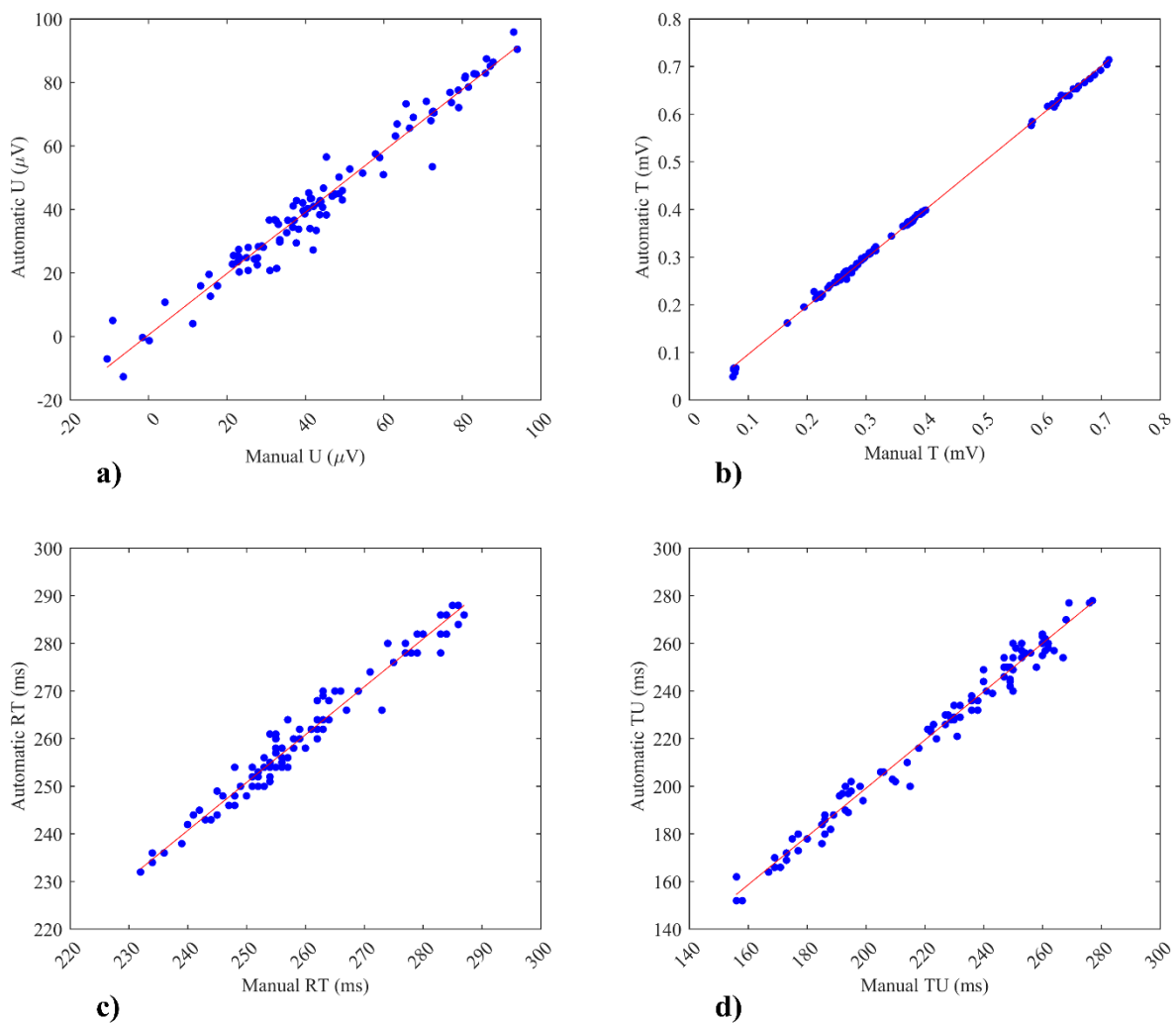
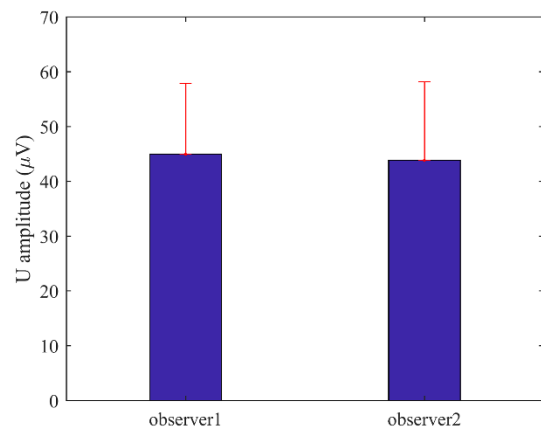


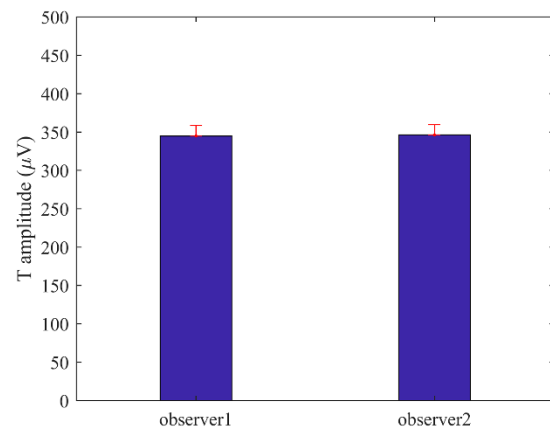
**Figure 4.5:** The correlation between manual (gold standard) and automatic measurements in the validation study for 100 beats. **a)** U wave amplitude,  $R=0.9802$ , **b)** T wave amplitude,  $R=0.9995$ , **c)** R-T interval,  $R=0.9794$  and **d)** T-U interval,  $R=0.9893$ .

**Table 4.2:** Statistical summary for manual measurements of two observers to measure the ventricular features in 100 beats.  $P$  value indicates the significance between the paired measurements using the Wilcoxon signed rank statistical test.

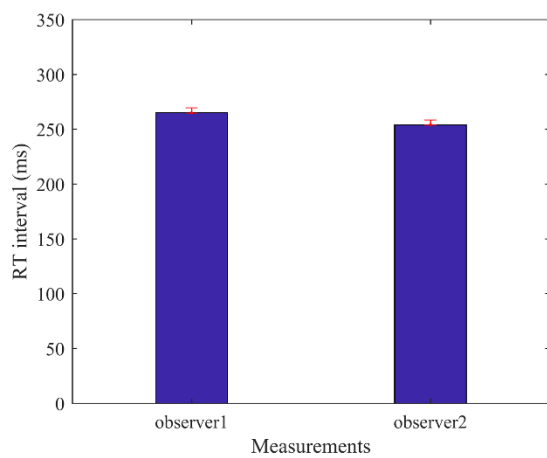
Feature	Observer 1 (PL)	Observer 2 (MSA)	$\Delta$ value mean $\pm$ SD	$p$ value	Interclass correlation (ICC)
	mean $\pm$ SD	mean $\pm$ SD		$p$	$R$
U ( $\mu$ V)	45 $\pm$ 13	44 $\pm$ 14	1 $\pm$ 1	0.1655	0.8392
T ( $\mu$ V)	345 $\pm$ 14	346 $\pm$ 14	-1 $\pm$ 9	0.064	0.801
R-T (ms)	265 $\pm$ 5	254 $\pm$ 5	11 $\pm$ 26	0.0000	0.8622
T-U (ms)	222 $\pm$ 5	226 $\pm$ 5	-4 $\pm$ 25	0.0698	0.7918



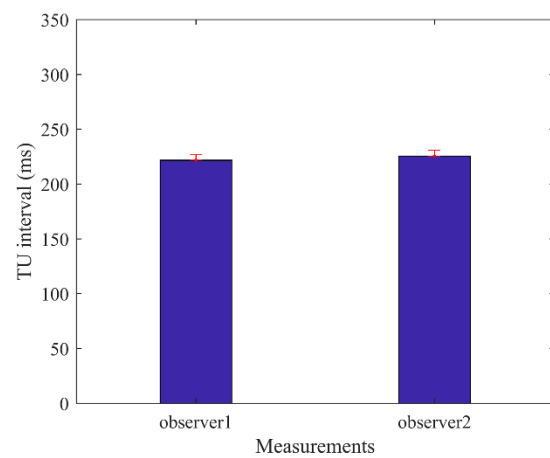
**a)**



**b)**



**c)**



**d)**

**Figure 4.6:** The manual measurements by two observers for **a)** U wave amplitude, **b)** T wave amplitude, **c)** R-T interval and **d)** T-U intervals. Bars and whiskers indicate mean and standard deviation (mean  $\pm$  SD) of the values across 100 beats.

### 4.2.3. Discussion

This study has described the ‘automatic ECG feature measurement algorithm’ developed to quantify ventricular repolarisation features in AF. The algorithm was used to measure U and T wave amplitudes and the intervals R-T and T-U in AF subjects. The algorithm’s ability to automatically measure the ventricular features was validated against a manual measurement for the same features. The manual measurement was implemented by two observers via bespoke software built for ventricular features measurements. The measurements, manual and automatic, were strongly correlated without significant difference between them.

The automatic algorithm showed the ability to process large numbers of beats to measure the repolarisation features in AF, particularly the challenging U wave. Evidently, the algorithm measurements were reliable as they were not statistically significantly different to the manual measurements for the same features.

This indicates that the automatic algorithm is reliable and validated to measure the repolarisation wave amplitudes (U amp and T amp) and the intervals (R-T and T-U). The automatic algorithm underestimated U wave amplitudes by average 1  $\mu$ V, which is a similar magnitude of difference between observers (see Table 4.2). While for T wave the amplitude difference was 2  $\mu$ V compared to 1  $\mu$ V between observers. R-T intervals were identical with no average differences between the manual and automatic measurement. However, there was an average 11 ms difference in R-T interval measurement between observer 1 and observer 2. The R-T interval difference between the two observers is related to the difference of their selections of the peak of T waves. The automatic algorithm underestimated T-U interval by average 1 ms relative to the manual measurement (see Table 4.1), whereas the differences with inter-observer was on average 4 ms (see Table 4.2).

Note that the quality of the averaged beat plays a significant in the peak detection and hence the accuracy of the features’ measurement. This is because the noisy beat leads to a higher amplitude for the detected peak due to the residual noise. Therefore, it is important to ensure averaging a sufficient number of beats to produce high quality beat. For more details, the study in section 4.4 of this chapter has investigated the number of beats required to generate high quality beats using beat averaging algorithm.

The algorithm offers a wide potential to satisfy the need of clinicians and researchers to investigate the repolarisation features including the challenging U wave, and their changes during the repolarisation process in such arrhythmia (AF).

The manual measurement was considered the ‘gold standard’ in the validation study [173]. The manual measurement software was designed with the flexibility to select and inspect the main

ventricular features. Additionally, the software provides the researchers with the potential to inspect features of the end of the T wave (TU nadir).

Although the manual measurement is considered as a gold standard in medical studies, it is subjected to the observers' experience which can provide variation in the results as presented above. Furthermore, manual examination is a time-consuming process for large amounts of data, therefore a validated automated measurement algorithm is needed to facilitate further medical research efficiently, and to ensure repeatable measurements.

The automatic measurement algorithm and the manual measurement software, both can be used to perform further studies to examine the repolarisation processing characteristics. The validation study was implemented using AF recordings; however, the two techniques developed are capable of measuring the repolarisation features in any ECG recordings. Critically, in AF recordings, both techniques require the removal of the atrial fibrillatory wave to achieve accurate detection and measurement for the desired features. This is why beat averaging algorithm was used to pre-process the AF recording before the measurement. Notably, beat averaging algorithm provides a useful tool to clean any recordings from the noise contamination and generate noise free beats.

Building on the results and discussion presented in this chapter, this study has proposed an automatic algorithm to measure the ventricular features in ECG recordings such as AF. The algorithm's automated measurement has been validated against manual measurement for the same features. The 'automatic ECG feature measurement algorithm' provides a useful tool to quantify the repolarisation waves and intervals. Hence, it will be used to measure the desired repolarisation features in the thesis studies.

### **4.3. Validation Study for the Beat Averaging Technique to Extract U Waves in AF Patients by Comparison with U Waves in the Same Patients During SR**

In Chapter one, section 1.3 the importance of being able to measure the U wave was established. It was discussed how the U wave cannot be recognised in AF, and the beat averaging technique demonstrated its ability to clean AF recordings in Chapter three (section 3.2.3).

With good quality SR recordings, the U wave can be easily seen without significant processing. However most clinical recordings present some noise which can also obscure U waves, and by applying the same beat averaging algorithm as for the AF recordings the resulting noise reduction allows for easier identification of U waves. It is hypothesised that U wave is present in SR are also present during AF in the same patient and also that basic U wave morphology such as polarity and amplitude are unchanged by the arrhythmia [1,54].

Having established a suitable technique for removing the atrial fibrillatory waves, the aim of the study is to validate the ‘beat averaging algorithm’ to reveal the U wave, by comparing the U waves extracted from AF recordings to the U waves that are observable in SR recordings for the same patients. This study was part of the published work under the title “*Validation of an algorithm to reveal the U wave in atrial fibrillation*” [1].

#### **4.3.1. Method**

##### **4.3.1.1. ECG Recordings**

The database used in this study was the AF/SR Database described in Chapter 2, section 2.3.2. As a brief reminder it contains data from 25 subjects for which both of AF and SR recordings were available for the same patient.

From this database, of the 11 local hospital recordings, lead V4 was analysed since it has the most prominent U wave [49,54]. Lead V4 was not available in the 14 PhysioNet recordings so the lead with most clearly observable U wave was analysed.

##### **4.3.1.2. ECG Processing**

The beat averaging algorithm was used to clean both the AF and SR recordings. The beat averaging algorithm was described comprehensively in Chapter three (section 3.2.3), however the methodological steps for both phases are described in the following sections since it is necessary to describe specific implementation according to the recording type (i.e. AF or SR).

### 4.3.1.2.1. AF Recording Analysis

The beat averaging algorithm was used to extract U waves from AF recording, by generating an averaged beat clean from the atrial activity using only beats with similar preceding R-R intervals. It is important to note that careful beat selection according the preceding beat interval and the subsequent accurate alignment of these beats is essential to ensure the optimum extraction for U wave and to reduce the heart rate impact on the U wave amplitude and timing. As will be shown in section 5.2.2.1 of Chapter five it is demonstrated that the preceding beat interval is a major determinant of ECG repolarisation characteristics, including the U wave, in AF.

As a reminder for the reader the processing stages illustrating the beat averaging algorithm are shown in Figure 4.7.

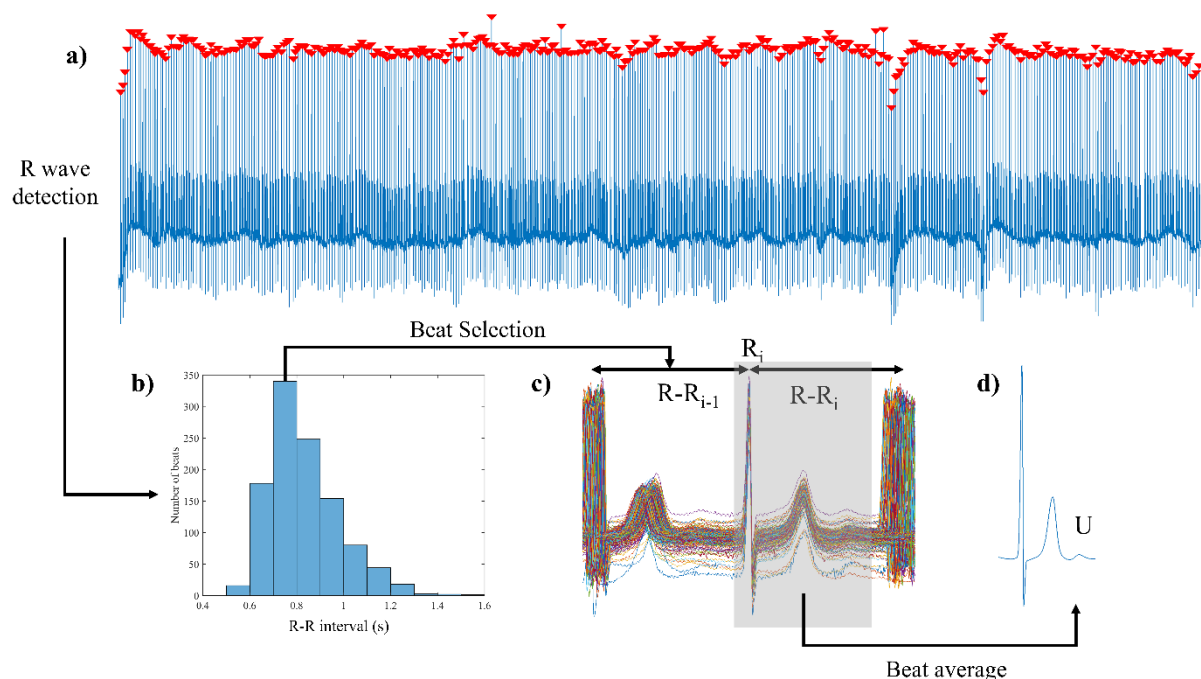


**Figure 4.7:** Signal processing stages to extract U waves from AF recordings. R wave peaks ( $\blacktriangledown$ ) were detected in the ECG lead (a) from which the R-R histogram (bin size  $R-R_{bin} = 100$  ms) was created (b). Beats meeting the selection criteria ( $R-R_{i-1} = R-R_{mode} \pm R-R_{bin}/2$  and  $R-R_i > R-R_{min}$ ) were extracted from the ECG lead and aligned to the R peak ( $R_i$ ) (c). The average beat (d) was calculated from the collection of beats over the interval corresponding to the grey area in (c) revealing the U wave.

The processing stages of average beat calculation consisted of:

- 1) R wave detection  
R wave peaks ( $R_i$ ) were detected automatically and inspected visually, as described in Figure 4.7-a. If present, ectopic beats and their adjacent beats were removed.

## 2) R-R histogram

The R-R intervals were calculated as  $(R-R_{i-1} = R_i - R_{i-1})$ . The R-R histogram with bin size ( $R-R_{bin}$ ) of 100 ms was created (Figure 4.7-b), and that facilitated classifying the number of beats at specific R-R intervals.

## 3) Qualifying beats selections

To ensure the average beat was constructed from the maximum number of beats with similar R-R intervals, ensuring maximum noise reduction, the beats from the R-R bin with the greatest number were selected (Figure 4.7-b and 4.7-c). In other words, the qualifying beats had  $(R-R_{i-1} = R-R_{mode} \pm 50 \text{ ms})$ , where  $(R-R_{mode})$  was the histogram bin with maximum number of beats.

To prevent the contamination of the U wave in the resulting average beat by QRS complexes of beats with short following interval ( $R-R_i$ ), following beats with interval ( $R-R_i$ ) less than a threshold ( $R-R_{min}$ ) of 650 ms were removed.

## 4) Averaged beat calculation and U wave identification.

All qualifying beats were aligned to their R wave peaks ( $R_i$ ) as shown in Figure 4.7-c. The averaged beat was calculated as a mean amplitude, sample-by-sample, across the collected beats (Figure 4.7-d), and the presence of U wave was identified from that generated averaged beat.

### 4.3.1.2.2. SR Recordings Analysis

The U wave can be easily discerned from good quality SR recordings without the need for significant processing. However, clinical recordings usually show some noise such as powerline and electromagnetic artefact and by using the same ‘beat averaging algorithm’ used to clean the AF recordings, such noise can be reduced. That allows the extraction of cleaner U waves. Therefore, SR recordings were processed by the same ‘beat averaging algorithm’ used for the AF recordings. However, it is essential to note that SR recordings have P waves compared to their absence in AF recordings, therefore, at fast heart rates in SR, the P wave can impinge on the U wave, and accordingly it was necessary to extend  $R-R_{min}$  interval to 750 ms to prevent the beat averaged U wave contamination by the following P wave.

### 4.3.1.3. The Validation Assessment

The presence and absence of U waves in the generated averaged beats was assessed visually and independently by two observers (MSA, PL) for each patient for both AF and SR recordings.

The validation assessment was defined according to the criteria: positive validation outcome, according to the presence of U waves having the same polarity in both AF and SR recordings for the same patient, otherwise a negative validation outcome was recorded.

Validation outcomes were collected in a contingency Table, and statistical significance of the agreement between U waves in AF and SR was assessed by McNemar’s test.

#### 4.3.1.4. U Wave Measurement

The difference in U wave amplitudes was assessed in SR and AF from the generated averaged beats. The amplitudes of the U waves were measured automatically and confirmed visually for both recordings in AF and SR for the same patient. Figure 4.8 illustrates the method of U wave measurements in both AF and SR averaged beats.

The amplitude of U wave was measured from the stable baseline to the U wave peak. The stable baseline (ref) was estimated from 10 samples window from the electrically inactive period before the onset of the *QRS complex* in AF recordings (Figure 4.8-a), and before the onset of *P wave* in SR recordings (Figure 4.8-b). The significance of the amplitude differences ( $\Delta$  amplitudes) between the AF and SR recordings was assessed by the paired t-test.

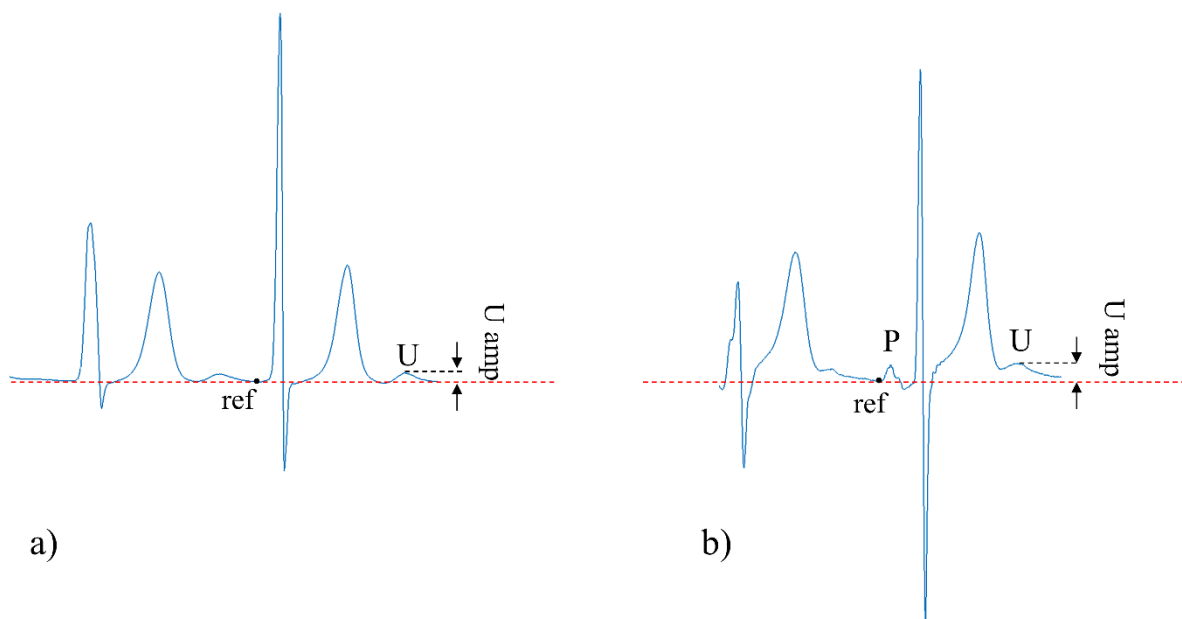


**Figure 4.8:** An illustration for U wave amplitude (U amp) measurement in two generated averaged beats. **a)** averaged beat example from AF recording. **b)** averaged beat example from SR recording from the same patient. ref = reference for the stable baseline amplitude (electrically quiescent period).

#### 4.3.2. Results

From the 25 patients processed for which recordings of AF and SR were available, 3 patients were excluded because the rapid heart rate during SR obscured the potential U waves by the following P waves in these patients.

After applying the ‘beat averaging algorithm’ to the AF and SR recordings to the remaining 22 patients, the results showed that all 22 patients had observable U wave in both AF and SR recordings. There were no discrepancies of reporting U waves presence between the two observers (MSA, PL).

Table 4.3 displays the contingency Table for the extracted U wave from AF and SR recordings. The statistics showed there is no significant difference in the presence of U wave in AF compared to SR in the same patients ( $p=0.88$ ) assessed by McNemar’s test.

**Table 4.3:** Contingency table of presence of U waves in AF and SR for 22 subjects of the validation study (McNemar’s test).

ECG	Visible U wave		Total
	Yes	No	
AF	22	0	22
SR	22	0	22
Total	44	0	44

Figure 4.9 demonstrates a representative example of the U wave extraction from AF and SR recordings for the same patient. The difficulties of discerning the U wave in AF are illustrated in Figure 4.9-a. It displays a 5 second period of ECG in which the irregular beat intervals and atrial fibrillatory wave cover the underlying U wave. However, after applying the beat averaging algorithm to the record, the U wave was revealed as shown in Figure 4.9-b. The U wave extracted from the AF recording is clear and, as expected, follows the T wave. Validation of the algorithm is provided in Figure 4.9-c and d which presents a 5 s period and average beat respectively for the same patient but in SR. The extracted U wave by the algorithm in AF were of the same polarity and morphology to that extracted from the SR recording, but with larger amplitude.

Note that 3 patients were removed from the study since they had no observable U wave during SR due to fast heart rate. Having applied the beat averaging algorithm to the AF recordings for these 3 patients, U waves were visible in the corresponding AF recordings. Figure 4.10 shows an example for one of these patients where, after application of the beat averaging algorithm, the AF recording had discernible U wave, whereas the SR recording had no observable U wave. The fast heart rate during SR is likely the reason that the U wave cannot be seen as it may be obscured by the P wave of the next cardiac cycle.

The U wave amplitudes showed a wide range between the patients for both AF and SR recordings. Figure 4.11 presents the paired relationship between the U wave amplitudes in SR and AF recordings. The amplitudes of U waves during AF were significantly larger than during SR (mean (SD), 55(39) vs 37(28)  $\mu\text{V}$ ,  $p=0.005$ ), with most patients (16/22, 73%) having larger U wave during AF in comparison to SR. This may imply a rate dependency of U wave since the average R-R in AF was 780 ms whereas in SR was 909 ms.

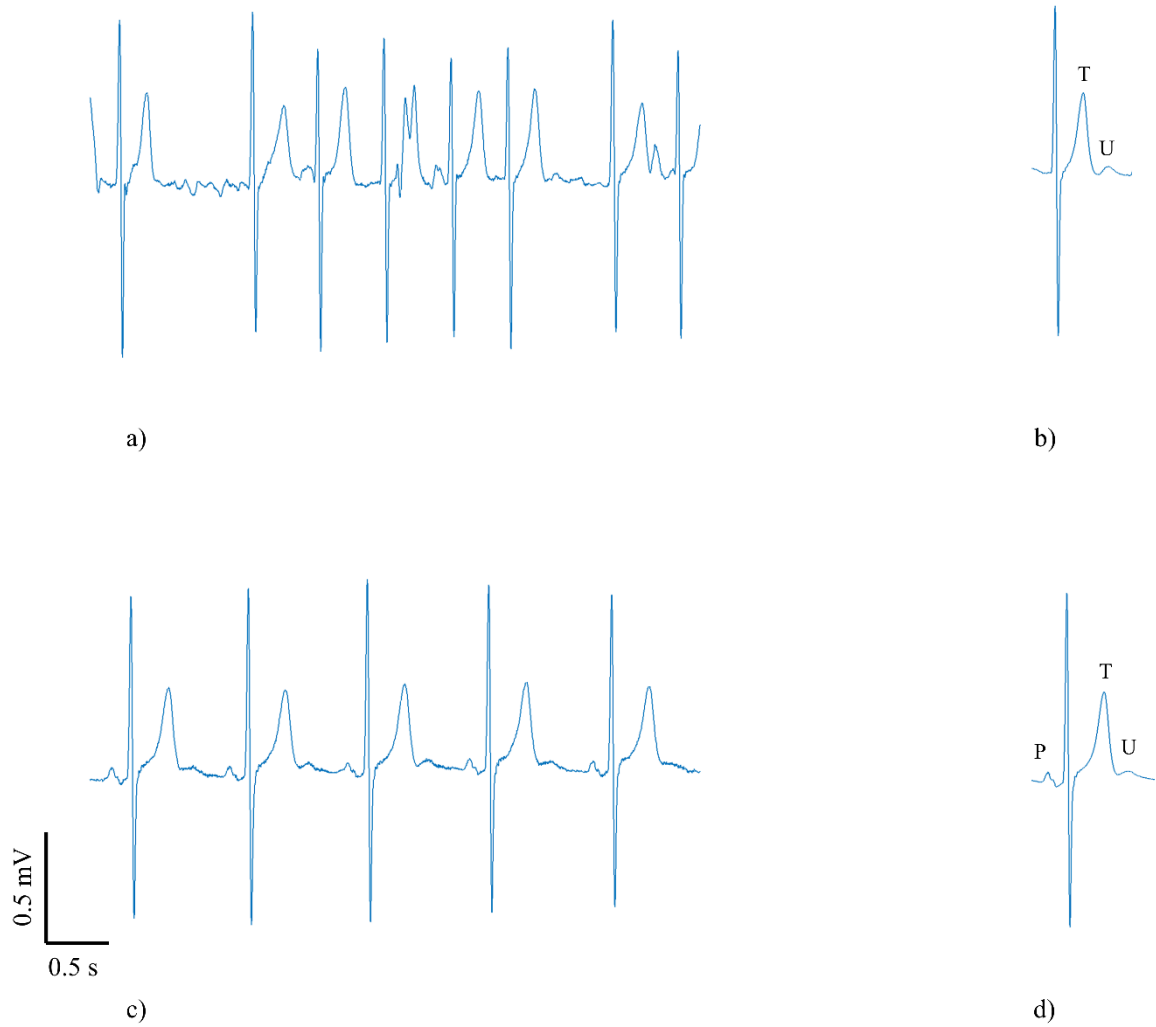


**Figure 4.9:** Example to illustrate the presence of U waves in a patient in both AF (top row) and SR (bottom row). **(a)** 5 s interval of ECG in AF in which it is impossible to discern the U waves and **(b)** the corresponding extracted average beat in AF with clear U wave following the T wave. **(c)** 5 s interval of ECG of the same patient during SR demonstrating clear U waves at each beat and **(d)** the corresponding average beat in SR showing a clear U wave with the same polarity and morphology as those in (b) and (c).

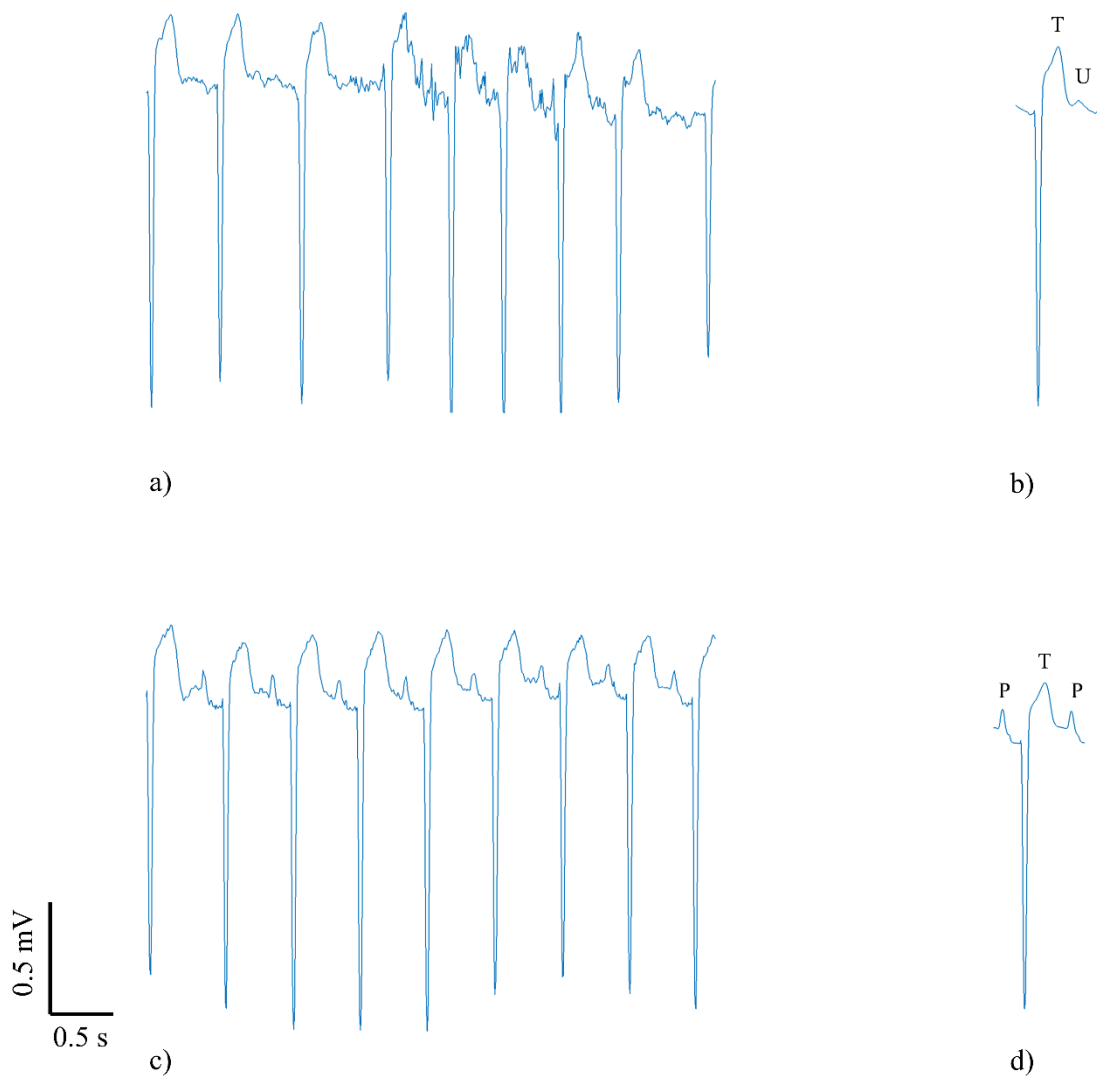


**Figure 4.10:** Example to illustrate the presence of U waves in a patient in AF (top row) and the apparent absence of U wave in SR (bottom row). **(a)** 5 s interval of ECG in AF in which it is impossible to discern the U waves and **(b)** the corresponding extracted average beat in AF with clear U wave following the T wave. **(c)** 5 s interval of ECG of the same patient during SR with no visible U waves at each beat and **(d)** the corresponding average beat in SR also showing no U wave. The U wave in SR is probably hidden by the following P wave of the next cardiac cycle.

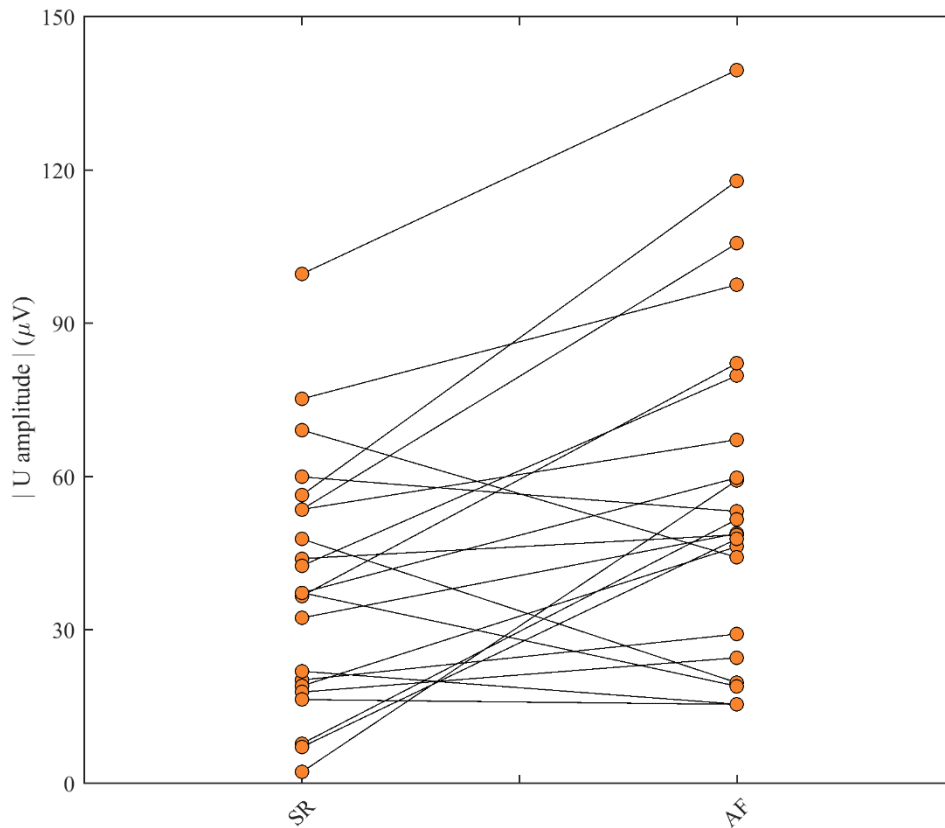


**Figure 4.11:** A paired comparison of U wave amplitudes measured during SR and AF for 22 patients in the validation study.

### 4.3.3. Discussion

This study validates the beat averaging algorithm as a method to reveal U wave in AF patients. Clearly, in all 22 patients U waves were observable during the episodes of AF recordings for which U waves could also be recognised in the corresponding SR recordings in the same patients.

U waves in AF had the same polarity and morphology as those in SR, but with larger amplitudes in majority of the subjects. Certainly, the increased amplitude in AF could not be regarded as the residual noise including atrial fibrillatory waves since none could be seen in the generated averaged beats after close visual inspection as presented in Figure 4.9. However, it might be due to the differences in heart rate ( $1/R-R$ ), where average R-R in AF was 780 ms whereas in SR was 909 ms if U wave is rate dependent. The rate dependency of ventricular repolarisation features is quantified in Chapter 5.

The U waves have rarely been described in patients with AF, and that is not surprising because of the measurement difficulties due to the atrial activity that masks U waves in AF. Now, with the beat averaging algorithm capability to clean the AF recordings from the fibrillatory waves, U wave can be detected and measured, which provides wide opportunities. First, for researchers

to explore possible mechanisms which might explain differences in U waves during AF and SR. Second, for clinicians to determine the extent of U wave abnormalities in AF patients, including those with permanent AF.

Interestingly, after applying the beat averaging algorithm to 3 patients, who showed no visible U wave in their SR recordings, a U wave was discernible in the corresponding AF recordings. Figure 4.10 illustrates an example of one of those patients. Although U waves could not be seen in these 3 SR recordings, it is likely that U waves were existent but buried by the P wave of the next cardiac cycle. Surawicz reported that U waves cannot be distinguished with fast heart rates [48].

The beat averaging algorithm satisfies a clinical need as it has been difficult to observe U wave in atrial fibrillation. Many studies had reported the importance of the U wave abnormalities and its diagnostic value, especially inverted U waves [52,86,87]. Although there was no detection for any U wave's abnormalities during the analysis, the algorithm has the capability to reveal abnormal U waves in AF patients as has been recommended by the major cardiac organisations [49,52]. As a minor limitation, since the algorithm generates an averaged beat by averaging a collection of beats, it is unlikely to detect U abnormalities with changing morphology beat by beat.

Moreover, the algorithm enables a wider insight to understand the genesis of U wave since AF is unique in its characteristics (i.e. rapid changing beat intervals) and can provide a useful model to study U waves in such condition. Interestingly, the preceding R-R interval is known to influence the dynamics of ventricular fillings [49,175,176], which may link to the genesis of U waves through the electro-mechanical hypothesis of the U wave [48,51,63]. The effect of changes in beat interval on ECG repolarisation characteristics, including U wave, are explored in section 5.2 of Chapter five.

In conclusion, the ventricular beat averaging algorithm developed in this project reveals U waves in AF patients and has been validated against SR recordings in the same patients. The amplitudes of U wave were larger than during SR. The algorithm enables the detection and reporting of U wave and their abnormalities in AF patients.

#### **4.4. The Number of Beats Required to Remove the Atrial Fibrillatory Activity to Allow the Effective Measurement of the U Wave in AF**

The beat averaging algorithm has been validated as an effective technique, allowing the extracted U wave to be successfully observed in the averaged beat. The algorithm provides ventricular beats with reduced atrial fibrillatory activity which can facilitate further studies into the repolarisation process and the ventricular features in AF, specifically U waves and T waves. U waves are particularly challenging due to their low amplitude.

The effectiveness of the technique relies on the accurate alignment and averaging of a number of ventricular beats, and consequently, the amplitude of the uncorrelated noise is reduced while the desired U wave is revealed in the resulting averaged beat. It has been hypothesised that the noise reduction level is dependent on the number of the averaged signal epochs [1,177,154], hence, the ‘number of beats’ is a key factor affecting directly the quality of the averaged beats, and accordingly the quality of resulting U wave.

Therefore, it is important to define the requirement for the number of beats needed for the beat averaging algorithm to generate averaged beats with sufficiently reduced atrial fibrillatory activity to enable effective extraction of U waves in AF. In fact, a large number of averaged beats may yield high level noise reduction but collecting a large number of beats requires long duration for ECG recordings in patients. Therefore, it has important implications for the clinical application of the algorithm since the number of beats determines the ECG recording duration.

Thus, the aim of this study was to establish the ‘number of beats’ that are required to extract U waves effectively using the beat averaging algorithm during AF. The approach was to generate an average beat from a large number of individual beats which benefits from high noise reduction (i.e. reduction of the contaminating AF activity). This is referred to as the *reference beat*. Then, average beats were generated using systematically reduced numbers of individual beats and compared to the *reference beat* in terms of U wave amplitude. It was hypothesised that as the number of beats used to generate the average beat is reduced, the U wave amplitude would increase due to higher levels of noise in the resulting average beat.

The study was part of the published research under the title “*Validation of an algorithm to reveal the U wave in atrial fibrillation*” [1].

## 4.4.1. Method

### 4.4.1.1. ECG Recordings

The analysis required long ECG recording durations in order to secure a large number of beats. Therefore, the Long Duration AF Database described in section 2.3.1 of Chapter two was used in this study. The dataset includes 12-lead ECG from 10 AF recordings, and lead V4 was analysed for this study.

### 4.4.1.2. ECG Processing

The ‘beat averaging algorithm’ was used repeatedly, each time with a reducing number of beats used to generate the average beat, to investigate the effect of the number of beats ( $N_{\text{beats}}$ ) on the revealed U wave in AF.

It is important to provide as many beats as possible during the analysis and the maximum number of beats at any particular preceding R-R interval is dependent upon two factors; i) the duration of the ECG recordings, and ii) the bin size used to collect the beats with specific R-R interval (i.e.  $R-R_{\text{bin}}$ ). These will be explained in the following methodological sections.

The methodology stages for this study were divided into three:

- a) ECG pre-processing
- b) Average beat generation using different numbers of beats in the beat averaging algorithm
- c) An assessment of the relationship between the resulting U wave amplitudes against the number of beats used

Fundamentally, in the ECG pre-processing stage (a), beat averaging algorithm used to remove atrial fibrillatory waves from AF recordings and provide clean ventricular beats. Below, the beat averaging algorithm is highlighted describing the changes required during the processing in order to collect and then generate the desired beats. However, the full methodological steps for beat averaging algorithm were described in section 3.2.3 of Chapter three. In stage (b) U waves were generated and measured using defined number of beats; and in final stage (c) the relationship between U wave amplitudes and number of beats was assessed.

It was hypothesised that as the number of beats used to generate the average beat reduced, U wave amplitude would increase due to higher levels of noise in the resulting average beat. This was expected since the automatic U wave measurement algorithm detects the peak (i.e. maximum) value, so any noise can be expected to increase the U wave amplitude depends upon frequency of noise. Therefore, relative to the U wave amplitude of the *reference beat*, a higher amplitude indicates U wave acquired some noise.

The three stages are described as following.

### **a) ECG pre-processing**

The processing in this stage is identical to the processing in section 4.3.1.2.1 of this chapter where AF recordings were analysed to remove atrial activity via beat averaging algorithm.

It is important to note the *size* of R-R<sub>bin</sub> (check Figure 4.7 in Section 4.3.1.2.1 of this chapter) was widened from 50 ms (the default algorithm bin size) to 100 ms, the reason was to collect more beats for defined R-R interval since the number of collected beats depends on the bin size. The potential consequence of this is that there is more dispersion of wave features in the average beat.

### **b) Average beat generation from different number of beats**

From the R-R bin with the maximum number of beats (Max N<sub>beats</sub>), 100 beats were collected. It is important to note that, across all recordings the maximum bin count was at least 100 beats so 100 beats were taken as the maximum number of beats to generate the reference average beat.

The beat averaging algorithm was systematically iterated with decreasing number of beats used for the averaging in each iteration, and the 100 beats considered a (reference) in the study. Trials were conducted where the number of beats was systematically reduced from 100 beats (reference) in steps of 10 down to 10 beats (i.e. N<sub>beats</sub> = {100, 90, 80, 70, 60, 50, 40, 30, 20, 10}).

Rather than remove some beats for trials where N<sub>beats</sub> was less than 100, multiple sub-trials were conducted in which all 100 beats were analysed across all the sub-trials. This was achieved by dividing the 100 beats into adjoining groups of 10 beats. For each N<sub>beats</sub> trial, 10 sub-trials were conducted, systematically including the suitable number of groups of 10 beats so by this within the 10 trials all the beats were used, as the example in Figure C.1 in appendix C shows.

At the end of stage b, 10 U waves were acquired, and their amplitudes were measured including the reference U (U amp<sub>reference</sub>).

### **c) Differences of U wave amplitudes**

The differences between U wave amplitudes for each N<sub>beats</sub> trail and the U amp<sub>reference</sub> (N<sub>beats</sub> = 100 beats) were calculated as  $\Delta U \text{ amp} = U \text{ amp} (N_{\text{beats}}) - U \text{ amp}_{\text{reference}}$ . The statistical difference with the respect to the zero mean amplitude difference was assessed by ‘within subject ANOVA’ and post-hoc *t*-test. The *p* value less than 0.05 considered statistically significant and all tests were two sided.

#### 4.4.2. Results

The analysis showed that changing number of beats ( $N_{\text{beats}}$ ) used to generate the averaged beat influences the extracted U wave amplitudes for all recordings. Figure 4.12 illustrates the effect on the U wave amplitudes by changing the number of beats (from 100 to 10 beats) used to construct the averaged beats for all 10 AF patients. Each subplot represents one AF patient. In all cases, the effect of decreasing the number of beats from 100 beats ( $N_{\text{beats}} = 100$ ) to 10 beats was to increase the U wave amplitudes gradually.

Combining all the subjects and analysing the difference of U wave amplitudes ( $\Delta U$  amps) relative to the reference U amplitudes ( $U \text{ amp}_{\text{reference}}$ ), Figure 4.13 shows there was a gradually increasing amplitude difference as the number of beats was reduced. The mean amplitude difference was  $5 \mu\text{V}$  when using 10 beats rather than 100 beats to generate the averaged U wave, which implies that the noise amplitude increased by average  $5 \mu\text{V}$ .

The statistics showed that the mean amplitude differences were significantly greater than zero across the trials ( $p=0.0000183$ , within subject ANOVA). In addition, the post-hoc analysis showed that there were no significant differences in the amplitudes with respect to the reference when at least 70 beats were used (mean (SD)  $\Delta U$  amps =  $0.2(0.4) \mu\text{V}$ ,  $N_{\text{beats}}=70$  beats,  $p=0.1063$ ). Figure 4.14 demonstrates three averaged beats generated from the same AF recording by averaging (a) 100 beats (b) 70 beats and (c) 10 beats. The averaged beats in (a) and (b) were almost identical, with clean U wave, whilst the averaged beat in (c) shows increment in the noise level however the U wave presence is readily discernible. The residual noise had high frequency, so was unrelated to the atrial fibrillatory activity.

When expressed as a percentage of the U wave reference amplitude, the mean amplitude increase was less than 1% when using 70 or more beats and was 14% when using only 10 beats. However, as is illustrated in Figure 4.14 U waves could be seen in some subjects even when 10 beats ( $N_{\text{beats}}=10$ ) were used regardless of the increase of the noise level.

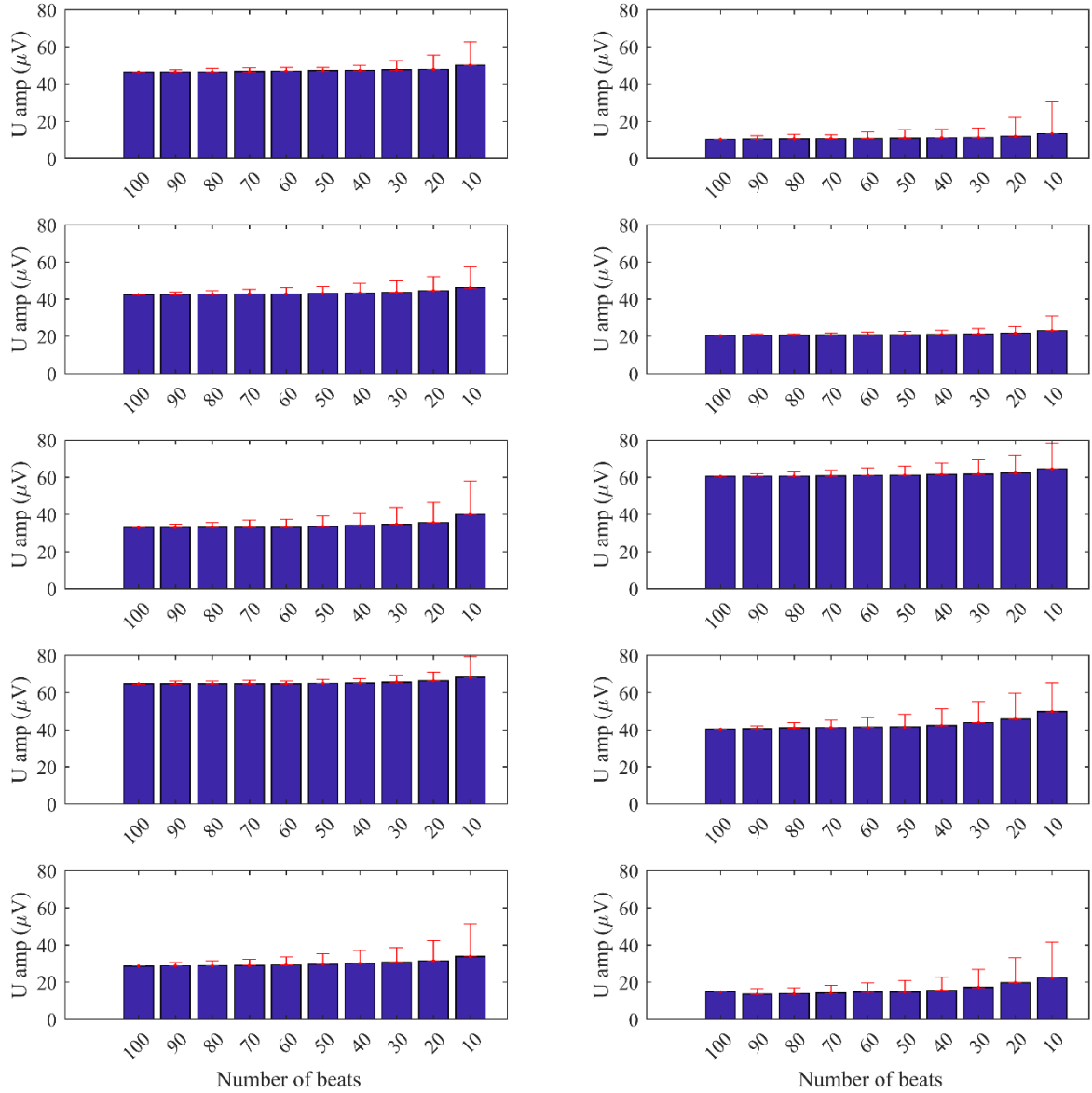


**Figure 4.12:** The U wave amplitudes (U amp) for 10 AF patients, each subplot represents one patient. The effect on U wave amplitude by reducing the number of beats from 100 to 10 used to generate the averaged beat is presented. Bars and whiskers indicate mean and standard deviation of amplitude across the 10 sub-trials for  $N_{\text{beats}} = \{90, 80, 70, 60, 50, 40, 30, 20, 10\}$ .

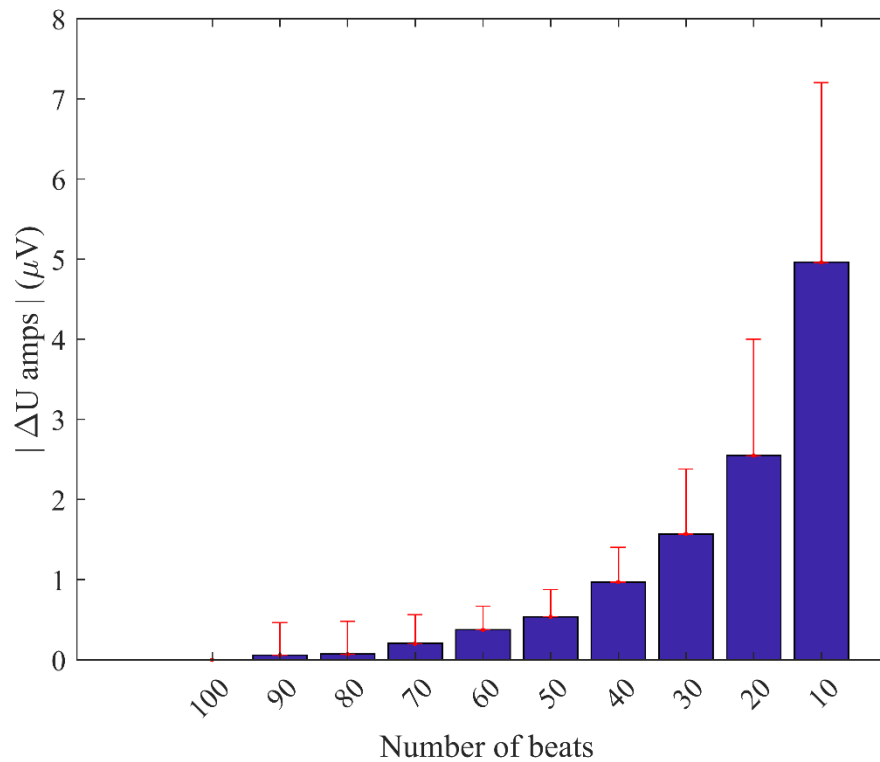


**Figure 4.13:** The difference in U wave amplitudes ( $\Delta U$  amps) relative to the reference amplitude ( $U \text{ amp}_{\text{reference}}$ ,  $N_{\text{beats}} = 100$ ) for reducing number of beats ( $N_{\text{beats}} = 90, 80, 70, 60, 50, 40, 30, 20, 10$ ). Bars and whiskers indicate mean and standard deviation of amplitude difference across the 10 patients.

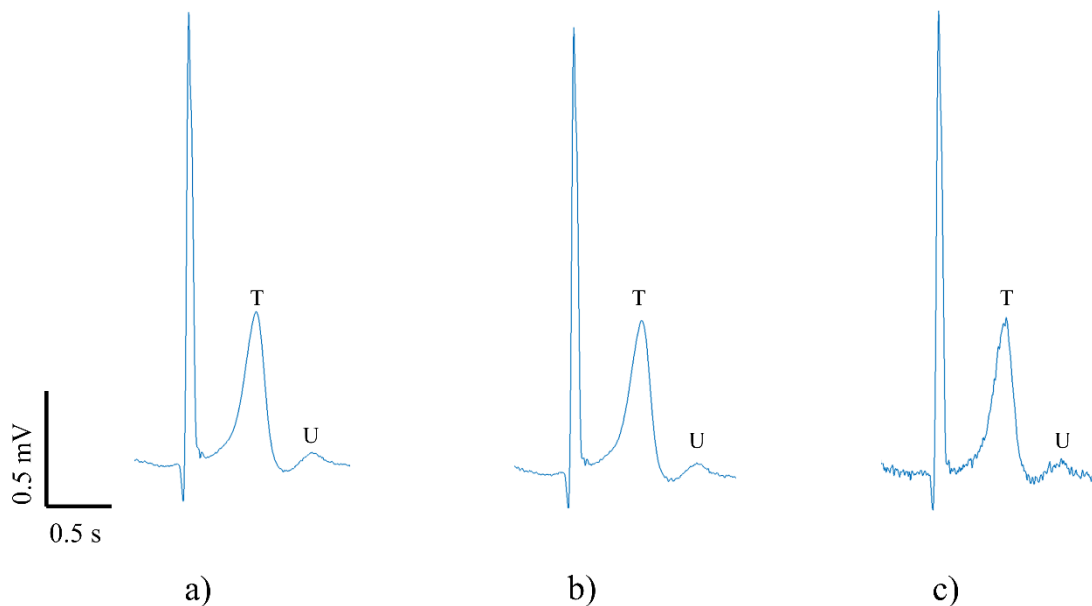


**Figure 4.14:** Three averaged beats generated from the same AF recording by averaging **a)** 100 beats, **b)** 70 beats and **c)** 10 beats. Increased noise level can be seen in **c)**, but the U wave is readily discernible.

### 4.4.3. Discussion

The ‘number of beats’ is a fundamental part to calculate the averaged beats using the developed beat averaging algorithm. The quality of these generated averaged beats depends on the number of beats that used for their calculation and hence U wave quality. The greater the number of beats, the greater the noise reduction. On the other hand, the greater the number of beats, the longer duration of recording which is required with associated resource implications. Therefore, it is important to identify the required number of beats that is effective for revealing the U wave in AF patients.

The ‘number of beats’ study showed that decreasing the number of beats from 100 to 70 did not significantly affect the U wave amplitude. However, in some recordings the U wave was effortlessly observable when the average beat was generated from few beats such as 10 beats with an average increase in noise amplitude of only 5  $\mu\text{V}$  or 14% of reference amplitude.

It is important to note that the data used are standard clinical recordings, and as such will be subject to typical clinical noise levels. Hence, the results should be generally applicable.

The data used are standard clinical recordings, and therefore they will be subject to different typical clinical noise levels (such as movement artifact, breathing artifact, powerline interference and muscle noise) [152]. The low amplitude noise such as atrial activity corruption with the frequency band of the signal and may completely obscure the signal. Thus, conventional filtering schemes fail when the signal and noise frequency spectra significantly overlap. Signal averaging is a noise reduction technique that has been widely adopted for use with repetitive physiological signals (e.g. ECG) without introducing signal distortion. Hence, the results should be generally applicable.

The beat averaging algorithm exploits the fact that the U wave is reliable, invariant feature in its occurrence in every ventricular beat at the end of the ventricular cycle after the T wave. In theory, the reduction of noise level, depends on the number of averaged signal epochs, where it can be reduced by a factor of  $\sqrt{N}$  where  $N$  is the number of epochs [152,177]. By averaging, the total noise components in the averaged ECG signal are reduced since the ECG features (including U wave) are uncorrelated to the noise (which includes the atrial fibrillatory waves). The noise is effectively averaged out depending on the number of ventricular beats.

It is the noise nature that makes signal averaging useful. Each time epoch (i.e. R-R) is intentionally aligned with the previous epochs so that the digitised samples from the new epoch are added to the corresponding samples from the previous epochs. Thus, the time-aligned repetitive signals  $S$  in each epoch are added directly together so that after 10 epochs (as an example), the signal amplitude is 10 times larger than for one epoch ( $10S$ ).

If the noise is random and has a mean of zero and an average rms value  $Noise$ , the rms value after 10 epochs is the square root of the sum of squares (i.e.  $\sqrt{10Noise^2}$ ). In general, after  $N$  repetitions the signal amplitude is  $NS$  and the noise amplitude is  $\sqrt{N} Noise$ . Thus, the SNR improves as the ratio of  $N$  to  $\sqrt{N}$  [154].

For example, averaging 100 repetitions of a signal improves the SNR by a factor of 10. This can be proved mathematically in appendix D [154].

Note that, the selection of 100 beats as reference was taken because of the unavailability of longer recordings for all AF subjects. Additionally, since in general lead V4 produces higher amplitude U waves than the other leads [17,31,54,49] it was used in the analysis.

This study has shown that the number of beats used to generate the average beat is an important consideration. The results can be used to guide the requirement for the number of beats to use for the medical investigations dependent upon the required application but in general U waves can be revealed with relatively low numbers of beats.

## 4.5. Chapter Summary

Three studies were conducted in this chapter. The *first* study (section 4.2) has proposed an automatic algorithm to measure the ventricular features in ECG recordings. The algorithm's automated measurement has been validated against manual measurement for the same features. The 'automatic ECG feature measurement algorithm' provides a useful tool to quantify the repolarisation waves and intervals. Therefore, it will be used to measure the desired repolarisation features in the thesis studies.

In the *second* study (section 4.3), the developed ventricular beat averaging algorithm reveals U waves in AF patients and has been validated against SR recordings in the same patients. The study showed the amplitudes of U wave were larger in AF than during SR. The algorithm enables the detection and reporting of U wave and their abnormalities in AF patients.

The *final* study (section 4.4) has shown that the number of beats used to generate the average beat is an important consideration for the beat averaged quality and hence extracted U wave. The results can be used to guide the requirement for the number of beats to use for the medical investigations dependent upon the required application but in general U waves can be revealed with relatively low numbers of beats.

## **Chapter 5**

# **Investigation of Rate Dependency of Ventricular Repolarisation Features in Atrial Fibrillation Patients and Healthy Subjects**

## **Chapter 5. Investigation of Rate Dependency of Ventricular Repolarisation Features in Atrial Fibrillation Patients and Healthy Subjects**

### **5.1. Introduction**

The beat averaging algorithm is exploited in this chapter to investigate beat interval dependency of ventricular repolarisation features in AF and healthy subjects.

The chapter includes two studies. The *first study* inspects the effect of beat interval on ventricular repolarisation characteristics in AF. The *second study* examines the effect of the heart rate changes due to exercise on U and T waves amplitudes in healthy subjects.

The rate dependency of the features in AF and healthy subjects are compared and provide evidence consistent with the mechano-electrical coupling influence on ventricular repolarisation features.

## **5.2. The Effect of Beat Interval on Ventricular Repolarisation Characteristics in Atrial Fibrillation**

As was discussed in section 1.5.2.1, AF is characterised by rapid changes in beat intervals from one beat to the next. Here this characteristic was exploited to investigate the effect of such rapid beat interval changes on ventricular repolarisation characteristics in AF. It was hypothesised that ventricular repolarisation characteristics such as T and U wave amplitudes and intervals exhibit a beat interval dependency. This dependency was confirmed by the present study. By reviewing potential mechanisms, it is postulated that ventricular filling and stretch, mediated by the preceding beat interval, are major determinants of ventricular repolarisation characteristics in AF. The aim of this study is to investigate the effect of the preceding and current beat interval changes on the repolarisation features in atrial fibrillation.

### **5.2.1. Methods**

#### **5.2.1.1. ECG Recordings**

The study required long duration ECG recordings to provide a large number of beats over a range of beat intervals. Thus, the Long Duration Database described in section 2.3.1 of Chapter two was used in this study. It contains 12-lead ECGs of 10 AF patients.

#### **5.2.1.2. ECG Processing**

The beat averaging algorithm was used in this analysis to clean AF recordings and generate clean averaged beats free from the atrial activity.

Each lead of the 12-lead ECG AF recording was analysed to generate 10 averaged beats formed using only beats with similar preceding beat interval (R-R). The preceding beat intervals were defined within ranges  $R-R \pm 25$  ms duration centred on 625, 675, 725, 775, 825, 875, 925, 975, 1025 and 1075 ms. Details of the averaging process have been extensively described in section 3.2.3 and the workflow of the ECG processing was illustrated in Figure 3.11 of Chapter three.

It was discussed in section 4.4 of Chapter four that the quality of the averaged beat is subject to the number of beats used to generate the average beat, i.e. the greater the number of beats employed for averaging, the higher quality of the resultant averaged beat. Therefore, in the current study only averaged beats generated from 10 or more individual beats were analysed.

From each average beat the main ventricular repolarisation features U and T wave amplitudes and intervals were inspected visually but detected and measured automatically by the automatic feature measurements algorithm described in section 4.2.1.2.2 of Chapter four. To highlight the measurement method, the amplitudes for U wave (U amp) and T wave (T amp) were

calculated from a stable baseline to their peaks. The stable baseline was estimated from a 10 samples window before the onset of the QRS complex. The intervals R-T and T-U were calculated as the duration between their peaks respectively. Figure 5.1 illustrates the features measured.

Additional data was provided by the manual measurement described in section 4.2.1.2.3 of Chapter four. Manual measurements of the TU nadir (amplitude and timing) were also analysed. However, these measurements were only available in a single lead, lead V4.

### **5.2.1.3. Statistical Analysis**

Boxplots of the change in measured features relative to the shortest beat interval bin ( $625 \pm 25$  ms) were used to show the relationship between the ventricular repolarisation characteristics and beat interval.

Statistical analysis was facilitated by grouping the measurements from the 10 beat interval bins into two groups: ‘Short R-R’ containing beat interval bins centred on 625, 675, 725, 775 and 825 ms, and ‘Long R-R’ containing beat interval bins centred on 875, 925, 975, 1025 and 1075 ms.

The terms ‘Short R-R’ and ‘Long R-R’ are subsequently used to refer to these two R-R interval groups. For each set of measurements (amplitudes and intervals) that related to ‘Short R-R’ and ‘Long R-R’, the mean, standard deviation (mean  $\pm$  SD) were calculated across the 10 AF patients for each lead (reported in the Tables 5.1 – 5.6 and the paired non-parametric Wilcoxon signed rank test was used between the paired groups in the tables).

Also, the differences in the mean amplitudes of U and T waves (designated  $\Delta$ ) were calculated (see Figures 5.4 and 5.6).

The statistical difference in the measured amplitudes and intervals of ventricular features was assessed by within subject ANOVA (i.e. the measurement (amplitudes or durations) in each lead was tested across 10 R-R intervals for 10 subjects using ‘within subject ANOVA’ test).

Additionally, to test the significance of rate dependent difference between U wave and T wave amplitudes (delta U and delta T in Figure 5.8), the paired non-parametric Wilcoxon signed rank test was used.

All statistical tests were two sided and  $p$ -values less than 0.05 considered statistically significant.

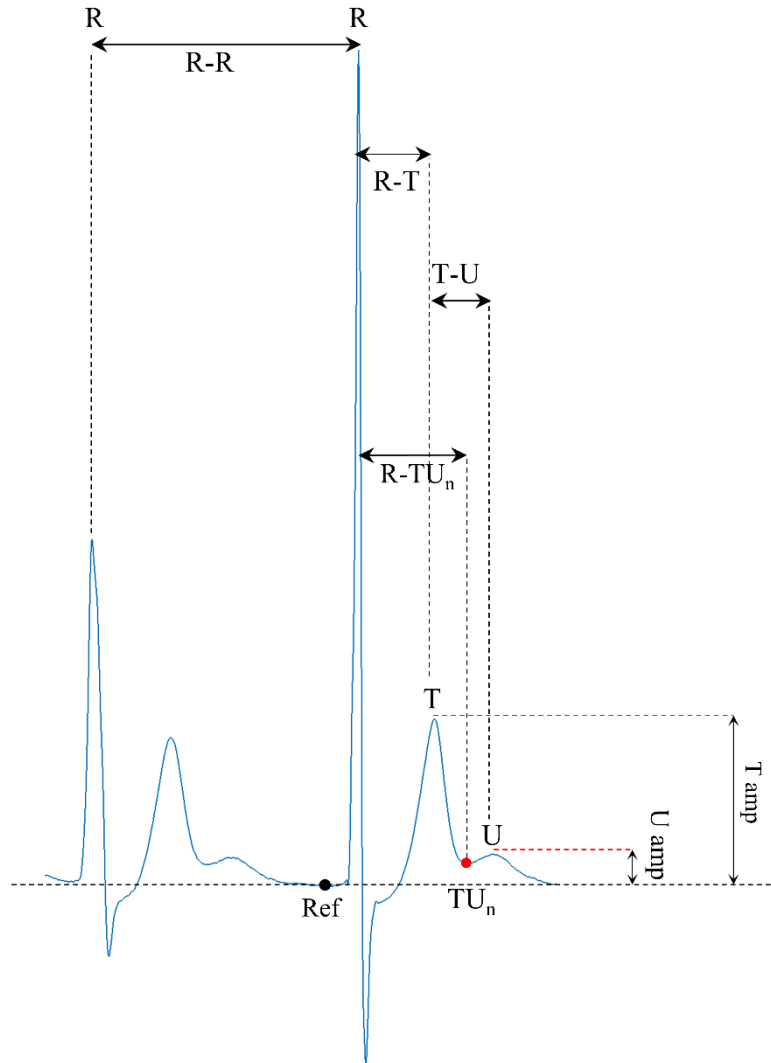


**Figure 5.1:** Illustration of the ventricular repolarisation characteristics of an average beat, indicating U wave amplitude (U amp), T wave amplitude (T amp), R-T interval (R-T) and T-U interval (T-U). Ref represents the reference for a stable baseline amplitude (electrically quiescent period).

#### 5.2.1.4. 'Preceding' vs 'Current' Beat Interval

So far in this thesis the importance of collecting beats of similar R-R interval from the *preceding beat* has not been demonstrated. To address this, the analysis described above (sections 5.2.1.2 and 5.2.1.3) was repeated but instead of generating average beats from collections of individual beats with similar *preceding* R-R interval, average beats were generated from collections of individual beats with similar *current* R-R interval. This distinction is illustrated in Figure 5.2. As a sub-study this part of the analysis was restricted to lead V4.

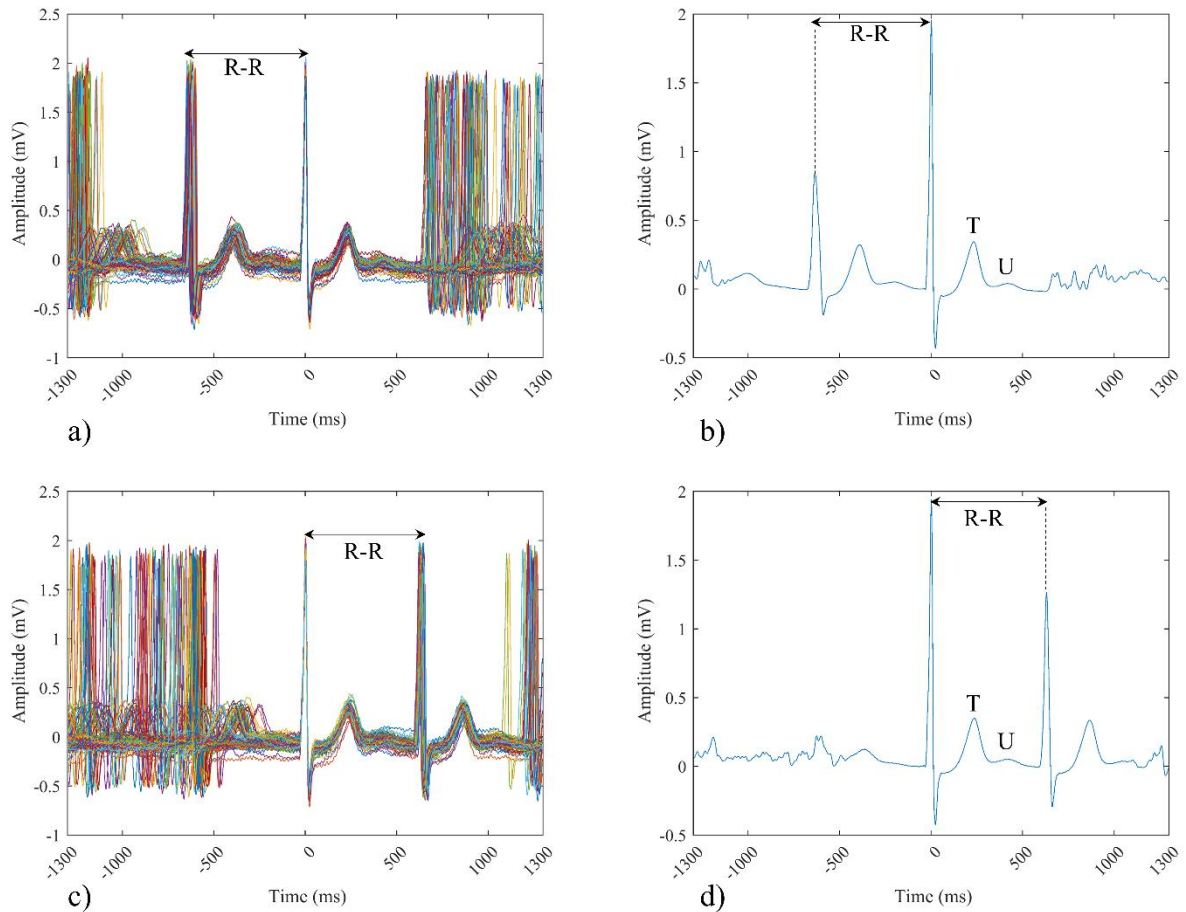


**Figure 5.2:** Example illustrates the difference in the method of collecting beats with respect to ‘Preceding’ R-R in the top row and ‘Current’ R-R interval in the bottom row for the beat averaging technique in one of the AF subjects. The beat averaging algorithm used the same recordings to **a)** collects the beats with respect to the preceding R-R (details in section 3.2.3) to generate an averaged beat which produced in **b)** showing U and T waves with respect to preceding R-R. In **c)** the beat averaging algorithm collects the beats with respect to current R-R and generate averaged beat produced in **d)** showing U and T waves with respect to current R-R.

## 5.2.2. Results

### 5.2.2.1. The Effect of the Preceding Beat Interval on Ventricular Repolarisation Features

The analysis showed that many ventricular repolarisation characteristics were influenced by preceding beat intervals in AF.

The increase of preceding R-R intervals exhibited a clear positive impact on U wave amplitudes, T wave amplitudes, R-T intervals and TU nadir (TU<sub>n</sub>) amplitudes, whereas T-U intervals and R-TU<sub>n</sub> intervals did not respond to the increase of preceding R-R.

Figure 5.3 illustrates an example showing the effect of the preceding beat intervals on the repolarisation features. The example presents two averaged beats generated from the same patient. One of the average beats was generated from beats with preceding R-R intervals of  $625 \pm 25$  ms, (Short R-R, blue trace) and one by preceding R-R intervals of  $1075 \pm 25$  ms (Long R-R, red trace). Clearly, the amplitude of U and T waves and the end of T wave amplitude (TU<sub>n</sub>) increased when preceded by the longer R-R interval. Similarly, the R-T interval is prolonged when preceded by the longer R-R.

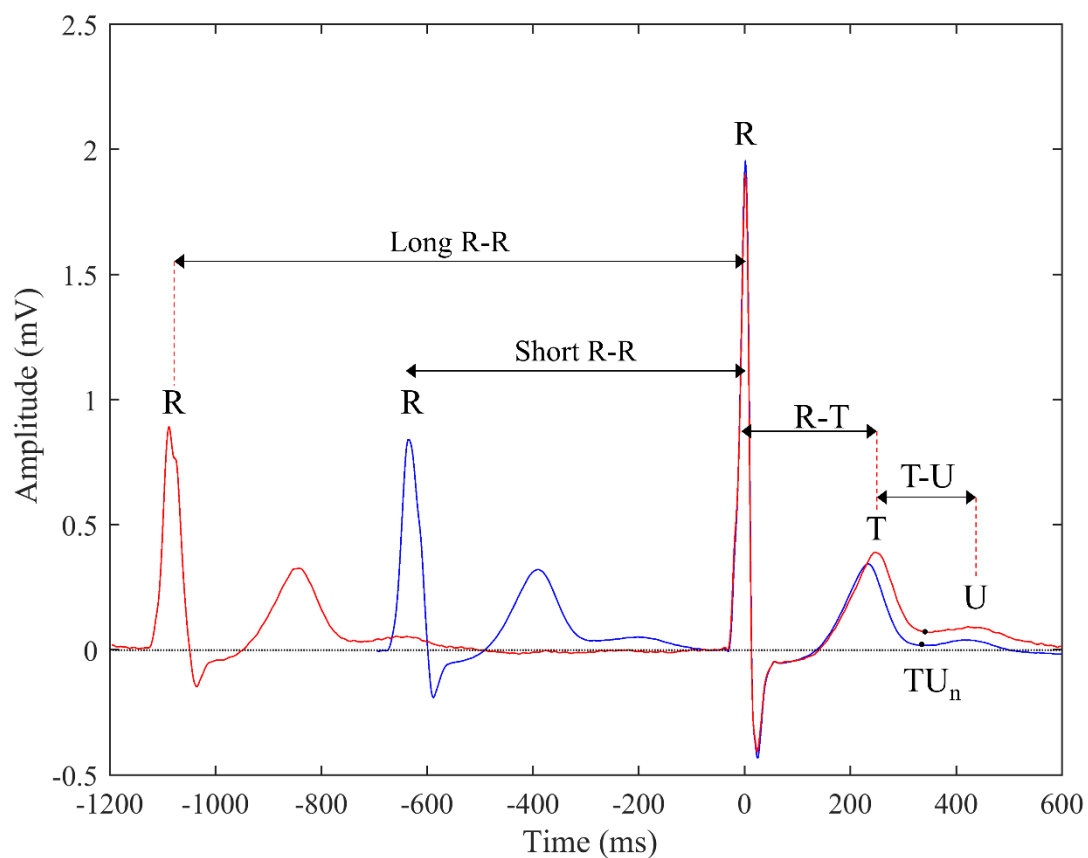


**Figure 5.3:** An example of two averaged beats for the same AF recording generated from beats with preceding beat intervals of  $625 \pm 25$  ms (Short R-R) and  $1075 \pm 25$  ms (Long R-R). T and U amplitudes, the end of T wave (TU<sub>n</sub>) and R-T interval were increased for beats preceded by the longer R-R interval relative to those for the shorter R-R interval.

The following sections provide the statistical analysis of each of the ventricular repolarisation features related to preceding beat interval.

### 5.2.2.1.1. U Wave Amplitudes

The U wave amplitudes showed a strong dependency on the preceding R-R interval in AF. U wave amplitudes increased as the preceding R-R intervals increased. Figure 5.4 illustrates U wave amplitude differences ( $\Delta U$  amp) for 12 leads across the 10 AF subjects. For the majority of leads (all leads except III, aVL, and V1),  $\Delta U$  amplitudes showed a gradual increase as preceding R-R intervals increased.

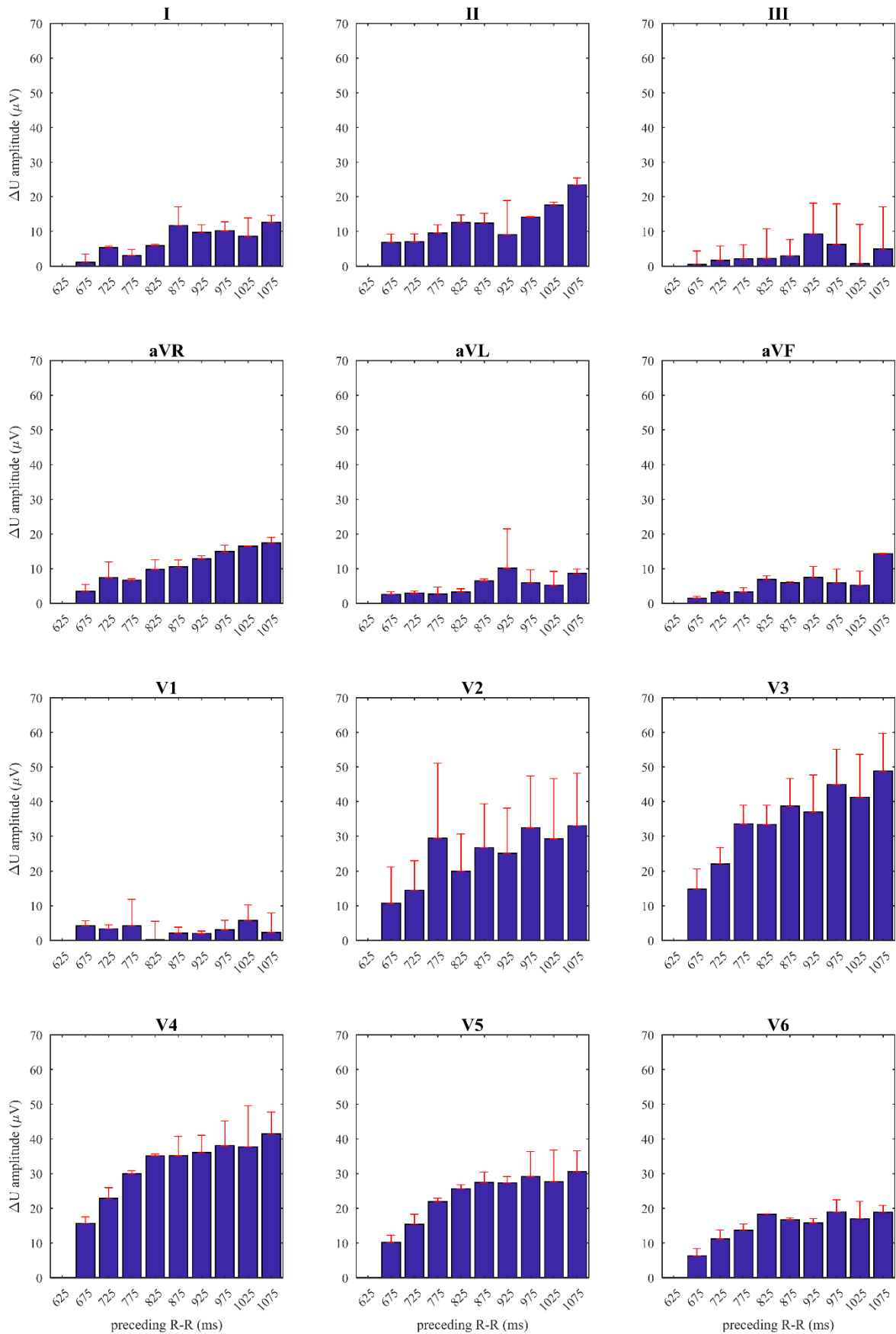
Table 5.1 presents the statistics of U wave measurements with respect to ‘Short R-R’ and ‘Long R-R’ for 12 leads across 10 AF subjects.

In 9 leads, the amplitudes of U wave showed a significant increase if they were preceded by ‘Long R-R’ relative to their amplitudes if they preceded by ‘Short R-R’ (using within subject repeated ANOVA). The statistical tests of the 12 leads were: lead I was ( $p < 0.0001$ ), lead II was ( $p < 0.0001$ ), lead III was ( $p = 0.3141$ ), lead aVR was ( $p < 0.0001$ ), lead aVL was ( $p = 0.1104$ ), lead aVF was ( $p = 0.0001$ ), lead V1 was ( $p = 0.5508$ ), lead V2 was ( $p < 0.0001$ ), lead V3 was ( $p < 0.0001$ ), lead V4 was ( $p < 0.0001$ ), lead V5 was ( $p < 0.0001$ ), and lead V6 was ( $p < 0.0001$ ).

**Table 5.1:** Summary statistics for U wave amplitudes (mean  $\pm$  SD) for ‘Short R-R’ and ‘Long R-R’ intervals in 12 leads for 10 AF patients. *P* value indicates significance between the U amplitudes related to the paired ‘Short R-R’ and ‘Long R-R’ using the Wilcoxon signed rank statistical test.

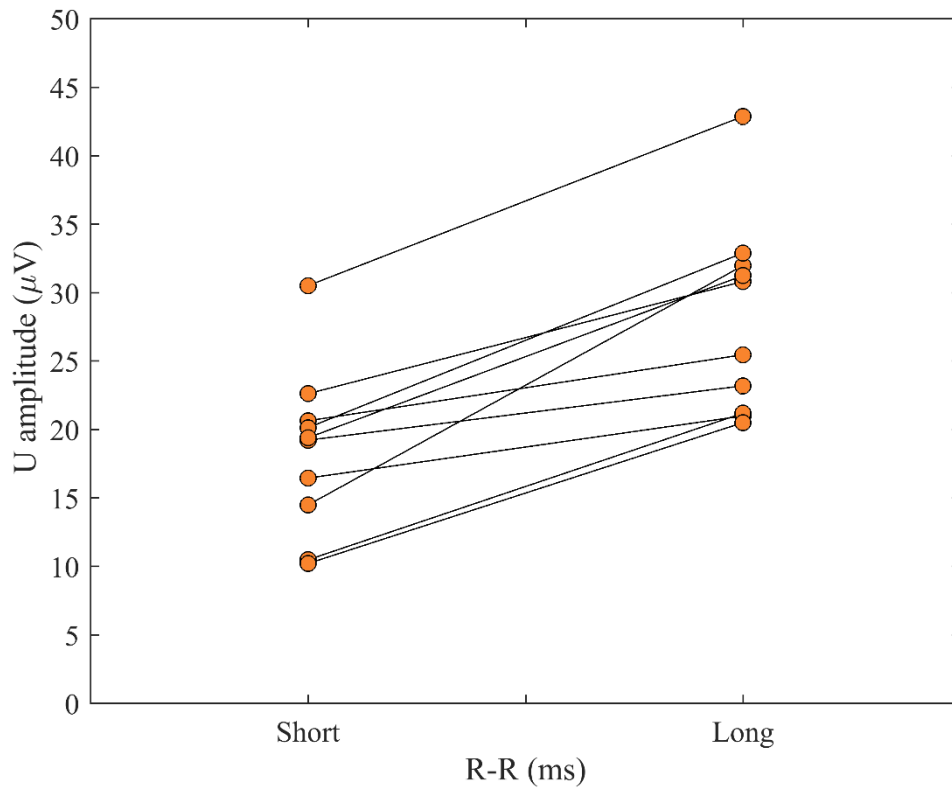
Leads	Short R-R	Long R-R	$\Delta U$ mean amp ( $\mu V$ )	<i>p</i> value
	mean $\pm$ SD ( $\mu V$ )	mean $\pm$ SD ( $\mu V$ )		
I	8 $\pm$ 6	16 $\pm$ 9	8 $\pm$ 6	0.0059
II	15 $\pm$ 9	23 $\pm$ 10	8 $\pm$ 4	0.0039
III	10 $\pm$ 8	14 $\pm$ 12	3 $\pm$ 7	0.3223
aVR	11 $\pm$ 6	20 $\pm$ 7	9 $\pm$ 7	0.0039
aVL	7 $\pm$ 7	12 $\pm$ 8	5 $\pm$ 5	0.0273
aVF	12 $\pm$ 10	17 $\pm$ 12	5 $\pm$ 5	0.0137
V1	5 $\pm$ 9	10 $\pm$ 12	5 $\pm$ 15	0.6953
V2	33 $\pm$ 23	48 $\pm$ 30	14 $\pm$ 14	0.0137
V3	44 $\pm$ 23	65 $\pm$ 30	21 $\pm$ 12	0.0039
V4	35 $\pm$ 15	52 $\pm$ 25	17 $\pm$ 15	0.0020
V5	24 $\pm$ 11	37 $\pm$ 21	14 $\pm$ 13	0.0059
V6	16 $\pm$ 8	24 $\pm$ 13	8 $\pm$ 8	0.0273

Figure 5.5 combines all U wave amplitudes measurements in paired relationship relative to ‘Short R-R’ and ‘Long R-R’ for 10 AF subjects. Each pair represents the mean U wave amplitude for one AF patient across the 12 leads. U wave amplitudes for ‘Long R-R’ were higher and statistically significant ( $p = 0.002$ , Wilcoxon signed rank paired statistical test) compared to ‘Short R-R’ in all subjects ( $28 \pm 7 \mu V$  vs  $18 \pm 6 \mu V$ ).



**Figure 5.4:** The effect of preceding R-R intervals on U wave amplitudes differences ( $\Delta U$  amp) in 12 ECG leads of 10 AF subjects. Bars and whiskers indicate mean and standard deviation of

amplitude difference across 10 AF subjects. The difference is measured relative to the 'reference amplitude' which is that for the shortest preceding interval (R-R = 625 ms). Preceding R-R intervals were (625, 675, 725, 775, 825, 875, 925, 975, 1025 and 1075 ms).



**Figure 5.5:** Paired relationship for U wave amplitudes relative to 'Short R-R' and 'Long R-R' intervals for 10 AF subjects. Each pair presents mean U wave amplitude for one AF subject across the 12 leads. 'Short R-R' were (625, 675, 725, 775, and 825 ms), and 'Long R-R' were (875, 925, 975, 1025 and 1075 ms). There was a significant increase in mean U wave amplitude from 'Short R-R' to 'Long R-R' ( $18 \pm 6 \mu\text{V}$  vs  $28 \pm 7 \mu\text{V}$ ,  $p=0.002$ ).

### 5.2.2.1.2. T wave Amplitudes

Similar to U waves, the T wave amplitudes showed a strong dependence on the preceding R-R interval in AF. T wave amplitudes increased as the preceding R-R intervals increased. Figure 5.6 illustrates T wave amplitude differences ( $\Delta T$  amp) for 12 leads across the 10 AF subjects. For the majority of leads (all leads except I, III, aVL and V1),  $\Delta T$  amplitudes showed a gradual increase as preceding R-R intervals increased.

Table 5.2 presents the summary statistics of T wave measurements with respect to ‘Short R-R’ and ‘Long R-R’ for 12 leads across 10 AF subjects.

In 8 leads, the amplitudes of T wave showed a significant increase if they were preceded by ‘Long R-R’ relative to their amplitudes if they preceded by ‘Short R-R’ (using within subject repeated ANOVA). The statistical tests of the 12 leads were: lead I was ( $p=0.3343$ ), lead II was ( $p=0.0031$ ), lead III was ( $p=0.5902$ ), lead aVR was ( $p<0.0001$ ), lead aVL was ( $p=0.8150$ ), lead aVF was ( $p=0.0001$ ), lead V1 was ( $p=0.3854$ ), lead V2 was ( $p<0.0001$ ), lead V3 was ( $p<0.0001$ ), lead V4 was ( $p<0.0001$ ), lead V5 was ( $p<0.0001$ ), and lead V6 was ( $p<0.0001$ ).

**Table 5.2:** Summary statistics for T wave amplitudes (mean  $\pm$  SD) for ‘Short R-R’ and ‘Long R-R’ intervals in 12 leads for 10 AF patients.  $P$  value indicates significance between the U amplitudes related to the paired ‘Short R-R’ and ‘Long R-R’ using the Wilcoxon signed rank statistical test.

Leads	Short R-R	Long R-R	$\Delta T$ mean amp ( $\mu V$ )	$p$ value
	mean $\pm$ SD ( $\mu V$ )	mean $\pm$ SD ( $\mu V$ )		
I	139 $\pm$ 82	141 $\pm$ 83	2 $\pm$ 9	0.4316
II	157 $\pm$ 109	163 $\pm$ 114	7 $\pm$ 9	0.0840
III	87 $\pm$ 98	88 $\pm$ 95	1 $\pm$ 10	0.9219
aVR	150 $\pm$ 78	156 $\pm$ 80	6 $\pm$ 8	0.0645
aVL	89 $\pm$ 65	90 $\pm$ 66	1 $\pm$ 10	0.6250
aVF	91 $\pm$ 107	98 $\pm$ 112	6 $\pm$ 7	0.0098
V1	90 $\pm$ 73	89 $\pm$ 74	-1 $\pm$ 7	0.6250
V2	286 $\pm$ 213	302 $\pm$ 208	16 $\pm$ 18	0.0371
V3	406 $\pm$ 210	424 $\pm$ 206	18 $\pm$ 25	0.0488
V4	336 $\pm$ 177	351 $\pm$ 192	15 $\pm$ 30	0.0840
V5	273 $\pm$ 198	287 $\pm$ 214	13 $\pm$ 25	0.0840
V6	180 $\pm$ 128	188 $\pm$ 136	8 $\pm$ 15	0.1055

Figure 5.7 combines all T wave amplitudes measurements in paired relationship relative to ‘Short R-R’ and ‘Long R-R’ for 10 AF subjects. Each pair represents the mean T wave amplitude for one AF patient across the 12 leads. T wave amplitudes for ‘Long R-R’ were higher but not significant compared to ‘Short R-R’ in all subjects ( $198 \pm 86 \mu V$  vs  $190 \pm 81 \mu V$ ,  $p=0.06$  using Wilcoxon signed rank paired statistical test).

There was however a significant increase in T wave amplitudes between the extreme preceding R-R intervals with (mean  $\pm$  SD) of:  $199 \pm 86 \mu\text{V ms}$  for preceding R-R of 1075 ms vs  $180 \pm 81 \mu\text{V ms}$  for the shortest preceding R-R of 625 ms ( $p=0.0098$  using Wilcoxon signed rank paired statistical test).

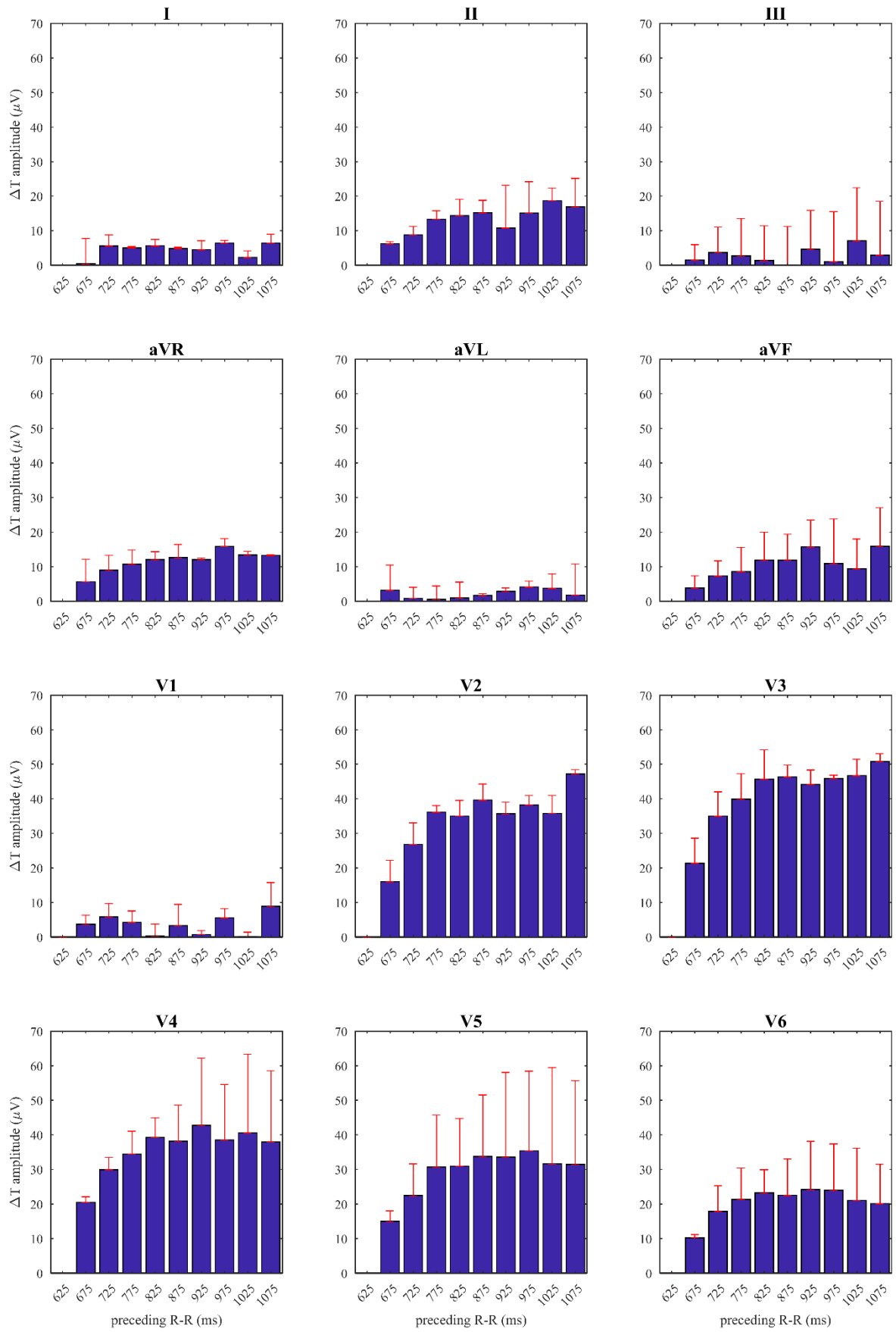


**Figure 5.6:** The effect of preceding R-R intervals on T wave amplitudes differences ( $\Delta T$  amp)

in 12 ECG leads of 10 AF subjects. Bars and whiskers indicate mean and standard deviation of amplitude difference across 10 AF subjects. The difference is measured relative to the ‘reference amplitude’ which is that for the shortest preceding interval (R-R = 625 ms). Preceding R-R intervals were (625, 675, 725, 775, 825, 875, 925, 975, 1025 and 1075 ms).

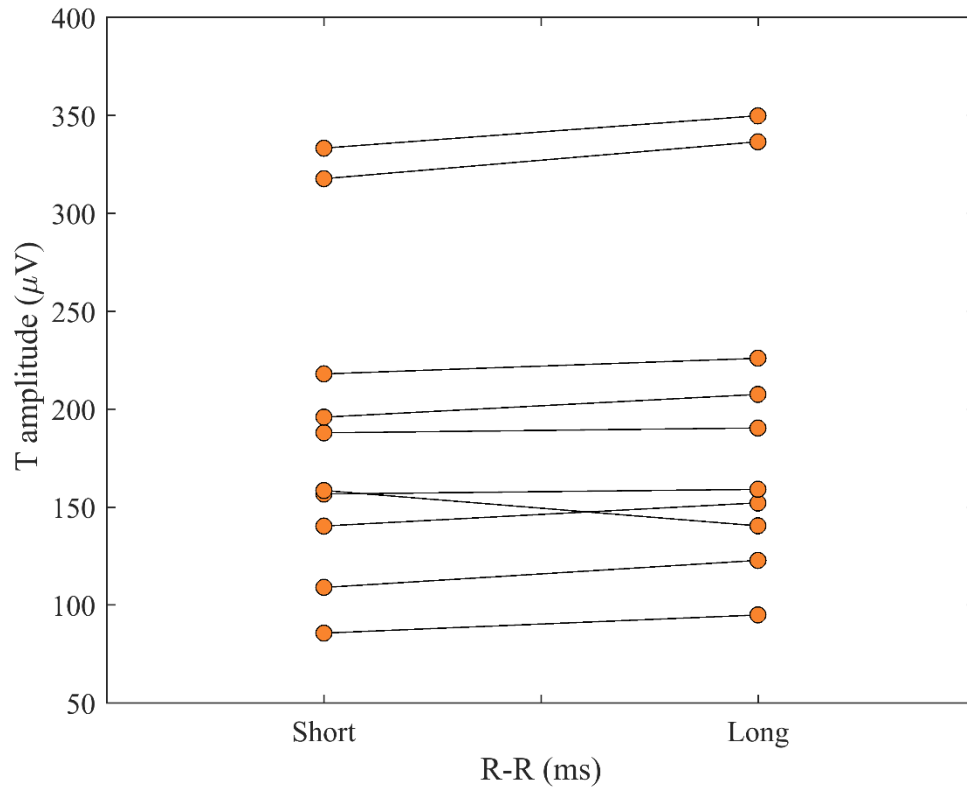


**Figure 5.7:** Paired relationship for T wave amplitudes relative to ‘Short R-R’ and ‘Long R-R’ intervals for 10 AF subjects. Each pair presents mean T wave amplitude for one AF subject across the 12 leads. ‘Short R-R’ were (625, 675, 725, 775, and 825 ms), and ‘Long R-R’ were (875, 925, 975, 1025 and 1075 ms).

### 5.2.2.1.3. Analysis of the Relative U Wave and T Wave Amplitude Changes with Respect to Preceding R-R Interval

Both the U and T wave amplitudes increased as the preceding beat interval R-R increased, during AF.

From Short to Long R-R intervals U wave amplitudes increased by (mean  $\pm$  SD)  $10 \pm 4 \mu\text{V}$  and T wave amplitudes increased by  $8 \pm 11 \mu\text{V}$  ( $p=0.8$ , using Wilcoxon signed rank paired statistical test). So, U waves and T waves increased by similar amounts. This is illustrated in Figure 5.8. It shows that U and T wave amplitudes increased by approximately the same value with respect to the change in the preceding beat intervals.

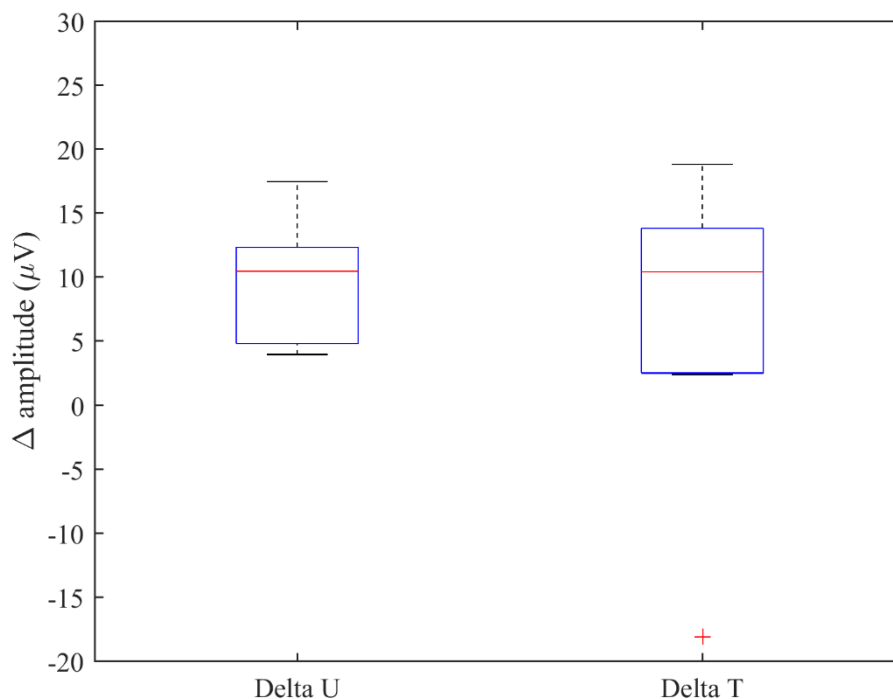


**Figure 5.8:** The amplitude differences delta U and delta T between ‘Short’ and ‘Long’ preceding R-R intervals. Data is the average across 12 leads in 10 AF subjects. The statistical test comparing the difference in means between delta U and delta T was ( $p=0.8$ ). On each boxplot, the central mark indicates the median, and the bottom and top edges of the box indicate the 25th and 75th percentiles, respectively. The whiskers indicate variability outside the upper (greatest value excluding outliers) and lower (least value excluding outliers) quartiles. The symbol ‘+’ indicates the outliers. The outlier represents a data point that differs significantly from other observations.

### 5.2.2.1.4. R-T and T-U Intervals

The R-T interval showed a strong dependency on the preceding R-R interval in AF. R-T interval increased as the preceding R-R intervals increased. Figure 5.9 illustrates R-T interval for 12 leads across the 10 AF subjects. For the majority of leads (all leads except aVF and V1), R-T interval showed a gradual increase as preceding R-R intervals increased.

Table 5.3 presents the summary statistics of R-T interval measurements with respect to ‘Short R-R’ and ‘Long R-R’ for 12 leads across 10 AF subjects.

In 10 leads, the interval of R-T showed a significant increase if they were preceded by ‘Long R-R’ relative to their amplitudes if they preceded by ‘Short R-R’ (using within subject repeated ANOVA). The statistical tests of the 12 leads were: lead I was ( $p<0.0001$ ), lead II was ( $p<0.0001$ ), lead III was ( $p=0.0306$ ), lead aVR was ( $p<0.0001$ ), lead aVL was ( $p=0.003$ ), lead aVF was ( $p=0.1816$ ), lead V1 was ( $p=0.5364$ ), lead V2 was ( $p=0.0215$ ), lead V3 was ( $p<0.0001$ ), lead V4 was ( $p<0.0001$ ), lead V5 was ( $p<0.0001$ ), and lead V6 was ( $p<0.0001$ ).

Figure 5.10-a combines all R-T intervals measurements in paired relationship relative to ‘Short R-R’ and ‘Long R-R’ for 10 AF subjects. Each pair represents the mean R-T interval for one AF patient across the 12 leads. R-T intervals for ‘Long R-R’ were higher compared to ‘Short R-R’ in all subjects ( $263 \pm 9$  ms vs  $257 \pm 11$  ms,  $p=0.002$  using Wilcoxon signed rank paired statistical test).

**Table 5.3:** Summary statistics for R-T interval (mean  $\pm$  SD) for ‘Short R-R’ and ‘Long R-R’ intervals in 12 leads for 10 AF patients. *P* value indicates significance between the R-R intervals related to the paired ‘Short R-R’ and ‘Long R-R’ using the Wilcoxon signed rank statistical test.

Leads	Short R-R	Long R-R	$\Delta$ R-T (ms)	<i>p</i> value
	mean $\pm$ SD (ms)	mean $\pm$ SD (ms)		
I	265 $\pm$ 12	273 $\pm$ 13	8 $\pm$ 4	0.0020
II	265 $\pm$ 13	272 $\pm$ 14	7 $\pm$ 2	0.0020
III	243 $\pm$ 32	285 $\pm$ 38	15 $\pm$ 15	0.0059
aVR	264 $\pm$ 12	272 $\pm$ 13	8 $\pm$ 3	0.0020
aVL	253 $\pm$ 20	262 $\pm$ 23	9 $\pm$ 5	0.0020
aVF	255 $\pm$ 30	260 $\pm$ 27	5 $\pm$ 10	0.0801
V1	264 $\pm$ 21	256 $\pm$ 46	-8 $\pm$ 41	0.4316
V2	238 $\pm$ 23	243 $\pm$ 23	4 $\pm$ 5	0.0371
V3	244 $\pm$ 30	250 $\pm$ 29	6 $\pm$ 3	0.0020
V4	257 $\pm$ 17	264 $\pm$ 17	7 $\pm$ 3	0.0020
V5	266 $\pm$ 15	274 $\pm$ 15	8 $\pm$ 2	0.0020
V6	268 $\pm$ 13	276 $\pm$ 14	8 $\pm$ 2	0.0020

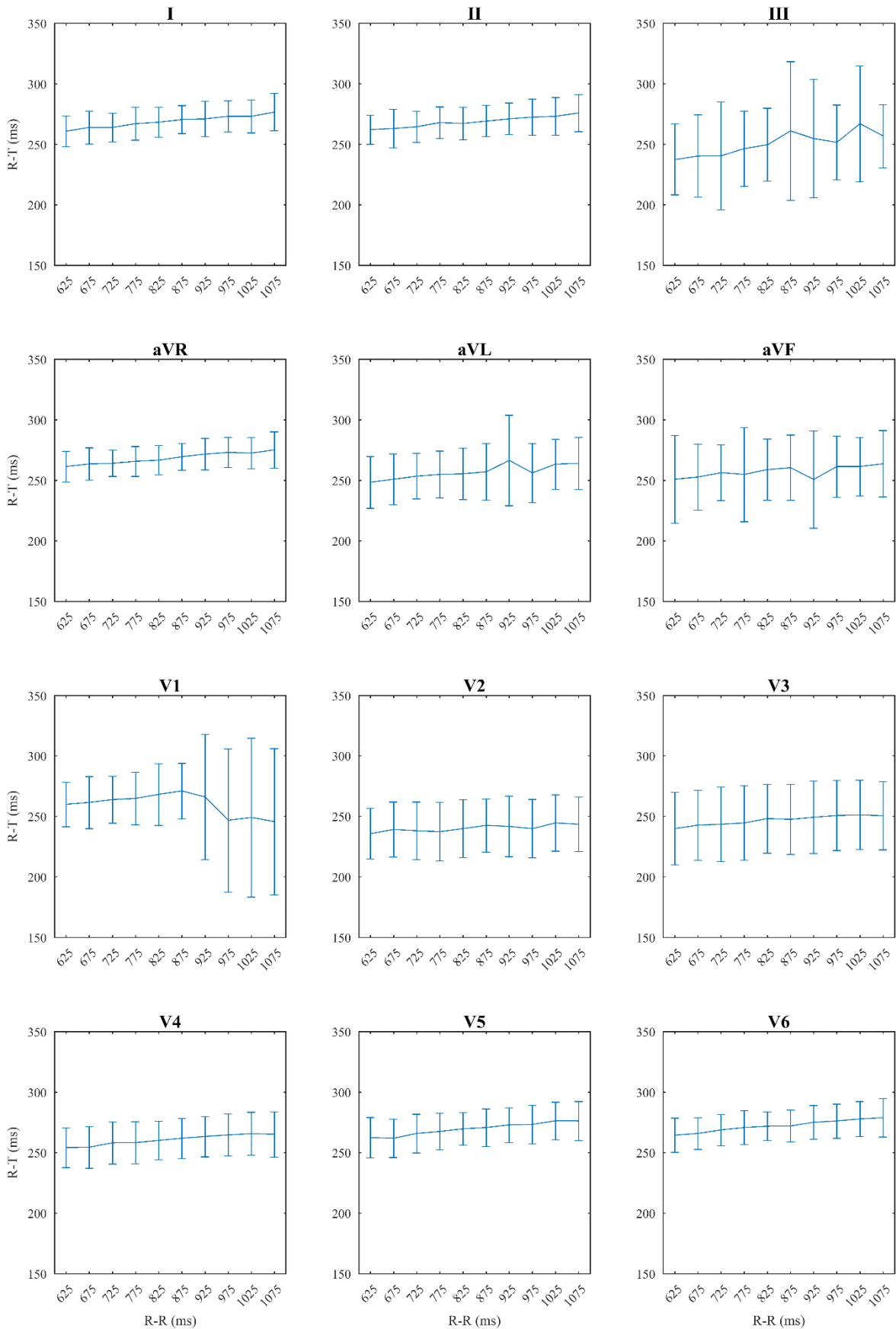


**Figure 5.9:** The effect of preceding R-R intervals on R-T intervals in 12 ECG leads. Whiskers indicate mean and standard deviation of amplitude difference across 10 AF subjects. Preceding

R-R intervals were (625, 675, 725, 775, 825, 875, 925, 975, 1025 and 1075 ms).

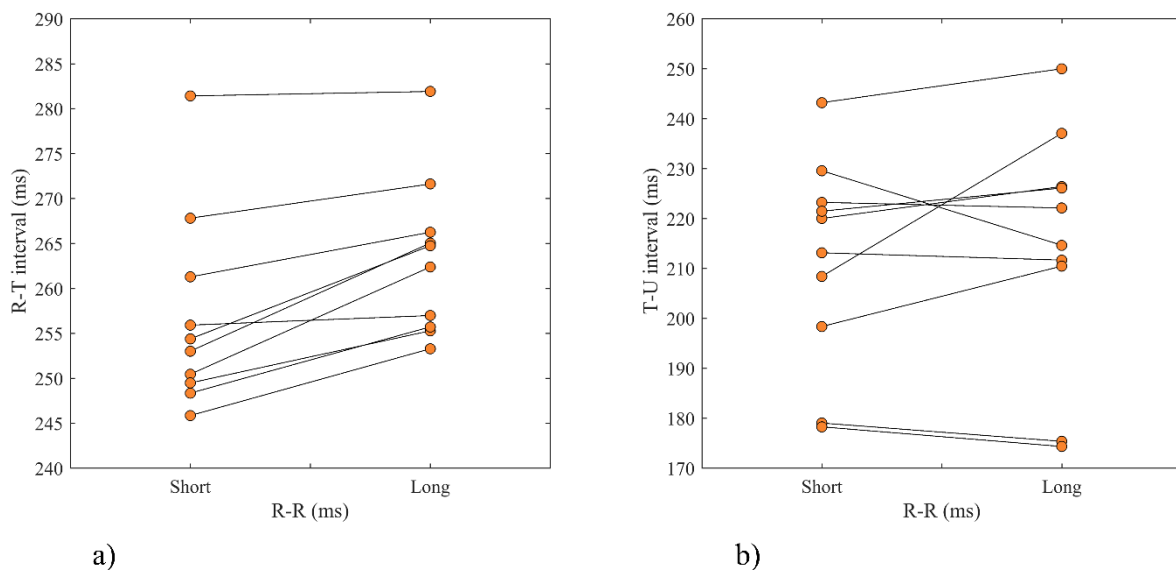


**Figure 5.10:** Paired relationship for R-T and T-U intervals relative to ‘Short R-R’ and ‘Long R-R’ intervals for 10 AF subjects. In **a)** each pair presents mean R-T interval for one AF subject across the 12 leads. There was a significant increase in mean R-T interval from ‘Short R-R’ to ‘Long R-R’ ( $257 \pm 11$  ms vs  $263 \pm 9$  ms,  $p=0.002$ ). In **b)** each pair presents mean T-U interval for one AF subject across the 12 leads. There was no significant increase in mean T-U interval from ‘Short R-R’ to ‘Long R-R’ ( $212 \pm 21$  ms vs  $215 \pm 24$  ms,  $p=0.43$ ). ‘Short R-R’ were (625, 675, 725, 775, and 825 ms), and ‘Long R-R’ were (875, 925, 975, 1025 and 1075 ms).

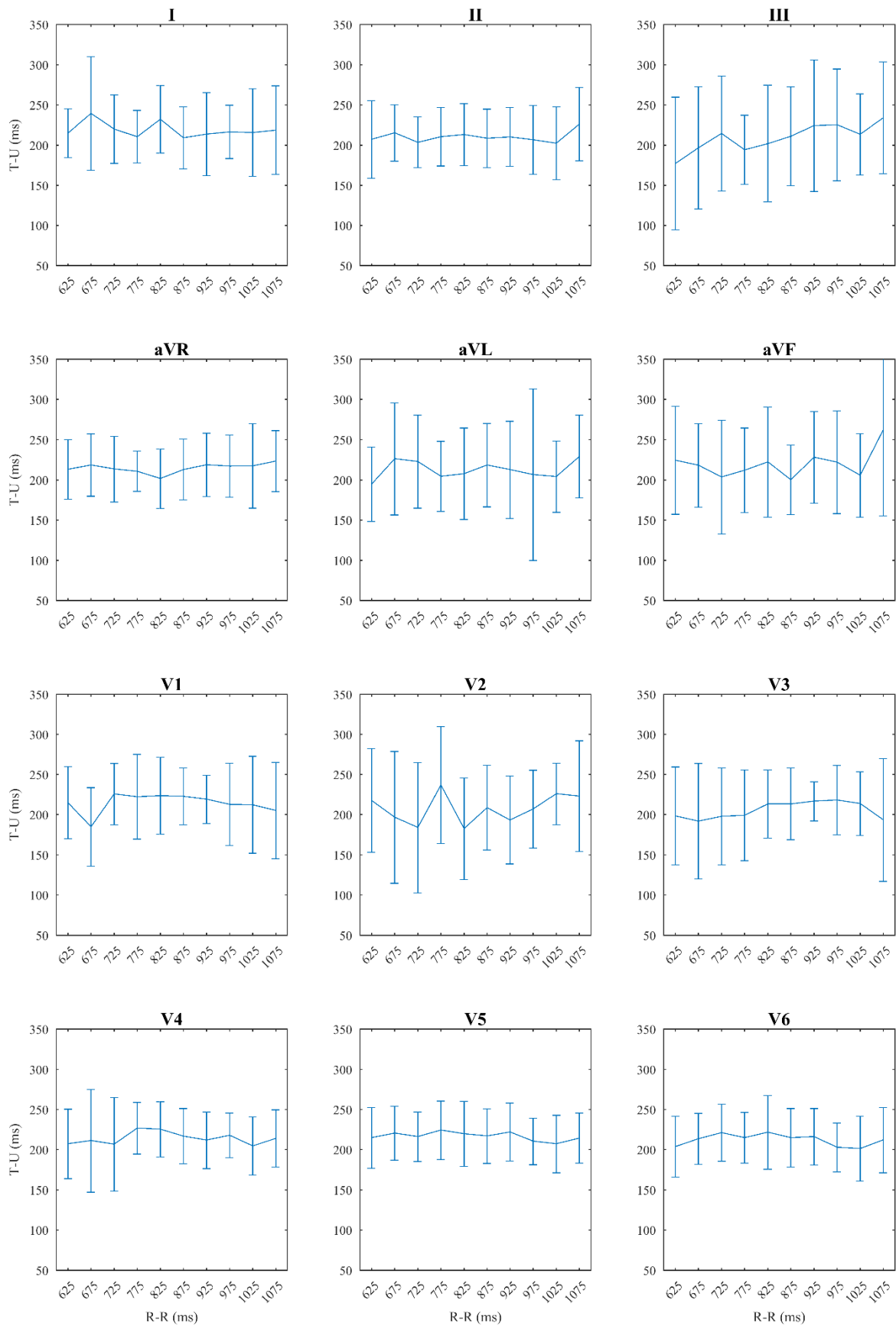
In contrast to R-T interval, T-U intervals were independent of the preceding R-R interval in AF. T-U interval did not respond to the preceding R-R intervals increasing. Figure 5.11 illustrates T-U interval for 12 leads across the 10 AF subjects. For all 12 leads, T-U interval showed no specific response as preceding R-R intervals increased.

Table 5.4 presents the summary statistics of T-U interval measurements with respect to ‘Short R-R’ and ‘Long R-R’ for 12 leads across 10 AF subjects.

In all 12 leads, the intervals of T-U were not statistically significant if they were preceded by ‘Long R-R’ relative to their amplitudes if they preceded by ‘Short R-R’ R’ (using within subject repeated ANOVA). The statistical tests of the 12 leads are: lead I was ( $p=0.4984$ ), lead II was ( $p=0.3440$ ), lead III was ( $p=0.1565$ ), lead aVR was ( $p=0.5829$ ), lead aVL was ( $p=0.9073$ ), lead aVF was ( $p=0.0946$ ), lead V1 was ( $p=0.5150$ ), lead V2 was ( $p=0.1776$ ), lead V3 was ( $p=0.8980$ ), lead V4 was ( $p=0.6134$ ), lead V5 was ( $p=0.4494$ ), and lead V6 was ( $p=0.2503$ ).

Figure 5.10-b combines all T-U intervals measurements in paired relationship relative to ‘Short R-R’ and ‘Long R-R’ for 10 AF subjects. Each pair represents the mean T-U interval for one AF patient across the 12 leads. T-U intervals for ‘Long R-R’ were not significantly different

compared to 'Short R-R' in all subjects ( $215 \pm 24$  ms vs  $212 \pm 21$  ms,  $p=0.43$  using Wilcoxon signed rank paired statistical test).



**Figure 5.11:** The effect of preceding R-R intervals on T-U intervals in 12 ECG leads of 10 AF subjects. Whiskers indicate mean and standard deviation of amplitude difference across 10 AF

subjects. Preceding R-R intervals were (625, 675, 725, 775, 825, 875, 925, 975, 1025 and 1075 ms).

**Table 5.4:** Summary statistics for T-U interval (mean  $\pm$  SD) for ‘Short R-R’ and ‘Long R-R’ intervals in 12 leads for 10 AF patients. *P* value indicates significance between the R-R intervals related to the paired ‘Short R-R’ and ‘Long R-R’ using the Wilcoxon signed rank statistical test.

Leads	Short R-R	Long R-R	$\Delta$ T-U (ms)	<i>p</i> value
	mean $\pm$ SD (ms)	mean $\pm$ SD (ms)		
I	223 $\pm$ 37	215 $\pm$ 43	-9 $\pm$ 36	0.4316
II	210 $\pm$ 34	211 $\pm$ 37	1 $\pm$ 14	0.8457
III	197 $\pm$ 54	222 $\pm$ 60	25 $\pm$ 32	0.0117
aVR	212 $\pm$ 34	218 $\pm$ 38	6 $\pm$ 23	0.3105
aVL	211 $\pm$ 42	214 $\pm$ 43	3 $\pm$ 47	0.6250
aVF	216 $\pm$ 51	224 $\pm$ 57	8 $\pm$ 31	0.2754
V1	214 $\pm$ 30	214 $\pm$ 37	0 $\pm$ 34	0.8262
V2	204 $\pm$ 49	212 $\pm$ 45	8 $\pm$ 28	0.2754
V3	200 $\pm$ 43	211 $\pm$ 26	11 $\pm$ 40	0.6250
V4	216 $\pm$ 42	213 $\pm$ 30	-3 $\pm$ 30	0.8457
V5	219 $\pm$ 33	214 $\pm$ 30	-5 $\pm$ 14	0.3594
V6	215 $\pm$ 32	210 $\pm$ 32	-5 $\pm$ 10	0.1602

### 5.2.2.1.5. TUn Amplitude and R-TUn Interval

The amplitude of the T wave end (TUn), and its interval, R-TUn interval, were measured in lead V4 for 10 AF subjects. Figure 5.12 displays the effect of preceding beat intervals on these repolarisation characteristics.

The TUn amplitudes showed a significant increase ( $p=0.000$  using within subject repeated ANOVA) with respect to increasing preceding R-R intervals as Figure 5.12-a shows. TUn amplitudes relative to ‘Long R-R’ were significantly higher compared to their amplitudes for ‘Short R-R’ as shown in Table 5.5

R-TUn intervals showed slight visible increasing with respect to the lengthening of preceding R-R intervals as Figure 5.12-b illustrates. However, the statistical test for R-TUn intervals compared to ‘Short R-R’ and ‘Long R-R’ was not significant ( $p=0.066$ , using within subject repeated ANOVA). Table 5.5 displays the R-TUn statistics.

There was however a significant increase in R-TUn intervals between the extreme preceding R-R intervals with mean  $\pm$  SD of: 392  $\pm$  27 ms for preceding R-R of 1075 ms vs 376  $\pm$  31 ms for the shortest preceding R-R of 625 ms ( $p=0.027$  using Wilcoxon signed rank paired statistical test).

R-TUn intervals relative to ‘Long R-R’ were higher compared to their amplitudes for ‘Short R-R’ as shown in Table 5.5.

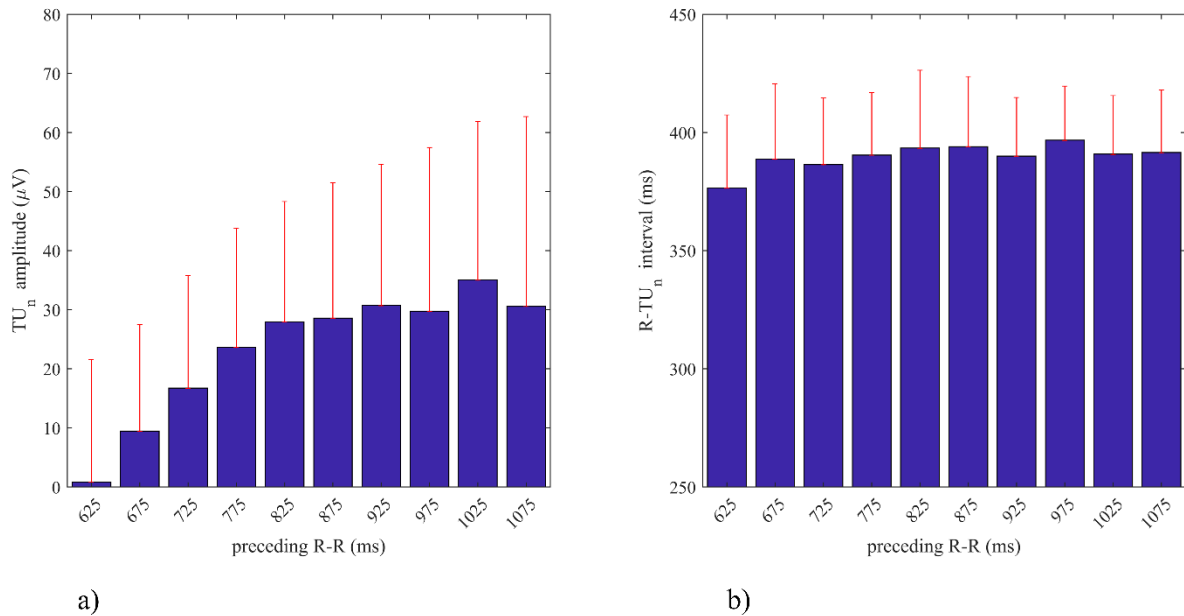


**Figure 5.12:** The effect of preceding R-R intervals on ventricular repolarisation features at the end of the T wave (TU nadir). **a)** TUn amplitudes and **b)** R-TUn intervals for lead V4 of 10 AF subjects. Bars and whiskers indicate mean and standard deviation (mean  $\pm$  SD) of amplitudes and intervals respectively across 10 AF subjects.

**Table 5.5:** Summary statistics for TUn amplitude and R-TUn intervals (mean  $\pm$  SD) for ‘Short R-R’ and ‘Long R-R’ in lead V4 for 10 AF patients. *P* value indicates significance between the R-R intervals related to the paired ‘Short R-R’ and ‘Long R-R’ using the Wilcoxon signed rank statistical test.

	Short R-R	Long R-R	$\Delta$ value	<i>p</i> value
	mean $\pm$ SD	mean $\pm$ SD		
TUn ( $\mu$ V)	16 $\pm$ 18	31 $\pm$ 26	15 $\pm$ 13	0.0098
R-TUn (ms)	387 $\pm$ 28	393 $\pm$ 24	6 $\pm$ 12	0.1602

### 5.2.2.2. ‘Preceding’ vs ‘Current’ Beat Interval

All the results presented so far relate to use of the *preceding* beat in the beat averaging algorithm. It was hypothesised that ventricular repolarisation features would not show a dependence on the ‘current’ beat interval, so this section analyses the rate dependency of

ventricular repolarisation features when selecting the *current* beat for use in the beat averaging algorithm.

The analysis confirmed that U and T wave amplitudes were independent of the current beat interval.

Figure 5.13 displays two averaged beats, one generated from ‘*current*’ beat intervals (a) and one generated from ‘*preceding*’ beat intervals (b). In Figure 5.13-a the amplitudes of U and T waves for a short current beat interval (R-R = 625 ms, blue trace) were almost identical to those of long current beat interval (R-R = 1075 ms, red trace). For comparison Figure 5.13-b shows U and T amplitudes generated from long and short *preceding* R-R intervals where clear difference in repolarisation features can be seen.

This result was confirmed when considering ‘*current*’ and ‘*preceding*’ R-R intervals on U wave and T wave amplitudes in lead V4 for the 10 AF patients as presented in Figure 5.14.

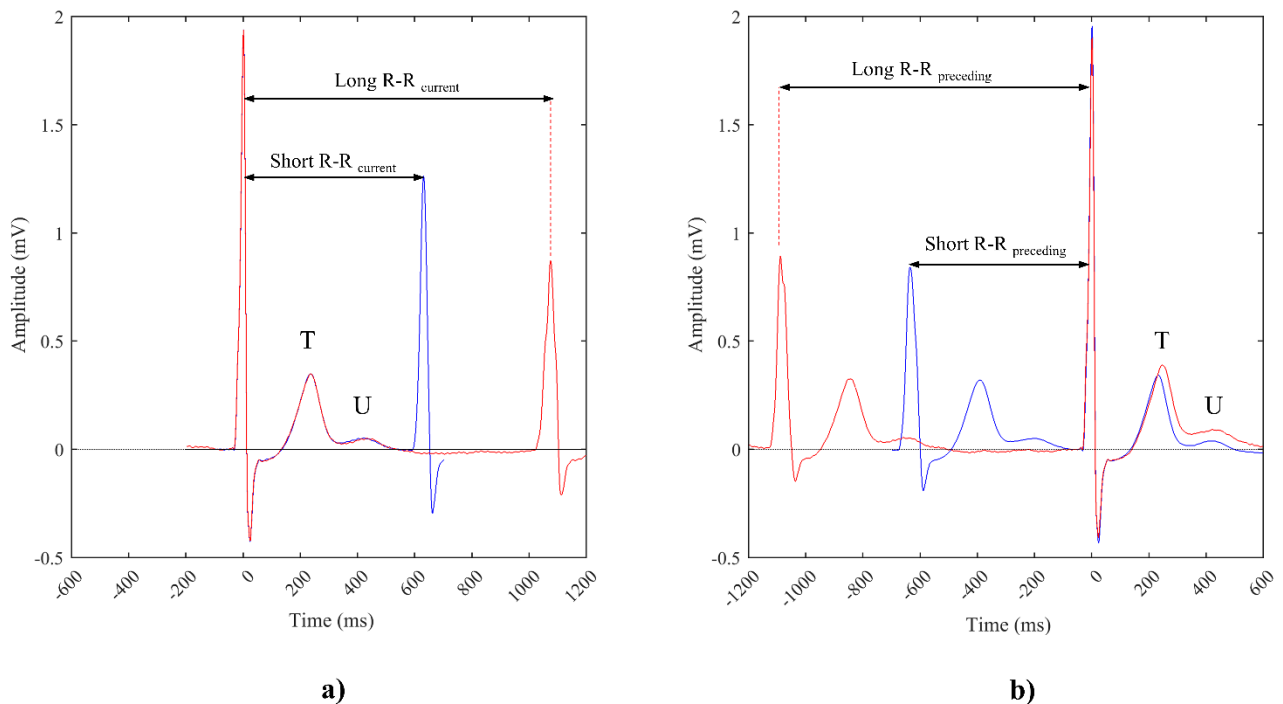


**Figure 5.13:** Examples of two averaged beats for same AF recording, generated for beats with short (625 ms) and long (1075 ms) beat intervals (R-R). The average beats were constructed from **a)** ‘*current*’ beat interval, and the resulting U and T waves were almost identical with no significant change between their amplitudes, and from **b)** ‘*preceding*’ beat interval, and the resulting U and T waves exhibit significant differences in ventricular repolarisation features between long and short R-R intervals.

Figure 5.14-a shows the response of U wave amplitudes to ‘*current*’ beat intervals. U wave amplitudes are independent of current R-R interval. As a comparison, Figure 5.14-b presents

the effect of ‘preceding’ beat interval on U wave amplitude for the same patients in same lead V4 and clearly the U wave amplitudes increased.

Similarly, Figure 5.14-c and 5.14-d show T wave amplitudes respond in a similar way with no rate dependence exhibited for ‘current’ beat intervals, whereas there is a clear rate dependence for ‘preceding’ beat intervals.

Table 5.6 presents the statistical analysis of U and T wave amplitudes (mean  $\pm$  SD) relative to ‘Short R-R’ and ‘Long R-R’ with respect to current and preceding R-R intervals.

There was no significant difference between amplitudes of U waves ( $p=0.7$ ) and T waves ( $p=1$ ) that related to ‘Short R-R’ and ‘Long R-R’ for current R-R. However, there was significant difference for both U and T amplitude ( $p < 0.0001$ ) for preceding R-R (using within subject repeated ANOVA test).

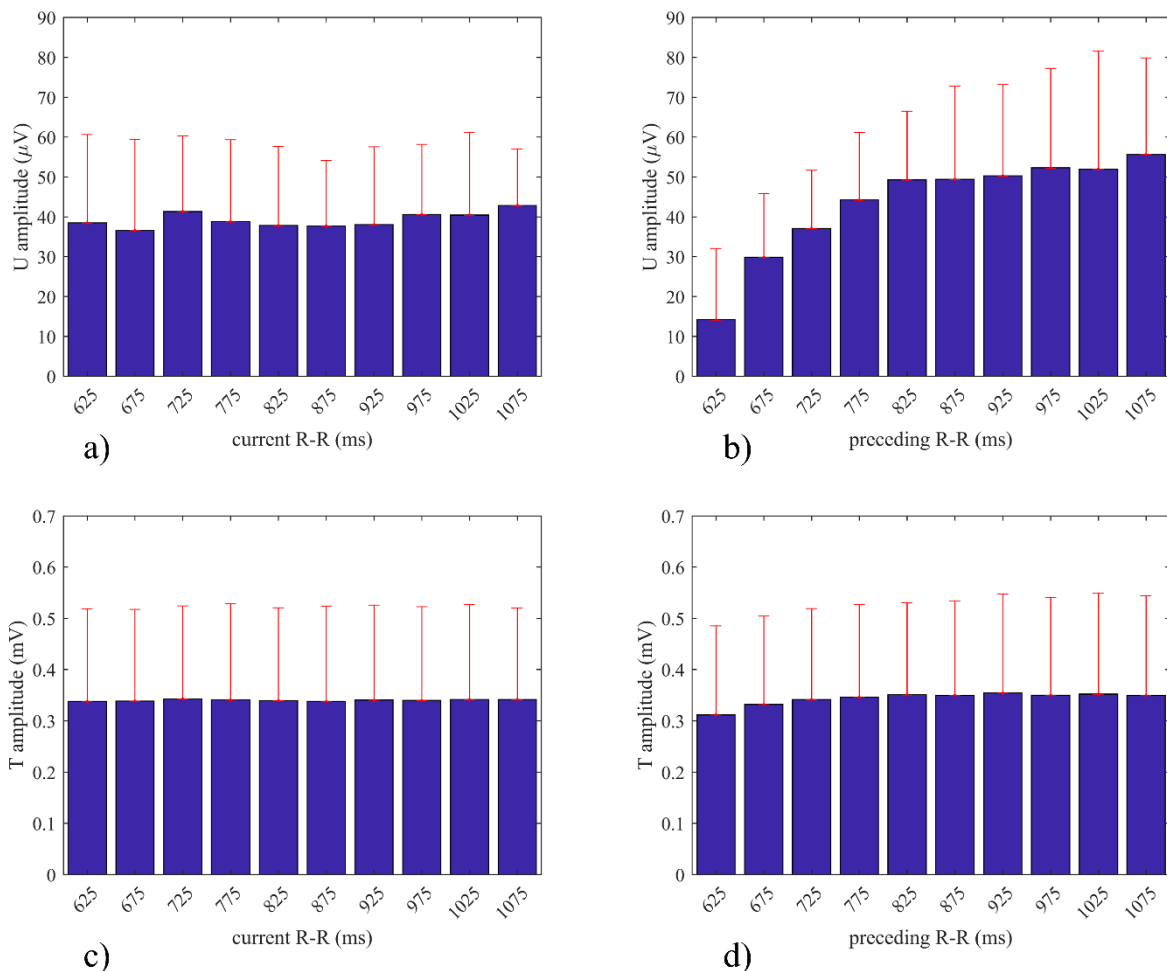


**Figure 5.14:** The effect of the ‘current’ and ‘preceding’ beat intervals on the amplitudes of U wave (top row) and T wave (bottom row) for 10 AF patients using lead V4. Bars and whiskers indicate mean and standard deviation (mean  $\pm$  SD) of amplitudes across subjects. **a)** displays the effect of ‘current’ beat interval on U wave amplitudes, **b)** shows the effect of ‘preceding’

beat interval on U wave amplitudes. **c)** displays the effect of ‘current’ beat interval on T wave amplitudes while **d)** the effect of ‘preceding’ beat interval on T wave amplitudes.

**Table 5.6:** Summary statistics of average beat U and T wave amplitudes (mean  $\pm$  SD) generated from ‘current’ and ‘preceding’ ‘Short R-R’ and ‘Long R-R’ intervals for 10 AF patients in lead V4. *P* value indicates significance between the R-R intervals related to the paired ‘Short R-R’ and ‘Long R-R’ using the Wilcoxon signed rank statistical test.

V4	Current R-R				Preceding R-R			
	Short R-R	Long R-R	$\Delta$ value	<i>p</i> value	Short R-R	Long R-R	$\Delta$ value	<i>p</i> value
U amplitude mean $\pm$ SD ( $\mu$ V)	39 $\pm$ 20	40 $\pm$ 17	1 $\pm$ 5	0.4922	35 $\pm$ 15	52 $\pm$ 25	17 $\pm$ 15	0.0020
T amplitude mean $\pm$ SD ( $\mu$ V)	340 $\pm$ 182	340 $\pm$ 184	0 $\pm$ 8	1	336 $\pm$ 177	351 $\pm$ 192	15 $\pm$ 30	0.0840

### 5.2.3. Discussion

This study has examined the effect of rate dependency of ventricular repolarisation features during AF. No previous studies have quantified the rate dependency of repolarisation features in AF. The main finding is that there was a significant rate dependency when considering the preceding beat interval. Most of ventricular repolarisation features were influenced by the ‘preceding’ beat intervals. The amplitudes of U wave, T wave, end of T wave (TUn) and R-T intervals showed a positive dependency on the preceding R-R interval.

However, when considering the ‘current’ beat interval all rate dependency of ventricular repolarisation features was lost.

These findings have significant implications for implementation of the beat averaging algorithm and its use in characterising the ventricular repolarisation features in AF patients. Firstly, that there is indeed a rate dependency of ventricular repolarisation features during AF which might give new mechanistic insight into ECG ventricular repolarisation features (including the U wave). Secondly, the beat averaging algorithm must always be implemented considering the *preceding* beat interval if rate dependency of ventricular repolarisation features is to be captured.

The remainder of this discussion relates the findings of the study to potential explanatory mechanisms of the observed rate dependency.

AF is characterised by irregular, rapid heart rate changes and large beat to beat variability in cycle length (see section 1.5.2 of Chapter one) which affects left ventricular performance

[178,179]. The large beat to beat variation (i.e. different cardiac cycle length) in AF (unlike sinus rhythm SR) provides a mechanism to investigate the effect of these interval changes on ventricular characteristics, since these interval changes are known to influence the left ventricular cardiac performance [178,179]. However, few studies have investigated the relationship between beat intervals and cardiac performance in AF [179-182].

In SR, left ventricular characteristics are nearly stable and there is little beat to beat variation during the cardiac cycle. This produces stable factors such as preload, contractility and afterload that characterise left ventricular performance (see Figure 1.22 and section 1.2.3.2 in Chapter one) [31,179]. In AF, however, the variation of beat to beat interval changes affects cardiac performance due to instability of these factors and hence causes the left ventricular characteristics to change rapidly [178,179].

In AF cardiac performance and left ventricular function are mainly dependent on the preceding beat interval rather than the current beat interval, since the length of preceding beat interval influences the preload (Section 1.2.3.2.1) or the diastolic filling [178-180].

Understanding the mechanical and electrical function of the left ventricle is essential to understand the behaviour of the repolarisation characteristics in this study. Here, the response of the left ventricle during repolarisation is highlighted from the mechano-electrical perspective as it provides insight into the study results.

Ventricular repolarisation is greatly affected by the preceding beat intervals [11,19,31,175,176,183,184]. Previous studies have shown there is a significant positive correlation between preceding R-R intervals and the amount of blood that fills the left ventricle before ventricular contraction in AF [183-186]. That amount of blood is defined as end-diastolic volume (EDV) as explained in section 1.2.3.2.1 and represents the passive filling phase during diastole in the cardiac cycle [3,8,31,187] (see the relation between the rapid filling phase and ventricular volume in Figure 1.21 and more details of the mechanical events of the cardiac cycle in section 1.2.3.1). In other words, a longer preceding R-R results in larger EDV (i.e. more blood fills in the left ventricle).

Blood flowing into the left ventricle stretches the ventricular wall causing an expansion during diastole according to the Frank-Starling's law (section 1.2.3.3) [8,31,175,176]. This stretch is a hemodynamic load on the myocardial wall at the end of diastole and is clinically known as 'preload' [20,31,187]. Preload reflects the degree of stretch of cardiac myocytes at the end of ventricular filling [20,31,184,187]. The level of stretching depends on the blood volume that fills the left ventricle, i.e. preload increases as left ventricle fills with more blood [8,28,162]. According to the Frank-Starling mechanism, the greater the stretch, the greater the force of the subsequent contraction of the left ventricle (see Figure 1.23) [20,31,175,183].

The force generated by cardiac muscles translates into **pressure** within the chamber [31,35,188]. As the volume within the chamber increases or decreases there is a corresponding change in cardiac muscle's length, and therefore sarcomere length. Figure 1.14 in Chapter one illustrates the cardiac muscle during relaxation and contraction. This in turn results in corresponding changes to ventricular wall stretch and chamber pressure [31,35,188]. Full

details of the relationship between the ventricular pressure and volume has explained in section 1.2.3.4 of Chapter one.

Ventricular pressure increases as ventricular volume is increased (see Figure 1.24-a and b) [31,35,188,189]. In AF, there is a positive correlation between the preceding R-R and left ventricular pressure [185,190] as Figure 5.15 shows. In other words, a long preceding R-R results in high left ventricular pressure. Note the similarity between the shape of the relationship of preceding interval to pressure shown in Figure 5.15 with those for the T and U waves presented in Figures 5.4 and 5.6. The relationship between preceding interval and pressure (Figure 5.15) is associated with the EDV increasing with respect to the preceding R-R, due to the Franck-Starling mechanism [185,190]. In other words, the increase of EDV (i.e. large blood volume in left ventricle) due to the long R-R is the key factor to increase the ventricular pressure.

The increase in pressure induces stretch in the left ventricle. Stretch activates mechanosensitive ion channels [63,78-80,97,191] that generate current flow through changes in membrane ion channel permeability which are involved in mechano-electrical coupling (MEC). This current flow generates a voltage gradient in the left ventricular myocardium manifested in the surface ECG [63,78-80,97,191].

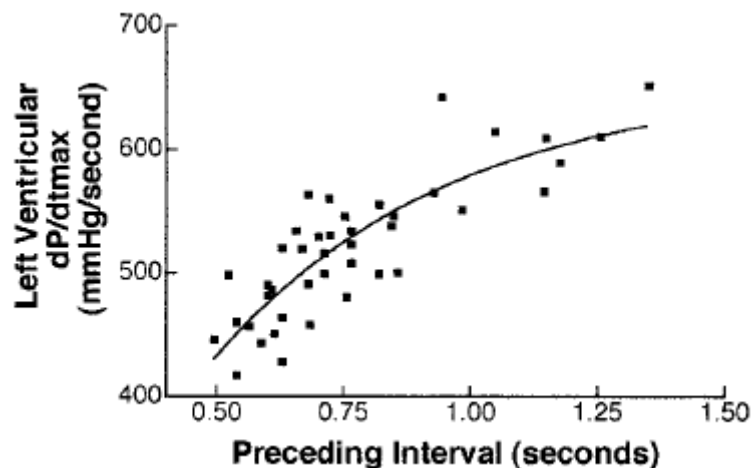


**Figure 5.15:** Relationship between left ventricular pressure (maximum rate of rise of left ventricular dP/dtmax) and preceding R-R interval in atrial fibrillation [185].

The results of the current study, which related ventricular repolarisation characteristics to preceding R-R intervals in AF, show a favourable association for the dynamics of mechanical and electrical activities explained above. The following sections address the response of the ventricular features observed in the current study to the mechanisms outlined above.

### 5.2.3.1. Rate Dependency of U Wave Features

The U wave coincides with the second heart sound and occurs after the T wave [48,49,52]. Left ventricle filling (preload) is closely related to the preceding R-R intervals as explained, therefore the filling time becomes very short when the heart rate is fast (i.e. short preceding R-R) [176,183,189].

In atrial fibrillation (AF), there is a positive correlation between the total left ventricular filling (i.e. EDV) and preceding cycle length (R-R intervals) [183,185,189], which means there is more filling (large blood volume) with long R-R intervals, and less filling (small blood volume) for short R-R intervals. The larger volume of the blood which flows into the left ventricle, will stretch the heart walls causing a greater expansion during diastole according to Frank-Starling's law and this increases the left ventricular pressure [31,176,190]. This will activate mechanosensitive ion channel which transduce that pressure and stretch into an electrical signal through changes in membrane ion channel via MEC [50,63,76,96,191]. As was described in Chapter one (section 1.3.3.3), one of the hypotheses of U wave generation is *mechano-electrical coupling*. This theory suggests that after-potentials caused by the stretching of the cardiac muscle of the left ventricle, gives rise to the U wave [48-50]. This means that the U wave is a manifestation of ventricular mechanical stretch [48,51,62]. Thus, substantial stretch may induce local membrane repolarisation, generating a voltage gradient in the left ventricular myocardium detected as the U wave in the surface ECG [48,51,63].

Meijborg et al [96] elucidated through experiment that stretch influences the repolarisation characteristics by MEC where the increase in left ventricular pressure leads to increased amplitudes and intervals of repolarisation.

In our study, the rate dependency of U wave features in AF, shows support for Meijborg's [96,97] theory. In effect, a rapid heart rate (short preceding R-R) leads to a smaller volume of blood entering the left ventricle resulting in less stretch of the left ventricular wall. Accordingly, there is less left ventricular pressure which translates into smaller U wave amplitudes. This is consistent to the small amplitudes of U wave related to 'Short R-R' intervals presented in the results (section 5.2.2.1.1). Whereas for 'Long R-R' intervals, a large volume of blood fills the left ventricle, which leads to greater stretch to the heart walls, high left ventricular pressure which translates into high U wave amplitudes. This is consistent with the higher amplitudes of U waves related to 'Long R-R' intervals in the presented results. Despite the range of U waves hypotheses, Surawicz [48] has shown that physiological U wave is heart rate dependant and suggested that the mechano-electrical coupling theory is a likely explanation for U wave origin. This is consistency with the project results although the current study was conducted on AF patients not healthy subjects in SR. The study in section 5.3 of this chapter looks at the effect of rate changes on ventricular repolarisations of healthy subjects in SR.

Our study showed that the T-U intervals were independent of the effect of the prolongation of preceding R-R intervals in AF. In other words, the distance between the U peak and T peak is relatively constant. So, as the position of the T wave peak extends (R-T interval) as the

preceding R-R interval prolongs, so does the U wave peak by a similar amount. Surawicz [48] stated in his characterisation of the normal U wave that the interval from the end of the T wave to the apex of the U wave is almost rate independent.

Additionally, the U wave amplitudes were independent of the prolongation of current R-R intervals. As explained above that left ventricular function is mainly dependent on the length of preceding R-R interval in which effects the preload or the passive filling in left ventricle before the new cardiac cycle starts. By selecting beats only based on the ‘current’ R-R interval, the preceding beat intervals (of those beats) will be highly variable, so what is observed in the resulting average beat is the average T and U wave considering many different preceding intervals.

### 5.2.3.2. Rate Dependency of T Wave Features

The results of rate dependency of T wave features in AF showed similar behaviour to U wave features.

Our study has shown that in AF, T wave amplitudes (T amp, TUn amp) and interval (R-T interval) increased with increasing preceding R-R intervals. Meijborg et al [96,97] observed, as explained above, that the stretch of the left ventricle influences repolarisation via MEC [79,192]. Increasing left ventricular pressure leads to prolongation of the repolarisation through MEC, and consequently to larger T amplitudes and longer repolarisation (or QT) intervals. An illustrative example from Meijborg [96] is reproduced in Figure 5.16.

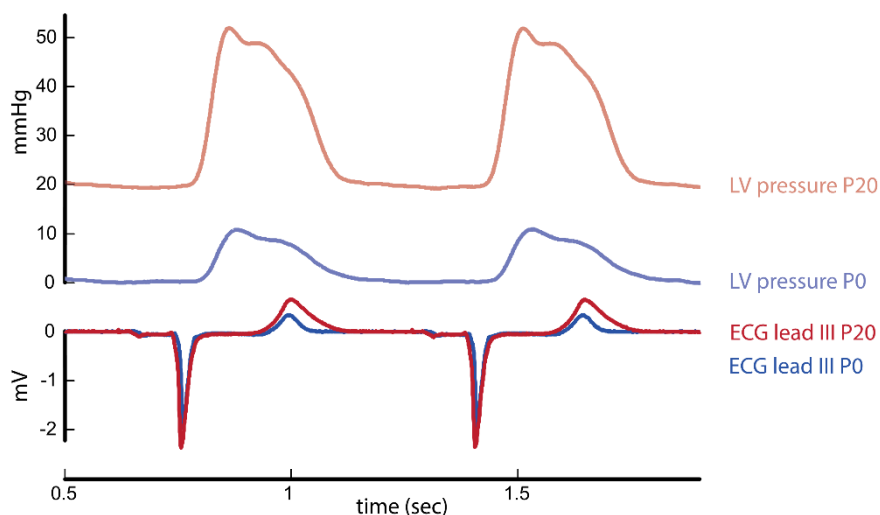


**Figure 5.16:** An example shows the left ventricular pressure changes and induced ECG changes. The simultaneous recordings of the left ventricular (LV) pressure and ECG (lead III) at a diastolic LV pressure of 0 mmHg (P0, blue trace) versus 20 mmHg (P20, red trace). The increased in LV pressure resulted in larger T-waves [96].

It is stated above that long preceding R-R leads to large volume of blood filling the left ventricle leading to large stretch for its walls, and accordingly high left ventricular pressure, which leads to prolong repolarisation intervals and increased T wave amplitudes. This is consistent with the study results where T wave amplitudes (section 5.2.2.1.2) were larger and R-T intervals (section 5.2.2.1.4) were longer related to ‘Long preceding R-R’ intervals. This presumably corresponds to the prolongation in repolarisation process, through increased ventricular dispersion and action potential [94,95]. On the other hand, for ‘Short R-R’ intervals, small volume of blood fills left ventricle, which leads to less stretch to the heart walls combined by smaller left ventricular pressure, and that leads to shorter R-T intervals and smaller T wave amplitudes compared to their values influence by ‘Long R-R’.

T wave amplitudes, similar to U wave amplitudes, were independent of the length of current beat intervals. As explained above, that left ventricular function is mainly dependent on the length of preceding beat interval, which effects the preload or the passive filling in left ventricular before the new cardiac cycle starts.

Therefore, it seems highly plausible that the rate dependency of repolarisation features (T and U wave) was due to ventricular filling dynamics induced by changes in the preceding beat interval. The beat averaging algorithm is able to capture these subtle amplitude and duration changes by careful selection of individual beats to use in the algorithm.

Further, the amplitudes at the end of the T wave (TUn) were influenced by the change of preceding R-R. The TU nadir (TUn) amplitude behaved similarly to both U and T waves, increasing with increasing preceding R-R intervals. This may suggest increased dispersion of repolarisation for beats with longer preceding R-R. In other words, it was subjected to the same effect of preceding R-R intervals and accordingly the same effect of left ventricular pressure as it represents part of repolarisation components. With ‘Long R-R’ intervals, a larger volume of blood flows into left ventricle, causing more stretch due to the greater expansion of the hearts walls, this leads to increase left ventricle pressure, in which results to greater amplitudes for TUn. While for ‘Short R-R’ intervals, smaller volume of blood flows into left ventricle, causing less stretch due to the smaller expansion of the hearts walls, this leads to less left ventricle pressure, in which results to smaller amplitudes for TUn compared to the effect of ‘Long R-R’.

The results showed that the intervals R-TUn were independent of the effect of the prolongation of preceding R-R intervals in AF.

QT lengthening is a widely known effect of heart rate slowing (R-R interval increasing) so our finding of increased R-T intervals is consistent with this. Our finding [132] of increased amplitudes at the peak and at the terminal part of the T wave may suggest increased dispersion of repolarisation for beats with longer preceding beat intervals, although other factors may also contribute to T wave amplitude changes [95]. A linear increase in T wave amplitude with increasing R-R interval was observed in healthy subjects during long term Holter monitoring [193], but beat interval changes in healthy subjects are generally small outside of exercise and slowly changing unlike those in AF. Nonetheless our results are consistent with the findings of

that study. In contrast, as will be shown in the next section of this chapter, healthy subjects during the post exercise recovery period exhibited the opposite response to increasing R-R interval because their T waves decreased in amplitude [131] (see study 5.3 of this chapter) suggesting exercise imparts a different response on ventricular repolarisation to heart rate changes and different to that we have observed during AF.

In summary, preceding beat intervals in AF have influenced most ventricular repolarisation features. The amplitudes of U wave, T wave, end of the T wave (TUn) and R-T intervals were increased alongside the prolongation of the preceding beat intervals. The R-TUn and T-U intervals were independent of preceding beat intervals. Average beats generated from 'current beat intervals' do not exhibit rate dependency highlighting the importance of using 'preceding' beat intervals in the beat averaging algorithm.

## **5.3. The Effect of the Heart Rate Changes Due to Exercise on the U and T Waves Amplitudes in Healthy Subjects**

It is difficult to study the effect of the heart rate (HR) changes on the ventricular features in SR recordings of healthy subjects due their stability. One method to change the heart rate substantially in SR is to stimulate the heart by exercise activity. So far, several studies investigated the effect of heart rate changes on the T waves in healthy subjects [91,92,128], however the U wave never been studied in such condition. Therefore, the aim of the study is to investigate the effect of heart rate changes, particularly that of preceding beat interval ( $HR=1/R-R$ ), on the amplitudes of the repolarisation waves (U and T) in healthy subjects following exercise. Their behaviour is compared to the effect of rate dependency shown in AF patients in the previous section (section 5.2).

### **5.3.1. Method**

#### **5.3.1.1. ECG Recordings**

The SR Exercise Database described in section 2.3.3 of Chapter two was used in this study. It contains 12-lead ECGs of 20 healthy subjects before and after exercise.

#### **5.3.1.2. ECG Processing**

The beat averaging mechanism that has been mainly described in section 3.2.3 of Chapter three, was used in this study with a few changes. Although the study relates to SR recordings, applying the beat averaging algorithm is useful to reduce the noise on the ventricular repolarisation features. Lead V4 was analysed, unless there was excessive artefact, then lead V2 or II were analysed (five subjects). The processing had two parts, the “pre-exercise” analysis and the “post-exercise” analysis, with the following description:

##### **5.3.1.2.1. Pre-Exercise Analysis**

The pre-exercise ECG records were used. The ECG recorded in the supine posture where the heart rate steady, is used as a reference record in the study. The length of pre-exercise records was 30 seconds. Figure 5.17 illustrates the method applied to a pre-exercise recording. At the *first stage* for each recording, R waves were detected, the beats collected automatically and aligned with the R wave peaks with visual confirmation, as illustrated in Figure 5.17-a.

The *second stage* of the analysis was to calculate the preceding R-R intervals as  $(R-R_{i-1} = R_i - R_{i-1})$  as shown in Figure 5.17-b. The first consecutive 30 beats were used to generate one averaged beat. The beat intervals were stable; however, a further requirement was to exclude beats with short following R-R intervals (referred to as  $R-R_i$  in Figure 5.17) that would

otherwise have P waves that could contaminate the averaged U wave. Therefore, beats with the  $R-R_i$  less than a threshold  $R-R_{\min}$  of 500 ms were excluded (if they exist). The qualified beats were aligned to their R peak ( $R_i$ ), and the averaged beat was calculated across the collected beats (Figure 5.17-c). The presence of the U wave was identified from the averaged beat (Figure 5.17-c).

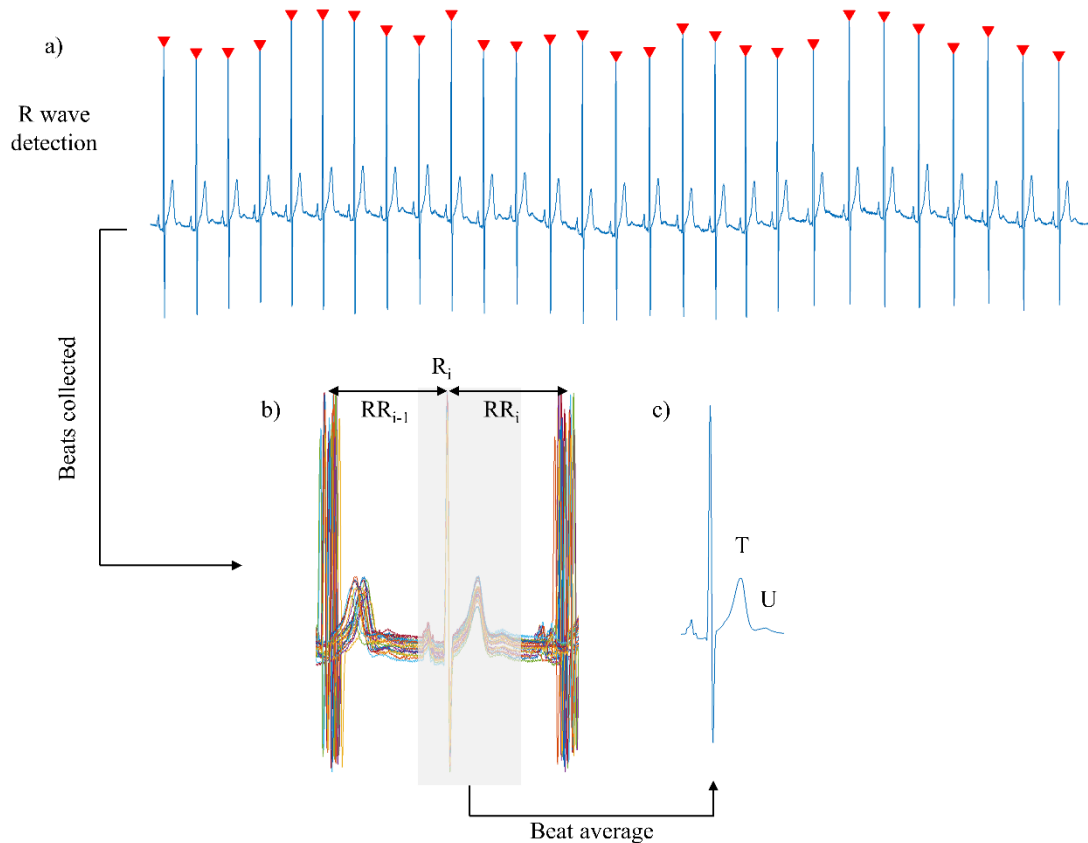


**Figure 5.17:** ECG signal processing to extract U wave from the pre-exercise records. R wave peaks ( $\blacktriangledown$ ) were detected in the ECG lead at the resting condition (a) R wave detection (b) qualified beats were extracted from the ECG lead and aligned to R peak ( $R_i$ ), (c) averaged beat calculated from the collected beats for the first consecutive 30 beats in the record, representing by the grey area in b) to reveal U wave in the averaged beat.

### 5.3.1.2.2. Post-Exercise Analysis

In the second part of the analysis, the post-exercise ECG records from the same subjects were used. The ECGs were recorded during recovery after exercise (treadmill exercise, see section 2.3.3). The length for post-exercise recordings was 360 seconds. The first 50 seconds from the record was used in the analysis, since the heart rate was rapid compared to the rest of the record where the heart rate starts to slow gradually after the exercise. The ECG processing was similar to section 5.3.1.2.1 for all stages. The first consecutive 30 beats were used to generate an average beat for the analysis. However, if there was an excessive artefact or strong baseline

wander in these beats, the second consecutive 30 beats were used instead. Figure 5.18 illustrates an example of the method applied to a post-exercise record.

The amplitudes of U waves and T waves were measured automatically from the baseline to U peak (or T peak) for the generated averaged beats in pre and post-exercise ECG records using the automatic measurement algorithm described in section 4.2 of Chapter four. A stable baseline amplitude was estimated from 10 samples window in the electrically inactive period before the onset of the P wave from the averaged beat.

The significance of differences in amplitudes of U and T waves between the prior and post-exercise recordings was assessed by paired *t*-test.

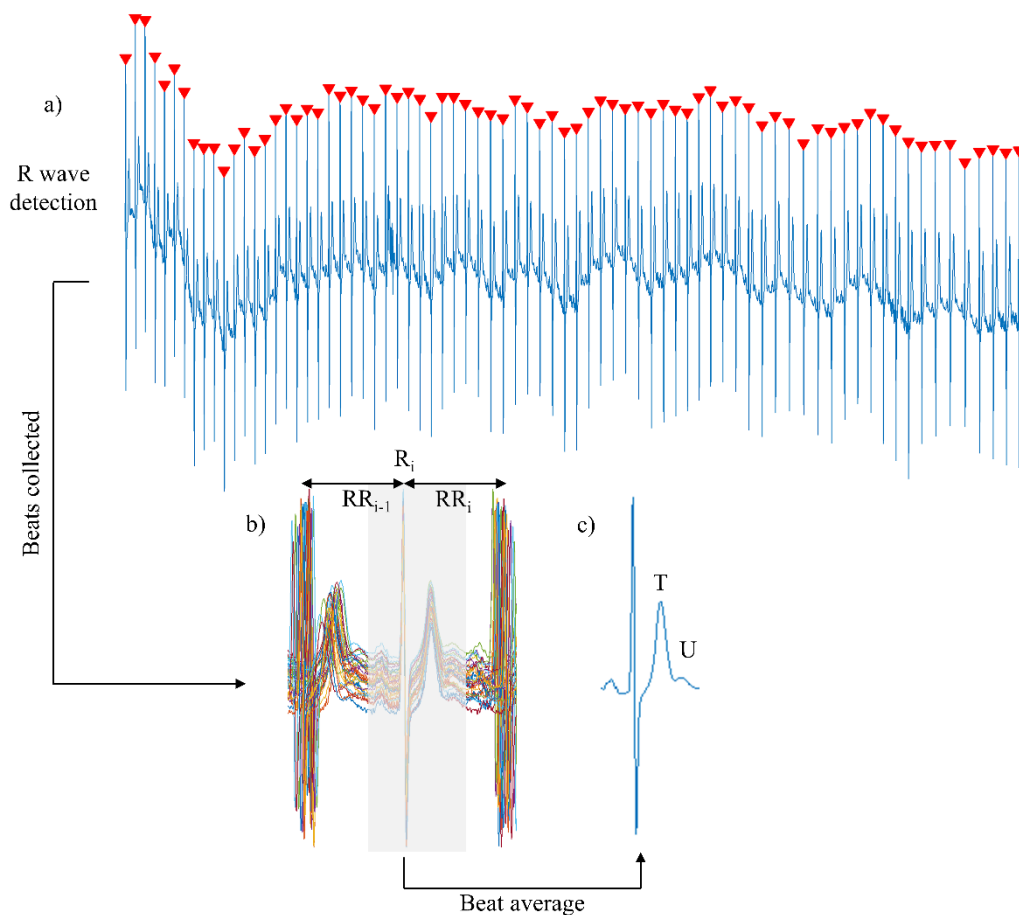


**Figure 5.18:** ECG signal processing to extract U wave from the post-exercise records. R wave peaks ( $\blacktriangledown$ ) were detected in the ECG lead at the recovery condition (a) R wave detection (b) qualified beats were extracted from the ECG lead and aligned to the corresponding R wave ( $R_i$ ), (c) averaged beat constructed from the collected beats represented by the grey area (in b) for the first or the second consecutive 30 beats in the record to reveal U wave.

## 5.3.2. Results

### 5.3.2.1. U Wave Amplitudes

After applying the beat averaging algorithm to the ECG recordings for 20 healthy subjects, all of them had visible U waves in both recordings, pre-exercise and post exercise. Table 5.7 lists the U amplitudes for all the subjects and the associated heart rate for pre and post-exercise. Figure 5.19 illustrates an example for two average beats during pre (a) and post exercise (b) for the same subject. In both averaged beats, U waves were visible.

For 20 healthy subjects, the statistical results showed that U wave amplitudes were significantly increased ( $p=0.0003$ , assessed by paired  $t$ -test) from  $36 \pm 14 \mu\text{V}$  (mean  $\pm$  SD) at the pre-exercise condition (heart rate  $63 \pm 8$  bpm), to  $80 \pm 48 \mu\text{V}$  at the post-exercise condition (heart rate  $100 \pm 9$  bpm) and ( $\Delta$  amplitudes  $44 \pm 45 \mu\text{V}$ ).

The example in Figure 5.19 represents the pre and post exercise averaged beats, where it is obvious that U wave has the higher amplitude during the post-exercise compared to the prior one. Figure 5.19-a shows an averaged beat for the pre-exercise with resting heart rate, the U wave is visible and measurable. Figure 5.19-b shows an average beat for the post-exercise condition for the same subject and again the U wave is visible, and its amplitude is higher than the U wave in (a).

Figure 5.20-a represents the paired relation between U wave amplitudes, and Figure 5.20-c represents the heart rates in the pre and post-exercise for 20 subjects. As the Figure shows, the U wave amplitudes increased in most of the subjects (18 of 20 subjects, see Table 5.7) during the post exercise condition when the heart rates are increased rapidly compared to their amplitude during the pre-exercise when the heart rates are steady.

### 5.3.2.2. T Wave Amplitudes

T wave amplitudes were measured similarly to the U wave amplitudes measurements for 20 subjects during the pre and post exercise condition. The statistical results showed significant increase in the T wave amplitudes from the pre-exercise ( $650 \pm 250$ )  $\mu\text{V}$ , compared to the post-exercise ( $700 \pm 160$ )  $\mu\text{V}$ ,  $p=0.006$ , assessed by paired  $t$ -test, and ( $\Delta$  amplitudes  $117 \pm 167 \mu\text{V}$ ).

The example in Figure 5.19 for the two average beats clearly shows the increase in the T wave amplitude during the post exercise (b) where the T wave was higher, while its amplitude in pre-exercise beat (a) was lower for the same subject.

Figure 5.20-b illustrates the paired relation between T wave amplitudes measured in the pre and post-exercise for the 20 subjects. The T wave amplitudes during the post-exercise condition (rapid heart rate) compared to the pre-exercise condition (slower heart rate) were higher in 16 subjects, and reduced amplitude in 4 subjects (see Table 5.7 and Figure 5.20-b and c).

**Table 5.7:** Summary of 20 healthy subject recordings during pre and post-exercise, HR= heart rate (beat/minute), U amp = U amplitude ( $\mu\text{V}$ ), and T amp = T amplitude ( $\mu\text{V}$ ).

Subject	Lead Analysed	Pre-Exercise			Post-Exercise			$\Delta$ amplitudes ( $\mu\text{V}$ )	
		HR (bpm)	U amp ( $\mu\text{V}$ )	T amp ( $\mu\text{V}$ )	HR (bpm)	U amp (mV)	T amp ( $\mu\text{V}$ )	$\Delta\text{U}$	$\Delta\text{T}$
1	V4	70	48	654	98	48	601	0	-53
2	II	56	19	451	96	78	701	59	250
3	V2	54	11	387	94	35	588	24	201
4	V4	64	39	789	108	78	726	39	-63
5	V4	48	47	720	106	168	890	121	170
6	V4	62	54	550	100	109	579	55	29
7	V4	56	36	321	91	88	688	52	367
8	V4	66	28	1226	110	43	996	15	-230
9	V4	70	27	278	104	32	482	5	204
10	V4	56	47	927	113	197	1085	150	158
11	V2	68	39	722	78	9	562	-30	-160
12	II	56	40	639	92	105	708	65	69
13	V2	68	53	503	101	67	621	14	118
14	V4	66	17	413	108	122	592	105	179
15	V4	62	50	739	114	77	744	27	5
16	V4	70	48	704	102	55	857	7	153
17	V4	58	22	284	96	67	503	45	219
18	V4	80	43	551	104	131	603	88	52
19	V4	68	25	243	90	64	709	39	466
20	V4	68	16	221	89	18	418	2	197

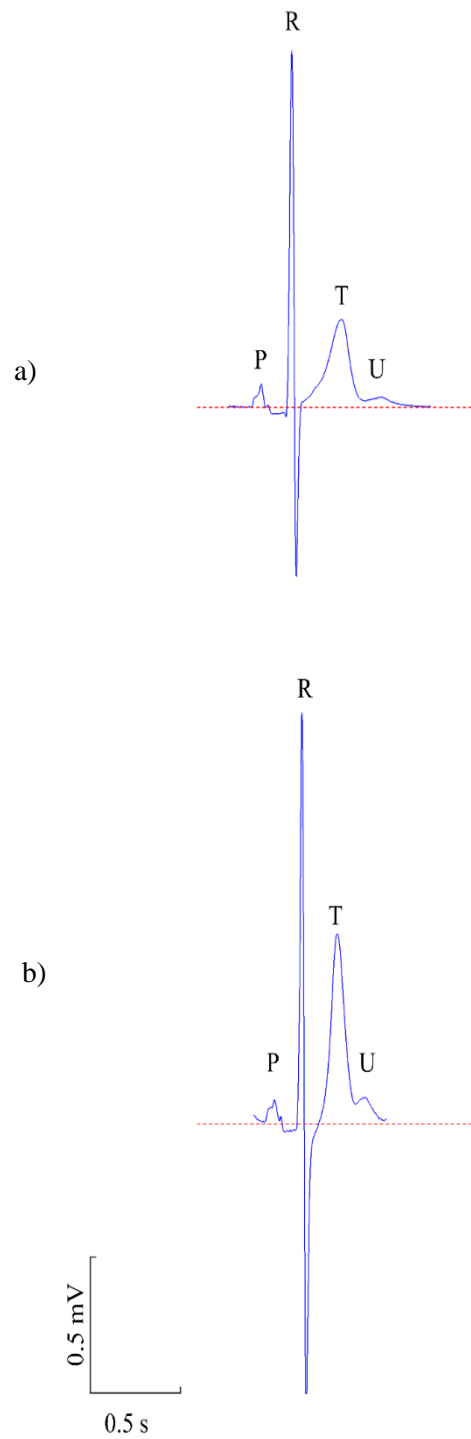


**Figure 5.19:** Two averaged beats for the pre and post-exercise recording for the same subject. **a)** averaged beat for pre-exercise recording, **b)** averaged beat for the post-exercise recording. U wave in both beats were visible and measurable, however its amplitude was higher in the post-exercise (b) compared to the pre-exercise condition (a), as was the T wave.

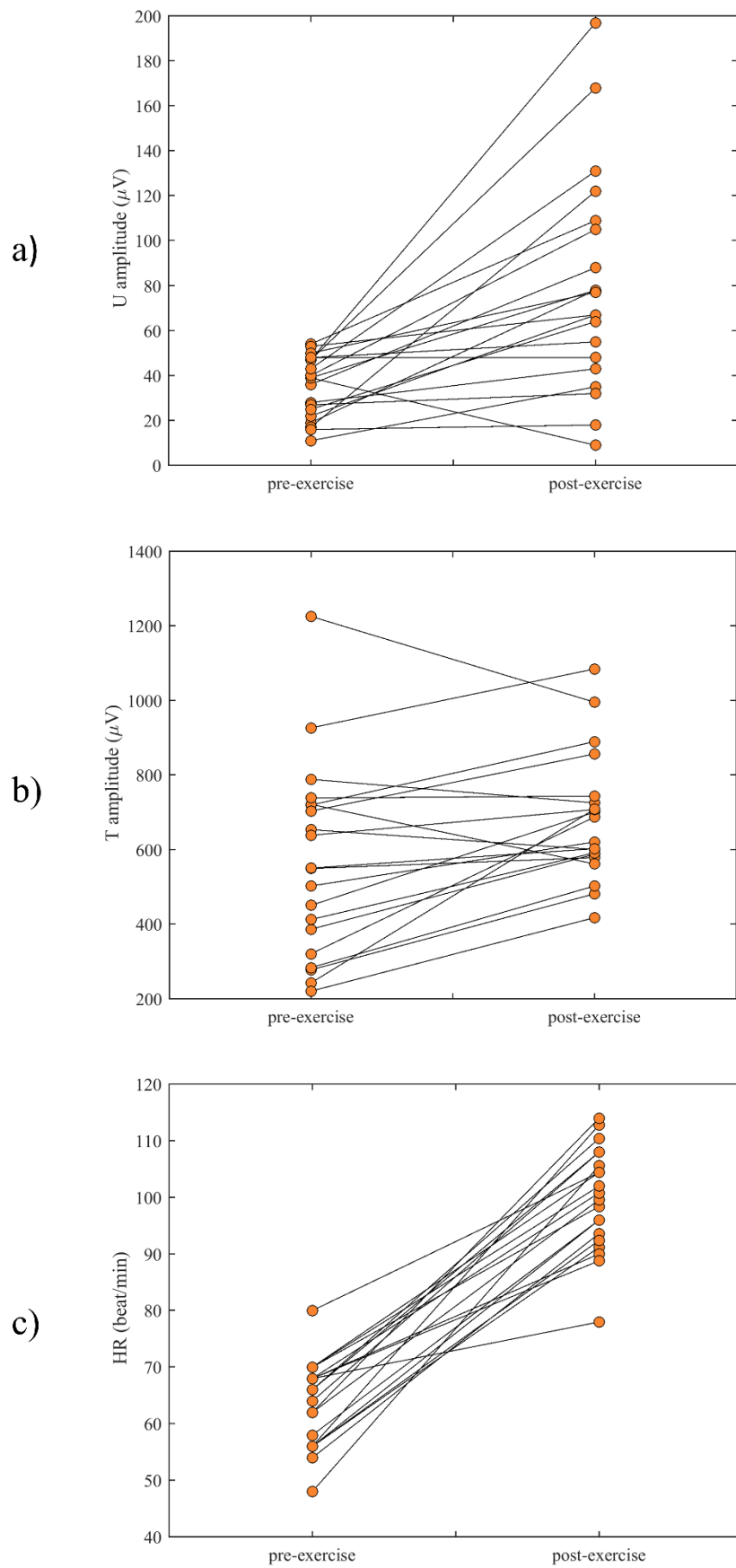


**Figure 5.20:** Paired relationship for U and T wave amplitudes and heart rates for 20 healthy subjects during the pre and post exercise. **a)** U wave, **b)** T wave, and **c)** heart rate (HR).

### 5.3.3. Discussion

The results showed that exercise-induced heart rate changes affect the repolarisation waves, where both of T and U wave amplitudes increased significantly when the heart rate rises.

The increase of T wave amplitudes may suggest there is increased dispersion of the repolarisation (DOR) with the increase of heart rate ( $HR=1/R-R$ ), since the concept of the T wave amplitude genesis depends on two variables: the DOR and the action potential duration (APD) [94,95, 131,194,195]. Heart rate and the action potential duration are linearly correlated [92,98,180] where the rise of the heart rate is shortening the action potential and the vice versa (see Figure 1.10 in Chapter one). Kitchin et.al [196] showed that T wave amplitude increases during the post-exercise due to the change of action potentials of the myocardial cells.

In a study of the effect of the action potential duration on the T wave [95,101], the authors found that T wave amplitude is proportional to the DOR and inversely proportional to the repolarisation time or the minimal action potential duration. This means that T wave amplitude increases with the short action potential. In other words, T wave amplitudes increased with high heart rate since heart rate is linearly correlated to the action potential duration. Our results are consistent with this study [95,101]. In addition, other studies to investigate the T wave morphology changes with respect to the heart rate changes for the healthy subjects [94,95,131] showed the same response to our results, where T amplitudes increased with faster heart rate. Furthermore, in a study as understand the effect of mechano-electrical coupling (MEC) on the repolarisation process and T wave [96,97], the investigation showed that increasing left ventricular pressure via MEC has an effect on the repolarisation, causing a prolongation for the repolarisation intervals and higher amplitudes for the T wave [96,97].

Physiologically, the cardiovascular system adapts to change during exercise to produce adequate energy to the working muscles by increasing the heart rate and cardiac output [36], as described in section 1.2.4.1 of Chapter one. The increase of cardiac output occurs because of the large end-diastolic volume EDV (see Figure 1.26) and that means large blood volume fills the left ventricle [36]. In other words, preload increases causing more stretch to the myocardium, and that helps the left ventricle to contract more fiercely according to Frank-Starling law of the heart [31, 36,41]. This hard contraction increases the left ventricle pressure during the rapid heart rate and according to [96,97], that will produce a higher T wave amplitude, which is consistent with study results of T wave in our study.

U wave amplitudes were visible and measurable in both pre and post-exercise recordings. Despite the rapid heart rate during the post-exercise, U waves were extracted, and their amplitudes were measured. The U wave has been reported to be present in 90% of healthy subjects at slow heart rates and stated that it cannot be seen at rapid heart rate [48,50]. However, in the current study U waves were observable in fast heart rate during post-exercise recordings (see Figure 5.19 and section 5.3.2.1). U wave amplitudes respond to the increase of the heart rate positively during the post-exercise, while they have lower amplitudes during the pre-exercise in most subjects. The U wave behaves similarly to the T wave, both are increased

when the heart rate is elevated in the post exercise period. U wave amplitudes were highly dependent on the heart rate.

Although the origin of U waves is uncertain, but the assumption is that U waves are a reliable feature at the end of the repolarisation cycle in every ventricular beat and undergoes the same changes of the repolarisation process, as the T wave. Since increases in heart rate will cause larger blood volume flows into the left ventricle, and accordingly causes more stretch to the myocytes during diastole (increases the preload) according to the Frank-Starling mechanism (see 1.2.4.1 of Chapter one). This expansion of the heart's walls will increase the pressure of the left ventricle and activates the mechanosensitive ion channels which transduce the pressure and the stretch into electrical signal [79-80] with higher amplitude [49,63,96,97]. Additionally, as the heart rate changes influences the action potential, Bernardo and Murray postulated in their study [82] that if larger after-potential occurred, the U wave amplitude becomes more distinct.

One of the hypotheses of the U wave genesis is mechano-electrical coupling MEC (see section 1.3.3.3 of Chapter one). This theory suggests that after-potentials caused by stretching of the left ventricle give the rise to the U wave. The presence of U wave in slow and fast heart rate, gives the indication that U wave is reliable feature of the ECG occurring at the end of the repolarisation phase after T wave, regardless of heart rate. The possible contribution of the MEC to generate U waves because of the myocyte stretch is high and can be more obvious during the post-exercise recording during the fast heart rate, where the combination of the MEC and high systolic pressure (left ventricular pressure) influence the repolarisation waves including U wave to be larger. The reason for the absence in some reported U wave during the rapid heart rate is because U wave and P wave become coincident, where the U wave buried under the P wave.

It seems plausible that the U wave is an electrical manifestation for ventricular mechanical stretch. The results of the U wave in this study show strong support to MEC hypothesis, and suggest it is part from the repolarisation process like the T wave, since they respond to rate changes in very similar ways.

As expected, there were no abnormal T or U waves in the recordings in this investigation, where both of the waves were upright with positive polarity. The observation of the increased T wave amplitudes may help to predict the change of DOR and that can help with early diagnoses of QT symptoms, since they are strongly linked to the fatal arrhythmia and sudden death [95,197]. Also, U wave abnormalities are associated with cardiac pathology, such as ischemia, hypertension and hypertrophy and due to the hypokalaemia or to the drug effects. The U wave has also been considered a potential marker of Torsade de Points [49,52,63,67]. This study did not detect abnormal U waves, as expected in a healthy subject group, however, it still important to understand the U wave characteristic since the major cardiac organisation such as American Heart Association (AHA), and Heart Rhythm Society (HRS) recommended that all U wave abnormalities should be reported during the ECG interpretation [49,52].

In study 5.2 in this chapter, U and T wave amplitudes were investigated with respect to the change of preceding beat intervals in AF. The amplitude results for both waves were in contrast of their amplitude in the healthy subjects. In the current study, U and T waves amplitudes were increasing with short preceding R-R (fast heart rate) and decreasing with long preceding R-R (slow heart rate). Whereas, in AF the amplitude of both waves was increasing with long preceding R-R (slow heart rate) and decreasing with short preceding R-R (fast heart rate). The possible reason for this behaviour linked to the stretching via MEC during ventricular filling dynamics for both cases (i.e. in healthy subjects and AF). However, the ventricular filling process is different for these two cases.

In AF, as the study 5.2 presumed, the left ventricular filling is greater with respect to long preceding R-R (slow heart rate) [190] (i.e. greater volume of blood fills the left ventricular, higher EDV) which cause a greater expansion to the heart's wall, leading to increase the stretching force of the cardiac muscle according to Franck-Starling law [185]. The increase of stretching leads to higher pressure in the left ventricle which effect positively the amplitude of the repolarisation features and produces higher amplitudes for U and T waves via MEC [96,97,185]. With short preceding R-R (fast heart rate), less amount of blood fills the left filling due to the short filling in which leads to less pressure in the left ventricle according to the small expansion of the cardiac muscle walls. This produces smaller amplitudes for T and U wave (more details in study 5.2).

Whereas in the current study, due to the cardiorespiratory system adaptation to the exercise, the heart rate increases (short preceding R-R) in order to increase the amount of blood that needed to provide the body's muscles with the required energy (i.e. metabolism). In other words, and as has been mentioned earlier in the study discussion, with the increase of heart rate in post exercise condition, the ventricles rapid filling increases (i.e. large blood volume fills the left ventricle). Consequently, the heart wall expanded and increased the stretch to the myocardium, and that helps the left ventricle to contract more fiercely according to Frank-Starling law of the heart. This expansion of the heart's walls will increase the pressure of the left ventricle producing higher amplitude (i.e. higher amplitudes of U and T wave) via MEC. Whereas less filling of the left ventricle during the pre-exercise when the heart rate is slower (long preceding R-R), leads to smaller stretch to the heart's wall in which reverse the results compared to the fast rate condition, producing lower amplitudes for the repolarisation waves (i.e. U and T waves) due to less pressure.

In conclusion, U wave is visible and measurable during the pre and post-exercise (normal and fast heart rate) in healthy subjects. The U wave similar to T wave, responded to the change of heart rate where their amplitudes increased with the increase of the heart rate. T and U wave are dependent on the heart rate.

## 5.4. Chapter Summary

The first study (section 5.2) in the chapter showed that preceding beat intervals in AF have influenced most of ventricular repolarisation features. The amplitudes of U wave, T wave, end of the T wave (TUn) and R-T intervals were increased alongside the increasing of the preceding beat intervals. The R-TUn and T-U intervals were independent of preceding beat intervals influence. The study confirmed that current beat intervals have no effect on the corresponding repolarisation features.

The second study (section 5.3) showed that U wave is visible and measurable during the pre and post-exercise (normal and fast heart rate) in healthy subjects. The U wave like T wave, responded to the change of heart rate where their amplitudes increased with the increase of the heart rate.

The T and U waves are dependent on the heart rate. They are moving and increasing together in AF and healthy subjects.

# **Chapter 6**

## **Future Perspectives**

## **Chapter 6. Future Perspectives**

### **6.1. Introduction**

This chapter highlights several ideas for further research that has arisen during this project. The proposed investigations can help to extend the thesis research in the same and different directions as they provide in many of them, a further insight to understand U waves in ECG.

### **6.2. U wave Abnormalities in Atrial Fibrillation**

Major cardiac organisations recommended U wave abnormalities should be reported during ECG interpretation [49,52]. We did not detect any abnormalities during this project, perhaps due to the limited number of patients considered during the studies. Having established reliable algorithms to clean AF recordings, detect and measure U waves would facilitate the detection of the abnormal U waves. Therefore, further studies are needed to establish the prevalence of U wave abnormalities in AF patients.

### **6.3. Further Investigation of U Wave Genesis (Cellular Basis)**

#### **6.3.1. Intracellular Calcium Dynamics and the U Wave**

The sarcomeres length by stretch would increase the  $\text{Ca}^{2+}$  flow during the relaxation phase and would accelerate  $\text{Ca}^{2+}$  waves [8,14,22,50]. Stretch induces an immediate increase in twitch force which is the result of a length-dependent increase in  $\text{Ca}^{2+}$  sensitivity of cardiac muscle, this is generally accepted as the cellular basis of the Frank-Starling mechanism [50].

We showed the U wave amplitude depends upon the preceding beat interval, both in AF and SR. The preceding R-R interval affects ventricular filling dynamics [175,176] and hence also on mechano-electrical coupling. We proposed that U wave amplitudes changes were linked to the stretching changes in the left ventricular walls during diastole via mechano-electrical coupling.

Wu and et.al [198] established the relationship between action potential duration and the duration of the intracellular  $\text{Ca}^{2+}$  transient. The study was used to simulate SQTS which is related to the mechano-electrical coupling influence. The authors concluded that persistent increases in intracellular calcium, and after-depolarisations, underly the U wave [198].

The influx of  $\text{Ca}^{2+}$  lengthens the total duration of the cardiac action potential, leading to the change in the cardiomyocyte as it plays a key role in mechanical contraction and stretching. Since the action potential is related to the heart rate changes, additional insight into the molecular links between cardiac mechano-electrical activity and the U wave in different heart

rates is required. Further studies are needed to inspect and measure beat interval dependency of the intracellular calcium and their effect on the U wave amplitudes.

### **6.3.2. The Imaging for U Wave in LQTS**

The prominent U wave and long QT interval (i.e. long R-R) are widely known characteristics of LQTS [53,71,80,86]. The mechano-electrical and the M cell hypotheses of the U wave both presumably influence the generation of U waves that are clinically observed.

In LQTS, the dispersion of repolarisation would provide a prolonged period of active ventricular relaxation during early diastole, which may strengthen ventricular filling displayed clinically as a high E/A ratio (the marker of the function of left ventricle) in the velocity by Doppler echocardiography, an ultrasound-based cardiac imaging modality [63].

By affecting heart tissue contractility during slow filling due to the long R-R interval in LQTS, delayed M cell repolarisation, which could be modulated by mechanical coupling, could serve other mechanical functions that would require further investigation. Therefore, inspecting LQTS subjects using the ultrasound, and investigate U wave in such condition would be helpful to add further understanding to the mechanical coupling during the ventricular filling.

### **6.4. The Depression of P-R (PQ) Interval in Healthy Subjects**

P-R interval or as electro-cardiographers preferred the term P-Q interval is the interval from the beginning of P wave to the beginning of QRS complex. [199] Although the P-R was not in the remit of the research presented in this thesis, during the analysis of the healthy subject recordings in study 5.3, we observed that P-R interval exhibited a depression in post-exercise compared to the pre-exercise. Figure 6.1 shows an example of two averaged beats for the same subject during the pre-exercise and post-exercise.

Inspection of P-R intervals during exercise and post-exercise has rarely investigated and addressed [200]. The major reason is the estimation of this interval is particularly hard at rapid heart rates because T and U waves tend to overlap the P wave, which biases P wave detection [200]. The P-R depression or elevation were indicated as a mark to atrial injury [201] or pericarditis [200].

In a preliminary study in 1960, Lloyd-Thomas [44] reported that ‘P-Q’ segment showed depression after exercise. The author regarded this depression as due to accentuation of the atrial T wave (Ta). According to a theory presented by Scherf and Schaffer [203], the area bounded by the P wave is equal in size but opposite in polarity to the area of the Ta wave. As the Ta wave shortens with tachycardia (fast heart rate), it must deepen in order to keep its area equal to and opposite to that of the P wave.

Further studies are therefore required to inspect the effect of the heart rate changes on the P-R interval due to exercise in healthy subjects. This may help to give an insight to the underlying mechanism of this P-R depression in healthy subjects due exercise.

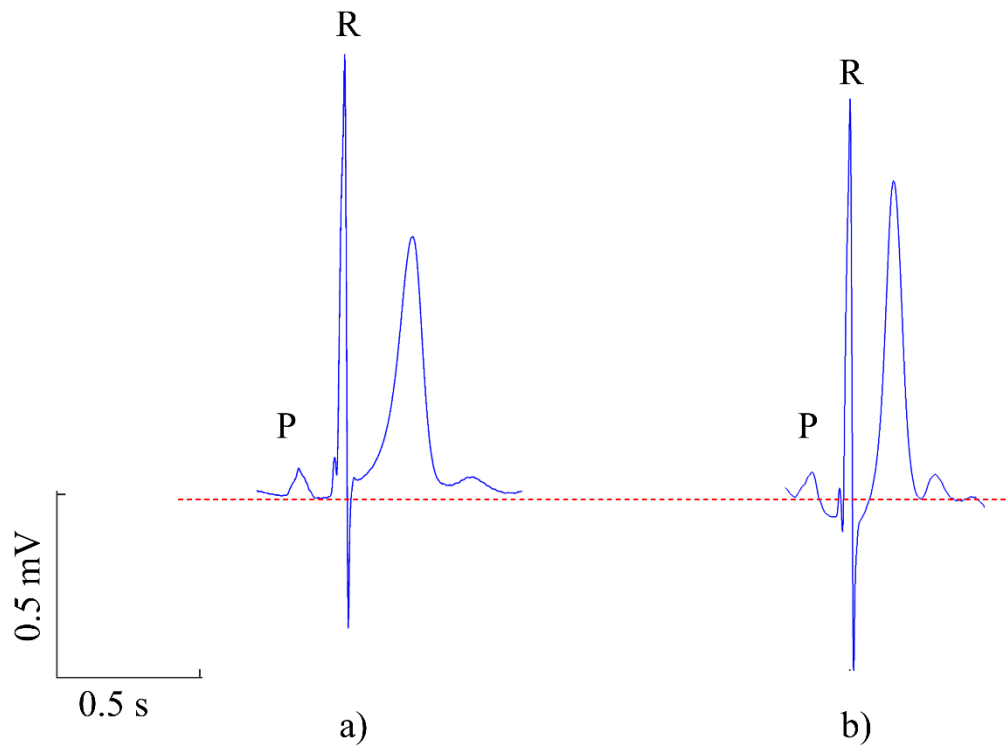


**Figure 6.1:** Example of two averages beats during **a)** pre-exercise and **b)** post-exercise for the same subject. The P-R interval showed depression in b) compared to a).

## **Chapter 7**

# **Research Summary and Final Discussion**

## Chapter 7. Research Summary and Final Discussion

Atrial fibrillation is a common arrhythmia characterised by rapid changes in ventricular beat intervals. It provides an opportunity to investigate the effect of rapid beat interval changes on the characteristics of ventricular repolarisation components, U and T waves.

The U wave in atrial fibrillation is hard to observe and measure because it is hidden under the fibrillatory waves that results from the continuous and rapid atrial activation, which contaminate the ventricular repolarisation features including T wave [1,54]. To measure U wave and other ventricular features of ECG accurately, these atrial fibrillatory waves must be removed. Therefore, the first target of the research was to provide a validated algorithm to clean the ECGs of atrial fibrillation patients. The research proposed three techniques to remove these fibrillatory waves and provide clean ECGs beats so the ventricular features can be measured. The techniques were PCA, ICA and beat averaging (BA). Their ability to remove the atrial activity was evaluated *visually*, by observing the presence of a clean U wave. This metric of the technique's efficiency was chosen as it represents the main interest of the thesis research.

The PCA and ICA techniques gave inferior results and U wave was poorly revealed. However, PCA in comparison to ICA showed better performance to reveal U wave despite the remaining noise. On the other hand, the BA technique was able to remove the atrial fibrillatory waves effectively and provide clean ventricular beats suitable for detection and measurement.

The BA technique effectiveness in noise reduction level is associated with the number of ventricular beats used during the averaging calculation to generate *one* ventricular averaged beat. Thus, long duration of recordings is required to provide greater noise reduction and to reveal high quality U wave. A limitation is the long duration needed to collect many beats for the averaging process. A further limitation is that it provides one averaged beat which limits the possibility to investigate the changes of ventricular repolarisation characteristics beat by beat. Nevertheless, the BA algorithm provided an effective tool to clean AF recordings from the atrial activity and had the capability to capture the subtle amplitude and duration changes related to preceding beat intervals. The BA algorithm facilitated further investigations to detect and measure ventricular components not only for AF but also for SR., since it provides noise reduction in, for example, exercise ECG recordings.

Having the ability to generate clean averaged beats, provided an opportunity to measure the desired ventricular components. The “automatic ECG feature measurement algorithm” has been established to measure U and T wave amplitudes and intervals automatically. The measurement was validated against manual measurement via bespoke Matlab software created to measure the ventricular components manually. Both measurement approaches provided a useful tool to detect and measure the ventricular components, especially U waves in AF and SR.

The algorithm was validated by comparing U waves extracted from AF recordings to U waves readily observable in SR recordings for the same patients. The U waves were visible in both AF and SR and U waves in AF had the same polarity as those in SR, but with increased amplitude in most subjects. With the ability to detect and measure U waves during AF, the algorithm provided the opportunity to explore potential mechanisms which might explain differences in U waves during AF and SR. It was hypothesised that the amplitude differences in AF and SR might be due to U wave rate dependency since the heart rates in AF and SR were significantly different.

BA algorithm effectiveness, as has been mentioned, is dependent on the number of beats collected and averaged, and accordingly affects the quality of the extracted U wave; thus, a study [1] was conducted to define the number of beats required for effective U wave extraction in AF recordings. The study showed that the number of beats is an important consideration since the greater the number of beats the greater the noise reduction. The study indicated that decreasing the number of beats from 100 to 70 did not significantly affect the U wave amplitude. However, the U wave was readily observable when the average beat was generated from as few as 10 beats with an average increase in noise amplitude of only 5  $\mu$ V. The study can be used to guide the clinicians to the requirement for the number of beats to use dependent upon the required application.

The BA algorithm satisfies an unmet clinical need because until now it has not been possible to measure U waves in AF. Many studies have noted the diagnostic value of U wave abnormalities, particularly inverted U waves [50,204-206]. Although we did not detect any abnormal U waves in our cohort, the algorithm facilitates the reporting of U wave abnormalities in AF patients as recommended by the important cardiac associations [52]. The algorithm facilitates the detection and reporting of U waves and their abnormalities in AF patients.

The establishment of a validated algorithm to allow reliable measurement of ECGs features, enabled the opportunity to inspect the effect of beat interval dependency on the repolarisation waves, especially U waves, during atrial fibrillation and to compare them to those in sinus rhythm of healthy subjects.

Two studies were conducted to investigate the changes of the ventricular beat interval in AF and healthy subjects. The studies exploited the beat averaging algorithm capability to capture the subtle amplitude and duration changes to address the study interest. The *first* study inspected the effect of beat interval changes on ventricular repolarisation characteristics, U and T waves amplitudes and intervals in AF. It was hypothesised that ventricular repolarisation characteristics such as T and U wave amplitudes and intervals exhibit a 'preceding' beat interval dependency. This dependency was confirmed by this study. The amplitudes of U wave, T wave, end of the T wave (TUn) and R-T intervals were increased alongside the increasing of preceding beat intervals. The R-TUn and T-U intervals were independent of preceding beat intervals influence. The study confirmed that 'current' beat intervals have no effect on the corresponding repolarisation features. Therefore, if the rate dependency of ventricular repolarisation features is to be captured, it is important to consider the preceding beat interval.

One of the methods to change the heart rate substantially in SR is by stimulate the heart by exercise, therefore, the second *study* was conducted to investigate the effect of the heart rates changes on the amplitudes of the repolarisation waves in healthy subjects during the exercise. The study compared the rate dependence of U and T waves in SR after exercise to the effect of the rapid beat interval changes in AF. The U wave was visible and measurable during the pre and post-exercise (normal and fast heart rate) in healthy subjects. The U wave like T wave, responded to the change of heart rates where their amplitudes increased with the increase of the heart rates in SR. However, in AF the amplitudes of U and T waves had the opposite response (i.e. decreased) to the increase of heart rate changes. The T and U waves are dependent on the heart rate in AF and SR.

The linking mechanism which potentially explains the observed rate dependencies in both AF and SR recordings is mechano-electrical coupling. In AF, long preceding beat interval results in more blood entering the ventricle, leading to increased stretch, increased ventricular pressure and associated action potential changes which result in increased amplitude and prolongation of ventricular repolarisation. In SR, long beat interval (heart rate in resting condition) results in less blood entering the ventricle compared to the filling during exercise, leading to less stretch to hearts wall, accordingly less ventricular pressure and associated action potential changes compared to during exercise, which result in less amplitude of ventricular repolarisation features.

In summary, the thesis studies provided useful algorithms to clean AF recordings and measure the ventricular components in either AF or SR. The challenging U wave was revealed in AF. The U and T wave amplitudes and intervals were measured with respect to preceding R-R showing a rate dependency in AF and SR. In AF, the amplitudes of U and T wave were increasing with respect to the increasing of preceding beat intervals, whereas they were decreasing in SR. This indicates that U wave follows T wave either in AF or SR, where they increased and decreased together in which suggesting they are subjected to the similar repolarisation process. The beat interval dependency of ventricular repolarisation features showed support to the mechano-electrical hypothesis during AF and SR.

# References

1. Al-Karadi MS, Wilkinson AJ, Caldwell J, Langley P. Validation of an algorithm to reveal the U wave in atrial fibrillation. *Sci Rep* 2018; **8**: 11946, doi:<https://doi.org/10.1038/s41598-018-30493-8>.
2. Marieb EN, Keller SM. *Essentials of Human Anatomy & Physiology*. 12th ed. Pearson Education: Essex, England, 2017.
3. Saladin KS. *Loose Leaf for Anatomy and Physiology: The Unity of Form and Function*. 8th ed. McGraw-Hill Education: New York, NY, 2017.
4. Martini F, Nath JL, Bartholomew EF. *Fundamentals of Anatomy & Physiology*. 10th ed. Pearson Education, 2015.
5. Tortora GJ, Derrickson B. *Principles of Anatomy and Physiology*. 15th ed. John Wiley & Sons, 2018.
6. Bronzino JD, Peterson DR. *Biomedical Engineering Fundamentals*. 3rd ed. CRC Press, 2006.
7. Malmivuo P, Malmivuo J, Plonsey R. *Bioelectromagnetism: Principles and Applications of Bioelectric and Biomagnetic Fields*. 1st ed. Oxford University Press, 1995.
8. Stanfield CL. *Principles of Human Physiology*. 5th ed. Pearson Education, 2013.
9. Moore KL, Dalley AF, Agur AMR. *Clinically Oriented Anatomy*. 7th ed. Lippincott Williams & Wilkins, 2014.
10. Widmaier EP, Raff H, Strang KT. *Vander's Human physiology: The Mechanisms of Body Function*. 15th ed. McGraw-Hill Education, 2019.
11. Koeppen BM, Stanton BA. *Berne & Levy Physiology*. 7th ed. Elsevier, 2017.
12. Drake R, Vogl AW, Mitchell AW. *Gray's Anatomy for Students*. 3rd ed. Elsevier Health Sciences, 2014.
13. Pinnell J, Turner S, Howell S. Cardiac Muscle Physiology. *Contin Educ Anaesth Crit Care Pain* 2007; **7**: 85–88, doi: <https://doi.org/10.1093/bjaceaccp/mkm013>.
14. Silverthorn DU. *Human Physiology: An Integrated Approach, Global Edition*. 7th ed. Pearson Higher Ed, 2015.
15. Sherwood L. *Fundamentals of Human Physiology*. 4th ed. Cengage Learning, 2011.
16. Porth C. *Essentials of Pathophysiology: Concepts of Altered Health States*. 4th ed. Lippincott Williams & Wilkins: Philadelphia, USA, 2014.
17. Davis D. *Quick and Accurate 12 Leads ECG Interpretation*. 4th ed. Lippincott Williams & Wilkins, 2005.
18. Heuer AJ. Interpreting the Electrocardiogram. In: *Egan's Fundamentals of Respiratory Care*. Elsevier Health Sciences, 2016.
19. Katz AM. *Physiology of the Heart*. 5th ed. Lippincott Williams & Wilkins, 2010.

20. Calvert JW, Lefer DJ. Overview of Cardiac Muscle Physiology. In: *Muscle*. Academic Press, 2012, pp 57–66, doi: <https://doi.org/10.1016/C2009-0-61900-0>.
21. Weiss JN, Garfinkel A, Karagueuzian HS, Chen P-S, Qu Z. Early afterdepolarizations and cardiac arrhythmias. *Heart Rhythm* 2010; **7**: 1891–9, doi: <https://doi.org/10.1016/j.hrthm.2010.09.017>.
22. Bers DM. Cardiac Excitation–Contraction Coupling. *Nature* 2002; **415**: 198–205, doi: <https://doi.org/10.1038/415198a>.
23. Goldberger AL, Goldberger ZD, Shvilkin A. ECG Basics: Waves, Intervals, and Segments. In: *Goldberger's Clinical Electrocardiography*. Elsevier, 2018, pp 6–10, doi: <https://doi.org/10.1016/B978-0-323-40169-2.00002-0>.
24. Goldberger AL, Goldberger ZD, Shvilkin A. How to Make Basic ECG Measurements. In: *Goldberger's Clinical Electrocardiography*. Elsevier, 2018, pp 11–20, doi: <https://doi.org/10.1016/B978-0-323-40169-2.00003-2>.
25. Webster JG. *The Physiological Measurement Handbook Series in Medical Physics and Biomedical Engineering*. 1st ed. CRC Press: Madison USA, University of Wisconsin, 2014.
26. Betts JG, Desaix P, Johnson JE, Korol O, Kruse D, Poe B *et al.* *Anatomy & Physiology*. 1st ed. CRC Press: Houston, Texas, 2013.
27. Lilly LS. *Pathophysiology of Heart Disease: A Collaborative Project of Medical Students and Faculty*. 5th ed. Lippincott Williams & Wilkins, 2011: London, 2011.
28. Luna AB de. *Clinical Electrocardiography: A Textbook*. 4th, illustr ed. John Wiley & Sons, 2012.
29. Madeiro JV, Cortez PC, Da Silva. JM. *Developments and Applications for ECG Signal Processing Modeling, Segmentation, and Pattern Recognition*. 1st ed. Academic Press, 2019 doi:<https://doi.org/10.1016/C2017-0-01102-3>.
30. Luna AB de, Batchvarov VN, Malik M. The Morphology of the Electrocardiogram. In: *The ESC Textbook of Cardiovascular Medicine*. Wiley, 2006, pp 1–32.
31. Klabunde R. *Cardiovascular Physiology Concepts*. 2nd ed. Lippincott Williams & Wilkins: Philadelphia, PA, 2011.
32. Fox S. *Human Physiology*. 14th ed. McGraw-Hill Higher Education, 2015.
33. Restrepo RD. Cardiac Output Measurement. In: *Wilkins' Clinical Assessment in Respiratory Care*. Elsevier Health Sciences, 2013, p 373.
34. King TC. *Cardiovascular Pathology*. 1st ed. Elsevier Health Sciences, 2007.
35. Crystal GJ, Heerdt PM. Cardiovascular Physiology: Integrative Function. In: *Pharmacology and Physiology for Anesthesia*. Elsevier Health Sciences, 2013, pp 366–374, doi: <https://doi.org/10.1016/C2009-0-41712-4>.
36. Plowman SA, Smith DL. *Exercise Physiology for Health Fitness and Performance*. 4th ed. Lippincott Williams & Wilkins, 2013.
37. Laughlin MH. Cardiovascular Response to Exercise. *Am J Physiol* 1999; **277**: S244-59, doi: <https://doi.org/10.1152/advances.1999.277.6.S244>.
38. Stein RA, Michielli D, Diamond J, Horwitz B, Krasnow N. The cardiac response to exercise

- training: echocardiographic analysis at rest and during exercise. *Am J Cardiol* 1980; **46**: 219–25, doi: [https://doi.org/10.1016/0002-9149\(80\)90061-2](https://doi.org/10.1016/0002-9149(80)90061-2).
39. McArdle WD, Katch FI, Katch VL. *Exercise Physiology: Nutrition, Energy, and Human Performance*. Lippincott Williams & Wilkins, 2010.
  40. Whyte G, Sharma S. *Practical ECG for Exercise Science and Sports Medicine*. 1st ed. Human Kinetics, 2010.
  41. Burton DA, Stokes K, Hall GM. Physiological Effects of Exercise. *Contin Educ Anaesth Crit Care Pain* 2004; **4**: 185–188, doi: <https://doi.org/10.1093/bjaceaccp/mkh050>.
  42. Katch VL, McArdle WD, Katch FI. *Essentials of Exercise Physiology*. 4th ed. Lippincott Williams & Wilkins, 2011.
  43. Simonson E. Effect of moderate exercise on the electrocardiogram in healthy young and middle-aged men. *J Appl Physiol* 1953; **5**: 584–588, doi: <https://doi.org/10.1152/jappl.1953.5.10.584>.
  44. Lloyd-Thomas HG. The effect of exercise on the electrocardiogram in healthy subjects. *Br Heart J* 1961; **23**: 260–70, doi: [10.1136/hrt.23.3.260](https://doi.org/10.1136/hrt.23.3.260).
  45. Palmer JH. U wave inversion. *Br Heart J* 1948; **10**: 247–51, doi: [10.1136/hrt.10.4.247](https://doi.org/10.1136/hrt.10.4.247).
  46. Barold SS. Willem Einthoven and the birth of clinical electrocardiography a hundred years ago. *Card Electrophysiol Rev* 2003; **7**: 99–104, doi: [10.1016/j.resuscitation.2007.10.014](https://doi.org/10.1016/j.resuscitation.2007.10.014).
  47. Einthoven W. The different forms of the human electrocardiogram and their signification. *Lancet* 1912; **179**: 853–861, doi: [https://doi.org/10.1016/S0140-6736\(00\)50560-1](https://doi.org/10.1016/S0140-6736(00)50560-1).
  48. Surawicz B. U wave: facts, hypotheses, misconceptions, and misnomers. *J Cardiovasc Electrophysiol* 1998; **9**: 1117–28. doi: [10.1111/j.1540-8167.1998.tb00890.x](https://doi.org/10.1111/j.1540-8167.1998.tb00890.x).
  49. Pérez Riera AR, Ferreira C, Filho CF, Ferreira M, Meneghini A, Uchida AH *et al*. The enigmatic sixth wave of the electrocardiogram: The U wave. *Cardiol J* 2008; **15**: 408–421.
  50. Kohl P, Sachs F, Franz M. *Cardiac Mechano-Electric Coupling and Arrhythmias*. 2nd ed. OUP Oxford: Oxford, 2011.
  51. Kohl P, Schimpf R, Borggrefe M. Is the U wave in the Electrocardiogram a Mechano-Electrical Phenomenon? In: *Cardiac Mechano-Electric Coupling and Arrhythmias*. OUP Oxford, 2011, pp 274–280.
  52. Rautaharju PM, Surawicz B, Gettes LS. AHA/ACCF/HRS recommendations for the standardization and interpretation of the electrocardiogram: Part IV: The ST segment, T and U waves, and the QT interval: a scientific statement from the American Heart Association Electrocardiography and Arrhythmias C. *J Am Coll Cardiol*; **53**: 982–991, doi: <https://doi.org/10.1016/j.jacc.2008.12.014>.
  53. Lewis T, Gilder MDD. The human electrocardiogram: a preliminary investigation of young male adults, to form a basis for pathological study. *Philos Trans R Soc B Biol Sci* 1912; **202**: 351–376, doi: [10.1098/rstb.1912.0011](https://doi.org/10.1098/rstb.1912.0011).
  54. Langley P, Bourke JP, Murray A. The U wave in atrial fibrillation. *Comput. Cardiol.* 2015;42:833–836, doi: [10.1109/CIC.2015.7411040](https://doi.org/10.1109/CIC.2015.7411040).
  55. Lepeschkin E. The U wave of the electrocardiogram. *Arch Intern Med* 1955; **96**: 600–617, doi: [10.1001/archinte.1955.00250160042004](https://doi.org/10.1001/archinte.1955.00250160042004).

56. Surawicz B. Bradycardia-dependent long QT syndrome, sudden death and late potentials. *J Am Coll Cardiol* 1992; **19**: 550–551, doi: 10.1016/s0735-1097(10)80270-0.
57. Surawicz B, Kemp RL, Bellet S. Polarity and amplitude of the U wave of the electrocardiogram in relation to that of the T wave. *Circulation* 1957; **15**: 90–97, doi: <https://doi.org/10.1161/01.CIR.15.1.90>.
58. Reinig MG, Harizi R, Spodick DH. Electrocardiographic T- and U-wave discordance. *Ann Noninvasive Electrocardiol* 2005; **10**: 41–46, doi: <https://doi.org/10.1111/j.1542-474X.2005.00596.x>.
59. Carrillo-Esper R. The U Wave in the Electrocardiogram more than an academic curiosity. *Médica Sur* 2015; **22**: 27–29.
60. Fred M., Kusumoto. *ECG Interpretation: From Pathophysiology to Clinical Application*. 1st ed. Springer Science & Business Media: NY , USA, 2009.
61. Foster DB. *Twelve-Lead Electrocardiography: Theory and Interpretation*. 2nd ed. Springer London, 2007.
62. Conrath C, Opthof T. The Patient U Wave. *Cardiovasc Res* 2005; **67**: 184–186, doi: 10.1016/j.cardiores.2005.05.027.
63. Schimpf R, Antzelevitch C, Haghgi D, Giustetto C, Pizzuti A, Gaita F *et al*. Electromechanical coupling in patients with the short QT syndrome: further insights into the mechano-electrical hypothesis of the U wave. *Heart Rhythm* 2008; **5**: 241–245, doi: 10.1016/j.hrthm.2007.10.015.
64. Antzelevitch C. Cellular basis for the repolarization waves of the ECG. *Ann N Y Acad Sci* 2006; **1080**: 268–281, doi: 10.1196/annals.1380.021.
65. Hoffman BF, Cranefield PF. *Electrophysiology of the Heart*. 1st ed. John Wiley & Sons, Incorporated, 1976.
66. Watanabe Y. Purkinje repolarization as a possible cause of the U wave in the electrocardiogram. *Circulation* 1975; **51**: 1030–7, doi: 10.1161/01.cir.51.6.1030.
67. Wu J, Wu J, Zipes DP. Early afterdepolarizations, U waves, and Torsades de Pointes. *Circulation* 2002; **105**: 675–676, doi: <https://doi.org/10.1161/circ.105.6.675>.
68. Antzelevitch C, Sicouri S. Clinical relevance of cardiac arrhythmias generated by afterdepolarizations: role of M cells in the generation of U waves, triggered activity and Torsade de Pointes. *J Am Coll Cardiol* 1994; **23**: 259–277, doi: [https://doi.org/10.1016/0735-1097\(94\)90529-0](https://doi.org/10.1016/0735-1097(94)90529-0).
69. Hopenfeld B, Ashikaga H. Origin of the electrocardiographic U wave: effects of M cells and dynamic gap junction coupling. *Ann Biomed Eng* 2010; **38**: 1060–70, doi: 10.1007/s10439-010-9941-5.
70. Brun P, Tribouilloy C, Duval AM, Iserin L, Meguira A, Pelle G *et al*. Left ventricular flow propagation during early filling is related to wall relaxation: A color M-mode Doppler analysis. *J Am Coll Cardiol* 1992; **20**: 420–432, doi: [https://doi.org/10.1016/0735-1097\(92\)90112-Z](https://doi.org/10.1016/0735-1097(92)90112-Z).
71. Fioretti P, Brower RW, Meester GT, Serruys PW. Interaction of left ventricular relaxation and filling during early diastole in human subjects. *Am J Cardiol* 1980; **46**: 197–203, doi: [https://doi.org/10.1016/0002-9149\(80\)90058-2](https://doi.org/10.1016/0002-9149(80)90058-2).
72. Surawicz B. Electrophysiologic substrate of torsade de pointes: Dispersion of repolarization or

- early afterdepolarizations? *J Am Coll Cardiol* 1989; **14**: 172–184, doi: [https://doi.org/10.1016/0735-1097\(89\)90069-7](https://doi.org/10.1016/0735-1097(89)90069-7).
73. Furbetta D, Bufalari A, Santucci F, Solinas P. Abnormality of the U wave and of the T-U segment of the electrocardiogram. *Circulation* 1956; **14**: 1129–1137, doi: <https://doi.org/10.1161/01.CIR.14.6.1129>.
  74. Antzelevitch C, Nesterenko V V., Yan G-X. Role of M cells in acquired long QT syndrome, U waves, and torsade de pointes. *J Electrocardiol* 1995; **28**: 131–138, doi: [https://doi.org/10.1016/S0022-0736\(95\)80038-7](https://doi.org/10.1016/S0022-0736(95)80038-7).
  75. Murphy JG, Lloyd MA. *Mayo Clinic Cardiology: Concise Textbook*. 4th ed. OUP USA, 2012, doi: 10.1093/med/9780199915712.001.0001.
  76. Lepschkin E. Genesis of the U Wave. *Circulation* 1957; **15**: 77–81, doi:<https://doi.org/10.1161/01.CIR.15.1.77>.
  77. Lepschkin E, Surawicz B. The duration of the Q-U interval and its components in electrocardiograms of normal persons. *Am Heart J* 1953; **46**: 9–20, doi: [https://doi.org/10.1016/0002-8703\(53\)90237-3](https://doi.org/10.1016/0002-8703(53)90237-3).
  78. Guharay F, Sachs F. Stretch-activated single ion channel currents in tissue-cultured embryonic chick skeletal muscle. *J Physiol* 1984; **352**: 685–701, doi: 10.1113/jphysiol.1984.sp015317.
  79. Lab MJ. Contraction-excitation feedback in myocardium. Physiological basis and clinical relevance. *Circ Res* 1982; **50**: 757–766, doi: <https://doi.org/10.1161/01.RES.50.6.757>.
  80. Kohl P, Bollensdorff C, Garry A. Effects of mechanosensitive ion channels on ventricular electrophysiology: experimental and theoretical models. *Exp Physiol* 2006; **91**: 307–321, doi: 10.1113/expphysiol.2005.031062.
  81. Bernardo D, Murray A. Computer model for study of cardiac repolarization. *J Cardiovasc Electrophysiol* 2000; **11**: 895–899, doi: 10.1111/j.1540-8167.2000.tb00069.x.
  82. Bernardo D, Murray A. Origin on the electrocardiogram of U-waves and abnormal U-wave inversion. *Cardiovasc Res* 2002; **53**: 202–208, doi: [https://doi.org/10.1016/S0008-6363\(01\)00439-4](https://doi.org/10.1016/S0008-6363(01)00439-4).
  83. Surawicz B, Knilans T. QT interval, U wave abnormalities, and cardiac alternans. In: *Chou's Electrocardiography in Clinical Practice*. Elsevier Health Sciences, 2008, pp 569–585.
  84. Gerson MC, Phillips JF, Morris SN, McHenry PL. Exercise-induced U-wave inversion as a marker of stenosis of the left anterior descending coronary artery. *Circulation* 1979; **60**: 1014–20, doi: <https://doi.org/10.1161/01.CIR.60.5.1014>.
  85. Kishida H, Cole JS, Surawicz B. Negative U wave: A highly specific but poorly understood sign of heart disease. *Am J Cardiol* 1982; **49**: 2030–2036, doi: [https://doi.org/10.1016/0002-9149\(82\)90225-9](https://doi.org/10.1016/0002-9149(82)90225-9).
  86. Sovari AA, Farokhi F, Kocheril AG. Inverted U wave, a specific electrocardiographic sign of cardiac ischemia. *Am J Emerg Med* 2007; **25**: 235–7, doi: <https://doi.org/10.1016/j.ajem.2006.11.004>.
  87. Gregory SA, Akutsu Y, Perlstein TS, Yasuda T, Yurchak PM. Inverted U waves. *Am J Med* 2006; **119**: 746–747, doi: <https://doi.org/10.1016/j.amjmed.2006.07.017>.
  88. Goldberger AL, Goldberger ZD, Shvilkin A. Drug Effects, Electrolyte Abnormalities, and Metabolic Disturbances. In: *Goldberger's Clinical Electrocardiography*. Elsevier, 2018, pp

- 104–113.
89. Kirchhof P, Franz MR, Bardai A, Wilde AM. Giant T–U waves precede Torsades de Pointes in Long QT Syndrome. *J Am Coll Cardiol* 2009; **54**: 143–149, doi: <https://doi.org/10.1016/j.jacc.2009.03.043>.
  90. Baltazar, F. R. *Basic and Bedside Electrocardiography*. 1st ed. Lippincott Williams & Wilkins, 2009.
  91. Yan G-X, Lankipalli RS, Burke JF, Musco S, Kowey PR. Ventricular repolarization components on the electrocardiogram: Cellular basis and clinical significance. *J Am Coll Cardiol* 2003; **42**: 401–409, doi: [https://doi.org/10.1016/S0735-1097\(03\)00713-7](https://doi.org/10.1016/S0735-1097(03)00713-7).
  92. Hlaing T, DiMino T, Kowey PR, Yan G-X. ECG Repolarization waves: their genesis and clinical implications. *Ann Noninvasive Electrocardiol* 2005; **10**: 211–223, doi: <https://doi.org/10.1111/j.1542-474X.2005.05588.x>.
  93. Lin W, Teo SG, Poh KK. Electrocardiography series. Electrocardiographic T wave abnormalities. *Singapore Med J* 2013; **54**: 606–10, doi: [10.11622/smedj.2013218](https://doi.org/10.11622/smedj.2013218).
  94. Bernardo D, Murray A. Explaining the T-wave shape in the ECG. *Nature* 2000; **403**: 40–40, doi: <https://doi.org/10.1038/47409>.
  95. Bernardo D, Langley P, Murray A. Effect of changes in heart rate and in action potential duration on the electrocardiogram T wave shape. *Physiol Meas* 2002; **23**: 355–364, doi: <https://doi.org/10.1088/0967-3334/23/2/311>.
  96. Meijborg VMF, Belterman CNW, de Bakker JMT, Coronel R, Conrath CE. Mechano-electric coupling, heterogeneity in repolarization and the electrocardiographic T-wave. *Prog Biophys Mol Biol* 2017; **130**: 356–364, doi: <https://doi.org/10.1016/j.pbiomolbio.2017.05.003>.
  97. Meijborg VMF. *The T wave : Physiology and Pathophysiology*. 2015.
  98. Sicouri S, Antzelevitch C. A subpopulation of cells with unique electrophysiological properties in the deep subepicardium of the canine ventricle. The M cell. *Circ Res* 1991; **68**: 1729–41, doi: <https://doi.org/10.1161/01.RES.68.6.1729>.
  99. Antzelevitch C. M Cells in the human heart. *Circ Res* 2010; **106**: 815, doi: <https://dx.doi.org/10.1161/01.CIRCRESAHA.109.216226>.
  100. Conrath CE, Opthof T. Ventricular repolarization: An overview of (patho)physiology, sympathetic effects and genetic aspects. *Prog Biophys Mol Biol* 2006; **92**: 269–307, doi: <https://doi.org/10.1016/j.pbiomolbio.2005.05.009>.
  101. Artyeva N V, Azarov JE. Effect of action potential duration on Tpeak-Tend interval, T-wave area and T-wave amplitude as indices of dispersion of repolarization: Theoretical and simulation study in the rabbit heart. *J Electrocardiol* 2017; **50**: 919–924, doi: <https://doi.org/10.1016/j.jelectrocard.2017.07.001>.
  102. Yamaguchi M, Shimizu M, Ino H, Terai H, Uchiyama K, Oe K *et al*. T wave peak-to-end interval and QT dispersion in acquired long QT syndrome: a new index for arrhythmogenicity. *Clin Sci* 2003; **105**: 671–676, doi: <https://doi.org/10.1042/CS20030010>.
  103. Yan G-X, Antzelevitch C. Cellular basis for the normal T wave and the electrocardiographic manifestations of the long-QT syndrome. *Circulation* 1998; **98**: 1928–36, doi: <https://doi.org/10.1161/01.CIR.98.18.1928>.
  104. Wheelan K, Mukharji J, Rude RE, Poole WK, Gustafson N, Thomas LJ *et al*. Sudden death

- and its relation to QT-interval prolongation after acute myocardial infarction: two-year follow-up. *Am J Cardiol* 1986; **57**: 745–50, doi: [https://doi.org/10.1016/0002-9149\(86\)90606-5](https://doi.org/10.1016/0002-9149(86)90606-5).
105. Algra A, Tijssen JG, Roelandt JR, Pool J, Lubsen J. QTc prolongation measured by standard 12-lead electrocardiography is an independent risk factor for sudden death due to cardiac arrest. *Circulation* 1991; **83**: 1888–94, doi: <https://doi.org/10.1161/01.CIR.83.6.1888>.
  106. Leif, Sörnmo. *Atrial Fibrillation from an Engineering Perspective*. 1st ed. Springer, 2018.
  107. Iwasaki Y-K, Nishida K, Kato T, Nattel S. Atrial fibrillation pathophysiology. *Circulation* 2011; **124**: 2264–2274, doi: <https://doi.org/10.1161/CIRCULATIONAHA.111.019893>.
  108. Kirchhof P, Benussi S, Kotecha D, Ahlsson A, Atar D, Casadei B *et al.* 2016 ESC Guidelines for the management of atrial fibrillation developed in collaboration with EACTS. *Eur Heart J* 2016; **37**: 2893–2962, doi: <https://doi.org/10.1093/eurheartj/ehw210>.
  109. Smith JG, Platonov PG, Hedblad B, Engström G, Melander O. Atrial fibrillation in the Malmö diet and cancer study: a study of occurrence, risk factors and diagnostic validity. *Eur J Epidemiol*; **25**: 95–102, doi: <https://doi.org/10.1007/s10654-009-9404-1>.
  110. Padmavathi K, Sri Ramakrishna K. Classification of ECG signal during atrial fibrillation using Autoregressive modeling. *Procedia Comput Sci* 2015; **46**: 53–59, doi: <https://doi.org/10.1016/j.procs.2015.01.053>.
  111. Lip GYH, Fauchier L, Freedman SB, Van Gelder I, Natale A, Gianni C *et al.* Atrial fibrillation. *Nat Rev Dis Prim* 2016; **2**: 16016, doi: <https://doi.org/10.1038/nrdp.2016.16>.
  112. Nattel S. New ideas about atrial fibrillation 50 years on. *Nature* 2002; **415**: 219–226, doi: <https://doi.org/10.1038/415219a>.
  113. Wakili R, Voigt N, Kääh S, Dobrev D, Nattel S. Recent advances in the molecular pathophysiology of atrial fibrillation. *J Clin Invest* 2011; **121**: 2955–68, doi: <https://dx.doi.org/10.1172%2FJCI46315>.
  114. Garratt C. *Mechanisms and Management of Cardiac Arrhythmias*. 1st ed. Wiley, 2001.
  115. Lévy S, Camm AJ, Saksena S, Aliot E, Breithardt G, Crijns H *et al.* International consensus on nomenclature and classification of atrial fibrillation; a collaborative project of the working group on arrhythmias and the working group on cardiac pacing of the European Society of Cardiology and the North American Society of. *Europace* 2003; **5**: 119–122, doi: <https://doi.org/10.1053/eupc.2002.0300>.
  116. Allessie MA, Boyden PA, Camm AJ, Kléber AG, Lab MJ, Legato MJ *et al.* Pathophysiology and prevention of atrial fibrillation. *Circulation*. 2001; **103**: 769–777, doi: <https://doi.org/10.1161/01.CIR.103.5.769>.
  117. Kannel W., Wolf P., Benjamin E., Levy D. Prevalence, incidence, prognosis, and predisposing conditions for atrial fibrillation: population-based estimates. *Am J Cardiol* 1998; **82**: 2N-9N, doi: [https://doi.org/10.1016/S0002-9149\(98\)00583-9](https://doi.org/10.1016/S0002-9149(98)00583-9).
  118. Schoonderwoerd BA, Smit MD, Pen L, Van Gelder IC. New risk factors for atrial fibrillation: causes of ‘not-so-lone atrial fibrillation’. *Europace* 2008; **10**: 668–673, doi: <https://doi.org/10.1093/europace/eun124>.
  119. Munger TM, Wu LQ, Shen WK. Atrial fibrillation. *J Biomed Res* 2014; **28**: 1–17, doi: <https://dx.doi.org/10.7555%2FJBR.28.20130191>.
  120. Katan MB, Schouten E. Caffeine and arrhythmia. *Am J Clin Nutr* 2005; **81**: 539–540, doi:

<https://doi.org/10.1093/ajcn/81.3.539>.

121. Ferrari R, Bertini M, Blomstrom-Lundqvist C, Dobrev D, Kirchhof P, Pappone C *et al*. An update on atrial fibrillation in 2014: From pathophysiology to treatment. *Int. J. Cardiol.* 2016; **203**: 22–29, doi: <https://doi.org/10.1016/j.ijcard.2015.10.089>.
122. Chen-Scarabelli C, Scarabelli TM, Ellenbogen KA, Halperin JL. Device-detected atrial fibrillation: What to do with asymptomatic patients? *J Am Coll Cardiol* 2015; **65**: 281–294, doi: <https://doi.org/10.1016/j.jacc.2014.10.045>.
123. Francis H, Burgess RG. The Ethics of Educational Research. *Br J Educ Stud* 1990; **38**: 284, doi: [http://10.1007/978-0-387-73317-3\\_42](http://10.1007/978-0-387-73317-3_42)
124. Devlin AS. *Research Methods: Planning, Conducting and Presenting Research*. 1st ed. Thomson/Wadsworth, 2006.
125. Masic I, Hodzic A, Mulic S. Ethics in medical research and publication. *Int J Prev Med* 2014; **5**: 1073–1082.
126. Christine G. Do IRBs protect human research participants? *JAMA - J Am Med Assoc* 2010; **304**: 1122–1123, doi:<http://10.1001/jama.2010.1304>.
127. Avanzas P, Bayes-Genis A, Pérez De Isla L, Sanchis J, Heras M. Ethical considerations in the publication of scientific articles. *Rev Esp Cardiol* 2011; **64**: 427–429, doi:<http://10.1016/j.rec.2011.02.005>.
128. Raudonis BM. Ethical considerations in qualitative research with hospice patients. *Qual Health Res* 1992; **2**: 238–249, doi: <https://doi.org/10.1177/104973239200200207>.
129. Mazur DJ. *Evaluating the Science and Ethics of Research on Humans: A Guide for IRB Members*. 1st ed. Johns Hopkins University Press, 2007, doi: <http://10.7326/0003-4819-148-10-200805200-00021>.
130. Goldberger AL, Amaral LAN, Glass L, Hausdorff JM, Ivanov PC, Mark RG *et al*. PhysioBank, physioToolkit, and PhysioNet: components of a new research resource for complex physiologic signals. *Circulation* 2000; **101**: e215–e220, doi: <https://doi.org/10.1161/01.CIR.101.23.e215>.
131. Langley P, Di Bernardo D, Murray A. Quantification of T wave shape changes following exercise. *Pacing Clin Electrophysiol* 2002; **25**: 1230–1234, doi: <https://doi.org/10.1046/j.1460-9592.2002.01230.x>.
132. Al-Karadi M, J Wilkinson A, Langley P. The effect of beat interval on ventricular repolarisation in atrial fibrillation. In: *2018 Computing in Cardiology Conference (CinC)*. 2018 doi:<http://10.22489/cinc.2018.294>.
133. Venkatachalam KL, Herbrandson JE, Asirvatham SJ. Signals and signal processing for the electrophysiologist. *Circ Arrhythmia Electrophysiol* 2011; **4**: 974–981.
134. Buendía-Fuentes F, Arnau-Vives MA, Arnau-Vives A, Jiménez-Jiménez Y, Rueda-Soriano J, Zorio-Grima E *et al*. High-Bandpass Filters in Electrocardiography: Source of Error in the Interpretation of the ST Segment. *ISRN Cardiol* 2012; **2012**: 1–10, doi: <http://dx.doi.org/10.5402/2012/706217>.
135. Anderson JL, Arnsdorf MF, Mason J a YW, Scheinman MM, Waldo AL. Signal-averaged electrocardiography. *J Am Coll Cardiol* 1996; **27**: 238–249.
136. Tompkins WJ. *Biomedical Digital Signal Processing: C-language Examples and Laboratory*

- Experiments for the IBM PC*. 2nd ed. Prentice Hall, 2006.
137. Chawla MPS. PCA and ICA processing methods for removal of artifacts and noise in electrocardiograms: A survey and comparison. In: *Applied Soft Computing Journal*. Elsevier, 2011, pp 2216–2226, doi: <http://10.1016/j.asoc.2010.08.001>.
  138. Cardoso J-F. Blind signal separation: statistical principles. *Proc IEEE* 1998; **86**: 2009–2025, doi: <https://doi.org/10.1109/5.720250>.
  139. Castells F, Laguna P, Sörnmo L, Bollmann A, Roig JM. Principal component analysis in ECG signal processing. *EURASIP J Adv Signal Process* 2007; **2007**: 074580, doi: <https://doi.org/10.1155/2007/74580>.
  140. Hyvärinen A, Karhunen J, Oja E. *Independent Component Analysis*. 1st ed. John Wiley & Sons, 2004.
  141. Hyvärinen A, Oja E. Independent component analysis: algorithms and applications. *Neural Networks* 2000; **13**: 411–430, doi: [http://10.1016/S0893-6080\(00\)00026-5](http://10.1016/S0893-6080(00)00026-5).
  142. Tadeusz J. Ulrych MDS. *Handbook of Geophysical Exploration: Seismic Exploration*. 36th ed. Elsevier: Alberta, Canada, 2005.
  143. Tanskanen JMA, Viik JJ. Independent Component Analysis in ECG Signal Processing. In: Millis RM (ed). *Advances in Electrocardiograms*. IntechOpen, 2012.
  144. Zarzoso V, Nandi AK. Noninvasive fetal electrocardiogram extraction: Blind separation versus adaptive noise cancellation. *IEEE Trans Biomed Eng* 2001; **48**: 12–18, doi: <https://doi.org/10.1109/10.900244>.
  145. Rieta JJ, Castells F, Sánchez C, Zarzoso V, Millet J. Atrial activity extraction for atrial fibrillation analysis using blind source separation. *IEEE Trans Biomed Eng* 2004; **51**: 1176–86, doi: <https://doi.org/10.1109/TBME.2004.827272>.
  146. Kostka PS, Tkacz EJ. Feature extraction based on time-frequency and Independent Component Analysis for improvement of separation ability in atrial fibrillation detector. In: *2008 30th Annual International Conference of the IEEE Engineering in Medicine and Biology Society*. IEEE, 2009, pp 2960–2963, doi: <https://doi.org/10.1109/IEMBS.2008.4649824>.
  147. Comon P. Independent component analysis, A new concept? *Signal Processing* 1994; **36**: 287–314, doi: [https://doi.org/10.1016/0165-1684\(94\)90029-9](https://doi.org/10.1016/0165-1684(94)90029-9).
  148. Langlois D, Chartier S, Gosselin D. An Introduction to Independent Component Analysis: InfoMax and FastICA algorithms. *Tutor Quant Methods Psychol* 2016; **6**: 31–38, doi: <http://10.20982/tqmp.06.1.p031>.
  149. Hyvärinen A. Fast and robust fixed-point algorithms for independent component analysis. *IEEE Trans Neural Networks* 1999; **10**: 626–634, doi: <https://doi.org/10.1109/72.761722>.
  150. Rutledge DN, Jouan-Rimbaud Bouveresse D. Independent Components Analysis with the JADE algorithm. *TrAC - Trends Anal. Chem.* 2013; **50**: 22–32, doi: <http://10.1016/j.trac.2013.03.013>.
  151. Bell AJ, Sejnowski TJ. An information-maximization approach to blind separation and blind deconvolution. *Neural Comput* 1995; **7**: 1129–1159, doi: <http://10.1162/neco.1995.7.6.1129>
  152. Rompelman O, Ros HH. Coherent averaging technique: A tutorial review Part 1: Noise reduction and the equivalent filter. *J Biomed Eng* 1986; **8**: 24–29, doi: [http://10.1016/0141-5425\(86\)90026-9](http://10.1016/0141-5425(86)90026-9).

153. Jané R, Rix H, Caminal P, Laguna P. Alignment methods for averaging of high resolution cardiac signals: A comparative study of performance. *IEEE Trans Biomed Eng* 1991; **38**: 571–579, doi: <http://10.1109/10.81582>.
154. Gomes JA. *Signal Averaged Electrocardiography: Concepts, Methods and Applications*. Springer Netherlands: Netherlands, 1993.
155. Ros H.H., Koeleman A.S.M. V den AT. The technique of signal averaging and its practical application in the separation of atrial and His-Purkinje activity. In: *Signal averaging technique in clinical cardiology*. Stuttgart, Schattauer Verlag, 1981, pp 3–14.
156. Breithardt G, Becker R, Seipel L, Abendroth RR, Ostermeyer J. Non-invasive detection of late potentials in man-a new marker for ventricular tachycardia. *Eur Heart J* 1981; **2**: 1–11, doi: <https://doi.org/10.1093/oxfordjournals.eurheartj.a061158>.
157. Jolliffe IT. *Principal Component Analysis*. 1st ed. Springer, 2002.
158. Langley P, Bowers EJ, Murray A. Principal component analysis as a tool for analyzing beat-to-beat changes in ECG features: Application to ECG-derived respiration. *IEEE Trans Biomed Eng* 2010; **57**: 821–829, doi: [10.1109/TBME.2009.2018297](https://doi.org/10.1109/TBME.2009.2018297).
159. Langley P, Bourke JP, Murray A. Frequency analysis of atrial fibrillation. In: *Computers in Cardiology 2000. Vol.27*. IEEE, 2002, pp 65–68, doi: <http://10.1109/CIC.2000.898456>
160. Haigh AJ, Murray A, Langley P. Feasibility of separating the atrial and ventricular components of the electrocardiogram. In: *Computing in cardiology*. Valencia, Spain, 2008.
161. Jain N, Jain N, Shakya DK. Denoising Baseline Wander Noise from Electrocardiogram Signal using Fast ICA with Multiple Adjustments. *Int J Comput Appl* 2014; : 34-39,doi:<http://10.5120/17348-7691>.
162. Castells F, Igual J, Rieta J, Sanchez C, Millet J. Atrial fibrillation analysis based on ICA including statistical and temporal source information. In: *2003 IEEE International Conference on Acoustics, Speech, and Signal Processing, 2003. Proceedings. (ICA SSP 03)*. IEEE, pp 93–6, doi: <http://10.1109/ICASSP.2003.1199876>.
163. Castells F, Mora C, Millet J, Rieta JJ, Sánchez C, Sanchís JM. Multidimensional ICA for the Separation of Atrial and Ventricular Activities from Single Lead ECGs in Paroxysmal Atrial Fibrillation Episodes. In: *Independent Component Analysis and Blind Signal Separation*. Springer, 2010, pp 1229–1236, doi: [https://doi.org/10.1007/978-3-540-30110-3\\_155](https://doi.org/10.1007/978-3-540-30110-3_155).
164. Rieta JJ, Castells F, Sánchez C, Igual J. ICA Applied to Atrial Fibrillation Analysis. In: *ICA 2003*. 2003, pp 59–64.
165. Seema Deshpande SOR. Removing Artifacts from the ECG By using Independent component analysis. *Int J Res Sci Adv Technol* 2013; **5**: 182–184.
166. Shynk JJ. *Probability, Random Variables, and Random Processes: Theory and Signal Processing Applications*. 1st ed. John Wiley & Sons, 2012.
167. Bugli C, Lambert P. Comparison between principal component analysis and independent component analysis in electroencephalograms modelling. *Biometrical J* 2007; **49**: 312–327, doi:<http://10.1002/bimj.200510285>.
168. Raschka S. *The Effect of Scaling and Mean Centering Prior to a Principal Component Analysis*. 1ed. 2014.
169. Theodoridis S. *Machine Learning: A Bayesian and Optimization Perspective*. 1st ed. Academic

- Press, 2015, doi:<https://doi.org/10.1016/C2013-0-19102-7>.
170. Walpole RE, Myers RH, Myers SL. *Probability & Statistics for Engineers & Scientists*. Prentice Hall, 2002.
  171. Hurri, J., Gavert, J., Sarela, J., and Hyvarinen A. The FastICA package for Matlab. 1998. [www.cis.hut.fi/projects/ica/fastica](http://www.cis.hut.fi/projects/ica/fastica).
  172. Malik M, Batchvarov VN. Measurement, interpretation and clinical potential of QT dispersion. *J. Am. Coll. Cardiol.* 2000; **36**: 1749–1766, doi: [http://10.1016/s0735-1097\(00\)00962-1](http://10.1016/s0735-1097(00)00962-1).
  173. Merri M, Benhorin J, Alberti M, Locati E, Moss AJ. Electrocardiographic quantitation of ventricular repolarization. *Circulation* 1989; **80**: 1301–1308, doi:<http://10.1161/01.cir.80.5.1301>.
  174. Murray A, McLaughlin NB, Campbell RWF. Measuring QT dispersion: Man versus machine. *Heart* 1997; **77**: 539–542, doi:<http://10.1136/hrt.77.6.539>.
  175. Iwase M, Aoki T, Maeda M, Yokota M, Hayashi H. Relationship between beat to beat interval and left ventricular function in patients with atrial fibrillation. *Int J Card Imaging* 1988; **3**: 217–26.
  176. Cieslinski A, Hui WKK, Oldershaw PJ, Gregoratos G, Gibson D. Interaction between systolic and diastolic time intervals in atrial fibrillation. *Br Hear* 1984; **51**: 431–438, doi: <https://doi.org/10.1136/hrt.51.4.431>.
  177. Jarrett JR, Flowers NC, John AC. Signal-averaged electrocardiography: History, techniques, and clinical applications. *Clin Cardiol* 1991; **14**: 984–994, doi: <https://doi.org/10.1002/clc.4960141209>.
  178. Rawles JM. A mathematical model of left ventricular function in atrial fibrillation. *Int J Biomed Comput* 1988; **23**: 57–68, doi: [10.1016/0020-7101\(88\)90063-3](https://doi.org/10.1016/0020-7101(88)90063-3).
  179. Ko HS, Lee KJ, Kim SW, Kim TH, Kim CJ, Ryu WS. Prediction of left ventricular peak ejection velocity by preceding and prepreceding RR intervals in atrial fibrillation: a new method to adjust the influence between two intervals. *J Korean Med Sci* 2002; **17**: 743, doi: <https://doi.org/10.3346/jkms.2002.17.6.743>.
  180. Freeman GL, Colston JT. Evaluation of left ventricular mechanical restitution in closed-chest dogs based on single-beat elastance. *Circ Res* 1990; **67**: 1437–1445, doi: <https://doi.org/10.1161/01.res.67.6.1437>.
  181. Kerr AJ, Simmonds MB, Stewart RAH. Influence of heart rate on stroke volume variability in atrial fibrillation in patients with normal and impaired left ventricular function. *Am J Cardiol* 1998; **82**: 1496–1500, doi: [https://doi.org/10.1016/s0002-9149\(98\)00693-6](https://doi.org/10.1016/s0002-9149(98)00693-6).
  182. Ganau A, Devereux RB, Pickering TG, Roman MJ, Schnall PL, Santucci S *et al.* Relation of left ventricular hemodynamic load and contractile performance to left ventricular mass in hypertension. *Circulation* 1990; **81**: 25–36, doi: <https://doi.org/10.1161/01.cir.81.1.25>.
  183. Gosselink ATTM, Blanksma PK, Crijns HJGM, Van Gelder IC, de Kam PJ, Hillege HL *et al.* Left ventricular beat-to-beat performance in atrial fibrillation: Contribution of frank-starling mechanism after short rather than long RR intervals. *J Am Coll Cardiol* 1995; **26**: 1516–1521, doi: [https://doi.org/10.1016/0735-1097\(95\)00340-1](https://doi.org/10.1016/0735-1097(95)00340-1).
  184. Montagu A. Textbook of Medical Physiology. *Am. J. Psychiatry.* 2014; **118**: 477–477, doi: <https://doi.org/10.1176/ajp.118.5.477>.

185. Brookes C., White PA, Staples M, Oldershaw PJ, Redington AN, Collins PD *et al.* Myocardial contractility is not constant during spontaneous atrial fibrillation in patients. *Circulation* 1998; **98**: 1762–1768, doi: <https://doi.org/10.1161/01.CIR.98.17.1762>.
186. Greenfield JC, Harley A, Thompson HK, Wallace AG. Pressure-flow studies in man during atrial fibrillation. *J Clin Invest* 1968; **47**: 2411–2421, doi: <https://doi.org/10.1172/JCI105924>.
187. Vincent JL. Understanding cardiac output. *Crit Care* 2008; **12**: 174, doi: <https://doi.org/10.1186/cc6975>.
188. Sivarajan V Ben, Schwartz SM, Hoffman JIE. Structure and Function of the Heart. In: *Pediatric Critical Care*. Mosby, 2011, pp 199–216.
189. Muntinga HJ, Gosselink AT, Blanksma PK, De Kam PJ, Van Der Wall EE, Crijns HJ. Left ventricular beat to beat performance in atrial fibrillation: dependence on contractility, preload, and afterload. *Heart* 1999; **82**: 575–80, doi: <https://doi.org/10.1136/hrt.82.5.575>.
190. Ishida Y, Meisner JS, Tsujioka K, Gallo JI, Yoran C, Frater RW *et al.* Left ventricular filling dynamics: influence of left ventricular relaxation and left atrial pressure. *Circulation* 1986; **74**: 187–96, doi: <https://doi.org/10.1161/01.cir.74.1.187>.
191. Craelius W, Chen V, El-Sherif N. Stretch activated ion channels in ventricular myocytes. *Biosci Rep* 1988; **8**: 407–414, doi: <https://doi.org/10.1007/bf01121637>.
192. Taggart P, Sutton PMI. Cardiac mechano-electric feedback in man: Clinical relevance. *Prog Biophys Mol Biol* 1999; **71**: 139–154, doi: [https://doi.org/10.1016/S0079-6107\(98\)00039-X](https://doi.org/10.1016/S0079-6107(98)00039-X).
193. Johannesen L, Grove U, Sørensen J, Schmidt M, Graff C, Couderc J-P. Analysis of T-wave amplitude adaptation to heart rate using RR-binning of long-term ECG recordings. *Comput Cardiol (2010)* 2010; **37**: 369–372.
194. Franz MR, Swerdlow CD, Liem LB, Schaefer J. Cycle length dependence of human action potential duration in vivo. Effects of single extrastimuli, sudden sustained rate acceleration and deceleration, and different steady-state frequencies. *J Clin Invest* 1988; **82**: 972–979, doi: <https://doi.org/10.1172/JCI113706>.
195. Zareba W, Moss AJ. Dispersion of repolarization. Relation to heart rate and repolarization duration. *J Electrocardiol* 1995; **28 Suppl**: 202–6, doi: [https://doi.org/10.1016/s0022-0736\(95\)80057-3](https://doi.org/10.1016/s0022-0736(95)80057-3).
196. Kitchin AH, Neilson JM. The T wave of the electrocardiogram during and after exercise in normal subjects. *Cardiovasc Res* 1972; **6**: 143–149, doi: <https://doi.org/10.1093/cvr/6.2.143>.
197. Cubeddu LX. QT prolongation and fatal arrhythmias: a review of clinical implications and effects of drugs. *Am J Ther* 2033; **10**: 452–7, doi: [10.1097/00045391-200311000-00013](https://doi.org/10.1097/00045391-200311000-00013).
198. Wu S, Hayashi H, Lin SF, Chen PS. Action potential duration and QT interval during pinacidil infusion in isolated rabbit hearts. *J Cardiovasc Electrophysiol* 2005; **16**: 872–878, doi: <https://doi.org/10.1111/j.1540-8167.2005.40811.x>.
199. Saunders WB. Normal Electrocardiogram: Origin and Description. In: *Chou's Electrocardiography in Clinical Practice*. Elsevier Health Sciences, 2008, pp 1–28, doi: <https://doi.org/10.1016/B978-1-4160-3774-3.X1000-3>.
200. Cabasson A, Meste O, Blain G, Bermon S. Quantifying the PR interval pattern during dynamic exercise and recovery. *IEEE Trans Biomed Eng* 2009; **56**: 2675–2683, doi: <https://doi.org/10.1109/TBME.2009.2028694>.

201. Rao. *Clinical Examinations in Cardiology*. 1st ed. Elsevier India, 2009.
202. Masek K. ECG Diagnosis: Acute Pericarditis. *Perm J* 2013; **17**: e146–e146, doi: <https://doi.org/10.7812/TPP/13-044i>.
203. Wasserburger RH, Ward VG, Cullen RE, Rasmussen HK, Juhl JH. The T-a wave of the adult electrocardiogram: An expression of pulmonary emphysema. *Am Heart J* 1957; **54**: 875–886, doi: [https://doi.org/10.1016/0002-8703\(57\)90192-8](https://doi.org/10.1016/0002-8703(57)90192-8).
204. Gürlek A, Oral D, Pamir G, Akyol T. Significance of resting U wave polarity in patients with atherosclerotic heart disease. *J Electrocardiol* 1994; **27**: 157–61, doi: [https://doi.org/10.1016/s0022-0736\(05\)80099-8](https://doi.org/10.1016/s0022-0736(05)80099-8).
205. Tamura A, Nagase K, Mikuriya Y, Nasu M. Relation between negative U waves in precordial leads on the admission electrocardiogram and time course of left ventricular wall motion in anterior wall acute myocardial infarction. *Am J Cardiol* 1999; **84**: 332–334, doi: [https://doi.org/10.1016/s0002-9149\(99\)00288-x](https://doi.org/10.1016/s0002-9149(99)00288-x).
206. Tamura A, Watanabe T, Nagase K, Mikuriya Y, Nasu M. Significance of negative U waves in the precordial leads during anterior wall acute myocardial infarction. *Am J Cardiol* 1997; **79**: 897–900, doi: [https://doi.org/10.1016/s0002-9149\(97\)00011-8](https://doi.org/10.1016/s0002-9149(97)00011-8).

# Appendices

# **Appendix A**

## **Research Approval**

*M Al-Karadi*  
*School of Engineering and Computer Science*

Date: 27/11/2018

Our Ref: FEC\_2019\_111

Dear Marwa,

**ETHICAL APPROVAL OF RESEARCH**

Following consideration of an application submitted by you for:

‘Measurement of U wave in atrial fibrillation’

I am pleased to confirm that your study was approved by Chair’s Action on behalf of the Faculty of Science and Engineering Ethics Committee.

This approval will be reported at the next Faculty Ethics Committee meeting.

Yours Sincerely



*PP*  
Dr L Holloway  
Chair of Faculty Ethics Committee  
Faculty of Science and Engineering

Cc: Dr Philip Langley, Supervisor

Dr L Holloway  
Chair of Faculty Ethics Committee  
Faculty of Science and Engineering  
01482 465377

## **Appendix B**

# **GUI User Guide of Manual Measurement**

## B.1 User Guide for Manual Measurement GUI

This section provides simple instructions and guidance to use the bespoke software that has been created to measure the repolarisation features in section 4.2.1.2.3 of Chapter four manually. The software designed using the Matlab environment. The written code (Matlab files) and the data (ECG signals) will be provided to the university of Hull as part of the research work.

## B.2 The Software Characteristics and Ability

The software created with the Matlab 2017a environment. It is important to note the following software characteristics before using the GUI:

- 1) Suitable for 10 patients with 10 intervals, however it could be improved for more (patients and beats) in the future.
- 2) The subjects and the beats for associated R-R intervals, will be presented automatically. But the desired points (clicks) of the ventricular features can be chosen manually.
- 3) The desired points mentioned above have specific order, therefore it demands **careful** selections (More details later).
- 4) It is important to save the results acquired from the processing, in the same user folder for efficient results.

## B.3 The GUI Guide

The following walkthrough steps will explain how the software works:

### B.3.1 Lunch the GUI

Run the software by type “*uafmanual*” or run it from the **Run** button in the Editor tab of the main Matlab bar. Figure B.1 shows the main user interface window for the software.

It is important to follow the following steps for efficient analysis, for **New Analysis** for manual selection.

#### 1) Enter Username

Enter the *initial letters* of your name by clicking on **Enter User** button, capital letters are preferable, for instance: MS, PL or AJW, see Figure B.2. The results in the structure array of the manual measurement, depends on the username.

Note that i) GUI will lock the data loading or the analysis without the username, see Figure B.3, and ii) in case that you interrupted, and wanted to resume the analysis, GUI will remember your initial letters.

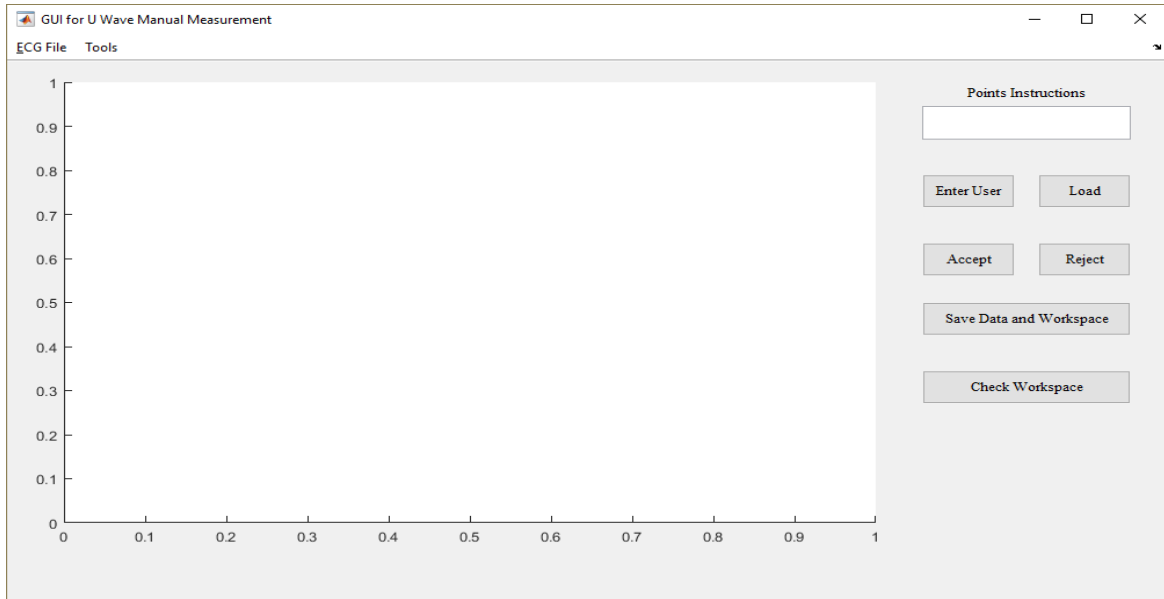


**Figure B.1:** Main user interface window

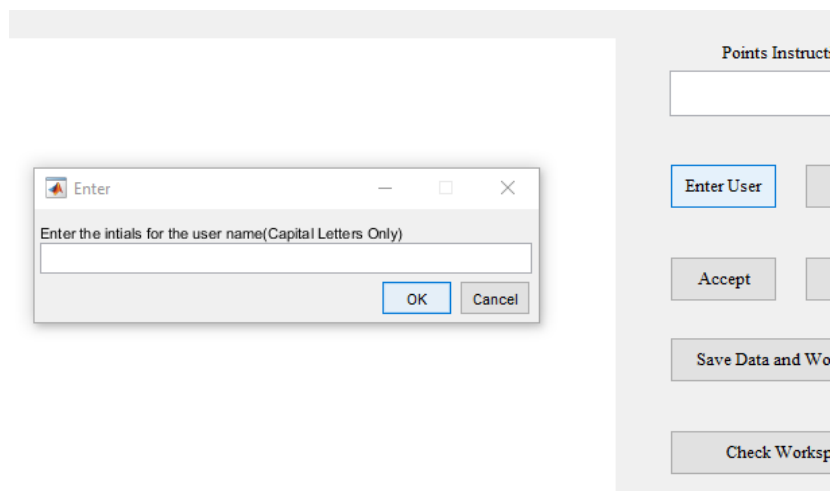


**Figure B.2:** Enter the username (Capital Initials)

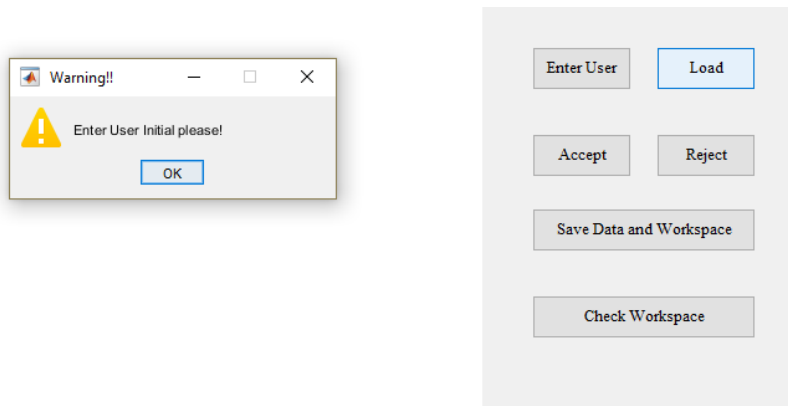


**Figure B. 3:** No loading data without the user initials

## 2) Loading Data

Load the provided data by clicking on **Load** button. Message information will appear first to give short guidance, as Figure B.4-a shows. In Figure B.4-b an example shows selecting 10-data structures (ECG beats), each structure represents AF subject for lead V4.

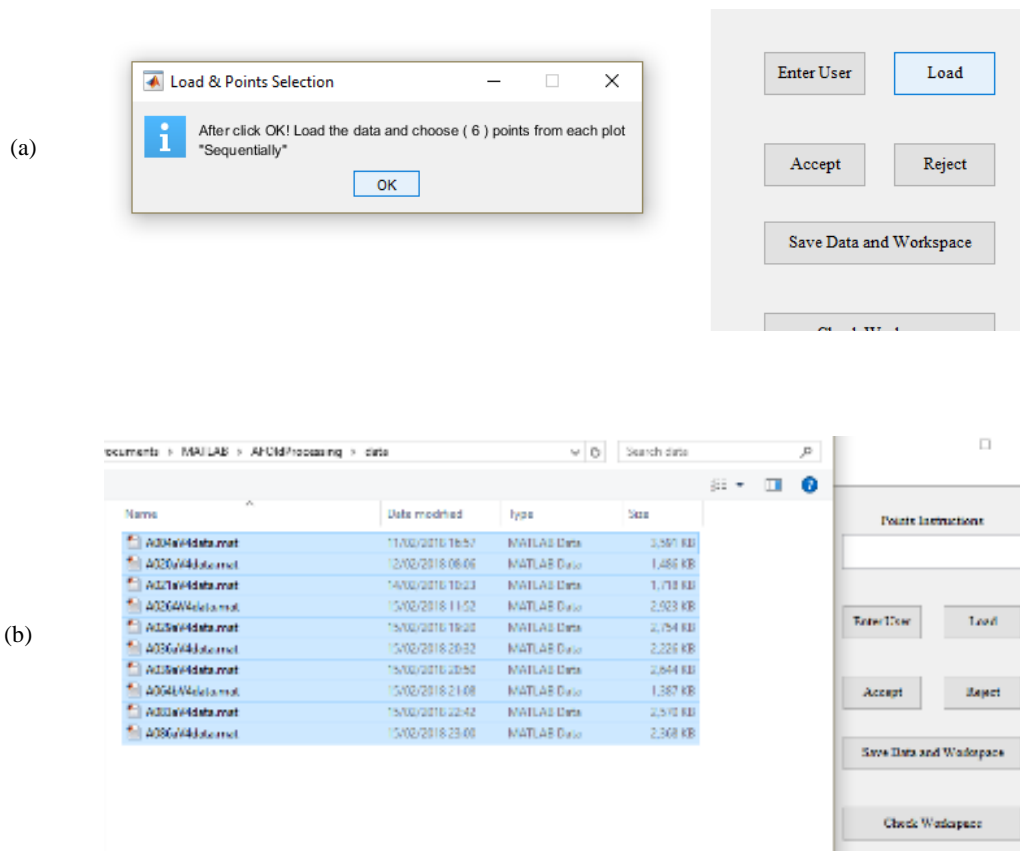


**Figure B.4:** Data loading and selecting

As soon as you upload the data, the first beat for the first patient will present automatically in the Figure area. Note that, the beats will be presented automatically for 10 increasing R-R intervals, from the intervals 625 to 1075 ms, for 10 AF subjects.

As Figure B.5 shows, the software waits your click for **six (6) points** (features marks) to be selected **sequentially**, so make sure to choose and click the right point. Also, there is **Text Instruction** in the upper right of the window that guide you for the next point, as shown in Figure B.6, in case that you forget the sequence of the points.

The sequence of the points wanted, in the following order:

- i) First baseline point ( $X_{b1}$ ).
- ii) Second baseline point, ( $X_{b2}$ )
- iii) T wave peak point, ( $X_T$ )
- iv) TU nadir point, ( $X_{TU_{nadir}}$ )
- v) U wave peak point, ( $X_U$ )
- vi) U wave end, ( $X_{U_{end}}$ )

The annotation shown in the Figure B.5, for the sake of explanation only, while the line marker will appear in the Figure of the GUI, to help the user to make a good judgment for the points selections.

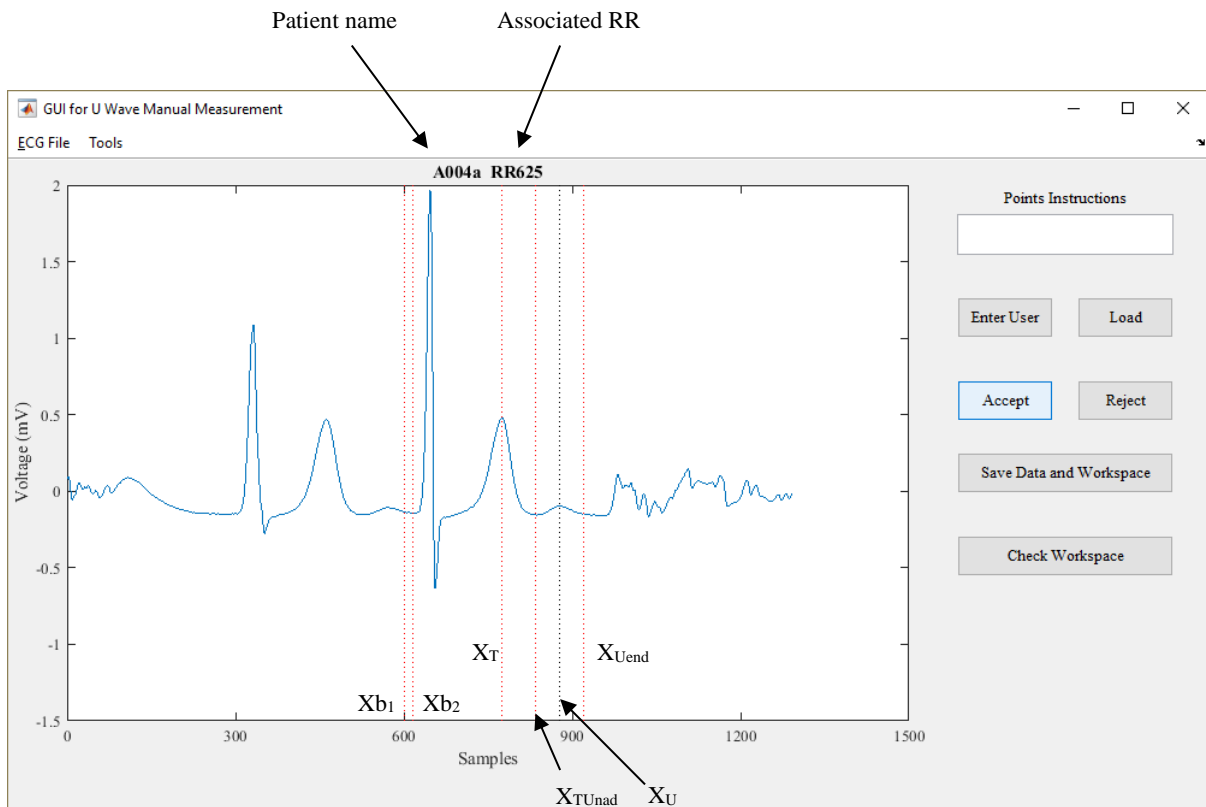


**Figure B.5:** Selecting 6 points (clicks) sequentially on the presented averaged beat

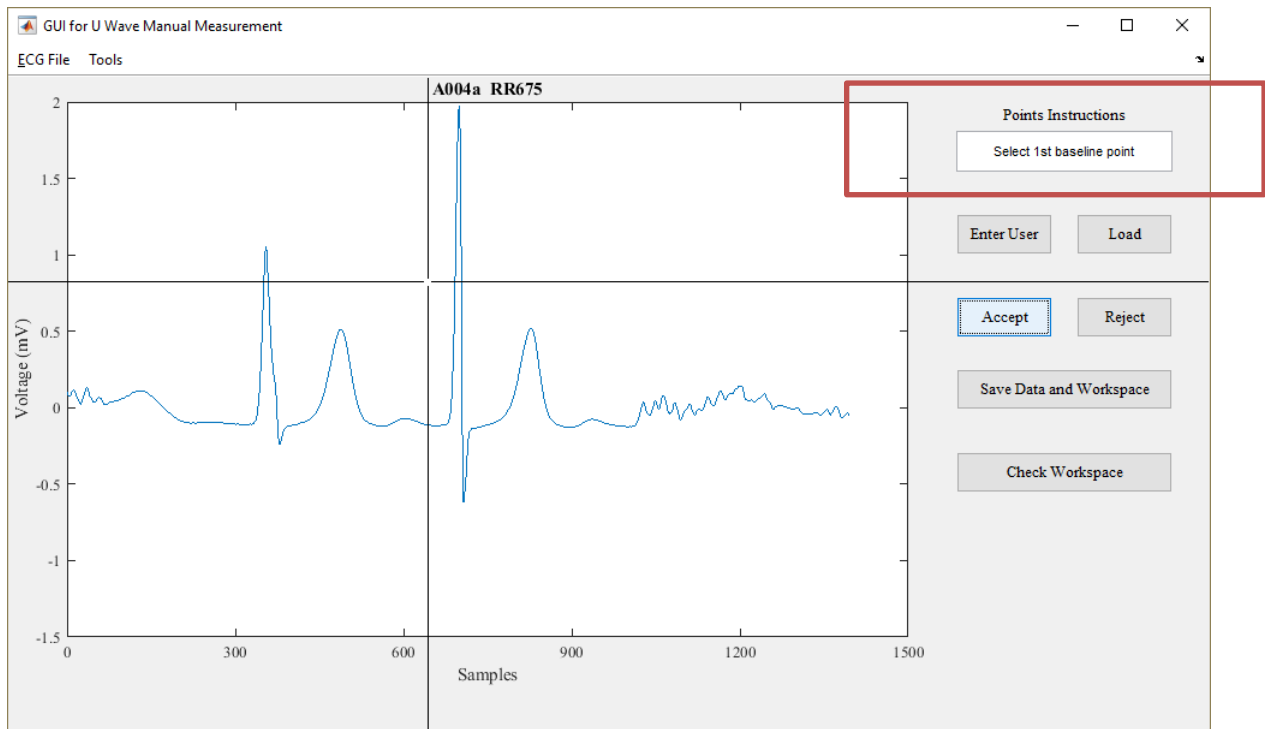


**Figure B.6:** Instructions text box

### 3) Accept / Reject Buttons

If the selection of these **6 points (clicks)**, are acceptable for the user and match the need of the points wanted, then press on **Accept button** to confirm and save the points, which can lead you to the next beat.

#### Reject button

If the **6 selections** have been mistakenly made or the user wanted to change the points, then **Reject button** will give the ability to re-select new 6 points again, and it should be in the same explained sequence.

Note that the Reject button will remove all the 6 markers and the data of the points, so you need to re-select new 6 points again, and then when you are satisfied, press **Accept button** to confirm the selections and save them.

The GUI will wait after points selection, until you '**Accept**' or '**Reject**' the selection to move on.

### 4) Save Data and Workspace Button

When you finish the analysis for *all the beats or part of them*, and you want to *quit* the GUI, you should **save the whole analysis** by press on the **Save Data and Workspace** button, see Figure B.7. The GUI will ask to choose a folder to save the data, so save them in the same environment of the GUI (i.e same folder of the code).

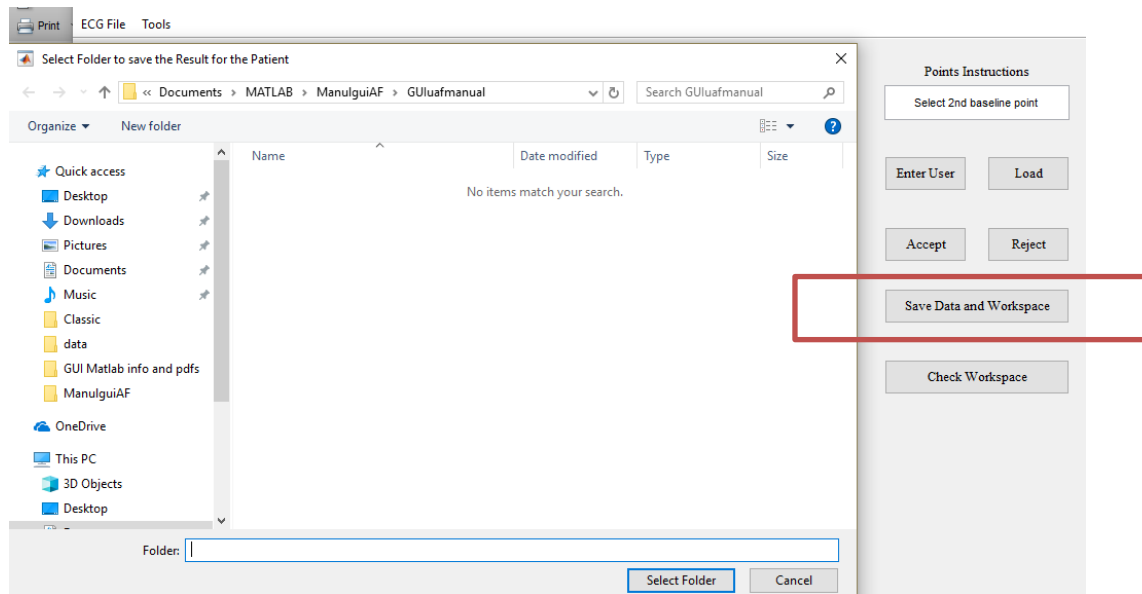


**Figure B.7:** Save the results from the analysis and the workspace window

## B.4 Results Structures Notes

If you finished selecting all the features, and analysed all the beats, the results will be saved in the same folder that you chose. The results will be saved in a structure array with following format (e.g):

**MAF.A004a.RR625.MS.ManualRslt.** Where:

- 1) **MAF**: the name of the structure array.
- 2) **A004a**: name of the subject (recording title), will be changed according to the patient name.
- 3) **RR625**: R-R interval, to classify the beat according to the specific intervals, since there are 10 R-R intervals. This will be changed from R-R 626 to R-R 1075. (Increasing by 50 ms)
- 4) **MS**: here is the initial for the username, so it could be any other letters according to the user. Which can help to identify the analyser.
- 5) **ManualRslt**: the final path where the x, and y coordinates (values) will be saved in the same order of clicking to have the points. See Figure B.8.
- 6) X values represents samples, while Y values represents the amplitudes in millivolts (Figure B.8).

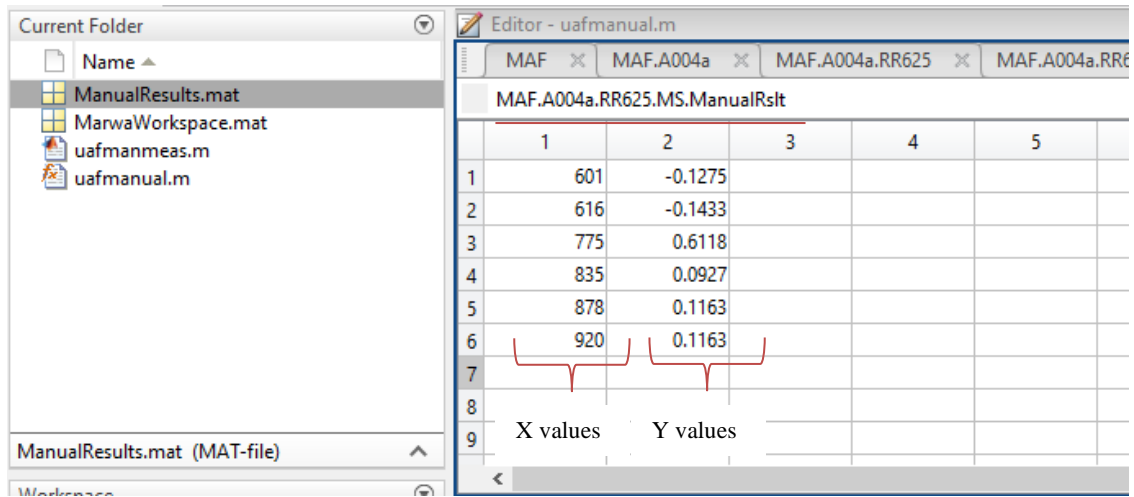


**Figure B.8.** Results structure in Matlab

If you did not finish the analysis, and you want to **quit and then resume the analysis** again, follow the next steps:

- 1) First you should save the results wherever you are in the analysis by press on the **Save Data and Workspace button**. That will guarantee, saving the data that you analysed, and help you to resume from the same beat and patient that you stopped with. Remember to save in the same folder.
- 2) When you want to **resume** the analysis, you should press on the **Check Workspace** button first. This step will look for the previous workspace that has been saved, see Figure B.9-a.

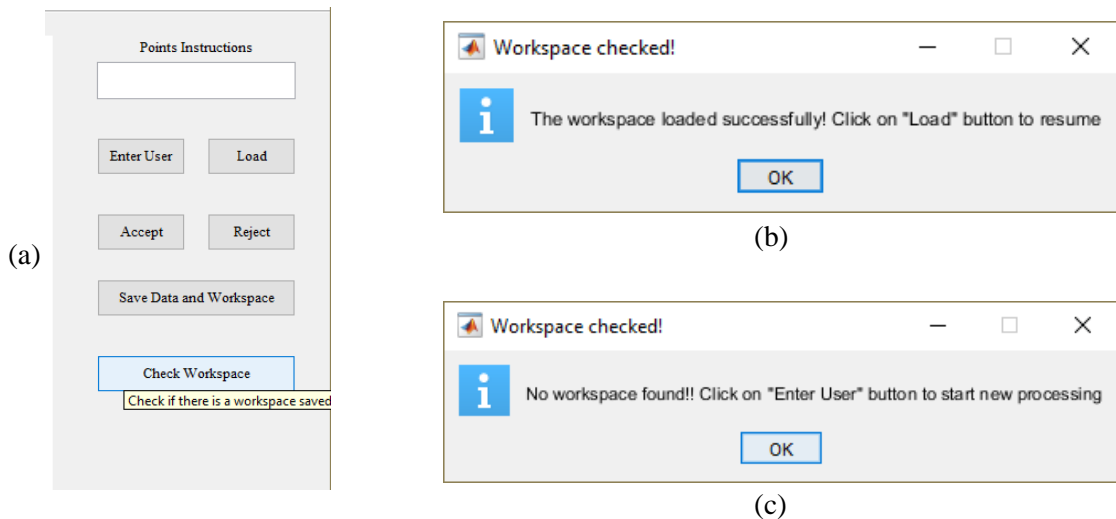


**Figure B.9:** Checking the Workspace

- 3) In case the GUI will find the workspace, it will give the confirmation message: that the data has been loaded, and then you can resume the processing, as B.9-b shows.
- 4) You need to re-load the data (ECGs) again, by using **Load button** as explained in step number (2) by loading data.
- 5) You will start from the **same** beat and patient that you stopped with, and then you can continue the processing normally, in the same steps order that has been mentioned above.
- 6) No need to re-enter the username initials in this case, because already it has been saved and re-uploaded.

You can use the **Check Workspace** button, at the beginning, even before username button in step (1).

- 7) If you have old workspace, it will upload it again.
- 8) If you have no workspace saved, it will give a message, to confirm that no workspace is available, and to start new manual analysis, see B.9-c.
- 9) Note: The recommendation for new analysis should start from step number (1) by entering new username.

# **Appendix C**

## **Beats Selection Matrix**

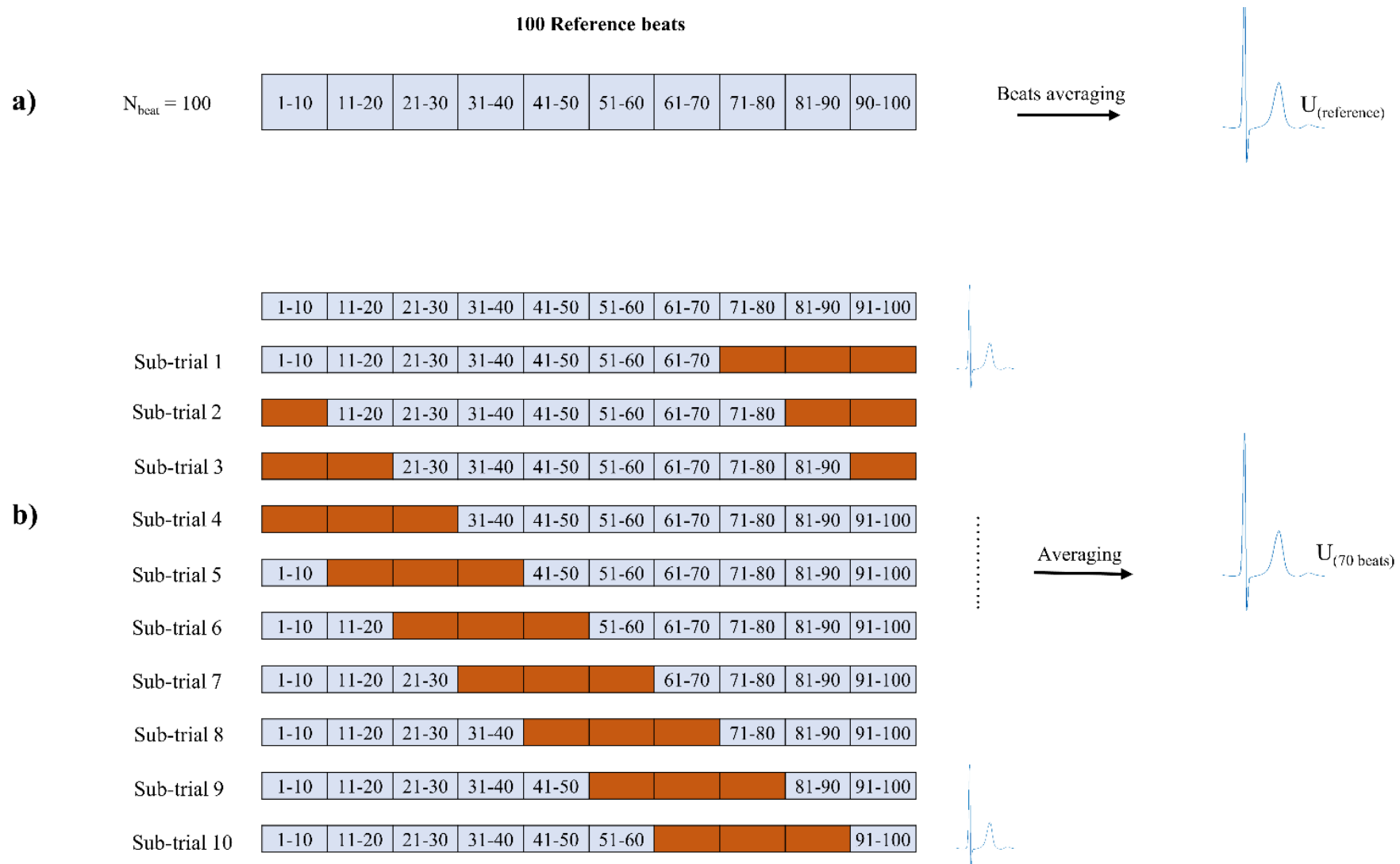


**Figure C.1:** Illustrates the selection of beats for 10 sub-trials when the number of beats = 70. **(a)** generating the reference ( $U_{\text{amp}_{\text{reference}}}$ ) from all 100 beats ( $N_{\text{beats}} = 100$ ). **(b)** the 10 sub-trials when the number of beats in the sub-trials was **70** beats ( $N_{\text{beats}} = 70$  beats). Each sub-trial generated an average beat which were compared to the reference U wave ( $U_{\text{amp}_{\text{reference}}}$ ).

## **Appendix D**

### **Proof: Increasing Number of Beats Reducing the Noise in Beat Averaging Technique**

Beat averaging improves the signal to noise ratio by a factor of  $\sqrt{N}$  where  $N$  is the number of epochs. The mathematical proof is as the following [154]:

The input waveform  $f(t)$  has a signal portion  $S(t)$  and a noise portion  $Noise(t)$ . Then:

$$f(t) = S(t) + Noise(t) \quad (1)$$

Let  $f(t)$  be sampled every  $T$  second. The value of any sample point in the time epoch ( $i = 1, 2, \dots, n$ ) is the sum of the noise component and the signal component.

$$f(iT) = S(iT) + Noise(iT) \quad (2)$$

Each sample point is stored in memory. The value stored in memory location  $i$  after  $N$  repetitions is:

$$\sum_{k=1}^N f(iT) = \sum_{k=1}^N S(iT) + \sum_{k=1}^N Noise(iT) \quad \text{for } i = 1, 2, \dots, n \quad (3)$$

The signal component for sample point  $i$  is the same at each repetition if the signal is stable and the epochs are aligned together perfectly. Then:

$$\sum_{k=1}^N S(iT) = NS(iT) \quad (4)$$

The assumptions for this development are that the signal and noise are uncorrelated and that the noise is random with a mean of zero. After many repetitions,  $Noise(iT)$  has rms value of  $\sigma_n$ .

$$\sum_{k=1}^N Noise(iT) = \sqrt{N\sigma_n^2} = \sqrt{N} \sigma_n \quad (5)$$

Taking the ratio of Equations (4) and (5) gives the SNR after  $N$  repetitions as:

$$SNR_N = \frac{NS(iT)}{\sqrt{N} \sigma_n} = \sqrt{N} SNR \quad (6)$$